The Triple Threat: Estrogen Deficiency, *APOE* Genotype, and Age on Cerebral Vascular Function

by

Mackenzie Nicole Kehmeier

A dissertation accepted and approved in partial fulfillment of the

requirements for the degree of

Doctor of Philosophy

in Human Physiology

Dissertation Committee:

Ashley E. Walker, Ph.D., Chair, Mentor

John R. Halliwill, Ph.D., Core Member

Carrie E McCurdy, Ph.D., Core Member

Alison Burggren, Ph.D., Core Member

Santiago Jaramillo, Ph.D., Institutional Representative

University of Oregon

Fall 2024

DISSERTATION ABSTRACT

Mackenzie Nicole Kehmeier

Doctor of Philosophy

Title: The Triple Threat: Estrogen Deficiency, APOE Genotype, and Age on Cerebral Vascular Function

As late-onset of Alzheimer's disease (LOAD) prevalence increases, efforts toward elucidating mechanisms underlying LOAD pathology are needed. Three of the greatest genetic risk factors for late-onset Alzheimer's disease are age, female sex, and the apolipoprotein E ε4 (*E4*) genotype. Two-thirds of LOAD cases are females, and perimenopause coincides with the prodromal phase of LOAD. Post-menopausal females with an *E4* allele have higher rates of LOAD compared with age-matched males with an *E4* allele, suggesting an interaction between *APOE genotype,* age*,* and estrogen deficiency. Cerebral endothelial function can alter cerebral blood flow (CBF) and compromise the blood-brain barrier. Cerebral endothelial dysfunction is a common link between the *E4* genotype, estrogen deficiency, and LOAD. However, the interaction effect of *APOE,* age*,* and estrogen on cerebral endothelial cell function and mitochondrial health is unknown. I hypothesized that estrogen fluctuation and deficiency modulate cerebrovascular function, and this function is further impaired in the presence of the *E4* genotype and age. The following aims were completed to test my hypotheses.

Aim 1: Determine the role of phytoestrogens and female sex hormones on cerebral vascular function. Aim 1 encompasses Chapters 2 & 3 of this dissertation and the main findings were two-fold. 1) The estrous cycle in female mice influenced large artery stiffness but not *ex vivo* endothelial function in resistance arteries. Thus, accounting for the estrous cycle for *ex vivo*

endothelial function is not needed but should be accounted for when measuring *in vivo* large artery stiffness. 2) Phytoestrogens, specifically soy in the rodent diet, influenced cerebral vascular function, insulin signaling, and cognitive function. This study also confirmed previous findings that ovariectomy impairs endothelial function and, for the first time, demonstrated that a soy diet prevents adverse effects of ovariectomy on insulin-mediated vasodilation.

Aim 2: Determine the interaction effect of APOE genotype and estrogen deficiency on cerebral vascular function, in vivo whole-body metabolism, and ex vivo cerebral vascular mitochondrial health. The findings from Aim 2 are shown in Chapter 4. In *E3* and *E4* female mice, I investigated how estrogen deficiency influenced endothelial and mitochondrial function. Overall, these results indicated that *APOE* genotype modulates the impact of estrogen on the cerebrovasculature. 17β-estradiol enhanced cerebrovascular function and mitochondrial function in *E3* mice, while *E4* mice conferred resistance to estrogen status.

Aim 3: Determine the interaction effect of aging and APOE genotype on cerebral vascular and cognitive function. Aim 3 is addressed in Chapter 5, and investigated the influence of age and *APOE* genotype on vascular function and cognition. The major results of this study demonstrated that age has a greater influence on cerebral vascular function than the *E4* genotype.

These series of studies highlight the importance of considering sex and age as a biological variable that can influence one's results. The major novel finding of these studies is that the *E4* allele confers resistance to estrogen status, and the broader impact of this finding is that consideration of *APOE* genotype is needed when prescribing hormone replacement therapy for menopausal females.

This dissertation includes previously published and co-authored material.

CURRICULUM VITAE

NAME OF AUTHOR: Mackenzie N Kehmeier

GRADUATE AND UNDERGRADUATE SCHOOLS ATTENDED:

University of Oregon, Eugene OR
Western Colorado University, Gunnison CO

DEGREES AWARDED:

Doctor of Philosophy, Human Physiology, 2024, University of Oregon
Master of Science, High Altitude Exercise Physiology, 2020, Western Colorado University
Bachelor of Science, Exercise Sports Science, 2019, Western Colorado University

AREAS OF SPECIAL INTEREST:

Vascular function
Sex differences
Aging

PROFESSIONAL EXPERIENCE:

Graduate Employee, Department of Human Physiology, University of Oregon. 2020-present.

Lab Instructor, Department of Human Physiology, University of Oregon, 2020-2022

Exercise Physiologist, Cardiac and Pulmonary Rehabilitation, Gunnison Valley Hospital, 2018-2020

Lab Instructor, Department of Biology, Western Colorado University, 2019

Graduate Assistant, High Altitude Exercise Physiology Lab, Western Colorado University, 2018-2019

Teacher Assistant, Department of Biology, Western Colorado University, 2018-2019

Research Assistant, High Altitude Exercise Physiology Lab, Western Colorado University 2017-2019

GRANTS, AWARDS, AND HONORS:

American Heart Association Predoctoral Fellowship, University of Oregon, 2023-2024

Cardiovascular Recgonition Award, Cardiovascular section, American Physiological Society 2024

Environmental & Exercise Physiology Section, American Physiological Society, Drs. Lou Stephenson and Margret (Peg) Kolka Women in Physiology Predoctoral Award, University of Oregon, 2023

FIrst Year Merit Award, University of Oregon, 2021

Beegle Travel Award, University of Oregon, 2024

Ursula (Sue) Moshberger Scholarship (University of ORegon, 2024

General University Scholarship, University of Oregon, 2023-2024

Jan Broekhoff Scholarship, University of Oregon, 2022

FIrst Year Merit Award, University of Oregon, 2021

PUBLICATIONS:

a. **Kehmeier MN**, Khurana A, Bedell BR, Cullen AE, Cannon AT, Henson GD, Walker AE. The effects of dietary soy content on cerebral artery function and behavior in ovariectomized female mice. *Am J Physiol Heart Circ Physiol*. 2023 Dec 29. doi:10.1152/ajpheart.00618.2023. PMID:38156886

b. **Kehmeier, M. N.,** Bedell, B. R., Cullen, A. E., Khurana, A., D'Amico, H. J., Henson, G. D., & Walker, A. E. (2022). In vivo arterial stiffness, but not isolated artery endothelial function, varies with the mouse estrous cycle. *American Journal of Physiology-Heart and Circulatory Physiology*, 323(6), H1057–H1067. https://doi.org/10.1152/ajpheart.00369.2022 PMID: 36240435

c. **Kehmeier MN**, Walker AE. Sex Differences in Large Artery Stiffness: Implications for Cerebrovascular Dysfunction and Alzheimer's Disease. *Front Aging*. 2021 Dec;2:791208.

doi: 10.3389/fragi.2021.791208. Epub 2021 Dec 1. PMID: 35072153; PMCID: PMC8782423.

d. Cole JA, **Kehmeier MN**, Bedell BR, Krishna Kumaran S, Henson GD, Walker AE. Sex Differences in the Relation Between Frailty and Endothelial Dysfunction in Old Mice. *J Gerontol A Biol Sci Med Sci*. 2022 Mar 3;77(3):416-423. doi: 10.1093/gerona/glab317. PMID: 34664649; PMCID: PMC8893262.

e. **Kehmeier MN**, Cannon AT, Kuhrana A, Cullen AE, Alkayed NJ, Walker AE. Cerebral artery function and stiffness is dependent on APOE genotype and ovariectomy status in mice. American Heart Association, Hypertension Scientific Sessions, 2023. https://doi.org/10.1161/hyp.80.suppl_1.122

f. **Kehmeier, M. N**., Dages, A., and Dalleck, L. (2020). Effects of Acute Reduced-Exertion High-Intensity Interval Training and Vigorous-Intensity Exercise on the Advanced Lipid Profile. *International Journal of Research in Exercise Physiology* 15*(2), 65-90.*

g. Seward, S., **Kehmeier, M.N,** and Dalleck, L. (2020). Effect of Community based-ventilatory threshold training program on metabolic syndrome risk factors. American College of Sports Medicine (ACSM). DOI: 10.1249/01.mss.0000678740.16420.0b

ACKNOWLEDGMENTS

I would like to give my deepest appreciation to all the incredible people who have helped support me throughout the process of this dissertation. First, I would like to give the biggest thanks to my mentor Dr. Ashley Walker, for her unwavering support and guidance. Dr. Walker has given me a beyond exceptional example of what it takes to be a successful female scientist, mentor, teacher, collaborator and mother. Thank you for taking a chance on me and allowing me the opportunity to develop as a researcher, scientist, and human under your care.

Second, I would like to thank all my committee members, Dr. John Halliwill, Dr. Carrie McCurdy, Dr. Alison Burggren, and Dr. Santiago Jaramillo, for their guidance and mentorship throughout my time here. Your time and energy to help me navigate my dissertation and development as a researcher is insurmountable.

Next, none of this work would have been possible without the staff in the animal facility here at the University of Oregon, and I am very grateful for all the tedious care they provide for our animals every day. I would also like to thank the American Heart Association for selecting me for a predoctoral fellowship, providing me support for the last two years here, so I could give all my time and passion to my research. Furthermore, I would like to thank all my friends and lab mates I have had the pleasure of crossing paths while being here. The people make a place, and this place is something I will be forever grateful for.

Lastly, I would like to acknowledge and thank all my co-authors. Science is a collaborative endeavor, and I wouldn't be able to complete this degree and dissertation without their help.

DEDICATION

I would like to dedicate this dissertation to the people I carry on with me, and to the people who allow me to grow. The first dedication is to my little cousins, my dreamers, Michelle and Kimber, who live on through me as the young girls they were, in search of their wildest dreams. Their love for life and who they would've been is something that reminds me to pursue my passions forcefully and to remain curious. My second dedication is to my dear friend Reid, who practiced greatness every day, in every aspect of his life, and inspires me to do the same. My last, and greatest dedication is my Aunt Barb and Marianne, who taught me to celebrate and embrace authenticity and kindness. I would not be half the woman I am today if it wasn't for them and the impact they have left on my life. Finally, to my support, my family. Mom, Dad, Kayla, and Casey are my roots and trunk to my tree. All of you have allowed me to grow and branch in all the ways I needed too, in order to get to where I am today. I could not have done this without any one of you, reminding me of who I am, who I want to be, and to keep pursuing a purpose greater than myself. This dissertation is for all of you.

TABLE OF CONTENTS

LIST OF FIGURES AND TABLES

I. INTRODUCTION

1.1 Specific Aims

As late-onset of Alzheimer's disease (LOAD) prevalence increases, efforts toward elucidating mechanisms underlying LOAD pathology are needed. Two of the greatest risk factors for LOAD are age and the *E4* genotype. The gene encoding for apolipoprotein E (*APOE)* has three isoforms in humans (*E2, E3, E4),* and ApoE itself serves as a functional protein in the body important for cholesterol and lipid flux. Two-thirds of LOAD cases are females, and perimenopause coincides with the prodromal phase of LOAD. Post-menopausal females with an *E4* allele have higher rates of LOAD compared with age-matched males with an *E4* allele, suggesting an interaction between *APOE genotype,* age*,* and estrogen deficiency. Cerebral endothelial function can alter cerebral blood flow (CBF), elevate oxidative stress, and compromise the blood-brain barrier. Cerebral endothelial dysfunction is a common link between *E4*, estrogen deficiency, and LOAD. The proposed mechanism for this interaction is that *E4* and estrogen deficiency cause metabolic dysregulation, increasing flux through oxidative phosphorylation. This, in turn, increases reactive oxygen species (ROS) production, which is known to contribute to endothelial dysfunction. However, the interaction effect of *APOE,* age*,* and estrogen on cerebral endothelial cell function and mitochondrial health is unknown. Understanding this interaction is vitally important as it will provide insight into LOAD mechanisms, generate therapeutic targets, and provide clinical equity to females.

The proposed study aims to identify the interaction effect of estrogen, age, and *APOE* genotypes on cerebral endothelial, cognitive, metabolic, and mitochondrial function. My central hypothesis is that the interaction of estrogen deficiency, age, and *E4* genotype,

compared to the individual effects, results in greater vascular impairments, poorer cognition, and greater mitochondrial dysfunction. By testing these hypotheses, I will develop a better understanding of LOAD mechanisms in females.

Aim 1: Determine the role of phytoestrogens and female sex hormones on cerebral vascular function. I hypothesize that periods of low estrogen and estrogen deficiency will have worse cerebral artery endothelial-dependent dilation (EDD) compared to estrogen sufficiency, and EDD impairments can be recovered with phytoestrogens. To test this hypothesis, I will assess *ex vivo* cerebral artery EDD in a) female mice that are in different stages of the estrous cycle and b) female mice that are intact, ovariectomized, or ovariectomized on a phytoestrogen diet.

Aim 2: Determine the interaction effect of *APOE* genotype and estrogen deficiency on cerebral vascular function, in vivo whole-body metabolism, and ex vivo cerebral vascular mitochondrial health. I hypothesize that *E4* estrogen-deficient mice will have worse cerebral artery EDD, the highest *in vivo* reliance on fat metabolism, and greater vascular mitochondrial dysfunction compared to *E3* or estrogen-sufficient mice. To test this hypothesis, I will assess a) cerebral artery EDD, b) in vivo whole-body metabolism, and c) ex vivo cerebral vascular mitochondrial function in *E3* and *E4* mice that are intact, ovariectomized, and ovariectomized with estradiol treatment.

Aim 3: Determine the interaction effect of aging and *APOE* genotype on cerebral vascular and cognitive function. I hypothesize that aged *E4* mice will have worse impairments in cerebral artery EDD, and cognitive function and elevations in neuroinflammatory markers compared to young *E4* mice and young and old *E3* mice. To

test this hypothesis, I will assess a) cerebral artery EDD and b) cognitive function in aged and young *E3* and *E4* female and male mice.

The proposed aims establish the relationship between age, estrogen, and *APOE* genotype on cerebrovascular dysfunction, metabolic mitochondrial impairments, cognition, and neuroinflammatory markers related to LOAD. These aims will help guide future research on how age, estrogen deficiency, and *APOE* genotype can alter arterial function and fuel utilization. This will allow for novel therapeutics and diagnostic measures to intervene before severe pathology of LOAD presents.

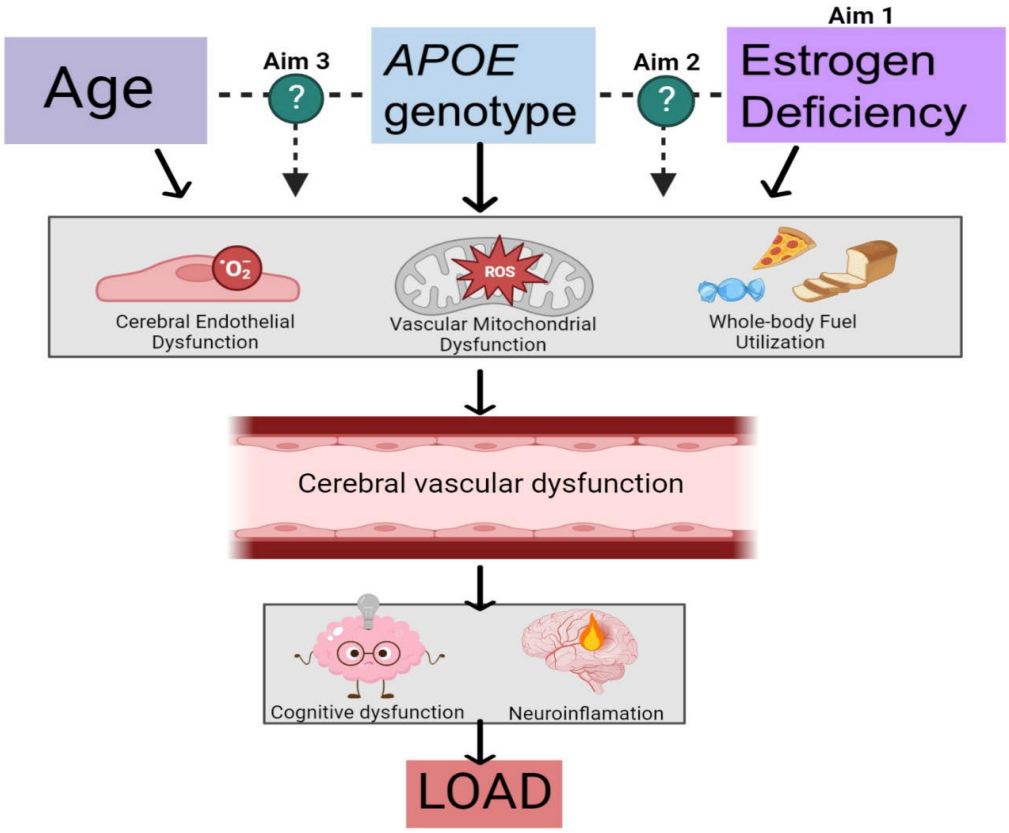

Figure 1.1. Aortic stiffness is lower during estrus. Schematic of the proposed for the relationship between age, *APOE* genotype, and estrogen deficiency. All these factors affect the outcomes individually, but my aims will investigate the interaction effect on the proposed outcome. Late-onset Alzheimer's Disease (LOAD).

1.2 Literature Review

1.2.1 Alzheimer's Disease and related Dementia

There is a current uproar in Alzheimer's Disease (AD) and dementia related research due to differing definitions of AD and the incomplete understanding of the disease. Thus, for this dissertation, we are defining AD as the following: A progressive brain disorder that causes impaired memory, thinking, and behavior. Amyloid Beta (Aβ) accumulation and tau tangles often accompany this disease. Aβ is generated from the amyloid precursor protein (APP), which is cleaved by α, β, and ɣ secretases. Cleavage of APP by β secretase generates insoluble Aβ42 that accumulates as Aβ plaques. Classical biomarkers like Aβ plaques and tau tangles are tied closely with early onset AD, which is AD that occurs before the age of 65 and accounts for 2% of AD cases. However, Aβ plaques and tau tangles can manifest with the more prevalent late-onset AD (LOAD). Interestingly, these pathological hallmarks are not necessary for clinical diagnosis of AD, suggesting other factors may underly the disease. While there is a myriad of risk factors for LOAD, three stand out, generating a triple threat in the development and onset of this disease. These risk factors are age, the *E4* genotype, and female sex.

Two decades ago, Farrer and colleagues reported a sex difference in the lifetime risk of AD in women (1). Women are two times more likely to develop AD. The *E4* genotype dramatically increases the risk of AD, and interestingly, women with a single copy of *E4* have a similar disease risk as men who have two copies of *E4*. Apolipoprotein E (apoE) is important to transport lipids and cholesterol and can contribute to cardiovascular disease risk (2). The interaction effect of estrogen and *APOE* genotype with age is incompletely understood and warrants further investigation. Notably, the current literature has left out a critical part of the picture: the investigation of the cerebral vasculature. Decreased cerebral blood flow (CBF) is the

first biomarker to change with the onset of AD (3). We and others (4) hypothesize that cerebrovascular function links cardiovascular risk factors to the observed cognitive decline. Thus, understanding the underlying mechanisms that alter CBF and how the triple threat interacts to impact cerebral vascular function, and health will provide crucial insight into personalized medicine and potential therapeutics.

1.2.2 Sex Hormones

Sex differences in AD and cardiovascular disease (CVD) risk are driven in part by changes in sex hormones (i.e. estrogen), which occur through the aging process. Other sex steroid hormones, like progesterone and androgens, influence vasculature and brain function (5, 6). For this dissertation, we will focus specifically on the role of estrogen in vasculature and the changes that occur in its absence. Estrogen signaling stimulates genomic and nongenomic cell signaling cascades, and its receptors are present in the vasculature and the brain (7, 8). Most of estrogen's action on the vasculature is attributed to action on the estrogen receptors (ER)α and g protein coupled estrogen receptor (GPER) (9). A decline of estrogen occurs with menopause, which is the cessation of the menstrual cycle, occurring around the age of 40-60 years in females. Perimenopause occurs 1-2 years before menopause and is accompanied by fluctuations in ovarian hormones, follicle-stimulating hormone (FSH), and luteinizing hormone (LH). This transitional phase and its accompanying hormone fluctuations cause a period of irregular hormone receptor imbalance, contributing to the many physiological and psychological symptoms associated with menopause, like cognitive dysfunction and hypertension (10–14). While humans experience the end of the menstrual cycle, rodents used in research experience a reproductive senescence known as estropause (rodent menopause), which is very different from humans (12). It is essential to consider these extraneous variables when performing translational physiology research.

Insight from previous clinical trials:

A series of clinical trials have been performed over the last three decades with efforts to highlight the effect of hormone replacement therapy (HRT) on postmenopausal women's health. Specifically, in 2002, a pivotal clinical trial known as the Women's Health Initiative (WHI) ended early (15). The importance of this trial has helped shape how we view HRT and brings to attention the complexity of estrogen signaling and its effects. Despite the beneficial knowledge this trial provided, it arguably pushed menopause and hormonal research back decades due to the extrapolated findings. The main headline from this trial was that estrogen causes breast cancer. While we can appreciate the complexity of hormone signaling, it is essential to note that women taking estrogen + progestin did experience a statistically significant, but maybe not clinically relevant, increase in breast cancer (15). However, women taking just estrogen supplementation, without progestin, experienced a relative decline in breast cancer prevalence. While the WHI did highlight the importance of potential HRT to mitigate menopausal symptoms, this clinical trial also was influential in highlighting that HRT in already post-menopausal females was not sufficient in helping reduce significant disease risk and was additive to disease progression (16, 17). Additional human clinical trials (HERS and HERS II) reported increased incidences and severity of neurological and vascular disease in women undergoing estrogen replacement therapy (18–23). This literature has brought forth the critical window hypothesis of hormone therapy (24). Thus, females who started estrogen therapy greater than ~10 years after entering menopause saw the adverse effects of estrogen therapy. In contrast, women who began therapy during the onset of their menopause redeemed the beneficial effects of estrogen (24). Despite the controversy, this highlights the need to investigate more mechanistic roles of estrogen.

1.2.3 Cardiovascular contributions to AD with special guest, estrogen:

Estrogen and the endothelium:

The vascular endothelium is a single layer of cells that provides a protective barrier to the smooth muscle cells (SMC) and supporting matrix proteins. The endothelial layer regulates blood flow, maintains tissue health, and ensures proper function. Dysfunctional endothelial cells lead to dysregulated cerebral artery responses (i.e., impaired vasodilation and altered vasoconstriction), ultimately leading to decreased CBF(25, 26). The primary mechanism for endothelial cell dysfunction with aging is an increase in reactive oxygen species (ROS),(27, 28) leading to decreased bioavailability of the vasodilator nitric oxide (NO) and elevated inflammation (29, 30). Endothelial-dependent dilation (EDD) is where mechanical force like the sheer stress of blood flow can stimulate eNOS, producing NO. NO then can travel to the SMC, activating cyclic guanosine monophosphate (cGMP), causing smooth muscle relaxation and arterial dilation. Endothelium-dependent dilation (EDD) decreases with age and estrogen deficiency (29, 31). The perimenopausal transition coincides with the onset of the loss of EDD, similar to the onset of AD (32, 33). Moreau and colleagues demonstrate that EDD, measured by FMD, declines in a stepwise manner with each stage of the menopausal transition (31). A placebo-controlled, double-blind, randomized clinical trial demonstrated that aromatase inhibition, which reduces estrogen, led to a 43% decrease in FMD in young, healthy men (34). These findings are important, but we must delve into estradiol's more mechanistic roles in endothelial signaling.

Estradiol has acute vasorelaxing properties via eNOS activation and subsequent NO production. Estrogen can upregulate eNOS expression, increasing nitric oxide bioavailability (35, 36). Estrogen diffuses through the cell membrane and binds to ERα. ERα interacts with and

activates PI3k, ultimately recruiting Akt at the membrane (37). Phosphorylation of Akt at serine 473 will then target eNOS, and phosphorylation of eNOS at serine 1177, changing the conformation of eNOS, enhancing its ability to convert L-arginine into NO and L-citrulline (38). Another important estrogen-specific receptor that results in vasodilation is GPER (39, 40). Activation of GPER participates in nongenomic estrogen related signaling, and *gper* deletion is associated with an increase in arterial stiffness, pulse pressure, and endothelial dysfunction (39, 41). Endothelial expression of GPER is lower in males and postmenopausal females compared with premenopausal females (42). It is widely accepted that estrogen binds to GPER at a lower affinity than classical estrogen receptors, it activates eNOS and NO production through the PI3k/Akt pathway, similar to ERα (43). The last classical estrogen receptor, Erβ, is thought to have negative vascular consequences (44). Declining circulating estrogen concentrations are associated with a shift in the ERα:ERβ ratio, more towards ERβ (44), which correlates with EDD loss. In addition to estrogen's effects on vasodilation, estrogen also strongly impacts vasoconstriction.

The balance of constrictors and estrogen's ability to influence them is important in the context of aging and disease. A primary constrictor in the vasculature is endothelin-1. A study in rats, with four groups: sham, ovariectomized, ovariectomy + estradiol, and ovariectomy + tamoxifen, demonstrated that ovariectomy enhanced cerebrovascular contractions to endothelin-1 and 17β-estradiol therapy reversed this effect (45). Estrogen can inhibit ET1 synthesis, partly explaining the increased constriction observed in the ovariectomy group. Another way estrogen affects the vasoconstrictor balance is via prostaglandins vs prostacyclin production through COX enzymes(18). Conversion of prostaglandins to prostacyclin promotes a vasodilatory response, while conversion to thromboxane elicits constriction (46). Researchers previously found in

middle cerebral arteries that 17β-estradiol decreased cerebrovascular tone by shifting the primary product of COX1 from prostaglandins to prostacyclin in rats (47). In rats with intact ovaries or those that have been ovariectomized, the ovariectomized rats had a decrease in vasopressin-induced thromboxane A2 release in the aorta (48). This decrease was due to lower COX-2 and thromboxane synthase enzyme mRNA expression in endothelial and SMC. Estrogen supplementation mitigated this effect (48). The ability of the artery to constrict properly to local stimuli and maintain vascular balance is critical, and the influence of estrogen on these constriction properties is often overlooked.

Oxidative stress is an imbalance of the body's reactive oxygen species (ROS) and antioxidants. Excessive levels of ROS oxidize cellular mitochondria components and DNA, contributing to the aging process (49). Different reactive oxygen species (ROS) types are essential for endothelial cell signaling. The first of interest is the superoxide radical (O2-), a result of incomplete reduction of oxygen in the electron transport system or a product of NADPH oxidase (NOX) (50). ENOS uncoupling can also produce superoxide, which increases the oxidative state of the cellular environment (51). NOX (Nox1 and Nox4) activity and function are lower in cerebral arteries from young female rats compared with young males (52). Additionally, higher superoxide levels increase the likelihood of reacting with NO to generate peroxynitrite (ONOO-) (53). ONOO- is a highly reactive molecule that not only results in cellular injury but also leads to vascular dysfunction by reducing NO. In 17β-estradiol treated ovariectomized rats, decreased superoxide production was observed due to lower NOX1 and NOX4 expression in the basilar artery (52). This is one example of estrogen’s ability to promote a lower oxidative environment by providing the cell with the necessary defense mechanism to combat oxidative stress.

Hydrogen peroxide (H2O2), the second ROS of interest, has both beneficial and detrimental vascular effects. Production of H2O2 in the vasculature occurs primarily through the enzyme superoxide dismutase (SOD). H2O2 production was initially thought to favor vasoconstriction pathways because of H2O2s prominent effects on thromboxane, COX, and overall contribution to an oxidative environment (54, 55). However, H2O2 production in a diseased state is an adaptive mechanism for increasing blood flow. In a diseased state like CVD, there is an increase in circulating ceramides. Ceramides are metabolized via sphingosine-1-phosphate (S1P), producing H2O2 (56). This H2O2 is released from the endothelium and diffuses to the SMCs to elicit hyperpolarization via opening BK_{Ca} channels, resulting in vasodilation (57). While these cellular mechanisms of oxidative balance are critical, we must consider that a primary site of ROS generation is the mitochondria.

Cerebrovascular mitochondrial function:

The human brain has a disproportionate energy demand relative to its size. It contributes to 2% of the body's weight, requires 20% of blood flow, and extracts about 50% oxygen and 20% of the body's available glucose, highlighting its high metabolic activity (58). Thus, it is unsurprising that mitochondrial dysfunction plays a significant role in impacting the oxidative balance in the brain. Estrogen interacts with its receptors to regulate mitochondrial biogenesis, the electron transport system (ETS), lipoprotein metabolism (59–64), and suppress ROS (65–68). The cerebral vessels are highly metabolically active, with more mitochondria in cerebrovascular endothelium than in other vascular beds (67, 69). Highly metabolically active cells are subjected to progressive cellular damage and dysfunction due to the increased production of mitochondrial ROS (67). Thus, the ability of estrogen to preserve endothelial function, specifically in the brain, has the potential to mitigate or enhance the development and progression of AD (70). Human

brain microvascular endothelial cells treated with 17β-estradiol have greater aconitase activity, indicating lower mitochondrial ROS, than sham treated controls (67, 68). Another study isolated mitochondria from cerebral blood vessels in ovariectomized rats vs controls. Control rats produced less succinate-driven mitochondrial H2O2 and had more Mn superoxide dismutase (Sod2) than ovariectomzed rats (65). The same study also found elevations in protein expression of cytochrome c and both subunits I and IV of complex IV in sham controls vs. ovariectomized rats (65). This study highlights the critical control estrogen must maintain appropriate mitochondrial function in cerebral blood vessels (67). Additionally, estrogen acts through the PGC-1 and NRF-1 pathways, which are important for modulating mitochondrial function, increasing mitochondrial efficiency, and reducing ROS production (67, 71, 72). Further, estrogens can regulate mitochondrial membrane microviscosity, improving bioenergetic function in skeletal muscle, but its role in this effect has yet to be investigated in the vasculature (73). Estrogens profound effects on regulating mitochondria function and antioxidant defenses captures the focus of many researchers due to its promising benefits.

Estrogen, vascular inflammation, and contributions AD:

The menopausal transition produces a storm of oxidative stress, the primary villain of vascular dysfunction (74). Increased ROS increases inflammatory signaling. Inflammatory signaling through tumor necrosis factor-α (TNFα) is the primary mediator of vascular dysfunction with aging and estrogen deficiency (75). TNFα can activate a signaling cascade, resulting in NFκB to release and translocate to the nucleus. Estrogen inhibits NFκB (75–78) suggesting a role for estrogen suppressing inflammation. Additional research has found that ovariectomy increased inflammatory cytokine IL1β in cerebral vessels in response to LPS injections(77). Overall, estrogen can aid in protection against cerebral vascular dysfunction by

reducing inflammation (79). While estrogen favors acting on the endothelial layer, its presence and absence also alter other vascular functions.

Large Artery Stiffness:

Aging of the vasculature results in increased arterial thickening and large artery stiffness. While CVD risk increases with age in both sexes, women experience an acceleration of stiffness post menopause (80). The SWAN heart study in 2019 aimed to determine whether women experienced changes in central arterial stiffness relative to their final menstrual period (80). Their results indicated that arterial stiffness significantly increased within one year of a female's final menstrual period. Healthy post-menopausal women's carotid artery compliance was lower with bilateral oophorectomy, and carotid artery β-stiffness was increased in the hysterectomy group (81). Hysterectomies allow for the preservation of the ovaries, but the removal of the uterus can still result in a decline in estrogen production due to inadequate blood supply. Thus, as women traverse menopause, ample evidence suggests they experience increases in arterial stiffness (82).

During menopause, large artery stiffness, mainly the aorta and carotid arteries, experience a decrease in elastin content, increased elastin fragmentation, and elevated collagen crosslinking, which increase vascular stiffness (32, 83, 84). This stiffness results in less pressure wave reflection and a decreased ability to dampen pulse pressure, resulting in a higher transmission of pulsatile energy (85). This increase in pulsatile pressure is transmitted into small resistant arteries, like the cerebral vessels, resulting in damage, dysfunction, and remodeling. This remodeling occurs in the artery's ECM and SMC.

Estrogen increases elastin content and inhibits collagen synthesis, as shown in animal studies (75, 86, 87). Thus, a reduction in estrogen lowers elastin content, elevates collagen deposition, and raises advanced glycation end products (AGEs), crosslinking the collagen. A

study in female monkeys noted increases in aortic collagen type 1 content compared with male counterparts with age (82, 88). Estrogen influences the regulation of collagen I, III, and matrix metalloproteases (MMP) 9 and 2 in cardiac tissue (89, 90). When estrogen levels drop, this regulatory effect diminishes. Additionally, estrogen deficiency increases intra-media thickness (IMT)(91). A study by Dubey 2000, revealed that estrogen acts by inhibiting MAPK, reducing SMC proliferation and migration from the media to the intima (92). They concluded that the affinity of the estrogen type alters the estrogen's ability to inhibit SMC proliferation.

Estrogens enhance vascular function by promoting an anti-oxidative environment, enhancing NO bioavailability, inhibiting SMC proliferation, and mitigating LAS. When considering the consequences of estrogen loss and outcomes on AD, we wondered how the *E4* genotype could promote poorer vascular outcomes related to AD.

1.2.4 What is Apolipoprotein E?

Apolipoprotein E is a protein involved in the metabolism of fats in the body and plays a significant role in the transport and distribution of cholesterol and other lipids (93). ApoE is found in both the peripheral tissues and the brain, with the cerebrovascular endothelium acting as the barrier between these two regions. ApoE is secreted primarily by the liver and macrophages in the periphery, whereas in the brain, it is largely produced by astrocytes. *APOE* polymorphisms result in three different *APOE* isoforms that differ by a single amino acid at residues 112 and 158, where cysteine or arginine are present (94). This difference in amino acids results in a change in structure and, thus, a change in protein function. *APOE* genotypes are as follows: *APOE ε2* (Cys112, Cys158), *APOE ε3* (Cys112, Arg158), and *APOE ε4* (Arg112, Arg158)(94). The *APOE* polymorphic alleles *E2*, *E3*, and *E4* have a worldwide frequency of 8%, 78%, and 14% respectively (1, 95). *E4* binds insufficiently to low-density lipoprotein receptors (LDLRs),

resulting in the deficient clearance of lipids, and in the case of AD, Aβ peptides, resulting in elevated oxidative stress and inflammation (96–98). While *E4* individuals have an increased prevalence of CVD, due to apoE's contributions to atherosclerosis, most of this review will focus on apoE's function in the brain and cerebrovasculature.

ApoE in the brain:

ApoE is crucial for brain function. Nearly every cell type in the brain has been reported to produce apoE (99, 100). Additionally, cholesterol homeostasis is pivotal for normal brain function. While the brain is only 2% of the body weight, 25% of all cholesterol is found in the brain(101, 102). Once apoE is secreted, apoE binds to cholesterol ATP-binding cassette protein (ABCA1), forming HDL particles in the ISF and CSF (101). Primary receptors for apoE are heparin sulfate proteoglycan (HSPG) and LDL receptors (LRP1), which promote cellular uptake and redistribution of cholesterol/lipids or convert cholesterol to oxysterols to clear through the blood-brain barrier (BBB) (101, 103, 104). Individuals with *E4* have increased cholesterol levels in the brain and body (105, 106). The *E4*'s change in apoE structure is poorly lipidated, suggesting one of its potential roles in disease and AD specifically.

APOE's role in inflammation and oxidative stress:

APOE modulates immune and inflammatory functions in the periphery and the CNS, further strengthening *APOEs* role in LOAD (107). The inflammatory marker, c-reactive protein, was measured from the Framingham Heart Study offspring cohort. Interestingly, individuals with the *E4* genotype had increased CRP levels, indicating this genotype is associated with higher baseline inflammation(108). Furthermore, in mice with the knock-in of *E3* and *E4*, *E4* mice had elevated measures of brain TNFα and IL6 secretion compared with *E3* mice (109). Studies demonstrate that microglia from E4s exhibit greater NFκB microglial expression than their *E3*

counterparts. This is potentially explained by *E4's* ability to bind to the promoter region of MAPK, activating the death domain (MADD and COMM domain containing 6 (COMMD6)), which are transcription factors that regulate gene expression via binding to NFκB (110, 111). *E4* can also decrease phagocytosis and increase glial activation, leading to an influx of inflammation and senescent cells in the AD brain (112, 113). *APOE4* was also reported to bind to the SIRT1 gene decreasing its expression and activity (110, 111). Sirt1 is involved in promoting autophagy, potentially explaining the role of *APOE4* in senescence and neurotoxicity(114). While the role of apoE on inflammatory processes has been widely investigated, the literature is still inconsistent, driving the field also to investigate the role of oxidative stress.

The *E4* genotype is correlated to elevated levels of oxidative stress, likely due to altered metabolism and immune response (115). Oxidative stress markers in *E4* cerebral vascular endothelial cells are elevated (100). Additionally, oxidative stress augments apoE secretion from adipocytes and apoE overexpression-protected cells from hydrogen peroxide-induced damage (116, 117). AD patients with the *E4* genotype have higher microglial lipid droplet accumulation and neurotoxic factors (118). Given the pleiotropic effects of the *APOE* gene, the field is moving to the proposition that the cell type from which apoE is generated plays a vital role in its functions. The multifaceted functions of apoE make it a potent modulator of cellular stress response that contributes to aging. As previously mentioned, the mitochondria are the primary site for ROS production. Thus, we must consider the influence of apoE and *APOE* genotype on mitochondrial function.

APOE and mitochondrial function:

While the symbiotic relationship of apoE and the mitochondria is not new, it is overlooked as a driver of AD. *APOE4* fragments have been found in the mitochondria of N2a

cells (110, 119). These *E4* cells have a reduction in mitochondrial complex I, IV, and V, supported by lower measures of oxygen consumption (OCR) compared to *E3* cells (120). Additional evidence, such as amplified ROS production, increased intracellular lipid droplets, and enhanced oxidative damage compared with the *E3* genotype, supports that the *E4* genotype is associated with mitochondrial dysfunction(100, 119, 121, 122). This metabolic dysfunction can be seen in *E4* individuals, who display lower brain glucose metabolism via FDG-PET scan, exemplifying a reduction in energy uptake.(123, 124). Mitochondrial dysfunction associated with *E4* has been well investigated in cell culture models and brain tissues; however, the role E4 plays specifically on cerebrovascular mitochondrial function remains unknown. ApoE is vital for the entire body's lipid flux, and we must understand how this protein and its varying isoforms impact the cerebrovascular since this is the barrier between the two distinct pools of apoE.

APOE in the vasculature:

The first biomarker of LOAD onset is alterations in cerebral perfusion (3), observed in older *E4* individuals. Previous research has provided limited knowledge of the impact and mechanisms of *APOE* genotype on vascular endothelial dysfunction. Most of the current literature regarding apoE, the cerebrovascular, and AD is about its effects on the integrity of the BBB (125, 126). In 2021, Montage and colleagues studied vascular dysfunction, Aβ pathology, neuronal dysfunction, and behavior in older (18-24mo) *E3* and *E4* knock-in mice alone and crossed with 5xFAD mice. Their findings show that old *E4* knock-in mice and *E4* x 5xFAD mice, compared to their respective *E3* lines, developed accelerated BBB breakdown associated with loss of pericyte capillary density, followed by subsequent reductions in CBF with and without Aβ presence (126). This group's work proposes the loss of BBB integrity is connected to the CypA-NFkB-MMP9 BBB degrading pathway in pericytes, and when activated, MMP9

degrades tight junction proteins. This is supported by the observed loss of zonulin-occludin (ZO)-1 and occludin in *E4* animals (125, 126). While this novel pathway and this group's work support a strong genotype effect and explanation of the mechanistic cause of BBB breakdown, the role of *apo*E in regulating blood flow in resistance arteries in the brain is warranted.

Other APOE effects in the Brain:

ApoE's role in AD onset and progression has been growing since apoE was discovered in the 1970s. ApoE transports lipids through the PNS and CNS and can also influence neuronal signaling via the reelin pathway acting through APOER2 (113). Reelin is essential for neuronal migration, dendritic spine development, and synaptic plasticity (113). *APOE4* limits reelin binding, decreasing synaptic plasticity(113, 127). ApoE also plays a vital role in microglia, and the APOE-TREM2 pathway drives dysfunctional microglia. This can be seen by the deletion of *APOE4* reducing microglial activation and neuroinflammation in the presence of Aβ and tau pathology (128). ApoE's effects in the brain is critical for proper function, and sex differences have emerged in apoE's functions.

1.2.5 Estrogen and *APOE*:

The *E4* allele has sex-dependent effects where the risk of developing AD is higher in *APOE4* expressing females than males (1, 129, 130). ApoE levels are lowest in the *APOE4* genotype compared to *E3*, and these differences are more pronounced in females (129, 131). Interestingly, action on ERα upregulates ApoE mRNA and protein expression (132). ERα expression is reported to be higher in AD and *APOE4* EFAD mice. This is proposed as a protective mechanism to increase apoE's presence (129, 133, 134). ERβ activation is associated with decreases in apoE levels, and it is hypothesized the HT effects on cognition could be blunted due to the reduced levels of apoE in *E4* carriers (132). Some studies have found *E4*

carriers more sensitive to HT protection (135–137). In contrast, others have found HT to interact negatively with apoE (133, 138–142), resulting in *E4* individuals being non-responsive to HT. This highlights the need to elucidate the mechanisms and consequences behind the interaction effect of sex hormones and *APOE* genotype.

1.3 The triple threat: Age, *APOE* genotype, and estrogen deficiency on cerebrovascular function

Given the lack of information on this triad of risk factors and how they interact, this dissertation and the following chapters aim to uncover the novel effects of apoE, its influence on the regulation of cerebral artery function, and the mechanisms underlying the alterations observed. Also, we aim to shed light on the often-overlooked sexual dimorphisms that exist in disease, specifically AD, and how the sex steroid hormone estrogen can interact with the *APOE* genotype to influence cerebral vascular and cognitive outcomes.

II. IN VIVO ARTERIAL STIFFNESS BUT NOT ISOLATED ARTERY ENDOTHELIAL FUNCTION VARIES WITH THE MOUSE ESTROUS CYCLE

From: **Kehmeier, M. N**., Bedell, B. R., Cullen, A. E., Khurana, A., D'Amico, H. J., Henson, G. D., & Walker, A. E. (2022). In vivo arterial stiffness, but not isolated artery endothelial function, varies with the mouse estrous cycle. American Journal of Physiology-Heart and Circulatory Physiology, 323(6), H1057–H1067. https://doi.org/10.1152/ajpheart.00369.2022 PMID: 36240435

2.1 Introduction

In the past, females were often excluded from research studies leading to a limited understanding of many physiological processes. In 2014, the National Institutes of Health announced a policy requiring both sexes to be represented in preclinical biomedical research for cells and animals, unless otherwise justified (143) and many scientific journals are beginning to add this requirement (144). Proper design of rodent studies that include females necessitates an acknowledgement of the hormonal fluctuation throughout the estrous cycle, and purposeful decisions about whether to control for these fluctuations. Therefore, it is crucial to elucidate the effects of the estrous cycle on physiological processes.

In women, the menstrual cycle phase impacts vascular function, in particular, stiffness of the large elastic arteries and endothelial function (145, 146). The large elastic arteries, specifically the aorta and carotid arteries, have a high elastin content contributing to their high compliance. Greater large artery stiffness corresponds with elevated systemic pulse pressure and increased risk for cardiovascular diseases and Alzheimer's disease (147). At the same time, endothelial cell function is important for regulating vascular tone and can modulate the compliance of arteries (148). Endothelial cells produce nitric oxide (NO), a potent vasodilator, through activation of endothelial nitric oxide synthase (eNOS). Impaired endothelial function, measured by endothelium-dependent vasodilation, is associated with cardiovascular and

cerebrovascular diseases (149). While numerous studies have examined changes to large artery stiffness and endothelial function during the menstrual cycle(145, 146, 150, 151), the effects of estrous cycle phase on these vascular outcomes in mice has yet to be investigated.

The impact of the menstrual or estrous cycle on vascular function likely arises from modulation by sex hormones (152). In mice, the estrous cycle is on average 5 days in length and composed of four stages: proestrus, estrus, metestrus, and diestrus. Circulating estrogen in mice is highest in the proestrus and estrus phases and lowest in diestrus (146). Other sex hormones also vary during the estrous cycle, such as progesterone and testosterone. Estrogens bind to estrogen receptor α (ERα, *Esr1* gene), estrogen receptor β (ERβ, *Esr2* gene), and estrogen G-protein coupled receptor (GPER, *Gper1* gene) in vascular cells. Activation of ERα and GPER increase NO bioavailability and deletion of *Gper1* is associated with higher arterial stiffness in mice (153, 154). Sex hormones are highly specific and have a high affinity for their receptors, allowing the slightest differences in sex hormone concentrations to induce physiological changes (155). Thus, despite the short duration of the mouse estrous cycle and low concentrations of circulating sex hormones, it is possible for the changes in circulating sex hormone concentrations and subsequent downstream receptor-mediated signaling to modulate physiological function between estrous cycle phases.

Due to the importance of including young female rodents in research, it is pertinent to understand the effects of the estrous cycle on vascular physiology and related outcomes. Therefore, the purpose of this study was to determine the effect of the mouse estrous cycle phase on arterial stiffness, vascular endothelial function, arterial estrogen receptor expression, and cognitive function. We hypothesized that estrous cycle stages with high circulating estrogen, namely proestrus and estrus compared with diestrus, would have lower aortic stiffness and higher

cerebral and mesenteric artery endothelial function. We further hypothesized that arterial estrogen receptor expression and eNOS expression/activation would be highest during proestrus/estrus compared with diestrus. As vascular function has overarching effects on other organs, we sought to determine the effects of the estrous cycle on cognitive function and motor coordination. We hypothesized that proestrus/estrus would be associated with higher cognitive function and better motor coordination.

2.2 Methods

Animals

Female C57BL/6 mice were purchased from Charles River and studied at 6-7 months of age (n=23). All mice were on a phytoestrogen free diet (Envigo, Teklad Global Soy Protein-Free Extruded Rodent Diet, 2920X) with food and water provided *ad libitum* and housed in the animal care facility on a 12/12-hour light-dark cycle at 24°C. Mice were euthanized by exsanguination under isoflurane immediately prior to vascular reactivity studies. In efforts to match the estrous cycles, female mice were induced into cycling by one cup of male bedding. All animal procedures conform with the Guide to the Care and Use of Laboratory Animals (8^{th} edition, revised 2011) and were approved by the Institutional Animal Care and Use Committee at the University of Oregon.

Estrous Cycle Tracking

The mouse estrous cycle was tracked via vaginal cytology at least 5 days prior to each test and at euthanasia. The vagina was flushed with a sterile transfer pipette containing sterile saline and the sample was expelled into a 36 well plate and placed on a slide for staining. Using rapid differential stain kit (Vet-One, Boise Idaho), the samples were stained per kit instructions. Once the slide was dry, samples we observed under LMi1 microscope (Lecia Microsystems,

Wetzlar, Germany) by two separate investigators and the cycle was determined. After analysis an additional two separate investigators confirmed cycle stage and any that were contradicting were verified by the University's veterinarian. Proestrus was identified by the presence of many nucleated epithelial cells, while estrus was identified by a predominance of cornified epithelial cells. Lastly, diestrus was determined by the presence of polymorphonuclear leukocytes (156, 157)(see supplemental figure S2.1). Metestrus was excluded from this study due to its limited duration within the estrous cycle.

Hormone Analysis

Plasma hormone concentrations for 17β-estradiol (E2), esterone (E1), progesterone, and testosterone were analyzed via Liquid Chromatography–Mass Spectrometry (LC-MS). Blood samples were collected via cardiac puncture with a heparin saline coated syringe. The blood was centrifuged, then plasma was collected and frozen in liquid nitrogen. All plasma analyses were performed by the Endocrine Technologies Core at Oregon National Primate Research Center at Oregon Health & Science University. Estradiol and esterone had low levels of detected and quantification for these is less accurate. The ratio of E2 to E1 was calculated and reported (see table 2.1).

Aortic stiffness

Aortic stiffness was measured *in vivo* by pulse wave velocity (PWV). In a cohort of mice (n=6), PWV was measured three times during a five-day period, with one day between each measurement, with the goal to make measurements in each phase of the cycle. However, given the short duration of proestrus, we did not collect enough measurements during this stage to include in the analysis, and thus, data for only estrus and diestrus are presented for the repeated-measures comparison. For the remaining mice, PWV measures were collected only once. Mice

were anesthetized using isoflurane (2% isoflurane in 100% oxygen) and laid supine on a temperature-controlled heating pad (35°C). Electrodes were placed on distal portions of limbs that recorded ECG, while two Doppler transducers were positioned on the aortic arch and abdominal aorta, and the distance between the two transducers was recorded. Using the Doppler signal processing workstation program (DSPW; Indus Industries, Webster, TX, USA), the time of a pulse to travel from the arch to the abdominal aorta was analyzed, and the time was then divided by the distance between the transducers. Two researchers analyzed all the files independently, and the average was taken.

Vascular Reactivity

Endothelium-dependent vasodilation was assessed in *ex vivo* isolated pressurized mesenteric arteries and posterior cerebral arteries, as described in detail previously (Cole et al 2021). Arteries were excised and cannulated onto glass micro pipettes in a myograph chamber (Danish MyoTechnology Inc.) filled with physiological salt solution. All arteries were preconstricted with phenylephrine (1-6 μM to obtain 20-40% preconstruction) and increases in luminal diameter in response to increasing concentrations of endothelium-dependent dilators acetylcholine (ACh: $1x10^{-9}$ to $1x10^{-4}$ M) and insulin ($1x10^{-9}$ to $1x10^{-5}$ M) were determined. After ACh and insulin responses, arteries were incubated for 30 minutes with 0.1 mM of N omega-Nitro-L-arginine methyl ester hydrocholoride (L-NAME). ACh and insulin responses were repeated in the presence of LNAME to determine the contribution of nitric oxide synthase to endothelium-dependent dilation. Endothelium-independent dilation was measured by the increases in lumen diameter to sodium nitroprusside ($1x10^{-10}$ to $1x10^{-4}$ M).

Motor Coordination

Motor coordination testing was performed using a rotarod (47650 Rota-Rod NG, Ugo Basile, Gemonio, Italy) over a two-day period. The first day was a training session, mice were required to stay on the rod rotating at 4 rpm for 90 seconds. The second day consisted of three trials, with a 10-minute rest between trials, where the rod accelerated during each trial from 4 to 40 rpm with a cut-off time at 5 minutes. The time was recorded for when the mouse fell from the rod or rotated around the rod two consecutive times (158).

Nesting behavior test

Nest building tests instinctual behavior and was performed over a 12-hour period. Mice were singly housed overnight in a cage with food, water, and a condensed cotton nestlet. In the morning, the researcher scored the nests and placed mice back in their communal cage. Nests were scored on a scale of 0-5, and the scoring criteria were as follows: 0- nestlet is untouched; 1- nestlet has been moved but no significant tearing; 2- significant tearing, but no formation of a nest; 3- significant tearing, indication of nest OR nest is in the corner of the cage; 4- significant tearing, formation of nest in the corner; 5- significant tearing, formation of nest in corner and the nest walls are high making a bowl like nest (159).

Protein Expression

The thoracic aorta was excised and cleaned of fat and blood and frozen in liquid nitrogen. Samples were homogenized in total protein extracting reagent buffer and protease inhibitor cocktail, and then water sonicated for 60 seconds twice at 50% power. Lysate protein concentration was assessed using a commercially available kit (Pierce BCA protein assay kit; Thermo Fisher, Waltham, MA). 4-20% Precast Criterion TGX gels were used for separation. Membranes were blocked with 5% goat serum in TBS-T. The transfer was verified with ponceau red stain, and then incubated in primary antibodies overnight in PBS containing 3% BSA.

Primary antibody concentrations are listed in supplemental table S2.2. Following incubation, membranes were washed and incubated with a species-appropriate HRP-conjugated secondary antibody. Following washes, membranes were incubated with Pierce Enhanced Chemiluminescence Western Blotting Substrate (Pierce ECL, Thermo Fisher) and imaged with an Odyssey Fc (LI-COR, Lincoln NE). Image J was used to determine protein band density and relative protein expression was calculated as protein density normalized to GAPDH density. Values were normalized to the group in diestrus. See supplement Table S2.2 for antibody list and validation.

Gene Expression

In samples of mesenteric arteries and cerebral arteries (combined middle cerebral artery, posterior cerebral artery, and basilar artery), mRNA gene expression was quantified for *Esr1*, *Esr2*, and *Gper1* through qPCR (see supplement Table S2.1 for primer sequences). RNA from cerebral arteries and mesenteric arteries was isolated by a standard protocol using Qiazol and RNAeasy Micro Kits (Qiagen, Hilden, Germany) and then quantified using a NanoDrop 2000 (Thermo Scientific, Waltham, MA). Reverse transcription was performed to produce cDNA with a Qiagen Quantitect Reverse Transcription Kit. The cDNA samples underwent real-time qPCR using ThermoFisher PowerUp Sybr Green and a Quantstudio 5 real-time PCR system (ThermoFisher Scientific, Waltham, MA). mRNA expression was calculated using the $2^{-\Delta\Delta CT}$ method. 18s mRNA was used as a housekeeping gene control, and values were normalized to the group in diestrus.

Statistical Analysis

Statistical analyses were performed with IBM SPSS (Version 26, Armonk, NY) and GraphPad Prism 9.0. One-way analysis of variance (ANOVA) between proestrus, estrus, and

diestrus groups were used unless otherwise noted. In cases of a significant F-value, post-hoc analyses were performed using a Tukey correction for preplanned comparisons. For the matched PWV measures, a paired t-test was used to compare cycle phases. A repeated measures ANOVA was used to determine group differences for dose responses. Pearson correlation analysis was used to assess bivariate relations of interest. Significance was set at $p<0.05$, and values are represented as mean ± SD. Outliers were identified as z score>2 and removed from the data set.

2.3 Results

Animal characteristics throughout the estrous cycle

There were no differences for body weight or any tissue weights, except for uterus weight, between the stages of the estrous cycle (all $p>0.05$, Table 2.1). Uterus weight was higher in the proestrus phase compared to estrus ($p=0.0014$) and diestrus ($p=0.007$). Plasma testosterone concentration was higher for mice in diestrus compared with mice in proestrus and estrus ($p=0.0003$, Table 1). Plasma esterone was elevated during the proestrus phase compared to the other two phases ($p=0.03$, Table 2.1).

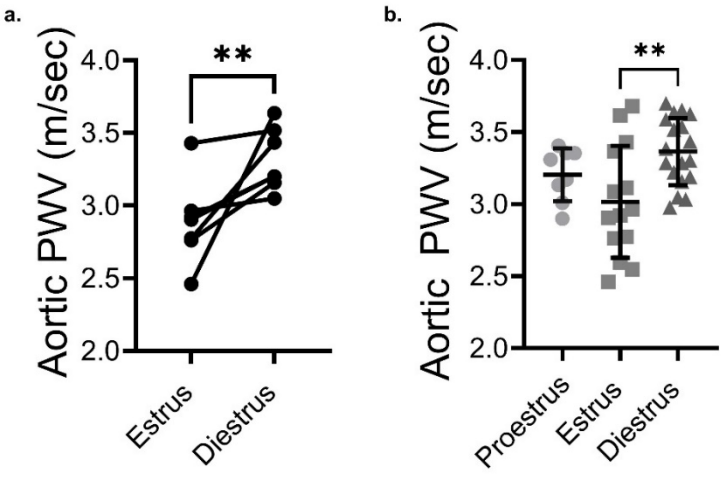

Figure 2.1. Aortic stiffness is lower during estrus. *A:* Repeated measures of aortic stiffness by pulse wave velocity (PWV) for mice in estrus and diestrus. n=6/group. *B*: Compiled aortic PWV for entire cohort during proestrus, estrus, and diestrus. n=8-18/group. One-way ANOVA revealed $p<0.01$(**). Data are mean ± SD.

In vivo arterial stiffness is dependent on estrous cycle phase

In a subset of mice that underwent repeated measures of arterial stiffness across the estrous cycle, aortic PWV increased from estrus to diestrus ($p=0.0046$, Fig 2.1 A). In the full subject sample, PWV was lower for the mice in estrus when compared with mice in diestrus ($p=0.0048$). Mice in proestrus did not differ from the other stages for aortic PWV ($p=0.32$ versus estrus, and $p=0.40$ versus diestrus, Fig 2.1 B). Heart rate did not differ between groups ($p=0.20$, data not shown).

Endothelial function ex vivo is independent of estrous cycle phase

The posterior cerebral artery and mesenteric artery responses to ACh did not differ between estrous cycle phases (dose response RM-ANOVA and maximal responses ANOVA, all $p>0.05$, Fig 2.2 A, B). The maximal ACh responses in the cerebral and mesenteric arteries did not correlate with uterus weight (posterior cerebral artery: $r=0.04$, $p=0.40$; mesenteric artery: $r=0.21$, $p=0.17$, progesterone (cerebral artery: $r=0.37$, $p=0.11$; mesenteric artery: $r=-0.14$, $p=0.30$), or testosterone (cerebral artery: $r=0.22$, $p=0.24$; mesenteric artery: $r=0.02$, $p=0.47$), further indicating no influence of the estrous cycle on endothelium-dependent vasodilation. Furthermore, the posterior cerebral artery and mesenteric artery responses to insulin were not different between estrous cycle phases (dose response RM-ANOVA and maximal responses ANOVA, all $p>0.05$, Fig 2.2 D, E). Likewise, the response to ACh and insulin in the presence of L-NAME was not different between estrous cycle phases for either artery (dose response RM-ANOVA and maximal responses ANOVA, all $p>0.05$, Fig 2.2 A, B, D, E). Endothelium-

independent vasodilation in response to sodium nitroprusside was also not different between groups for either artery (dose response RM-ANOVA and maximal responses ANOVA, all p>0.05, Fig 2.2E, F). Sensitivity (EC50) and preconstriction also did not differ between estrous cycle phases for any dose response (all p>0.05, supplemental Table S2.3). These data reveal that *ex vivo* endothelium-dependent and endothelium-independent vasodilatory responses in resistance arteries are independent of the estrous cycle phase.

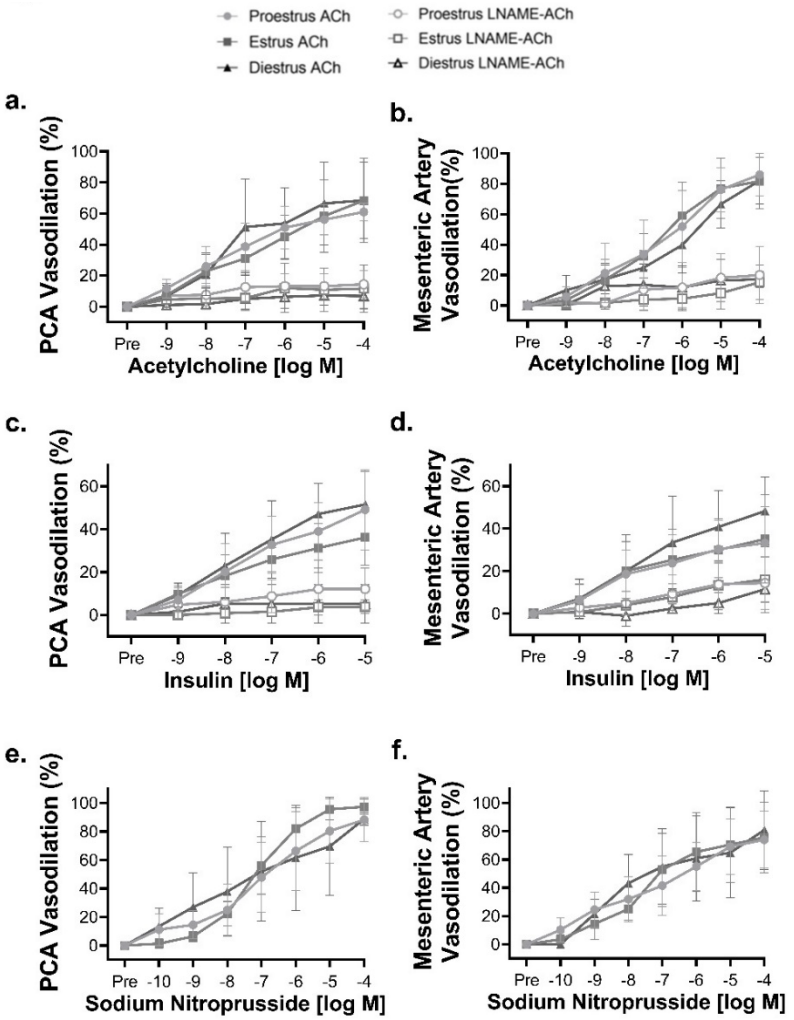

Figure 2.2. *Ex vivo* resistance artery endothelial function does not differ with estrous cycle phase. Endothelium-dependent dilation to acetylcholine (ACh), in the presence and absence of nitric oxide synthase inhibitor L-NAME, in the *A:* posterior cerebral artery (PCA) and *B:* mesenteric artery from mice in proestrus, estrus, or diestrus. Endothelium-dependent dilation to insulin in the *C:* PCA and *D*: mesenteric artery, and endothelium-independent dilation to sodium nitroprusside in the *E:* PCA and *F*: mesenteric artery from mice in proestrus, estrus, or diestrus. Repeated measure ANOVA showed no differences were found between groups. n= 7-9/group. Data are mean ± SD.

<u>*Small Artery gene expression*</u>

Gene expression did not differ between estrous cycle phases for *Esr1* and *Gper1* in either the cerebral or mesenteric arteries (all p>0.05, Figure 2.3 A, D), while mesenteric artery *Esr2* was not detectable. Cerebral artery *Esr2* gene expression for mice in estrus was 57%

lower than diestrus (p=0.008) and 54% lower than proestrus (p=0.04, Fig 2.3 B). *Gper1* expression in the mesenteric arteries during proestrus was lower than diestrus (p=0.03, Fig 2.3 E).

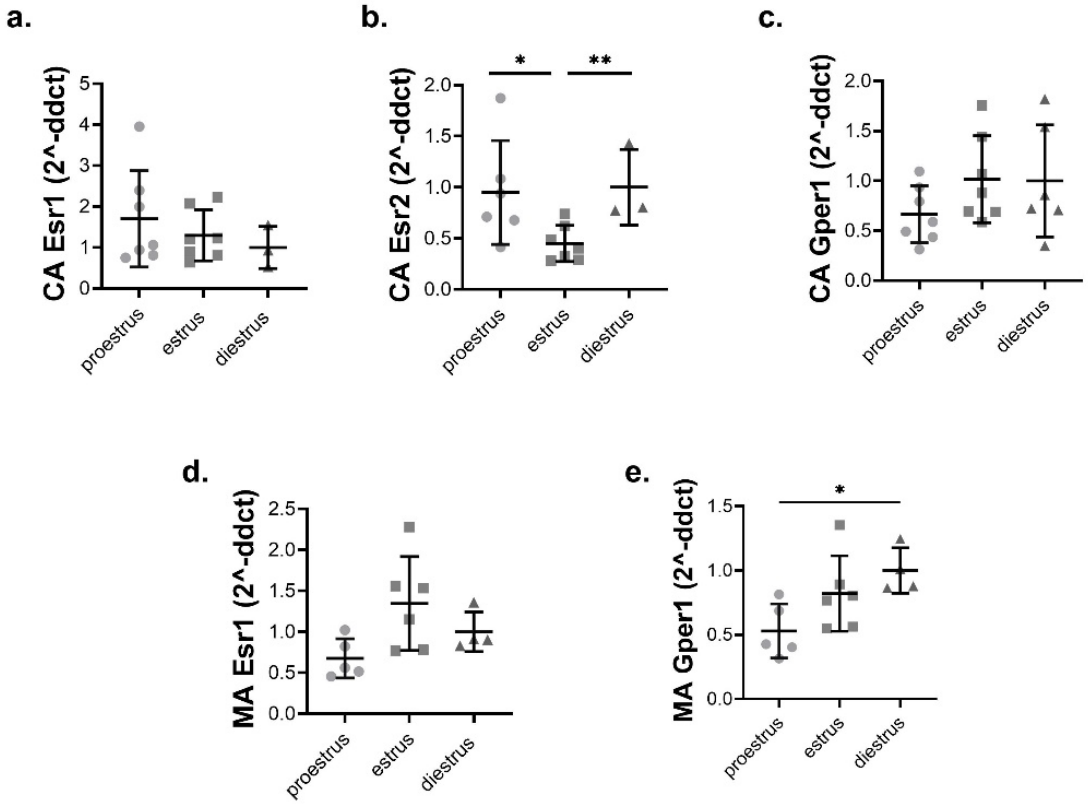

Figure 2.3. Resistance artery estrogen receptor gene expression during the estrous cycle; lower *Esr2* expression in cerebral arteries during estrus. Cerebral artery (CA) gene expression of *A*: *Esr1* (estrogen receptor α), *B*: *Esr2* (estrogen receptor β), and *C*: *Gper1* (GPER) from mice in proestrus, estrus, or diestrus. Mesenteric artery (MA) gene expression of *D*: *Esr1* and *E*: *Gper1* from mice in proestrus, estrus, or diestrus. *Esr2* was below threshold for detection in the MA. n=3-7/group. *p<0.05. A one-way ANOVA with Tukey's multiple comparison was used to test statistical significance. Data are mean ± SD.

Large artery protein expression

Aorta protein expression for ERα did not differ with estrous phase (p=0.34, Fig 2.4 A), but p-Erα (Ser167) was elevated during the estrus phase compared with proestrus (p=0.04, Fig 2.4 B). The ratio of p-ERα to total ERα was not different between phases (p=0.85, Fig 2.4 C).

Aorta protein expression of Akt, p-Akt (Ser 473), eNOS, p-eNOS (Ser1177), and their ratios did not differ between the stages of the estrous cycle (all p>0.05, Fig 2.4 D-I).

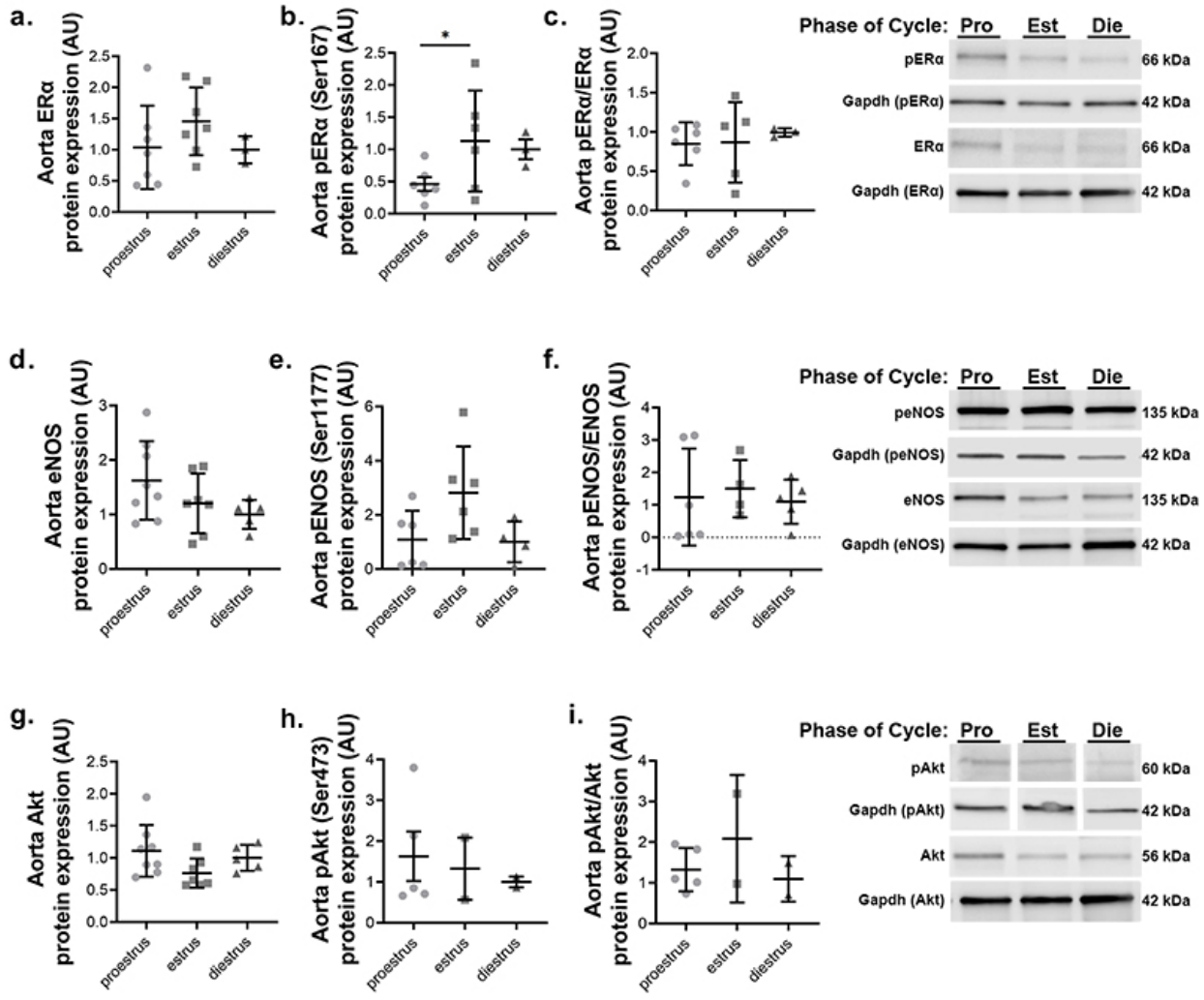

Figure 2.4. Aorta protein expression during the estrous cycle; higher pERα expression in the aorta during estrus. Aorta protein expression for *A*: estrogen receptor α (Erα), *B:* phosphorylated ERα at serine 167 (pERα), and *C*: pERα:ERα ratio, *D*: Endothelial nitric oxide synthase (eNOS), *E:* phosphorylated eNOS at serine 1177 (eNOS)(peNOS), F: pENOS:eNOS ratio, *G*: Akt, *H*: phosphorylated Akt at serine 473 (pAkt), and pAkt:Akt ratio for mice in proestrus (P), estrus (E), and diestrus (D). Representative blot to the right. n= 2-8 /group. *p<0.05. pAkt and its Gapdh was taken from supplemental figure 6 lanes 1 (P), 3 (D), and 5 (E). A one-way ANOVA with Tukey's multiple comparison was used. Data are mean ± SD.

Motor Coordination and Cognitive Function is independent of estrous cycle

Motor coordination, measured by the accelerating rotarod test, did not differ between estrous cycle stage (p=0.80, Fig 2.5A). Cognitive function, tested by nest building, also did not differ between estrous cycle stages (p=0.34, Fig 2.5 B).

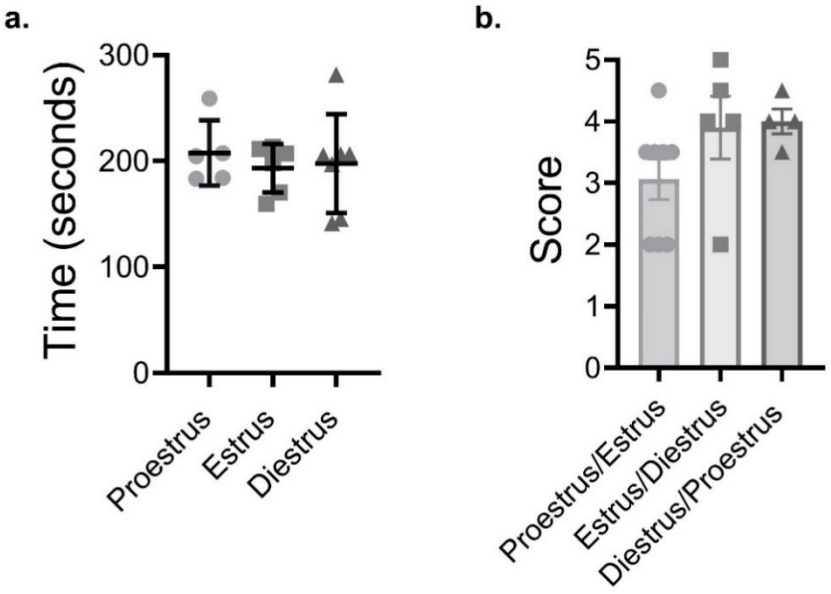

Figure 2.5. Motor coordination and cognitive function did not differ with estrous cycle phase. *A*: Amount of time on the rod during the accelerating rotarod test in mice during proestrus, estrus, and diestrus. *B*: Nest building score for mice grouped by estrus cycle phase at start of test and phase at completion. n= 4-8/group. No differences were found between groups using a one-way ANOVA. Data are mean ± SD.

2.4 Discussion

The major finding of this investigation is that aortic stiffness measured *in vivo* is lower in the estrus phase of the estrous cycle compared with the diestrus phase. In contrast, we found no differences between estrous cycle phases for resistance artery endothelial function measured *ex vivo* in either cerebral or mesenteric arteries. Cerebral artery gene expression of *Esr2* was lowest in the estrus phase, while gene expression of *Gper1* was higher during the estrus phase compared with proestrus. *Esr1* was not different between estrous cycle phases in small resistance arteries. Our results also reveal that phosphorylated ERα was elevated in the aorta in the estrus phase, but eNOS and Akt expression did not appear to be affected by the estrous cycle with the aorta.

Lastly, we found no differences between estrous cycle phases in motor coordination or cognitive function. Taken together, these results suggest that the mouse estrous cycle impacts large elastic artery stiffness, but not small resistance artery endothelial function, and these effects are accompanied by differences in estrogen receptor gene expression and post-translational modifications.

Large artery stiffness: modulation by hormonal fluctuations

Increased large artery stiffness is associated with cardiovascular diseases and poor overall health (147). With increasing age, large arteries become stiffer while circulating concentrations of sex steroid hormones decline progressively (160, 161) suggesting a potential relationship between large artery stiffness and lower levels of circulating sex hormones. Previous studies in human premenopausal females reveal that PWV (brachial-femoral or carotid-femoral) and aortic augmentation index were lower during the ovulatory or luteal phases (i.e., high estrogen phases) compared with during menses, suggesting that estrogen fluctuations during the menstrual cycle impact arterial stiffness (145, 150, 151). These results are similar to our findings of higher PWV in the diestrus phase, equivalent to the menses phase of a human. However, there are inconsistent findings in this regard in human studies, with some studies finding no effect of the menstrual cycle on arterial stiffness (162–166). Potential explanations for the varying results include inadequate tracking of the cycles, diets containing soy, or small sample sizes (167, 168). It is important to note that the mice in this study were on a phytoestrogen free diet, while the typical research mouse diet contains phytoestrogen soy protein. Thus, it remains unknown the effects of estrous cycle on artery stiffness in mice fed a diet containing soy protein. In summary, our results indicate that the mouse estrous cycle impacts large artery stiffness and accounting for the estrous cycle in future studies will allow for further insights into how sex steroid hormones modulate the

vasculature. More importantly, failure to account for the estrous cycle or phytoestrogen diet in studies of *in vivo* large artery stiffness may increase the variability of the data and mask potential results.

Mechanisms of modulation of large artery stiffness

Due to the short duration of the estrous cycle, it is unlikely that structural changes to the aorta account for the differences in stiffness between estrous cycle phases. As such, the most likely mechanism for the effects of the estrous cycle on PWV is a change in arterial tone. Circulating estrogen affects arterial tone, primarily by inducing vasodilation through actions on receptors ERα and GPER1 (9). ERα expression is increased in human endothelial cells during the late follicular phase (169). In contrast, we did not find a difference in aortic ERα expression between mouse estrous cycle phases. This may be due to our measurement of the whole aorta in mice compared with the measurement of isolated endothelial cells in human subjects in the previous study. We did find that ERα phosphorylation at Serine 167 was highest in the aorta during the estrus phase. In the presence of estradiol, the estrogen receptors undergo a conformational change, enhancing the likelihood of being phosphorylated, and once phosphorylated the receptor is more likely to affect nuclear transcription (170). Thus, our findings suggest greater activation of ERα in the aorta during the estrus phase. The non-genomic activity of ERα includes the phosphorylation of Akt, which in turn phosphorylates eNOS leading to greater NO production which can occur within minutes after exposure to estrogen (171). In addition, ERα genomic signaling upregulates eNOS and superoxide dismutase expression (172). Gavin and colleagues demonstrated that endothelial cell ERα expression is positively related to brachial artery endothelium-dependent dilation, as well as eNOS and p-eNOS (Ser1177) endothelial cell expression in healthy human females (169). eNOS expression is also higher in

the brain during the proestrus phase compared with diestrus in rats (173), and NO may play a pivotal role in the regulation and timing of the estrous cycle (174, 175). Thus, our results indicate that aortic ERα phosphorylation is modulated by the estrous cycle, while previous studies suggest the menstrual cycle modulates ERα expression concomitant with changes to eNOS expression.

GPER1 also participates in nongenomic estrogen related signaling and impacts large artery function (176). Aortas from middle-aged and old female mice have lower expression of GPER protein when compared to aortas from young female mice, and the vasodilatory responses to GPER agonist G-1 is impaired in aged female mice (176). Furthermore, young female mice have a lower PWV compared with young male mice, and this sex difference is abolished by GPER deletion (177). GPER deletion also results in an elevated pulse pressure, an indicator of greater large artery stiffness, in response to angiotensin II, but only in female mice (153). Unfortunately, we were unable to reliably measure GPER protein expression in this study. Thus, GPER has impacts on vascular tone and arterial stiffness; however, it remains unknown what role GPER protein expression plays in the aorta across the estrous cycle.

ERβ is also thought to impact vascular function but is also lowly expressed in the larger arteries (176), further suggesting the primary roles of ERα and GPER in large artery stiffness change during the estrous cycle. In general, ERβ is thought to negate the actions of Erα-mediated transcription (178) and have negative vascular consequences (179). Alterations in ER subtype expression with age and declining circulating estrogen concentration may mediate a shift in the ERα:ERβ ratio, towards more ERβ (179). This shift towards more ERβ may promote an adverse vascular phenotype and contributes to the development of hypertension and vascular injury, as previously found in the uterine arteries (44, 180). Given the low expression of ERβ in large

arteries, we were not able to detect ERβ in our aorta samples. Thus, the relationship between estrogen receptors with aging and estrous warrants further investigation.

In addition to estrogen receptors and NO, changes to other vasodilators and hormones with the estrous cycle impact arterial tone. For example, cyclooxygenases have a role in the increased middle cerebral artery velocity during the late follicular phase of the menstrual cycle (181). Hydrogen peroxide-induced vasodilation may also change during the estrous cycle as estrogen increases superoxide dismutase expression resulting in increased conversion of superoxide to hydrogen peroxide (172). It is also important to note the fluctuation of other hormones throughout the estrous cycle and their impacts on arterial tone. The effects of progesterone on endothelial function remain controversial (182), but majority of previous research shows progesterone can elicit negative effects on endothelial function (183, 184). Increased testosterone concentrations also correlate with endothelial dysfunction (182, 183, 185). Yet to be thoroughly investigated is the impact of luteinizing hormone and follicular stimulating hormone on endothelial function and arterial health. Thus, future studies are needed to determine the exact hormones and signaling involved in the changes to arterial stiffness during the estrous cycle.

Ex vivo small artery function and the estrous cycle

Despite the effects of the estrus stage on PWV, downstream small resistance artery endothelial function did not differ between estrous cycle phases in this study. These results could be due to the removal of the artery from the *in vivo* exposure to hormones when performing the *ex vivo* studies. Alternatively, estrogen potentially has a greater impact on conduit artery endothelial function compared with small resistance arteries (186, 187). Importantly for our study, the resistance artery results are consistent between two different endothelium-dependent

vasodilators, ACh and insulin. A meta-analysis of the impact of the menstrual cycle on vascular endothelial function found that conduit artery flow-mediated dilation was greatest during the late follicular phase. In contrast, this meta-analysis revealed no effect of the menstrual cycle on forearm or leg blood flow (186). A previous study also observed that the estrous cycle modulated the neurovascular response to angiotensin II, specifically angiotensin II-induced cerebral endothelial dysfunction and impaired neurovascular coupling was spared during proestrus and estrus phases compared with diestrus (188). One explanation for the conflicting results is that these previous studies were performed *in vivo* (i.e., with estrogen present) compared with our *ex vivo* studies. Thus, future studies could explore the acute vs. chronic effects of the hormonal environment on vascular function throughout the estrous cycle.

Resistance artery estrogen receptor expression

Our data revealed that *Esr2* expression was modulated by the estrous cycle in cerebral arteries, *Esr1* gene expression was independent of the estrous cycle in cerebral arteries and mesenteric arteries. As a lower ERα:ERβ ratio contributes to an adverse vascular phenotype, the lower *Esr2* expression during estrus could serve as a vascular protective mechanism (44). While our results for cerebral artery endothelium-dependent dilation do not have the same pattern as these *Esr2* expression results, there are other potential cerebrovascular benefits of changes to estrogen receptor expressions, such as metabolic and antioxidant benefits (59–61, 73, 189, 190). The ability to detect *Esr2* gene expression in the cerebral vasculature aligns with previous studies indicating relatively higher expression in the brain for *Esr2* (191). The cerebral artery samples collected in this study could include other brain cells that surround these arteries; thus, it is unknown which specific cells are expressing *Esr2* in these tissue samples. An implication of this

finding is that treatments that activate estrogen receptors could have differential effects depending on which receptors are being highly expressed in that tissue.

We found that *Gper1* expression was elevated during periods low estrogen (i.e., the diestrus phase). It was previously shown in mesenteric arteries that females better endothelium-dependent dilation in middle age compared with males, but these sex differences are absent in *Gper1* knockout mice (39), suggesting that GPER plays a pivotal role in endothelial function in females. However, in our study, despite differences in *Gper1* gene expression, no differences in endothelial function in mesenteric arteries was found between estrous cycle stages, thus dissociating *Gper1* expression from endothelial function.

Estrous cycle stage, cognitive function, and motor coordination

In this study, estrous cycle stage had no effect on cognitive function measured by nest building, consistent with previous findings (192). Furthermore, motor coordination assessed by accelerating rotarod was not affected by the estrous cycle also in line with past literature (193, 194). It is important to note the difficulty in measuring nest building across the estrous cycle due to the short duration of the cycle phases and the likelihood of switching between phases during the 12-hour test period. Overall, our data suggests that the estrous cycle does not need to be accounted for with motor or cognitive tasks.

Challenges of measuring steroid hormones

The measurement of sex hormones and estrous cycle staging in rodents presents a number of challenges. The most commonly used technique to measure serum sex hormones in rodents is immunoassays, but these often overestimate steroid hormone levels due to the lack of specificity (195–202). As such, it has been recommended that all studies reporting steroid hormones as an endpoint use mass spectrometry based assays to ensure specificity and

reproducibility (203). The inconsistencies in the literature related to sex hormone concentrations during the mouse estrous cycle may arise from the varied accuracy of different measurement techniques (157, 204–210). Furthermore, serum sex hormone concentrations may vary widely within an estrous cycle stage (211) indicating that a single measurement for each stage is not sufficient for capturing the hormone status. Thus, caution should we used when measuring sex hormones by immunoassay or using sex hormones to stage the estrous cycle.

Limitations

Our study has a few limitations that should be noted. We did not measure passive stiffness or examine structural differences in the aorta. Thus, while we believe the short duration of the estrous cycle precludes structural changes to the aorta as the mechanisms for differences in stiffness, we do not have evidence from this study to support this hypothesis. Our samples for gene and protein expression are whole arteries, and thus, we cannot determine estrogen receptor abundance within specific cells, for example endothelial cells vs. smooth muscle cell expression. Another limitation of our study is the inability to measure protein expression in cerebral arteries due to limited tissue availability, and thus we cannot confirm that the differences seen in gene expression are indicative of protein expression. We fed the mice in this study a phytoestrogen free diet to limit the confounding effects. However, standard rodent chows often contain phytoestrogen soy that may modulate the influence of the estrous cycle on the vasculature. Lastly, our findings may be specific to the C57BL/6 strain and we encourage further investigation with other rodent strains.

2.5 Conclusions

These results suggest that the estrous cycle should be accounted for when measuring *in vivo* large artery stiffness in young female mice. However, given that estrous cycle stage did not

affect *ex vivo* measures of endothelial function in small arteries, it appears that accounting for estrous cycle in these outcomes is not needed. Changes to estrogen receptor expression or activation may contribute to these vascular outcomes, specifically we find that during the estrous cycle Erβ gene expression fluctuates in cerebral arteries and p-Erα protein expression is modulated in the aorta. In summary, it is important to consider sex as a biological variable and accounting for hormonal fluctuation during *in vivo* measurements of vascular function will likely improve the quality of results. Acknowledging the effect of the estrous cycle on vascular function may explain the variability found within female rodents and further the understanding of the effects of sex hormones on vascular function.

Author contributions

MNK, BRB, and AEW conceived and designed the research; MNK, BRB, AEC, AK, HJD, GDH, and AEW collected data and analyzed; MNK, BRB, and AEW interpreted results; MNK prepared figures, MNK, BRB, and AEW drafted manuscript. MNK, BRB, AEC, AK, HJD, GDH, and AEW edited and revised manuscript, and approved of the final version.

Supplemental data: https://doi.org/10.6084/m9.figshare.20324889.v2

Table 2.1. Animal Characteristics

Variable	Proestrus	Estrus	Diestrus
n	8	8	7
Age, months	6.0 ± 0.3	5.9 ± 0.2	5.9 ± 0.2
Body mass, mg	23.9 ± 1.7	24.2 ± 1.7	24.4 ± 1.1
Heart mass, mg	0.11 ± 0.01	0.12 ± 0.02	0.12 ± 0.01
Percent heart:body mass	0.47 ± 0.05	0.50 ± 0.07	0.51 ± 0.03
Spleen mass, mg	0.09 ± 0.02	0.11 ± 0.02	0.10 ± 0.01
Percent spleen:body mass	0.41 ± 0.07	0.44 ± 0.06	0.42 ± 0.03
WAT mass, mg	0.76 ± 0.24	0.76 ± 0.36	0.77 ± 0.19
Percent WAT:body mass	3.16 ± 0.88	3.08 ± 1.37	3.14 ± 0.67
Gastroc mass, mg	0.15 ± 0.02	0.18 ± 0.04	0.17 ± 0.03
Percent gastroc:body mass	0.67 ± 0.11	0.75 ± 0.15	0.70 ± 0.13
Uterus mass, mg	0.10 ± 0.01	0.08 ± 0.01*	0.08 ± 0.01*
Percent uterus:body mass	0.43 ± 0.04	0.33 ± 0.05*	0.32 ± 0.03*
Esterone (ng/mL)	0.002 ± 0.001	0.001 ± 0.0004*	0.001 ± 0.001*
Estradiol (ng/mL)	0.008 ± 0.001	0.001 ± 0.000	0.002 ± 0.003
E2:E1 ratio	2.64 ± 1.74	0.49 ± 0.01	1.45 ± 0.76
Progesterone, ng/ml	2.32 ± 1.15	5.42 ± 2.80*	4.40 ± 2.70
Testosterone, ng/ml	0.016 ± 0.012	0.024 ± 0.096	0.094 ± 0.050†

WAT: white adipose tissue, Gastroc: gastrocnemius. E2: estradiol. E1: esterone. *$p<0.05$ vs. Proestrus, †$p<0.05$ vs. Estrus. Values are mean±SD.

III. THE EFFECTS OF DIETARY SOY CONTENT ON CEREBRAL ARTERY FUNCTION AND BEHAVIOR IN OVARIECTOMIZED FEMALE MICE

From: **Kehmeier MN**, Khurana A, Bedell BR, Cullen AE, Cannon AT, Henson GD, Walker AE. The effects of dietary soy content on cerebral artery function and behavior in ovariectomized female mice. *Am J Physiol Heart Circ Physiol*. 2023 Dec 29. doi:10.1152/ajpheart.00618.2023. PMID:38156886

3.1 Introduction

As females age, they transition through menopause, experiencing an increase in cardiovascular, metabolic, and neurodegenerative disease risk (212–214). Vascular impairments underlie many of these diseases(3). Cerebrovascular impairment occurs with menopause (215), likely due to the decline in estrogen that induces endothelial cell dysfunction (35). Therefore, a better understanding of the actions of estrogen and estrogen deficiency will provide further insight into mechanisms of cerebrovascular dysregulation.

The hormonal changes that occur post-menopause can be modeled by ovariectomy in rodent models. Previous studies have shown that ovariectomy in mice results in impaired endothelial function, and this endothelial dysfunction is prevented by treatment with estradiol (216, 217). Estrogens bind to estrogen receptor α (Erα) and G protein-coupled estrogen receptor (GPER) in vascular endothelial cells to exert their vasodilatory effects through increased nitric oxide (NO) production (153, 154). Estradiol also exerts anti-inflammatory and antioxidant effects, for example, inducing up-regulation of mitochondrial superoxide dismutase (SOD2) in the vasculature (218). Thus, ovariectomy impairs vascular function by downregulating these estrogen signaling pathways. When examining the effects of ovariectomy, it is important to consider external factors that may influence the estrogen pathway.

Among standard rodent chows, there is a large variance in soy content. For example, in our diet at the University of Oregon, the ingredient with the second highest concentration is

soybean meal (Lab Diet, PicoLab Rodent Diet 20, 5053) compared with other common diets where soybean meal is the sixth ingredient (e.g., NIH-31 Irradiated Open Formula, Inotiv, 7017). Soybean meal is rich in polyphenol isoflavones, known as phytoestrogens which can mimic the effects of estrogen (219). Specifically, our diet contains the phytoestrogen genistein, known to bind to Erα (220). Furthermore, genistein is known to improve endothelial function (221).These phytoestrogens have antioxidants effects by activating estrogen receptors to upregulate SOD expression (222). However, the effects of a soy diet are inconsistent throughout the literature, with a previous study in cerebral arteries finding no effect of a high soy diet on vasodilator or vasoconstrictor function after ovariectomy in rats (223). Thus, given these inconsistencies, the effects of soybean meal on vascular outcomes needs to be clarified.

The onset of menopause is associated with insulin resistance and metabolic deficiencies (224). Insulin signaling has only recently become a topic of interest for cerebral vascular endothelial function, since cerebral glucose uptake primarily occurs through GLUT1, which is insulin independent. However, recent studies demonstrate a role for insulin signaling in cerebral endothelial function, where endothelial dysfunction coincides with the onset of insulin resistance (225, 226). Furthermore, intranasal delivery of insulin increases cerebral blood flow and broadly improves cognitive function (227, 228). Insulin is known to increase NO production, a phenomenon that does not always require an intact insulin receptor (IR) (229). The activation of nitric oxide synthase (NOS) by insulin primarily occurs via phosphorylation by kinases such as proto-oncogene- protein kinase Src (cSrc), phosphoinositide 3-kinases (PI3k), and protein kinase B (Akt), similar to how estrogen signaling activates NOS (37). However, the impact of ovariectomy and soy diet on insulin signaling in the cerebral vasculature has yet to be investigated.

Due to the importance of considering the effect of diet in menopausal research, it is pertinent to understand the impact of diet on ovariectomized mice for proper experimental design of future studies. Therefore, the purpose of this study was to determine the effects of a standard chow diet containing soy on cerebral endothelial function, cerebral artery gene expression, hippocampal protein expression, and nesting behavior in female mice after ovariectomy. We hypothesized that ovariectomy would lead to impaired cerebral endothelial function, including the vasodilatory response to insulin. We further hypothesized that a standard chow diet containing soy would prevent endothelial dysfunction in ovariectomized mice. Furthermore, as cerebrovascular function is known to influence neurobehavioral function, we hypothesized that nesting behavior would be better in the sham and ovariectomy group on the soy diet compared with the ovariectomy group.

3.2 Methods

Animals

Female C57BL/6J mice were purchased from Jackson Lab and studied at 6-7 months of age (n=43). Mice were ovariectomized or underwent sham surgery at 4 months and were studied 8 weeks after surgery. Mice were fed a phytoestrogen-free diet (Envigo, Tekalad Global Soy Protein-Free Extruded Rodent Diet, 2920X) or fed our standard rodent chow that contains a high amount of soybean meal (Lab Diet, PicoLab Rodent Diet 20, 5053). See Supplemental Table 3.1 for detailed nutritional information. Food and water were provided ad libitum, and mice were housed on a 12/12-hour light-dark cycle at 24° C. Mice were euthanized by exsanguination under isoflurane immediately prior to vascular reactivity studies. The estrous cycle was tracked at the time of pulse wave velocity measures and at sacrifice for Sham mice (230). All animal procedures conform with the Guide for the Care and Use of Laboratory Animals (8th edition

revised 2011) and were approved by the Institutional Animal Care and Use Committee at the University of Oregon.

Ovariectomy

Female mice were randomly assigned to Sham fed a phytoestrogen-free diet (Sham), ovariectomy fed a phytoestrogen-free diet (OVX), or ovariectomy fed a standard chow diet (OVX+Soy). Ovariectomy procedures were performed at 4 months of age. Prior to the ovariectomy procedure, mice were anesthetized with 2% isoflurane. Heart rate, breathing rate, and body temperature were monitored throughout the surgery. Two incisions (~5mm) mid-flank, parallel to the spine, were made, and the skin was gently separated from the underlying muscle. The ovarian fat pad was gently exteriorized with the ovary and oviduct. A small hemostat was placed between the uterine horn and the oviduct, while absorbable surgical sutures (VetOne) were used to ligate the oviduct proximal to the hemostat. The ovary and oviduct were excised, and a drop of 2% bupivacaine was applied. The muscle wall was then closed with the absorbable suture, and an additional dose of bupivacaine was applied to the incision site of the muscle wall. Following this, the skin layer was closed. This process was repeated for the remaining ovary on the opposite flank. Once the surgery was complete, the mouse received 0.5 mL of sterile saline. Mice were monitored daily until a veterinarian approved the return to normal housing conditions. For sham surgeries, the ovary and oviduct were exteriorized and re-inserted back into the body cavity, and the muscle wall was closed as described above.

Plasma Hormones & Glucose

Blood samples were collected via cardiac puncture with a heparin saline-coated syringe. The blood was centrifuged, then plasma was collected and frozen in liquid nitrogen and stored at -80°C. Plasma hormone concentrations for 17β-estradiol (E2), estrone (E1), and progesterone

were analyzed via Liquid Chromatography–Mass Spectrometry (LC-MS). Plasma insulin and glucose were analyzed via ELISA. All plasma analyses were performed by the Endocrine Technologies Core at Oregon National Primate Research Center at Oregon Health & Science University. Estradiol and estrone had low levels of detection, and quantification for these was less accurate, while non-detected levels were excluded from means. The ratio of E2 to E1 was calculated and reported (see Table 3.1).

Vascular Reactivity

Endothelium-dependent vasodilation was assessed in *ex vivo* isolated pressurized posterior cerebral arteries, as described in detail previously (230, 231). Arteries were excised and cannulated onto glass micropipettes in a myograph chamber (Danish MyoTechnology Inc.) filled with a physiological salt solution. All the arteries were pre-constricted with phenylephrine (1-6 μM) to obtain 20-40% pre-constriction of starting luminal diameter. Increases in luminal diameter in response to increasing concentrations of endothelium-dependent dilators acetylcholine (ACh: $1x10^{-9}$ to $1x10^{-4}$ M) and insulin (1 to 10000 ng/mL) were determined. Insulin doses were prepared from a 4mg/mL stock (Insulin, human recombinant, zinc solution, Gibco), by diluting in physiological salt solution containing bovine serum albumin. After ACh and insulin responses, arteries were incubated for 30 minutes with 0.1 mM of N omega-Nitro-L-arginine methyl ester hydrochloride (L-NAME). ACh and insulin responses were repeated in the presence of LNAME to determine the contribution of NOS to endothelium-dependent dilation. Endothelium-independent dilation was measured by the increases in luminal diameter to sodium nitroprusside (SNP) ($1x10^{-10}$ to $1x10^{-4}$ M).

Passive Stiffness

Passive arterial stiffness was measured *ex vivo* in the PCA's by the resting lumen diameter and medial wall thickness while increasing intraluminal pressure (232). Passive stiffness was measured following a 60-minute incubation of calcium free solution to eliminate myogenic tone. Each artery was recorded from 5 to 100 cmH_2O (3.7-73.5mmHg) in 5 cmH_2O increments. From this stress-strain curves, Beta-stiffness, and elastic modulus were calculated as previously described (233).

Gene Expression

In samples of cerebral arteries (combined middle cerebral artery, anterior cerebral arteries, and basilar artery), and mesentery arteries, mRNA gene expression was quantified for superoxide dismutases (*Sod*) *1, 2, & 3*, estrogen receptor alpha (*Esr1*), glucose transporter 1 (*Slca2a1*), insulin receptor (*Irs*), NADPH oxidases (NOX2), and protein-coupled estrogen receptor (GPER)through qPCR (see Supplemental Table S3.2 for primer sequences). RNA from cerebral arteries was isolated by a standard protocol using Qiazol and RNAeasy Micro Kits (Qiagen, Hilden, Germany) and quantified using a NanoDrop 2000 (Thermo Scientific, Waltham, MA). Reverse transcription was performed to produce cDNA with a Qiagen Quantitect Reverse Transcription Kit. The cDNA samples underwent real-time qPCR using ThermoFisher PowerUp Sybr Green and a Quantstudio 5 real-time PCR system (ThermoFisher Scientific, Waltham, MA). mRNA expression was calculated using the $2^{-\Delta\Delta CT}$ method. 18s mRNA was used as a housekeeping gene control, and values were normalized to the Sham group.

Protein Expression

The hippocampus was carefully dissected from the other brain tissue, and the aorta was properly cleaned of fat, and both were then flash-frozen in liquid nitrogen. Samples were homogenized in protein extracting buffer and protease inhibitor cocktail, then internally

sonicated twice at 50% power for 60 second intervals. Hippocampal lysates were centrifuged at 3,000 rpm for 10 minutes at 4°C, and the supernatant was removed. Lysate protein concentration was assessed using a commercially available kit (Pierce BCA protein assay kit; Thermo Fisher, Waltham MA). Bio-Rad stain-free TGX gels were used for protein separation. The stain was activated to ensure protein separation and then transferred onto a nitrocellulose membrane. Membranes were imaged after transfer to verify the total protein transferred, and then membranes were blocked in with 5% bovine serum albumin (BSA) in TBS-T for 50 minutes, then incubated in the primary antibodies overnight in PBS containing 3% BSA. Primary antibody concentrations were as follows: Gapdh 1:2000; IRS1 1:1000; pAkt 1:1000; Akt 1:1000; pErα 1:1000; Erα 1:500; P85 (PI3k) 1:1000, eNOS (1:1000), p-eNOS(S1177) (1:1000). Following incubation, membranes were washed and incubated with a species-appropriate HRP-conjugated secondary antibody. Following washes, membranes were incubated in Azure Chemiluminescence (Azure Biosystems, Dublin, CA) and imaged with a ChemiDoc Imaging system (ChemiDoc, BioRad, Hercules CA). Image J was used to determine protein band density and relative protein expression was calculated as protein density normalized to GAPDH density. Values were normalized to the Sham group. See Supplemental Table S3.3 for antibody list and validation.

Cognitive function

Nest building is a test of instinctual behavior and was performed over a 12-hour period. Mice were singly housed overnight in a fresh cage containing a condensed cotton nestlet. The following morning, the researcher scored the nests. The same researcher scored all nests. The intrapersonal coefficient of variation in our laboratory is 0% for this test. Nests were scored on a scale of 0-5 with the following criteria: 0- nestlet is untouched; 1- nestlet has been moved but no

significant tearing; 2- significant tearing, but no formation of a nest; 3- significant tearing, indication of nest OR nest is in the corner of the cage; 4- significant tearing, formation of nest in the corner; 5- significant tearing, formation of nest in corner and the nest walls are high making a bowl like nest (159).

Aortic Stiffness

Aortic stiffness was measured *in vivo* by pulse wave velocity (PWV) (230). Mice were anesthetized using isoflurane (2% isoflurane in 100% oxygen) and placed supine on a temperature-controlled heating pad (37°C). Electrodes were placed on distal portions of limbs that record ECG, while two Doppler transducers were positioned on the aortic arch and abdominal aorta. The distance between the transducers was recorded. Using the Doppler signal processing workstation program (DSPW; Indus Industries, Webster, TX, USA), the time of a pulse to travel from the arch to the abdominal aorta was analyzed, and the time was then divided by the distance between the transducers. Two researchers analyzed the files independently, and the average was taken.

Statistical Analysis

Statistical analyses were performed with IBM SPSS (Version 26, Armonk, NY) and GraphPad Prism 9.5. After checking for normality, a one-way analysis of variance (ANOVA) between Sham, OVX, and OVX+Soy groups was used unless otherwise noted. In cases of a significant F-value, post-hoc analyses were performed using a Tukey correction for preplanned comparisons. Repeated Measures ANOVA was used to determine group differences for dose responses. Significance was set at $p<0.05$, and values are represented as mean ± SEM. Outliers were identified as z score>2 and removed from the data set.

3.3 Results

Animal characteristics

OVX and OVX+Soy mice had significantly smaller uteri compared with the Sham group, confirming successful ovariectomies ($p<0.0001$, Table 3.1). The OVX and OVX+Soy groups had significantly more white adipose tissue compared with the Sham group ($p<0.0001$, Table 3.1). The sham mice had a significantly lower body weight compared with the OVX group ($p=0.03$) and the OVX+Soy group ($p=0.03$). There were no differences in other tissue weights between groups ($p>0.05$, Table 3.1). Serum sex steroid hormone ranges were as expected based on our previous results (230). The Sham group trended to have higher estrone, estradiol, and progesterone compared with both ovariectomy groups (all $p> 0.05$, Table 3.1). There were no group differences in plasma insulin and glucose concentrations between groups (all $p> 0.05$, Table 3.1).

Cerebral Artery Endothelial function

The PCAs from OVX mice had impaired endothelium-dependent dilation to ACh compared with the Sham group (max: $p=0.210$, dose-response: $p=0.002$ Figure 3.1A and D). PCA vasodilation to ACh did not differ between the Sham and OVX+Soy groups, nor between OVX and OVX+Soy groups ($p>0.05$, Figure 3.1A and D). Maximal endothelium-dependent vasodilation to insulin was 27% lower in PCAs of OVX mice compared with the Sham mice (max: $p=0.05$, dose-response $p=0.005$ Figure 3.1 B and E). Interestingly, maximal PCA dilation to insulin was 27% higher in OVX+Soy mice compared with the OVX group (max: $p=0.04$, dose-response: $p=0.001$), and no difference in the vasodilation response to insulin was observed in the Sham group ($p>0.05$, Figure 3.1B and E). Endothelium-independent dilation in response to SNP was not different between groups (dose-response and maximal responses, all $p>0.05$),

indicating that the differences in vasodilation were due to endothelial cell impairment. The response to ACh and insulin in the presence of L-NAME was nearly absent for all groups and was not different between groups (dose-response and maximal responses, all > 0.05, Figure 3.1A, B), suggesting that the group differences in vasodilation are due to differences in NO

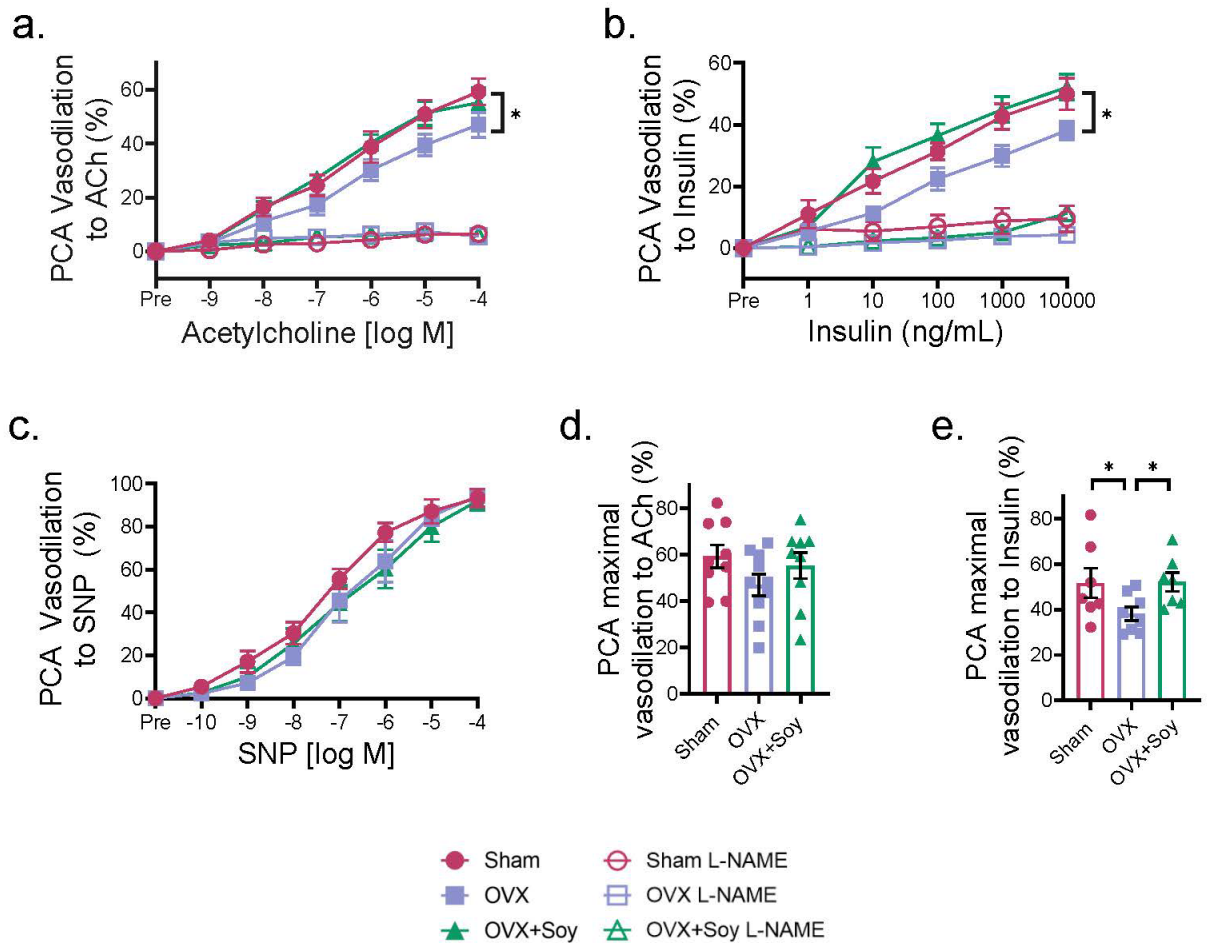

Figure 3.1. Cerebral artery endothelial function is impaired with ovariectomy but preserved with a soy diet. Young female mice underwent sham or ovariectomy (OVX) surgery and were fed a soy-free diet, while a separate cohort underwent OVX surgery and were fed a high-soy diet (OVX-Soy). In isolated posterior cerebral arteries (PCA), endothelial-dependent dilation was measured in response to (A) acetylcholine (ACh) and (B) insulin, in the presence and absence of nitric oxide synthase inhibitor L-NAME. (C) Endothelium-independent dilation was measured in response to sodium nitroprusside (SNP). PCA maximal vasodilation to ACh (D) and insulin (E). Repeated measure ANOVA of dose responses and one-way ANOVA of maximal responses found that the ACh response differed between Sham and OVX, while insulin responses in OVX differed from both Sham and OVX+Soy. *p<0.05 between Sham v OVX; # p<0.05 between OVX and OVX+Soy. n= 8-11/group. Data are mean ± SEM.

bioavailability. Sensitivity (EC50) to vasodilators and the amount of pre-constriction also did not differ groups (all p>0.05, Supplemental Table S3.4). These results reveal that cerebral artery endothelial function is impaired after ovariectomy due to lower NO bioavailability. The most intriguing finding is that a standard chow diet containing soy prevents the decline in insulin-mediated vasodilation after ovariectomy.

Small Artery Gene Expression

Cerebral artery gene expression for insulin receptor (*Insr*) was significantly higher in the OVX+Soy group compared with the Sham group (p=0.03) and showed a trend towards higher expression compared with the OVX group (p=0.09, Figure 3.2E). Additionally, superoxide dismutase 2 (*Sod2*) expression trended lower in the OVX group compared with the Sham group (p=0.07), but there were no differences compared with the OVX+Soy group (p>0.05, Figure 3.2B). *Sod1* and *Sod3* did not

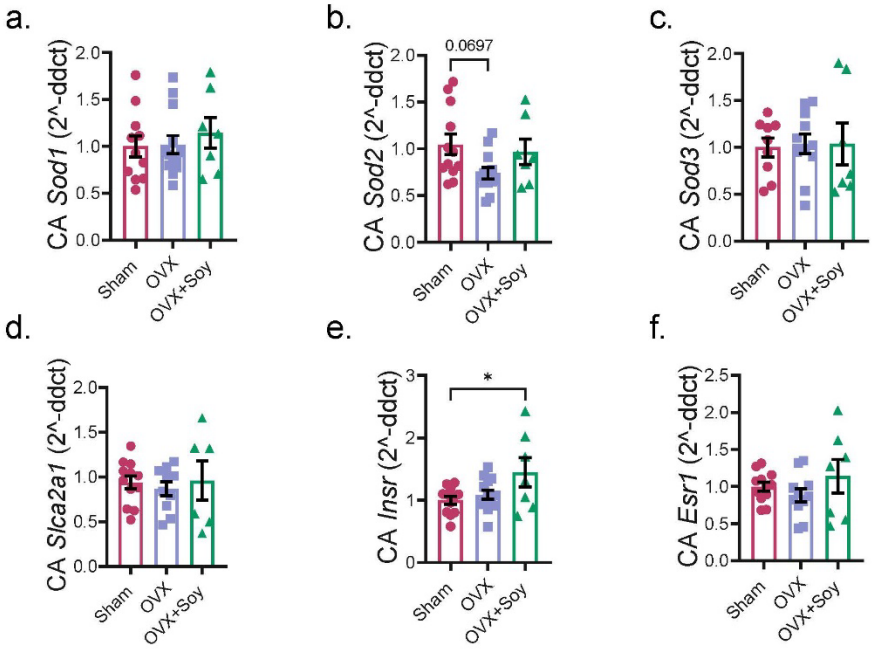

Figure 3.2. Cerebral artery gene expression differs with ovariectomy status and dietary soy. Cerebral artery (CA) gene expression of (A) superoxide dismutase (*Sod)1*, (B) *Sod2,* (C) *Sod3*, (D) glucose transporter type 1 (GLUT1, *Slca2a1*), (E) insulin receptor (Insr), and (F) estrogen receptor α (*Esr1*). *Sod1*, *Sod3*, *Slca2a1*, and *Esr1* were not different between groups. *Sod2* trended lower in the OVX (soybean meal free) group compared with the Sham (soybean meal free) group. *Insr* was significantly higher in the OVX+Soy group compared with the non-soy diet Sham and OVX groups. One-way ANOVA with Tukey multiple comparisons test. *p<0.05. n=8-13/group. Data are mean ± SEM.

differ between groups (all p>0.05, Figure 3.2A & C). Lastly, cerebral artery expression of Slca2a1 (GLUT1 transporter) and estrogen receptor alpha (Esr1) did not differ between groups (all p>0.05, Figure 3.2 D,F). In small mesentery arteries, gene expression for *Gper1* was higher in the Sham group compared to OVX group (p=0.04), and the OVX+Soy group (0.01), and *Nox2* was not different between groups (Figure 3.3).

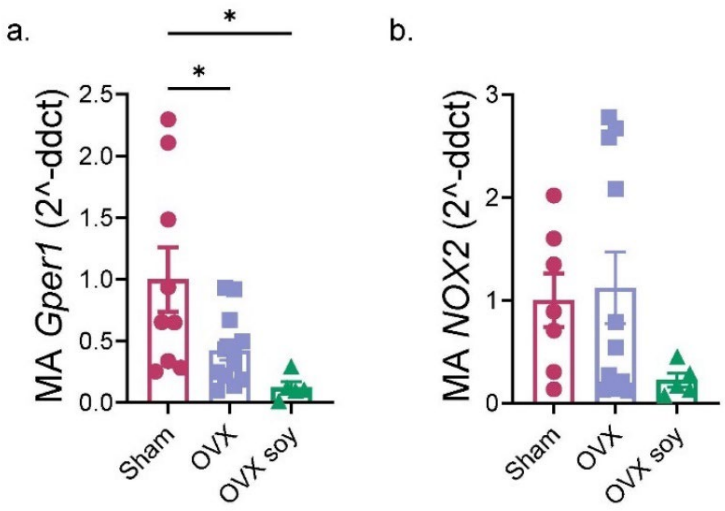

Figure 3.3. Mesentery artery gene expression differs with ovariectomy but not dietary soy. Mesentery (MA) gene expression for (A) g-protein-coupled estrogen receptor (*Gper1*) and (B) NADPH oxidase 2 (*Nox 2*). *Gper1* was significantly higher in the Sham group compared to the OVX group and OVX+Soy group. One-way ANOVA with Tukey multiple comparisons test. *p<0.05. n=8-13/ group. Data are mean ± SEM.

Hippocampal Protein Expression

Hippocampal protein expression for total ERα trended to be higher in the OVX+Soy group compared with the OVX group (p=0.12), and the Sham group did not differ from either OVX groups (P>0.05, Figure 3.4 A). P-ERα (Ser167) and the ratio of p-ERα to total ERα did not differ between the groups (all p>0.05, Figure 3.4 B & C). Hippocampal protein expression of AKT, p-AKT (Ser473), and its ratio also did not differ between groups (all p>0.05, Figure 3.4 D-F). Lastly, hippocampal IRS1 and the p85 subunit of PI3k did not differ in any group (all > 0.05, Figure 3.4G & H).

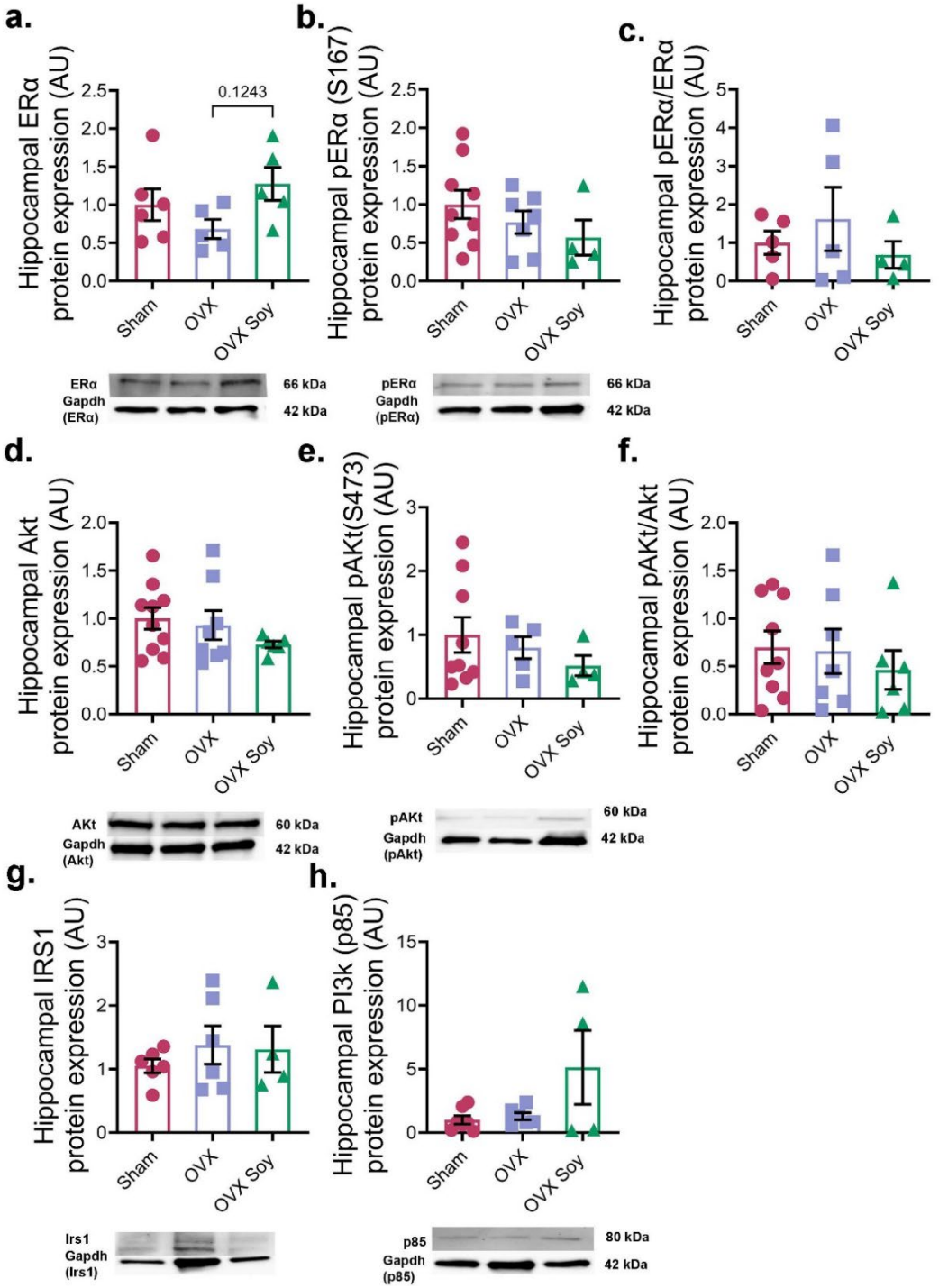

Figure 3.4. Hippocampal protein expression is independent of ovariectomy status and dietary soy. (A) Hippocampal protein expression for estrogen receptor α (ERα) trended to be elevated in ovariectomized mice fed high dietary soy (OVX+Soy) compared with OVX (soybean meal free) mice. However, (B) phosphorylated ERα at serine 167 (pERα) and (C) pERα:ERα ratio did not differ between groups. (D) Akt, (E) phosphorylated Akt at serine 473 (pAKT), (F) pAKT: AKT ratio, (G) insulin receptor substrate 1 (IRS1), and (H) PI3k (p85) did not differ between groups. Representative blots are below each graph and are aligned to the groups above. One-way ANOVA with Tukey's multiple comparison analysis. *$p<0.05$. n= 4-10 per group. Data are mean ± SEM.

Aortic Protein Expression

Aortic protein expression for phosphorylated-eNOS (P-eNOS) at serine 1177 (Ser1177), and total eNOS did not differ between groups (all >0.05, Figure 3.5 A, B). However, the ratio of phosphorylated eNOS to total eNOS trended higher in the OVX+Soy group compared with the OVX group (p=0.058, Figure 3.5C).

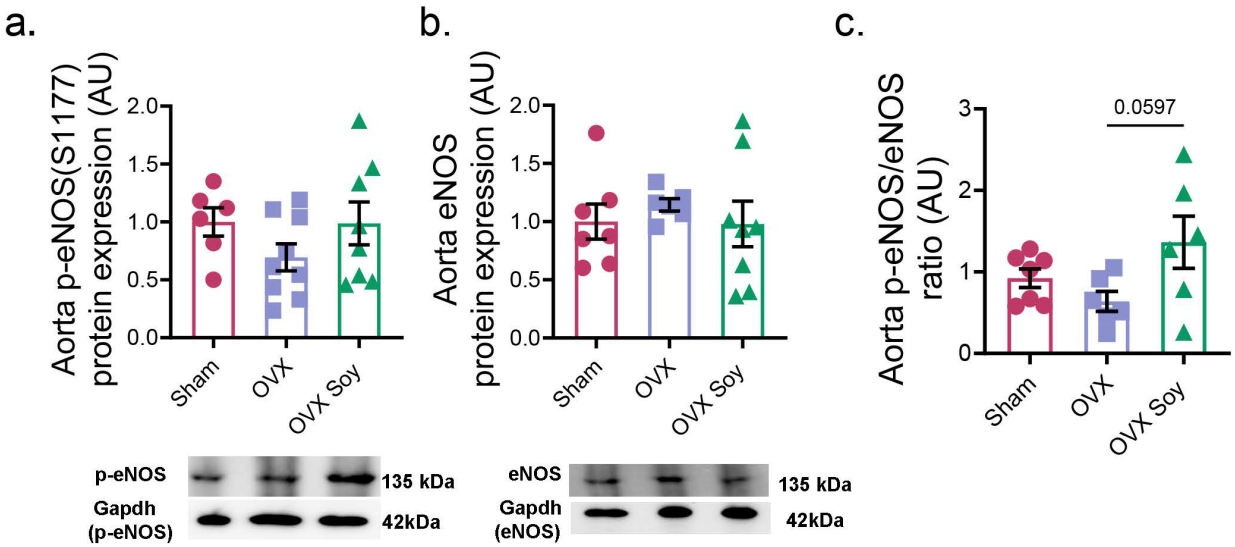

Figure 3.5. Aorta eNOS phosphorylation is influenced by soy diet. (A) Phosphorylated endothelial nitric oxide synthase at serine 1177 (P-eNOS(S1177)) and (B) total eNOS did not differ between groups. (C) p-eNOS:eNOS ratio trended to be elevated in the ovariectomized with high dietary soy (OVX+Soy) group compared to the OVX group. One-way ANOVA with Tukey's multiple comparison analysis. *p<0.05. n=6-9/ group. Data are mean ± SEM.

Artery stiffness is independent of ovariectomy and diet

Large artery stiffness, measured by aortic pulse wave velocity, did not differ between groups (all p>0.05, Figure 3.6B). Furthermore, the passive stiffness of the PCAs, determined by the elastic modulus and β-stiffness index, did not differ between groups (all p>0.05, Supplemental Figure 1).

Cognitive Function is impacted by a soy diet

Cognitive function, tested by nest building, was higher in the OVX+Soy group compared with the Sham group (p=0.025) and the OVX group (p=0.04, Figure 3.6A). These data reveal that a standard chow diet containing soy improved nest building in mice regardless of ovariectomy status.

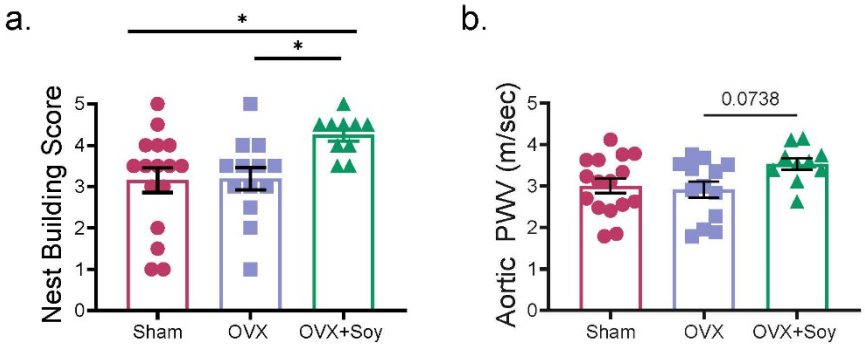

Figure 3.6. Cognitive function and aortic stiffness with ovariectomy status and dietary soy. (A) Nest building behavior was better in the ovariectomized with high dietary soy (OVX+Soy) group compared with the sham and OVX (soybean meal free) groups. (B) Aortic stiffness, measured by pulse wave velocity (PWV) did not differ between groups. One-way ANOVA with Tukey's multiple comparison analysis. *p<0.05. n=10-16/ group. Data are mean ± SEM.

3.4 Discussion

The major findings of this study are that ovariectomy impairs cerebral endothelial function, and that a diet containing soy prevented the impairment in vasodilatory function in response to insulin after ovariectomy. Furthermore, we found that the OVX+Soy group had higher cerebral artery gene expression for *Insr*, while *Sod2* trended to be lower in the OVX group. Our results also revealed a trend for OVX+Soy to have higher ERα hippocampal protein expression when compared with the OVX group. Additionally, our results revealed a trend toward higher activated eNOS in the OVX+Soy group compared with the OVX group. The OVX+Soy mice also performed better on an instinctual behavior test. Lastly, contrary to our

hypothesis, we found no differences in aortic or cerebral artery stiffness with ovariectomy or soy diet. Taken together, these results suggest that dietary soy and ovariectomy status influence cerebral artery function and cognitive function, and researchers need to consider the effect of dietary soy on vascular outcomes when interpreting research results from studies in rodents.

Estrogen and endothelial function

Females are more protected from insulin-related metabolic syndromes and cardiovascular diseases at young ages than their male peers, but this protection is reduced after menopause (234). There is considerable evidence to support that the loss of estrogen results in impaired endothelial function across many models (217, 235–238). Specifically, previous studies demonstrate that ovariectomy impairs endothelium-dependent vasodilation in resistance vessels of female rodents (239). In the present study, we found that ovariectomy led to impaired cerebral artery vasodilation in response to Ach, but not to SNP, indicating impaired endothelium-dependent dilation with no effect on endothelium-independent dilation. Additionally, declines in estrogen lead to diminished antioxidant production, impacting the overall balance of oxidative stress. Reactive oxygen species are known to reduce NO bioavailability through direct interactions, and loss of ERα signaling downregulates SOD expression, further impairing redox balance (218). Similarly, we found a trend for lower *Sod2* gene expression in cerebral arteries after ovariectomy in the present study. Ovariectomy has also been shown to increase superoxide production in the basilar artery of rats, and treatment with 17β-estradiol decreased this superoxide production (240).In addition, post-menopausal females have less tetrahydrobiopterin (BH4), an essential co-factor for eNOS (241). In the absence of BH4, eNOS becomes uncoupled and produces superoxide rather than NO, as well as prevents eNOS uncoupling (242). These insults contribute to the vicious cycle of oxidative stress and inflammation within the vascular

wall that can modulate estrogen-ER signaling, impair vascular function, and even influence disease pathologies such as atherosclerosis (243). Thus, there is substantial evidence that endothelial dysfunction occurs post-ovariectomy and post-menopause, suggesting that interventions that activate estrogen signaling are promising for improving cerebrovascular function in older females.

Soy and Vascular function

With the increased interest in differences between sexes, it is increasingly important that researchers consider how basic variables, like diet, can influence our findings (143). Previous studies have highlighted the beneficial influence of phytoestrogens on vascular function. Catina and colleagues found a reduction in ACh-mediated dilation in aortic rings from ovariectomized rats, and this impairment was prevented by treatment with a soy extract (237). Equol, the primary active metabolite postulated to be responsible for the cardiovascular benefits of soy, vasodilates basilar arteries *in vivo* and enhances NO-mediated dilation (244). In contrast, Schreihofer and colleagues found no effect of a high soy diet or estradiol administration on vasoconstriction or vasodilation responses in middle cerebral arteries after OVX in rats (223). Our findings are similar to this previous study in that soy did not impact endothelial-dependent dilation in response to ACh in the present study. Based on previous literature and our study, we conclude that there are inconsistencies in the effects of soy on endothelium-dependent vasodilation in cerebral blood vessels.

Similar to estrogen, there is abundant evidence that the phytoestrogens in soy activate and upregulate eNOS (245–247). Our data may suggest that a soy diet increases eNOS activation at serine 1177 in ovariectomized animals, but it should be noted that our findings are only a trend and did not reach statistical significance. Schroihofer, et. al., found that a high soy diet leads to a

higher ERα gene expression in the hippocampus but not in the cerebral vessels (223). Similarly, our results show that *Ers1* (ERα) expression in the cerebral arteries was not different between groups. Although we did see a trend for higher ERα protein expression in the hippocampus with a high soy diet, there were no effects of soy on phosphorylated Erα or Akt/p-Akt in the hippocampus, suggesting that the soy diet did not change Erα activation in the brain. Thus, we conclude that soy diet has minimal effects on estrogen receptor signaling in the cerebral vessels, and more studies are warranted to better understand the mechanisms by which a soy diet affects cerebrovascular function.

Insulin signaling and cerebrovascular function

Insulin signaling in the brain and cerebral vasculature is a growing topic of interest, particularly given the relationship between diabetes and Alzheimer's disease (42). Insulin signaling exists throughout the vascular tree. However, the effects of insulin-mediated vasodilation are best characterized in the skeletal muscle, where vasodilation of arteries and arterioles is important for increased blood flow and glucose delivery (248). Vasodilation by insulin occurs primarily through the activation of NOS via phosphorylation by kinases such as cSrc, PI3k, and Akt (37). We found insulin to be a potent vasodilator in the posterior cerebral arteries, which was primarily mediated via NO. This is supported by results from Katakam and colleagues, who found that insulin vasodilates cerebral arteries, and this vasodilation does not occur in endothelium-denuded cerebral arteries (226). It is important to note that this previous study was in relatively metabolically healthy male rats, and it is essential to consider what happens in cases of insulin resistance.

Insulin resistance not only leads to whole-body metabolic dysregulation but also impairs insulin-mediated vasodilation. Interestingly, insulin can also stimulate endothelin-1 (ET-1) via

Ras/MAPK signaling, which is associated with a pro-inflammatory state (248, 249). Thus, endothelial insulin signaling is a balance of vasodilators and vasoconstrictors. In healthy individuals, the net result is vasodilation; however, in the case of insulin resistance, vasoconstriction predominates due to reduced activity of NO signaling and enhanced ET-1 insulin signaling (248, 250). A recent study demonstrated that female mice are protected against overnutrition and obesity-induced impairments in the vasodilatory response to insulin (251). These findings suggest that estrogen in young females may preserve insulin-mediated responses despite the presence of metabolic stressors.

The major novel finding of our study is that a high soy diet preserves cerebral artery vasodilation to insulin after ovariectomy. While these are the first studies to examine the effects of soy on insulin-mediated vasodilation, the results are aligned with previous studies demonstrating that soy improves whole-body insulin sensitivity in ovariectomized rats (252). Our findings further indicate that a soy diet preserves insulin-mediated vasodilation by maintaining NO signaling and is associated with greater insulin receptor expression. Thus, the enhanced insulin-mediated vasodilation with a soy diet is potentially due to the higher expression of insulin receptors, leading to increased eNOS activation. However, the exact mechanisms by which soy consumption improves insulin actions remain unclear, and more research is required to understand the impact of insulin resistance on the brain vasculature.

Large artery stiffness

Greater large artery stiffness elevates systemic pulse pressure and increases cardiovascular, cerebrovascular, and neurodegenerative disease risk (253). Recent evidence from The SWAN Heart study reveals that arterial stiffness accelerates within one year of menopause (80). A systematic review of human clinical trial data examined the efficacy of dietary and

nutrient interventions for the treatment of arterial stiffness. The data revealed that soy was one of the few factors that reduced arterial stiffness (252, 254). Since the menopausal transition is associated with increased large artery stiffness in humans (255), we hypothesized that ovariectomy would result in elevated PWV. Contrary to our hypothesis, ovariectomy and soy diet did not affect PWV in our study. While the human literature is more consistent, in rodents there are many conflicting results regarding the effects of ovariectomy and soy on arterial stiffness. A previous study found that aortic PWV was lower with a soy diet but was not affected by ovariectomy status (252). In contrast, a different study found that omega-3 fatty acids, which are high in soy, prevented the arterial stiffening induced by ovariectomy (256). Contrary to these findings, another study found ovariectomy reduced arterial stiffness (257). Potential factors leading to these inconsistencies include the age at which the mice were ovariectomized and the length of time the animals were on the diet. Our mice were young and otherwise healthy, potentially explaining the discrepancies between our findings and recent clinical trials. Overall, the evidence supporting the benefits of soy for arterial stiffness is stronger in humans than in rodents.

Soy diet and cognitive function

To our surprise, our data revealed that mice on a soy diet had better nest-building scores, a measure of instinctual behavior in mice, compared with both OVX and Sham control mice. In contrast, a recent study compared mice assigned to three different diets, one of which was a high soybean meal diet, and found no influence of diet on nest-building behavior (258). However, this previous study did not examine the influence of ovariectomy on these outcomes. A potential mechanism for the cognitive benefits of soy is through its phytoestrogen properties, as it is known that estrogen enhances learning, memory, and mood (259). ERα is particularly important

in regulating behavior and function (260). We observed trends to higher protein expression of ERα in the hippocampus with the soy diet. Thus, we could postulate that estrogen receptor signaling underlies the better nest building. These results highlight the importance of diet in assessments of cognitive function. Given the variability between institutions for the diets fed to rodents, more consideration of diet will enhance scientific rigor and reproducibility (258).

Limitations

There are some limitations to our study that need to be noted. First, we did not study a Sham+Soy group as we were primarily interested in the effects of a soy diet following ovariectomy. As a result, we cannot determine the interaction effect of OVX and soy diet in this study. Secondly, we also did not measure testosterone or aromatase; thus, we are unsure of the amount of testosterone being converted to estradiol and how this influenced our findings. Third, although soybean meal content was the primary difference between diets, other differences (see Supplementary Table 1) could influence the results. Another addition to the soy diet was dried beet pulp, which is known to be high in nitrates, potentially contributing to NO production, however literature on this remains controversial. Fourth, all mice were on the soy-containing diet until ovariectomy or Sham surgery, when mice were switched to the soy-free diet based on group assignment. The soy diet during development could have protective properties that influenced the outcomes after ovariectomy. Fifth, how sex hormones contribute to vascular function during development warrants further investigation. Sixth, we did not measure superoxide directly, and believe this measure would be beneficial for future studies. Lastly, due to the low protein content of the cerebral arteries, we were not able to examine changes in protein expression in this tissue.

It is also important to highlight our high doses for insulin (1000 and 10000 ng/mL) are higher than those used in previous studies (226). Physiological fasting plasma insulin in humans ranges from 5-10 μU/mL (0.27 ng/mL) (261). Post-prandial plasma insulin can be 55 μU/mL (~2.2ng/mL) or higher in humans (262), and insulin can be higher than 230 μU/mL (8 ng/mL) during a glucose tolerance test in high-fat fed mice (263). Thus, in our study, the first two insulin doses are considered physiologically relevant, while the three higher doses are supraphysiological.

3.5 Conclusion

The results of these studies demonstrate the beneficial effects of dietary soy on cerebrovascular function, insulin signaling, and cognitive function. We confirmed previous findings that ovariectomy impairs cerebral artery endothelial function. For the first time, we demonstrated that a diet containing soy prevents the adverse effects of ovariectomy on insulin-mediated vasodilation. Our results also provide insights into the potential mechanisms for these vascular effects, such as increased insulin receptor expression with soy diet and decreased estrogen receptor and antioxidant expression after ovariectomy. We also find that dietary soy improves instinctual behavior, suggesting potential benefits to cognitive function. The results of these studies highlight the need to consider soy content in the diet when studying cerebrovascular function. Together, these results imply that the effects of diet on vascular function may explain potential inconsistencies found between studies, particularly in female rodents.

Author Contributions

MNK, AK, and AEW conceived and designed the research; MNK, AK, BRB, AEC, ATC, GDH and AEW collected data and analyzed; MNK and AEW interpreted the results;

MNK prepared the figures; MNK and AEW drafted the manuscript; MNK, AK, BRB, AEC, ATC, GDH, and AEW edited and revised manuscript and approved of the final version.

Supplemental Data: https://doi.org/10.6084/m9.figshare.24223264.v2

Table 3.1. Animal Characteristics

	Sham	OVX	OVX + Soy Diet
n	17	17	10
Age (months)	6.13 ± 0.2	6.35 ± 0.3	5.84 ± 0.08
Body mass (g)	24.2 ± 1.1	26.5 ± 2.2*	27.0 ± 3.6*
Heart mass (mg)	0.13 ± 0.01	0.12 ± 0.01	0.13 ± 0.01
Percent heart: body mass	0.52 ± 0.05	0.46 ± 0.06	0.49 ± 0.11
Liver mass (mg)	1.23 ± 0.12	1.30 ± 0.22	1.36 ± 0.14
Percent liver: body mass	5.13 ± 0.5	5.10 ± 0.71	5.18 ± 1.2
Spleen mass (mg)	0.10 ± 0.004	0.11 ± 0.03	0.10 ± 0.01
Percent spleen: body mass	0.41 ± 0.05	0.41 ± 0.12	0.37 ± 0.1
WAT mass (mg)	0.81 ± 0.29	1.53 ± 0.49*	1.58 ± 0.51*
Percent WAT: body mass	3.30 ± 1.03	5.70 ± 1.67*	6.30 ± 2.0*
Gastroc mass (mg)	0.18 ± 0.04	0.18 ± 0.04	0.19 ± 0.03
Percent gastroc: body mass	0.73 ± 0.15	0.69 ± 0.18	0.73 ± 0.22
Soleus mass (mg)	0.01 ± 0.004	0.01 ± 0.003	0.01 ± 0.004
Percent soleus: body mass	0.05 ± 0.02	0.04 ± 0.01	0.04 ± 0.02
Uterus mass (mg)	0.08 ± 0.02	0.03 ± 0.02*	0.01 ± 0.01*
Percent uterus mass: body weight	0.36 ± 0.1	0.12 ± 0.1*	0.07 ± 0.03*
Estrone (ng/mL)	0.0016 ± 0.0005	0.0014 ± 0.0004	0.0012 ± 0.0004
Estradiol (ng/mL)	0.003 ± 0.002	0.001 ± 0.0001	ND
E2/E1 ratio	1.875	0.714*	ND
Progesterone (ng/mL)	4.01 ± 2.1	3.05 ± 0.83	3.05 ± 1.3
Glucose (mg/dL)	205.3 ± 37.8	186 ± 46.7	197.5 ± 18.3
Insulin (ng/mL)	0.36 ± 0.2	0.46 ± 0.3	0.38 ± 0.2

Table 1: Characteristics of animals used for studies. Data are presented as mean ± SD. Not detected (ND). *$p < 0.05$ vs Sham, † $p<0.05$ vs. ovariectomy (OVX), #$p < 0.0001$ denotes significant difference between Sham and Soy OVX and OVX. White adipose tissue (WAT), Gastrocnemius (gastroc), esterone (E1), 17β-estradiol (E2)

IV. *APOE4* GENOTYPE CONFERS RESISTANCE TO THE VASCULAR AND METABOLIC BENEFITS OF 17β-ESTRADIOL

4.1 Introduction

APOE genotype is the most significant genetic risk factor for late-onset Alzheimer's disease (LOAD), where *E4* increases risk 3 to 10-fold for one and two alleles (95, 130, 225). Two-thirds of LOAD cases are females, and the perimenopausal transition coincides with the onset of LOAD (264). Post menopausal females with an *E4* allele have higher rates of LOAD compared with age matched males with an *E4* allele, suggesting an interaction between *E4*, estrogen deficiency, and LOAD (1, 265). A potential intervention to combat the negative effects of menopause on AD is estrogen/ hormone replacement therapy (HRT). Conflicting reports exist on how *APOE* genotype modulates the effects of estrogen loss on neural functions. The literature indicates that estrogen status has greater effects in *E4* than *E3* (137, 266, 267), has the same effect in both *E3 & E4* (268), or has negative effects in *E4* while having positive effects in *E3* (133, 138, 139, 141, 142). While literature is contradictory, studies have not investigated the effects of *E4* and estrogen on the cerebral vasculature, a major piece of the puzzle.

The first biomarker of LOAD is altered cerebral blood flow, closely followed by metabolic changes in the brain (3). Altered CBF results from cerebrovascular dysfunction contributing to AD (269). Cerebrovascular dysfunction emerges from lower nitric oxide availability, elevations in ROS, and an overall promotion of an oxidative and pro-inflammatory environment (270). NO bioavailability decreases with each menopausal phase and is restored in the presence of estrogen (31). Estrogen can also aid in increasing NO bioavailability, and promotes an antioxidant, anti-inflammatory environment (75, 77, 271). Lastly, estrogen has major influences on mitochondrial function, the primary ROS producer (73, 272).

Metabolic dysfunction is a common feature of the AD brain, caused by impairments in delivery and utilization of glucose. Decreased brain glucose metabolism is measured by F-FDG-PET imaging, and alterations are found in the early stages of AD (3, 273). Specifically, *E4* perimenopausal females exhibit a lower brain metabolic rate compared to *E3* (33, 274, 275). Since glucose uptake is impaired in menopausal and AD brains, this piques questions into how energy demands are being maintained for cellular functions?

Mitochondrial dysfunction is a well-studied contributor to many diseases, but particularly AD. *E4* expression is associated with altered mitochondrial dynamics and dysfunction in astrocytes (276) and neurons (119). However, little is known about *E4's* impact on mitochondrial health and function in the cerebral vasculature, the barrier that divides the periphery and brain. Mitochondria influences vascular tone and health (277), potentially linking their dysfunction to the altered cerebral hemodynamics observed in *E4* carriers. Aging alters the cerebral vasculature to impair mitochondrial function (278), but this has yet to be investigated in the *E4* genotype and estrogen status was not accounted for. Thus, understanding the interaction of *APOE* genotype and estrogen on the cerebral vascular mitochondria could provide novel insight into the dysregulation that occurs during menopause and AD.

The purpose of this study was to investigate the interaction effect of *APOE* genotype and estrogen status in cerebral vascular function and metabolism. We hypothesized that ovariectomized *E4* female mice had poorer vascular and mitochondrial function than their *E3* and estradiol-treated *E4* counterparts. We further hypothesize that *E4* mice exhibit overall worse cerebral vascular and mitochondrial function compared to *E3* mice, measured by *ex vivo* pressure myography and respirometry (oroboros). We expected that *E4* females would show poorer cognition than their *E3* counterparts, while estradiol-treated *E3* mice would perform better

cognitively than their sham and ovariectomy (OVX) *E3* groups. We also hypothesized that impairments in *E4* females were partially due to elevated inflammatory markers. Lastly, we predicted that *APOE* genotype and estrogen status will influence both cerebral and large artery stiffness.

4.2 Methods

Animal Characteristics

We purchased *E3* (JAX#029018) and *E4* (JAX#027894) mice from the Jackson Laboratories and established a breeding colony. We studied homozygous *E3* and *E4* female mice ~6 months of age. All mice were on a standard chow diet (Lab Diet, PicoLab Rodent Diet 20, 5053) until they received ovariectomy or sham surgery at 4 months old, after which, mice were fed a high fat, high cholesterol diet (Atherogenic Rodent Diet, Teklad, TD.02028; 42.6% kcal from Fat). Food and water were provided ad libitum, and mice were housed on a 12/12-hour light-dark cycle at 24°C. Mice were euthanized by exsanguination under isoflurane immediately prior to vascular studies. All animal procedures conform with the Guide for the Care and Use of Laboratory Animals (8th edition revised 2011) and were approved by the Institutional Animal Care and Use Committee at the University of Oregon. See table 4.1 for animal characteristics.

Ovariectomy & Estradiol Implants

Female mice were randomly assigned to Sham (Sham), ovariectomy (OVX), or ovariectomy supplemented with 17β-estradiol (OVX+estradiol). OVX procedures were performed at 4 months of age. Prior to the ovariectomy procedure, mice were anesthetized with 2% isoflurane. Heart rate, breathing rate, and body temperature were monitored throughout the surgery and were performed as previously explained (279). Mice were monitored daily until a veterinarian approved the return to normal housing conditions. Subcutaneous estradiol implant

surgeries occurred one-week post ovariectomy. Mice were again anesthetized with 2% isoflurane, and a small incision was made (~3mm) on the posterior cervical area of the mouse. A subcutaneous space was created, and a 60-day slow releasing 0.36mg 17β-estradiol pellet (Innovative Research of America, Sarasota, FL) was inserted in the subcutaneous space. The incision was closed, and mice were monitored until a veterinarian approved their return to their home cage.

Plasma Hormones & Total Cholesterol

Blood samples were collected via cardiac puncture with a heparin saline-coated syringe. The blood was centrifuged, then plasma was collected and frozen in liquid nitrogen and stored at -80°C. Plasma hormone concentrations for 17β-estradiol (E2), estrone (E1), and progesterone were analyzed via Liquid Chromatography–Mass Spectrometry (LC-MS). Total cholesterol was measured via ELISA. All plasma analyses were performed by the Endocrine Technologies Core at Oregon National Primate Research Center at Oregon Health & Science University. Hormone levels that were undetected were entered as 0, and the ratio of E2 to E1 was calculated and reported (see Table 4.1).

Cerebrovascular Reactivity

Endothelium-dependent vasodilation was assessed in ex vivo isolated pressurized posterior cerebral arteries, as described in detail previously (230, 231). Arteries were excised and cannulated onto glass micropipettes in a myograph chamber (Danish MyoTechnology Inc.) filled with a physiological salt solution. All the arteries were pre-constricted with phenylephrine (1-6 μM) to obtain 20-40% pre-constriction of starting luminal diameter. Increases in luminal diameter in response to increasing concentrations of endothelium-dependent dilators acetylcholine (ACh: $1x10^{-9}$ to $1x10^{-4}$ M) and insulin (1 to 10000 ng/mL) were determined.

Insulin doses were prepared from a 4mg/mL stock (Insulin, human recombinant, zinc solution, Gibco), by diluting in physiological salt solution containing bovine serum albumin. After ACh and insulin responses, arteries were incubated for 30 minutes with 0.1 mM of N omega-Nitro-L-arginine methyl ester hydrochloride (L-NAME). ACh and insulin responses were repeated in the presence of LNAME to determine the contribution of NOS to endothelium-dependent dilation. Endothelium-independent dilation was measured by the increases in luminal diameter to sodium nitroprusside (SNP) ($1x10^{-10}$ to $1x10^{-4}$ M). See supplemental table S4.1 for artery characteristics.

Cerebrovascular Mitochondrial function

To measured *ex vivo* cerebrovascular mitochondrial function, we used the oroboros (O2k, OROBOROS Innsbruck, Austria). Brain arteries were carefully dissected from the brain and placed in ice-cold BIOPS (10mM Ca-EGTA buffer, 0.1 μM calcium, 20mM imidazole, 20 mM taurine, 5 mM K-MES, 0.5 DTT, 6.56 mM MgCl2, 5.77 mM ATP, 15 mM phosphocreatine, pH 7.1), followed by permeabilization with 30 ug/mL saponin in BIOPS for 30 minutes, followed with a 30-minute wash in MIRO5. The arteries were then spun down briefly and placed in the respirometry chamber. All data were collected at 37° C in a super oxygenated environment (200-400 μmol/L O2). Mitochondrial integrity was confirmed by measurement of respiratory responses to cytochrome c. Each chamber received the same titration protocol probing for carbohydrate metabolism with the following sequential additions: 5mM pyruvate, 2mM malate, 10 mM glutamate, 5 mM ADP, 10 mM cytochrome c, 10 mM succinate, 1 mM FCCP, 10uM rotenone, 10 uM antimycin A, and 10 uM myxthiazol. This provides an in-depth evaluation of cerebral artery respiratory capacity and substrate control during OXPHOS, as well as the extent of non-phosphorylating respiratory leak, and noncoupled enzymatic capacity of the ETS. Once

respiratory measures were completed, the cerebral arteries were removed, spun down and frozen for further analysis.

DNA Content and mRNA Expression

After respirometry data collection, CA were thawed, the MIR05 was removed, and 200 ul of Quizol was added to the samples, and DNA isolation was performed according Quiros et al. (280). Samples were homogenized and water sonicated for 2 minutes at 50%. 0.2mL of chloroform per 1mL of Trizol was used, and samples were centrifuged for 15 minutes @ 12,000g. 0.3 mL of 100% Ethanol per 1 mL of TRIzol reagent. Follow gentle inversion and incubation for 3 minutes, samples were centrifuged again for 5 minutes @ 2000g to pellet the DNA. After pelleting the DNA went through a series of wash steps, followed by solubilization in 70 ul in RNA free H2O. DNA content was quantified by nanodrop (Nanodrop 2000 Spectrophotometer, ThermoFisher Scientific, Waltham, MA). The DNA samples underwent real-time PCR (Quantstudio 5, ThermoFisher Scientific, Waltham, MA) for mitochondrial DNA by 16S and ND1, and for nuclear DNA by HK2 (see supplemental table 4.2 for primer sequences). The $\Delta\Delta Ct$ was calculated ($\Delta Ct = Ct(mtDNA \text{ gene}) - Ct(nDNA \text{ gene})$; $\Delta\Delta Ct = \Delta Ct(\text{Sample of interest}) - \Delta Ct(\text{Control sample})$). In additional mice, we conducted gene expression measurements to identify the components of our samples. Using a similar technique as the sample collection of Cerebrovascular Mitochondrial Function, arteries that were dissected from the brain, then underwent RNA isolation, reverse transcription and qPCR. Gene expression was performed for the following genes: pecam1 (endothelial cells), acat2 (smooth muscle cells), gfap (astrocytes), Rbfox3 (neurons), and a1f1 (microglial)(Supplemental Table S4.2).

Protein Expression

Protein expression was measured for the hippocampus and aorta by Western blot. The hippocampus was carefully dissected from the other brain tissue, and the aorta was dissected and cleaned of perivascular fat. Both were then flash-frozen in liquid nitrogen. Samples were homogenized in protein extracting buffer and protease inhibitor cocktail, then internally sonicated three times at 70% power for 10 second intervals. Lysate protein concentration was assessed using a commercially available kit (Pierce BCA protein assay kit; Thermo Fisher, Waltham MA). Bio-Rad stain-free TGX gels were used for protein separation. The stain was activated to ensure protein separation and then transferred onto a PVDF membrane. Membranes were imaged after transfer to verify the total protein transferred, and then membranes were blocked in with 1.5% milk in TBS-T for 20 minutes, then incubated in primary antibody overnight in PBS containing 3% BSA. Primary antibodies for the hippocampus can be seen in table 4.2. Following incubation, membranes were washed and incubated with a species-appropriate HRP-conjugated secondary antibody (see table S4.3). Following washes, membranes were incubated in Azure Chemiluminescence (Azure Biosystems, Dublin, CA) and imaged with a ChemiDoc Imaging system (ChemiDoc, BioRad, Hercules CA). Image J was used to determine protein band density and relative protein expression was calculated as protein density normalized to GAPDH density. Values were normalized to the *E3* sham group. See table 4.3 for antibody list and validation.

Passive Stiffness

Passive arterial stiffness was measured ex vivo in the PCA's by the resting lumen diameter and medial wall thickness while increasing intraluminal pressure(232). Passive stiffness was measured following a 60-minute incubation of calcium free solution to eliminate myogenic tone. Each artery was recorded from 5 to 100 cmH2O (3.7-73.5mmHg) in 5 cmH2O increments.

From this stress-strain curves, Beta-stiffness, and elastic modulus at low pressure (EM_{LP}) and at high pressure (EM_{HP}) were calculated as previously described (233).

Aortic Stiffness

Aortic stiffness was measured *in vivo* by pulse wave velocity (PWV) (230). Mice were anesthetized using isoflurane (2% isoflurane in 100% oxygen) and placed supine on a temperature-controlled heating pad (37°C). Electrodes were placed on distal portions of limbs that record ECG, while two Doppler transducers were positioned on the aortic arch and abdominal aorta. The distance between the transducers was recorded. Using the Doppler signal processing workstation program (DSPW; Indus Industries, Webster, TX, USA), the time of a pulse to travel from the arch to the abdominal aorta was analyzed, and the time was then divided by the distance between the transducers. Two researchers analyzed the files independently, and the average was taken. Sham mice's estrous stage was noted at the time of PWV measure (230).

Oral Glucose Tolerance Test

Mice were fasted for ~4 hours. Blood was obtained from a tail cut and assessed for baseline glucose levels using iPet pro glucometer (Ultimed incorporated, Excelsior, MN). The mice then received 2 mg/g of 0.15 mg/uL dextrose solution via intraperitoneal injection. At 15, 30, 45, 60, 90, & 120 minutes post-injection, blood glucose was measured from the already punctured tail cut. Glucose curves were created, and area under the curve (AUC) was calculated.

Indirect Calorimetry

Prior to *ex vivo* studies mice were singly housed in an environmental cabinet for 5 days. Using metabolic cages (Promethion, Sable Systems, Las Vegas NV), we measured food and water intake, body weight, oxygen consumption (VO2), carbon dioxide production (VCO2), and water vapor during the 12:12-h light-dark cycles. Metascreen software (Sable Systems Inc.) was

used for data collection. Data was then processed with ExpeData and Macro Interpreter (Sable Systems Inc.), analyzed on an hourly basis. VO2, VCO2 production, and expenditure (kcals/hour) were normalized to body weight (kg). The first 24 hours were excluded from data analysis for an acclimatization period.

Cognitive Function

Learning and spatial memory was assessed via Morris Water Maze. Mice underwent a 3-day training period, where they performed 3 trails every session, with 2 sessions per day. On the fourth day, a probe trial was performed in the morning, where the mice swam for 60-seconds. Also, on the fourth day in the afternoon session the beacon trial was performed, where the platform was marked and the time it took the mouse to get to the platform was acquired. All sessions were analyzed and recorded on EthoVision XT12 software (Noldus, Wageningen, the Netherlands)(281).

Anxiety was measured via open field testing. Mice were placed in a $40cm^2$ square arena with a white matte floor and walls. Mice were in the arena for 10 minutes and their exploration was recorded using Ethovision XT12 software. The center of the 20x20 cm square was marked with software, and exploration criteria were defined as the amount of time the center of the mouse's body was inside the square area. Mice that spend more time exploring (more time in the center of the arena) have lower levels of anxiety (281).

Instinctual Behavior

Nest building is a test of instinctual behavior and was performed over a 12-hour period. Mice were singly housed overnight in a fresh cage containing a condensed cotton nestlet. The following morning, the researcher scored the nests. The same researcher scored all nests. Nests were scored on a scale of 0-5 with the following criteria: 0- nestlet is untouched; 1- nestlet has

been moved but no significant tearing; 2- significant tearing, but no formation of a nest; 3- significant tearing, indication of nest OR nest is in the corner of the cage; 4- significant tearing, formation of nest in the corner; 5- significant tearing, formation of nest in corner and the nest walls are high making a bowl like nest (159).

Motor Coordination

Motor coordination testing was performed using a rotarod (47650 Rota-Rod NG, Ugo Basile, Gemonio, Italy) over a two-day period. The first day was a training session, and mice were required to stay on the rod rotating at 4 rpm for 90 seconds. The second day consisted of three trials, with a 10-minute rest between trials, where the rod accelerated during each trial from 4 to 40 rpm with a cut-off time at 5 minutes. The time was recorded for when the mouse fell from the rod or rotated around the rod two consecutive times (223).

Statistical Analysis

Statistical analyses were performed with GraphPad Prism 10. A two-way analysis of variance (ANOVA) was used to determine the interaction effects and independent effects of genotype and estrogen status. In the case of a significant F-value, post-hoc analyses were performed using a Tukey correction for preplanned comparisons. A repeated measures ANOVA was used to determine group differences for dose responses. Significance was set at $p<0.05$, and values are represented as mean ± SD. Outliers were identified as a z score >2 and were removed from the data set.

4.3 Results

Animal Characteristics

E4 mice had higher body mass than *E3* mice (genotype effect p=0.001; Table 4.1). For white adipose tissue mass, there were main effects of estrogen and genotype (estrogen effect

p=0.004, genotype effect p=0.0005), and white adipose tissue mass was highest in the *E4* OVX group (Table 4.1). Confirming successful ovariectomy surgeries, uterus mass and plasma 17β-estradiol were lower in ovariectomized mice (estrogen effect p=0.002, p=0.02). A main effect of estrogen was seen for liver weight (estrogen effect p=0.007), spleen (estrogen effect p=0.0002), and total cholesterol (estrogen effect p=0.04), all increasing in the OVX+estradiol group. Lastly, plasma progesterone increased in the Sham groups (estrogen effect p=0.04)(Table 4.1).

Cerebral artery endothelial function is impaired by ovariectomy in E3 mice but not E4 mice

PCAs from *E3* mice differed from *E4* mice in their vasodilatory responses to ACh, and as demonstrated by an interaction effect of *APOE* genotype and estrogen status (p=0.05). There was also a main effect of estrogen status (p=0.01) and a trend for a main effect of genotype (p=0.11) for the vasodilation in response to ACh (Figure 4.1A & B). Specifically, *E3* OVX mice had about 20% less dilation than the *E3* shams (max: 0.02, dose-response: p=0.0002), and about 18% less dilation than the *E3* OVX+estradiol treatment mice (max p=0.02, dose-response: p=0.0002). Among the *E4* mice, PCA dilation to ACh did not differ with OVX or estradiol status (all p>0.05). When comparing the OVX+estradiol, the *E4* OVX+estradiol mice dilated less to ACh than the *E3* OVX+estradiol mice (max: p=0.09, dose-response: p=0.002). For the PCA dilation in response to insulin, there was a main effect of genotype (p=0.04) and a trend for a main effect of estrogen status (p=0.08), however no interaction effect was observed (Figure 4.1C &D). The vasodilation response to ACh and insulin in the presence of LNAME was nearly absent for all groups and was not different between groups (dose-response and maximal responses, all > 0.05, Figure 4.1B, D), suggesting that the group differences in vasodilation are due to differences in NO bioavailability. Endothelium-independent dilation in response to SNP was not different between groups (dose-response and maximal responses, all p>0.05), indicating that the

differences in ACh-mediated vasodilation were due to endothelial cell impairment. Sensitivity (EC50) to vasodilators and the amount of pre-constriction also did not differ between groups (all p>0.05, supplemental Table S4.1).

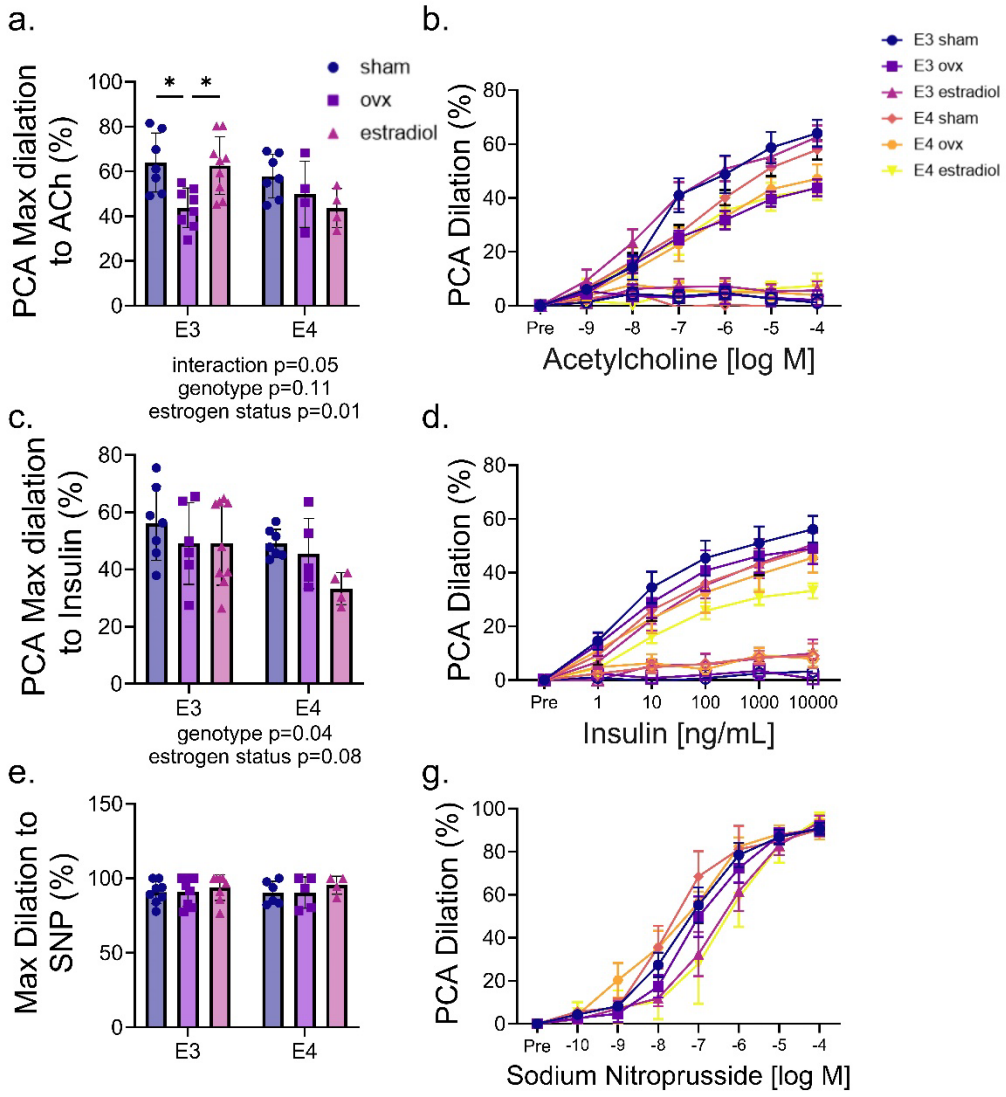

Figure 4.1. Cerebral artery endothelial function is impaired with ovariectomy and rescued with estradiol treatment in *E3* females but not *E4* females. Female homozygous *E3* and *E4* mice who received a sham, ovariectomy (OVX), or estradiol were studied at 6 mo. In isolated posterior cerebral arteries (PCA's), endothelium-dependent dilation was measured to a, b) increasing doses of acetylcholine (ACh) and c,d) insulin, in the presence and absences of nitric oxide inhibitor, LNAME. Endothelium-independent dilation in response to increasing doses to SNP. A repeated measures ANOVA for the dose responses and a two-way ANOVA for the maximal responses was used to determine independent and interaction effects, and Tukey's post-hoc analysis was performed. *p<0.05, **p<0.01, ***p<0.001. n=4-9/group. Data are mean ± SD.

Cerebral artery respiration is altered by estrogen status in E3 but not E4 female mice

For all the following results, the dissected arteries contained primarily SMC's (acat2) and EC's (pecam1), whose expression was significantly higher than expression from the hippocampus (SMC's: p<0.0001, EC's: p<0.0001). Our samples had traces of astrocytes (gfap), neurons (Rbfox3), and microglia (A1f1), but the expression was significantly lower than what was expressed in the hippocampus (gfap: p=0.01, rbfox3: p=0.0008, a1f1: p=0.005) (Supplemental figure S4.1).

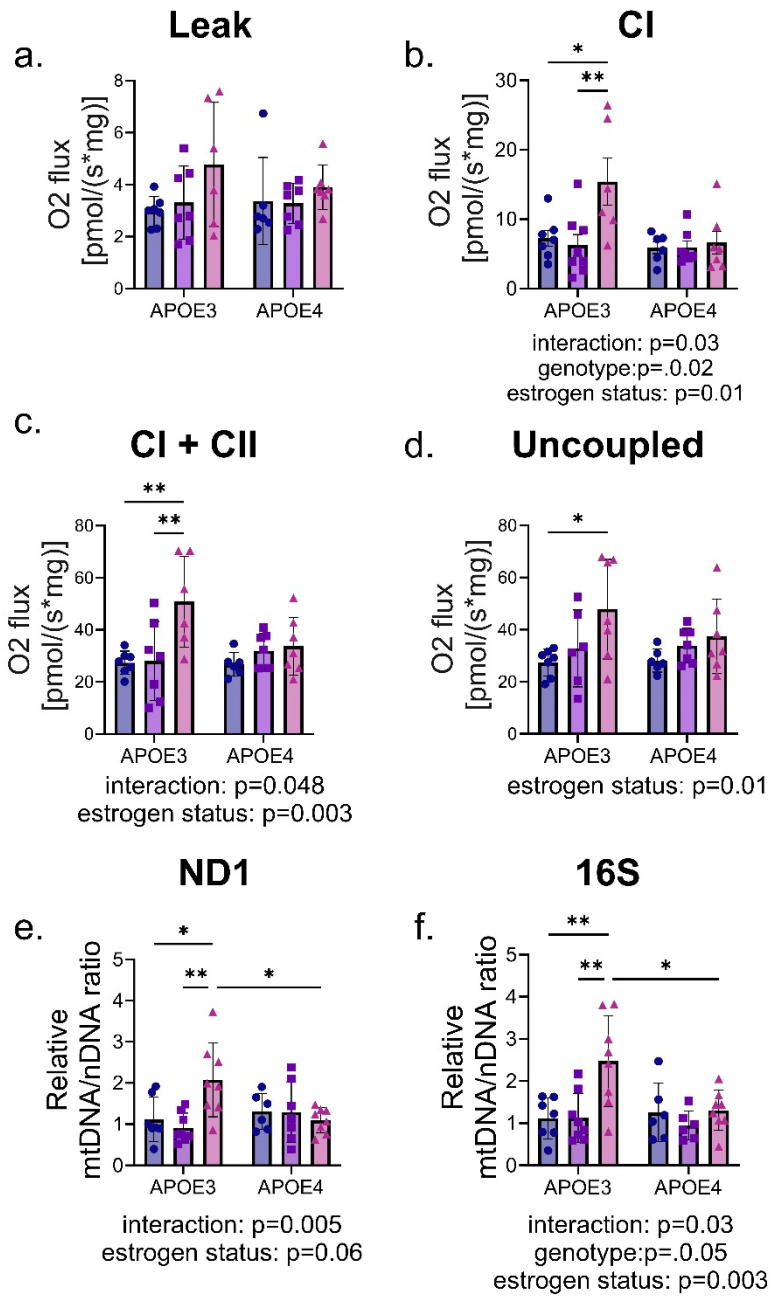

Figure 4.2. Estrogen status and *APOE* genotype interact to influence cerebral artery mitochondrial function. ETS activity for mitochondrial a) leak, b) CI, c) CI+CII and d) uncoupled maximal respiration. Mitochondrial DNA: nuclear DNA content for e) 16s and f) ND1. A two-way ANOVA was used to determine independent and interaction effects, and Tukey's post-hoc analysis was performed. *p=0.05, **p=0.01. n=5-7/group. Data are mean ± SD.

Estrogen status and *APOE* genotype interacted to impact CI coupled respiration (interaction p=0.03) and CI+CII coupled respiration (p=0.05) in cerebral arteries (Figure 4.2 B, C). For CI and CI+CII coupled respiration, there was a main effect of estrogen (CI p=0.01, CI+CII p=0.003) and CI had a main effect of genotype (p=0.02)(Figure 4.2 B & C). *E3* OVX+estradiol mice had greater CI and CI+CII respiration than the *E3* sham mice (CI p=0.03, CI+CII p=0.006) and *E3* OVX mice (CI p=0.007, CI+CII p=0.009)(Figure 4.2 B & C). There was also a main effect of estrogen status in uncoupled respiration, where estradiol supplementation elevated maximal respiration, primarily driven by the *E3* OVX+estradiol group (p=0.01)(Figure 4.2 D). Interestingly, among *E4* mice, CI, CI+CII, or uncoupled respiration did not differ with estrogen status (all p>0.05)(Figure 4.2 A-D). There were no differences in leak between groups (all > 0.05)(Figure 4.2 A). After respiration experiments, mtDNA was measured relative to relative nuclear DNA in the arteries, revealing similar trends. There was an interaction effect of estrogen status and *APOE* genotype for mtDNA genes 16s and ND1 (p=0.03, p=0.005)(Figure 4.2 E & F). Mice receiving estrogen had greater 16s and ND1 content compared to the other groups (main effects: p=0.003, p=0.06). *E3* OVX+estradiol mice had more 16s and ND1 content than *E3* shams (p=0.004, p=0.03), *E3* OVX (p=0.003, p=0.004), and *E4* OVX+estradiol mice (p=0.01, p=0.02).

Hippocampal protein expression differs by APOE genotype

Hippocampal expression of NFκB p65 and p50 were elevated in *E4* mice compared to *E3* mice (genotype effect p65 p=0.009, p50 p=0.10), and trend to interaction was observed in *E4* OVX, where p65 was greater (interaction effect p=0.10)(Figure 4.3A &B). LRP1 expression was higher in *E4* mice than *E3* mice (genotype effect p=0.005)(Figure 3E). *APOE* genotype and estrogen influenced hippocampal protein expression of ApoE (interaction effect p=0.03) and

trended higher in *E4* mice than *E3* mice (genotype effect p0.15)(Figure 4.3F). NFκB p105 expression trended to be influenced by estrogen status, where ovariectomized mice had greater expression (estrogen status effect p=0.06)(Figure 4.3C). Hippocampal expression of NDSFU1, citrate synthase , Cox1, and Cox2 did not differ between groups (all p>0.05)(Figure 4.3I-K).

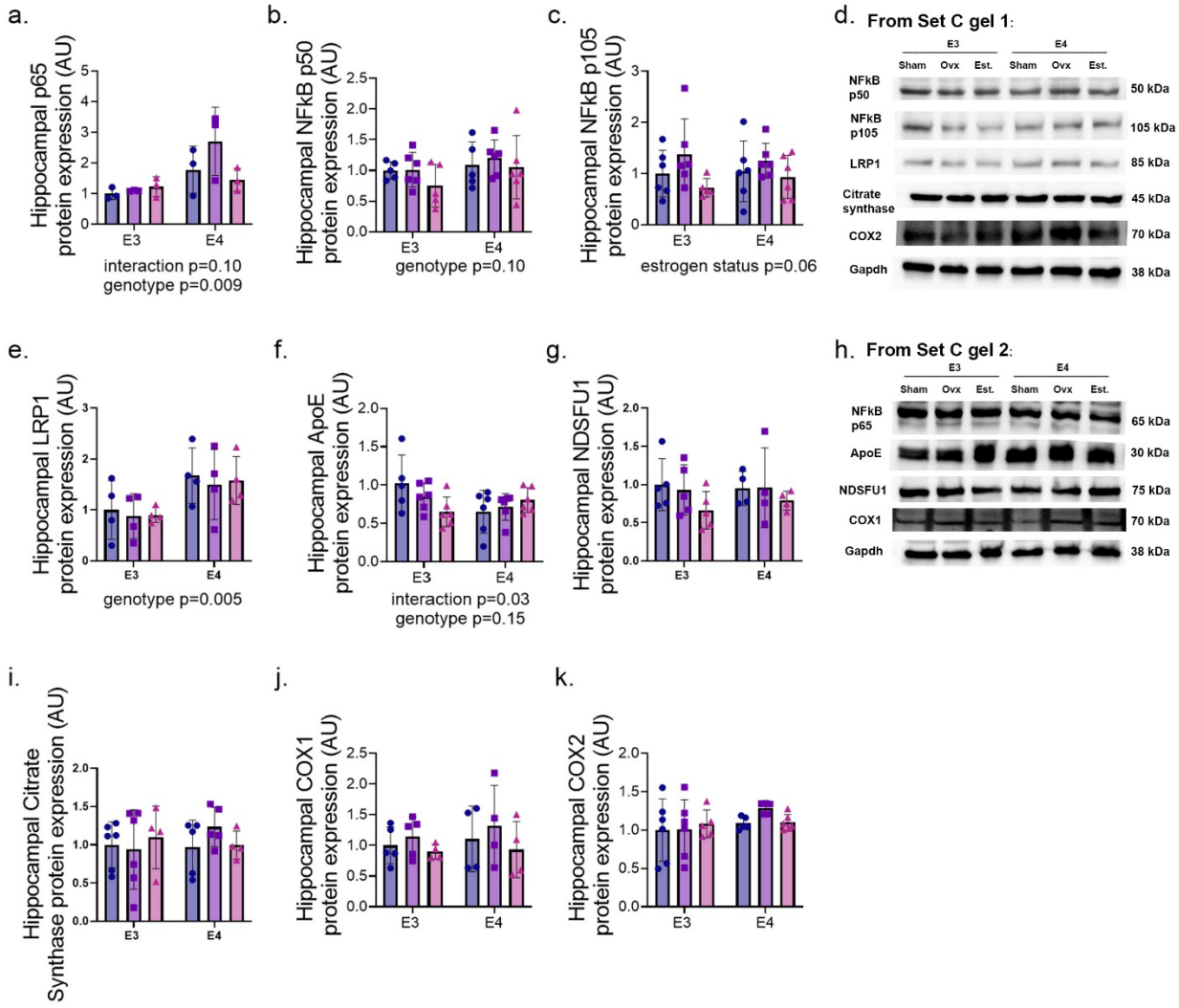

Figure 4.3. Hippocampal inflammation and ApoE protein expression are altered by *APOE* genotype and estrogen status. Hippocampal protein expression for a) p65, b) NFkB p52, c) NFkB p105, e) LRP1, f) Apoe, g) mitochondrial complex-I protein NDSFU1, i) COX1, j) COX2, and k) citrate synthase. Representative blot images on the right (d & h). A two-way ANOVA was used to determine independent and interaction effects, and Tukey's post-hoc analysis was performed. *p=0.05. n=3-7/group. Data are mean ± SD.

Aortic Protein expression

Aortic protein expression for and phosphorylated-eNOS (peNOS) at serine 1177 (S1177) trended greater in *E3* mice (genotype effect p=0.07)(Figure 4.4A), but did not differ for total eNOS or peNOS:eNOS ratio (all p>0.05)(Figure 4.4B & C). Phosphorylated-Akt (pAkt) at serine 473 (S473) was greater in the *E4* mice compared to the *E3* mice(genotype effect p=0.03; Figure 4D) but were not different for total Akt or pAkt:Akt ratio

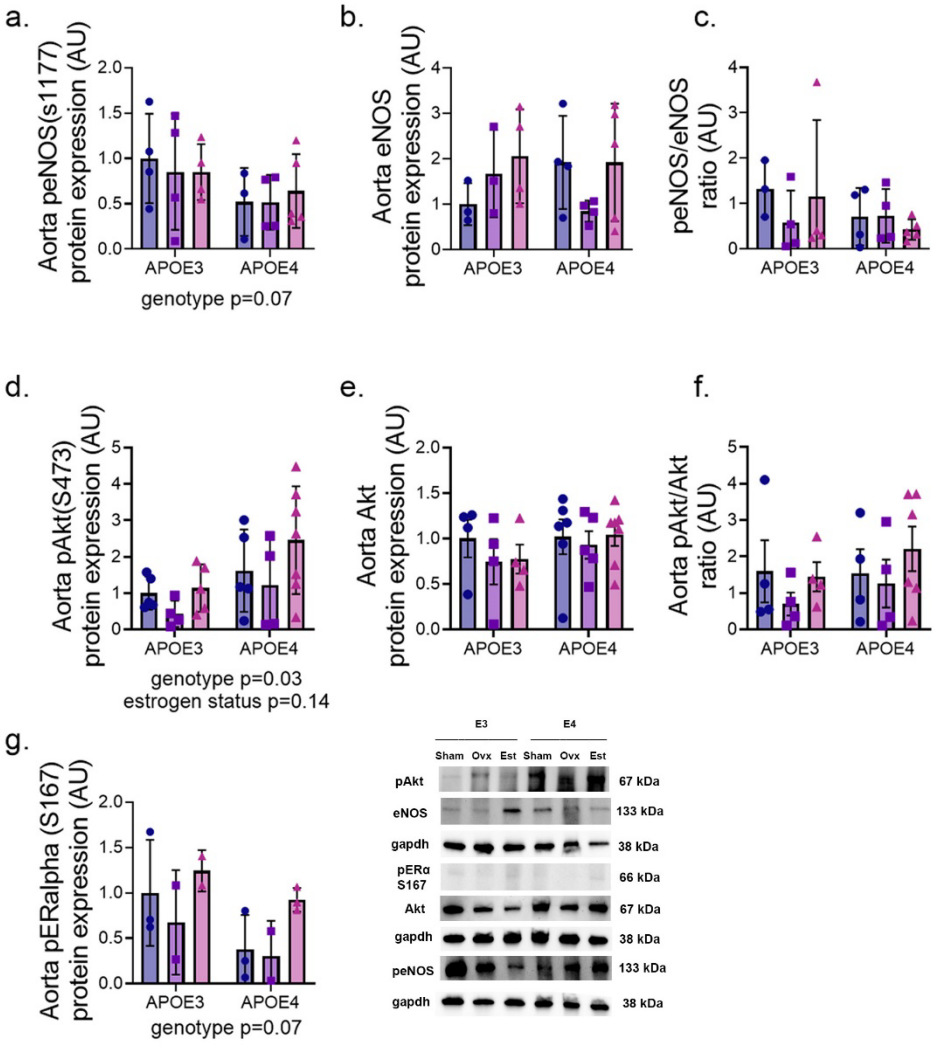

Figure 4.4. Phosphorylated eNOS differs by *APOE* genotype, and pAKt is altered independently by *APOE* genotype and estrogen status. Aorta protein expression for: a) phosphorylated endothelial nitric oxide synthase (eNOS) at serine 1177 (pENOS), b) total eNOS, c) peNOS:eNOS ratio, d) phosphorylated Akt at serine 473 (pAkt), e) Akt, f) pAkt:Akt ratio, and g) phosphorylated estrogen receptor alpha (Erα) at serine 167 (pERα). Representative blot images are below each graph. A two-way ANOVA was used to determine independent and interaction effects of *APOE* genotype and estrogen status. A Tukey's post-hoc analysis was performed. n=2-7/group. Data are mean ± SD.

(all p>0.05)(Figure 4.4E & F). Phosphorylated Erα trended higher in *E3* mice compared to *E4* mice (estrogen status effect p=0.07)(Figure 4G).

Cerebral artery stiffness is influenced by APOE genotype and estrogen status

We measured PCA passive stiffness *ex vivo,* and β-stiffness did not differ between groups (all p>0.05; Figure 4.5C). PCA EM_{LP} and EM_{HP} were dependent on estrogen status and *APOE* genotype (EM_{LP} interaction effect p=0.001; EM_{HP} interaction effect p=0.005; Figure 4.5 D, E). PCA EM_{LP} was greater in *E4* OVX mice compared to *E4* shams (p=0.02) but was not different from the *E4* OVX+estradiol mice (p>0.05). Data were generated from stress-strain curves in Figure 4.5A & B.

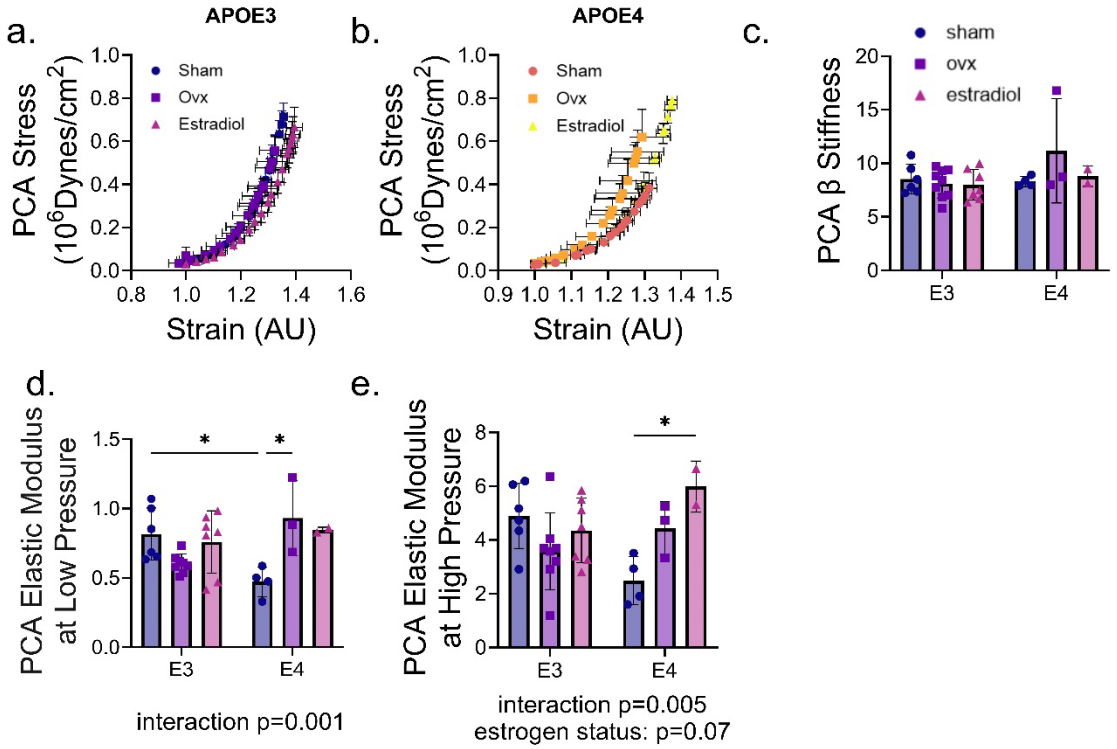

Figure 4.5. Posterior cerebral artery elastic modulus, a measure of stiffness, is influenced by *APOE* genotype and estrogen status. a, b) In PCAs incubated in calcium-free solution, a passive response to determine the structural components on the artery was performed, generating a stress-strain curve. From this curve, β -stiffness and elastic modulus were calculated. *APOE* genotype and estrogen status had no influence on c) PCA β –stiffness. There was an interaction effect of *APOE* genotype and estrogen status on elastic modulus at d) low and e) high pressure. A two-way ANOVA was used to determine independent and interaction effects of *APOE* genotype and estrogen status on PCA stiffness measures. *p<0.05. n=3-9/group. Data are mean ± SD.

Large artery stiffness is influenced by estrogen status

In vivo large artery stiffness, measured by aortic pulse wave velocity, did not differ by estrogen status or genotype (Figure 4.6C). We measured carotid artery passive stiffness *ex vivo* and carotid β-stiffness did not differ between any groups (all p>0.05). For carotid artery EM_{LP} and EM_{HP}, there were main effects of

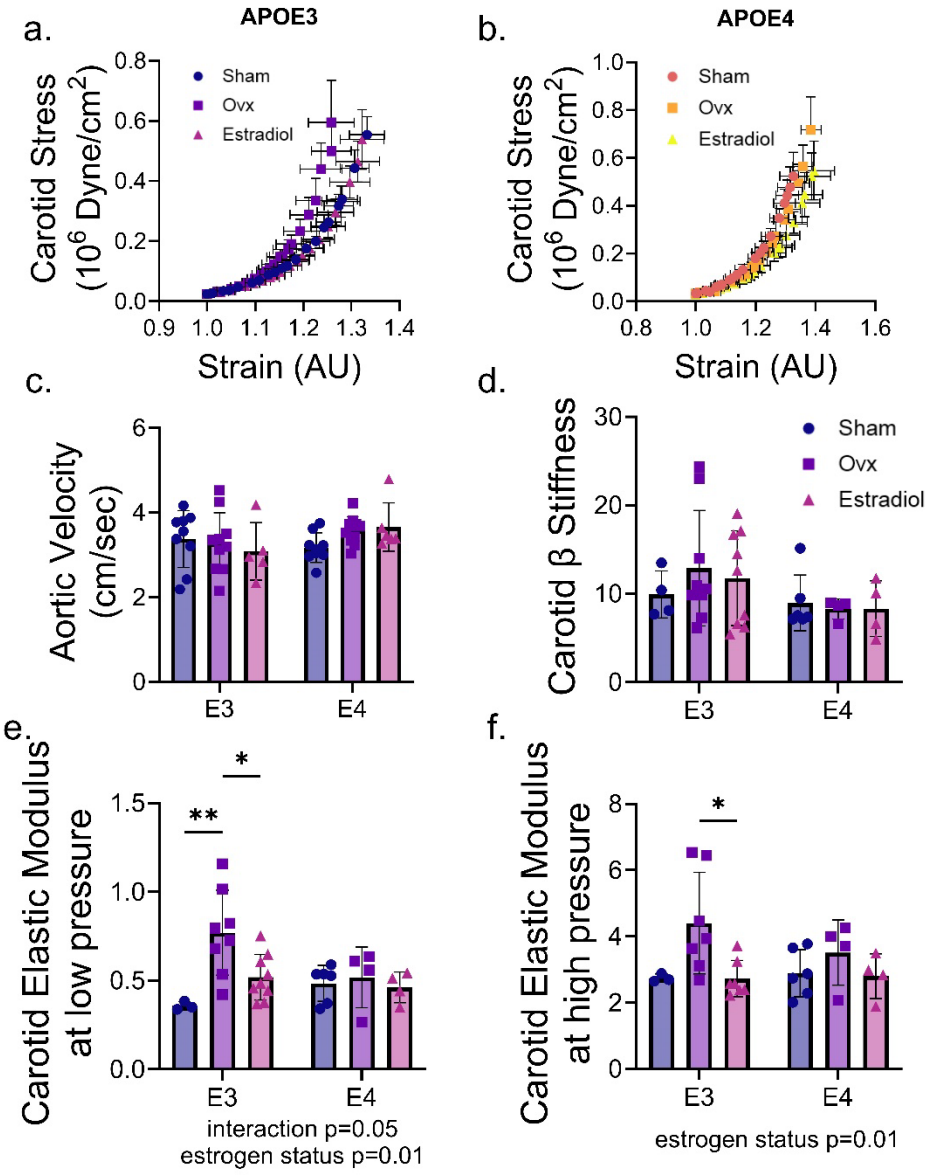

Figure 4.6. Carotid artery elastic modulus is affected by estrogen status. Aortic pulse wave velocity was measured, and c) is not affected by age or estrogen status. Carotid arteries were incubated in calcium free solution, and a passive response was performed. a,b) A stress-strain curve was generated, and β-stiffness and elastic modulus were calculated. d) Carotid β-stiffness was not different between groups. Carotid artery elastic modulus e) at low pressure revealed an interaction of estrogen status and *APOE* genotype, and a main effect of estrogen status alone. f) Carotid artery elastic modulus at high pressure was dependent on estrogen status, being elevated in the ovariectomy group. A two-way ANOVA was used to determine independent and interaction effects of estrogen status and genotype on stiffness parameters. *p<0.05, **p<0.01. n=4-11/group, data are mean ± SD.

estrogen status (EM_{LP}: p=0.01; EM_{HP}: p=0.01) (Figure 4.6 E & F). For carotid artery EM_{LP} there was also an interaction effect of estrogen status and *APOE* genotype (interaction effect p=0.05)(Figure 4.6 E). *E3* OVX mice had a higher carotid artery EM_{LP} than the *E3* sham (p=0.007) and *E3* OVX+estradiol groups (p=0.03)(Figure 4.6 F). For EM_{HP}, *E3* OVX mice had greater stiffness than the *E3* OVX+estradiol group (p=0.03) but not the *E3* sham group (p=0.15)(Figure 4.6F). The carotid artery EM measures did not differ between *E4* groups (all p>0.05). Data were generated from stress-strain curves in Figure 4.6A & B.

In-vivo metabolic measures are not influenced by APOE genotype or estrogen

In-vivo whole-body metabolism was measured in a subset of the mice by indirect calorimetry. There was a trend for estrogen status on oxygen consumption, with the OVX group trending to lower oxygen consumption than the sham and estradiol groups (estrogen effect p=0.09; Figure 4.7A). All other calorimetry parameters (CO2 production, energy expenditure (EE), and respiratory exchanges ratio (RER)) did not differ between any groups (all p>0.05)(Figure 4.7B-D). We performed glucose tolerance tests in the mice as well. Resting glucose, glucose clearance, and glucose area under the curve (AUC) did not differ between any groups (all p>0.05)(Figure 4.7E-G).

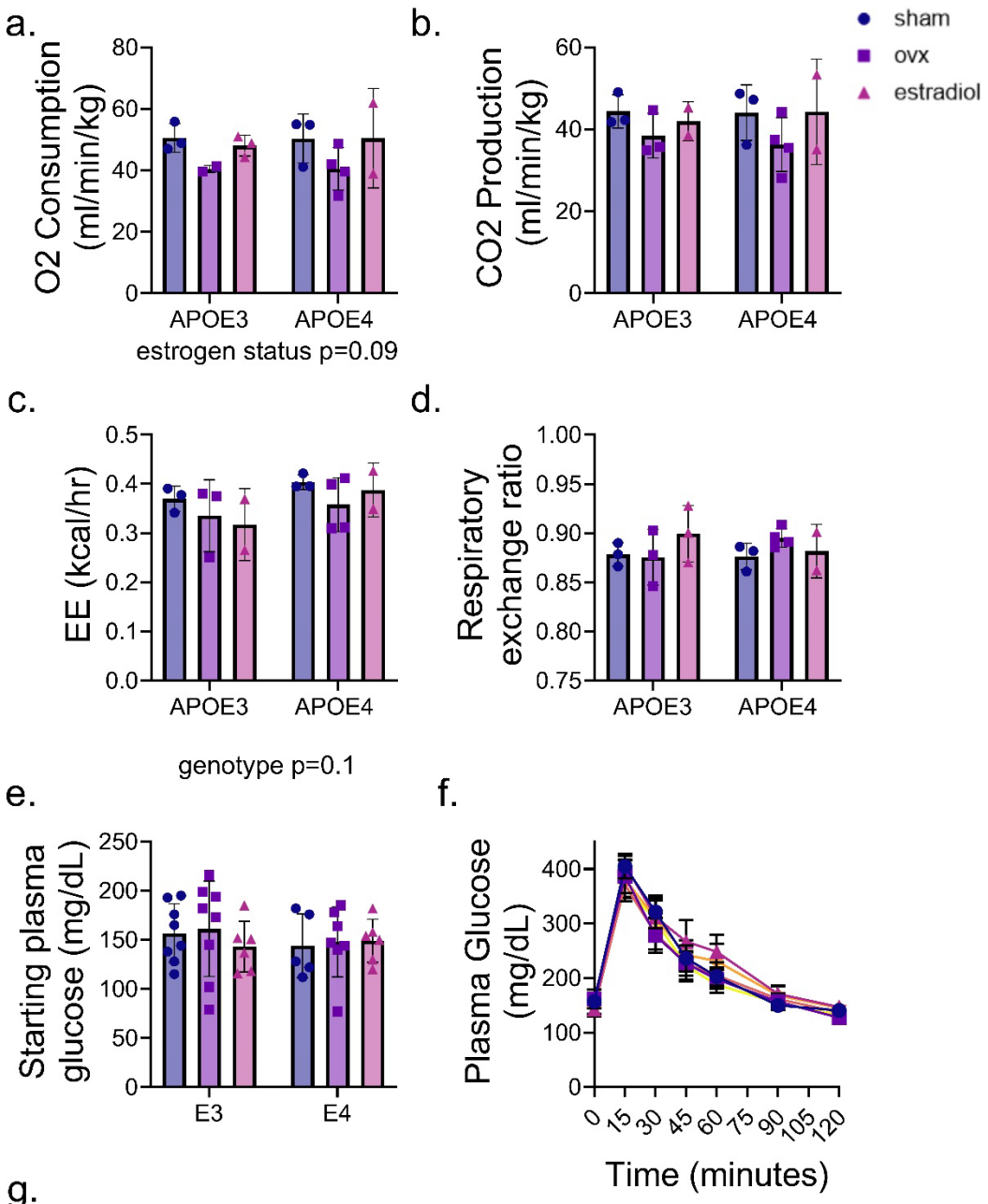

Figure 4.7. In-vivo metabolic measures are not influenced by *APOE* genotype or estrogen. These metabolic measures were measured by indirect calorimetry. a) VO2 and b)VCO2, normalized to body weight, are not different between groups. c) Energy expenditure and d) respiratory ratio (RER) are also not altered by estrogen and apoe genotype. Glucose tolerance tests were also performed in these mice. e) Resting glucose, and f,g) glucose area under the curve were not different between groups. *p<0.05. n=2-9/group. Data are mean ± SD.

APOE genotype and estrogen status did not influence cognitive function or motor coordination

We used the Morris water maze test to assess learning and spatial memory (Figure 4.8). In the 60 second probe trial, *E4* estradiol mice spent significantly less time in the target quadrant compared to the other quadrants (p=0.01; Figure 4.8D). All the other mice spend equal time or more time in the target quadrant than the other quadrants. Estrogen and

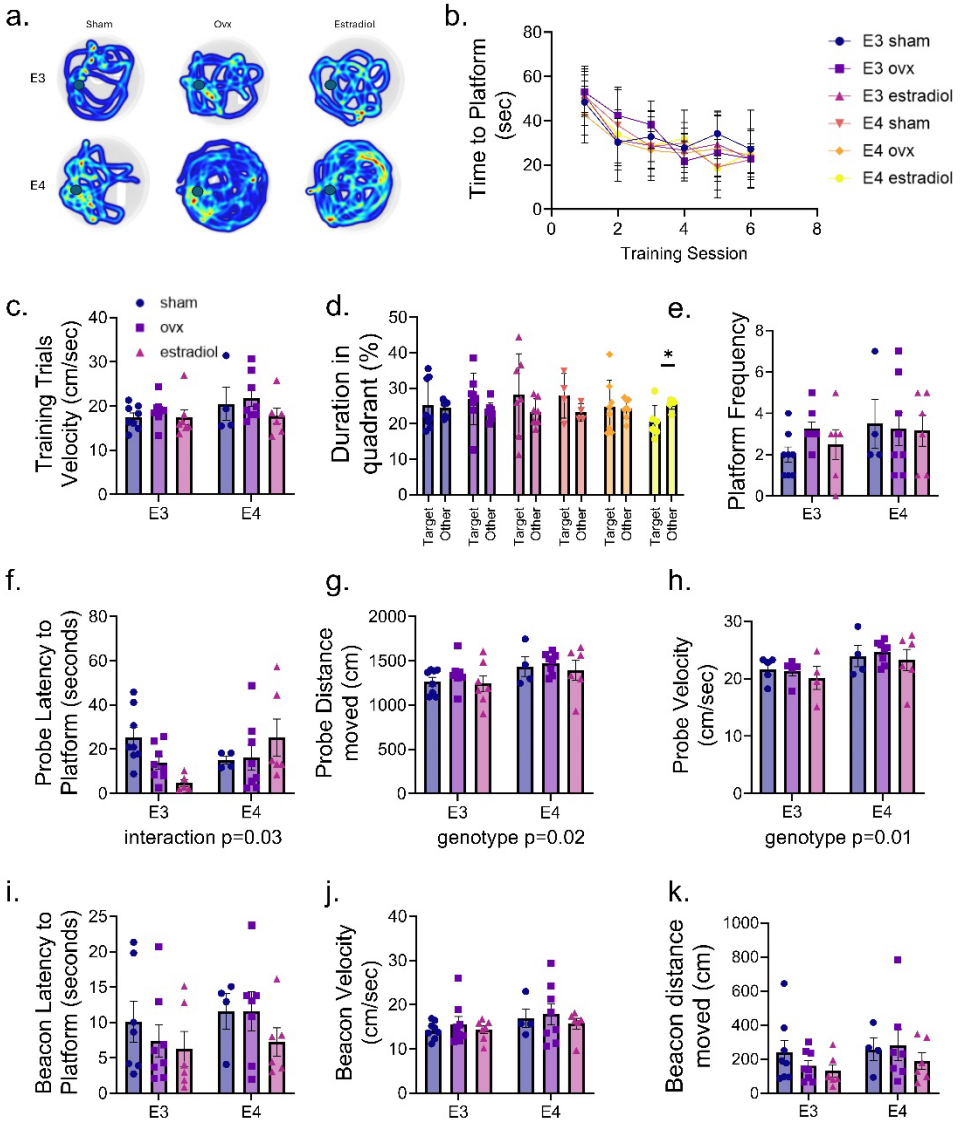

Figure 4.8. Learning and spatial memory were not greatly influenced by *APOE* genotype and estrogen status. a) Morris water maze heat maps traces for each genotype and estrogen status for their probe trial can be seen. No differences were seen in the training b) time to platform or c) training velocity. Probe trial outcomes are d) %time spent in each quadrant, e) platform frequency, f) latency to platform, g) probe distance moved, and h) probe velocity. Beacon trial outcomes are i) latency to platform, j) velocity, and k) beacon distance moved. A two-way ANOVA was used to determine independent and interaction effects of estrogen status and genotype on learning and memory. A one-tailed t-test was used for panel (d) to determine the time spent in the target vs other quadrant. *p<0.05, **p<0.01. n=4-8/group, data are mean ± SD.

APOE genotype influenced the latency to platform in the probe trial, where estrogen had more benefit in *E3* mice (interaction effect p=0.03; Figure 4.8F). *E4* mice had a greater distance moved and velocity during the probe trial (genotype effect p=0.02, p=0.01; Figure 4.8 G & H). There were no differences between groups in the outcomes of the Beacon or training trials (all p>0.05; Figure 4.8 B,C, I-K).

There were no differences in anxiety behavior, as indicated by the time spent in center of the open field arena, between groups (all p>0.05; Figure 4.9C-E). Additionally, there were no differences in object recognition, a measure of hippocampal-dependent memory assessed by Novel Object Recognition, between groups (all p>0.05; Figure 4.9 F & G).

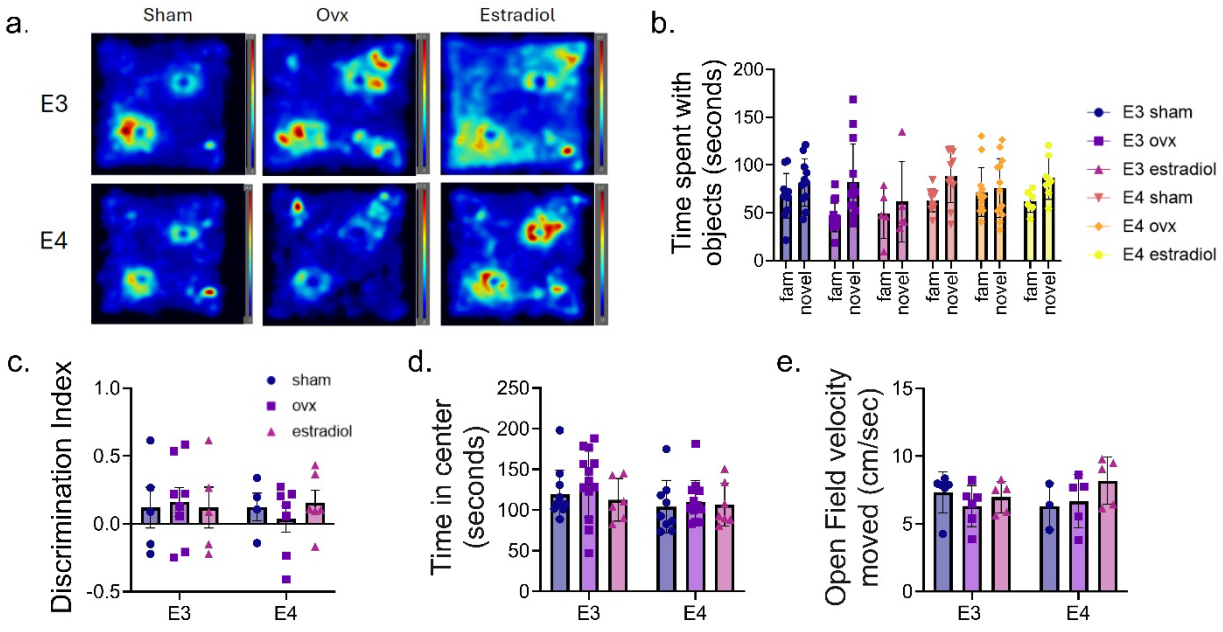

Figure 4.9. Object memory and anxiety were not dependent on *APOE* genotype or estrogen status. a) Novel object recognition representative heat maps. NOR b) time spent with familiar (fam) vs novel objects, followed by c) discrimination index calculation. Open field d) time in center and e) velocity. A two-way ANOVA was used to determine independent and interaction effects of estrogen status and genotype on hippocampal memory. *p<0.05, **p<0.01. n=3-8/group, data are mean ± SD.

Instinctual behavior, a measure of cognitive function, measured by nest building, was not different between any groups (all p>0.05; Figure 4.10A). Motor coordination, measured by rotarod, was also not different between groups (all p>0.05; Figure 4.10B).

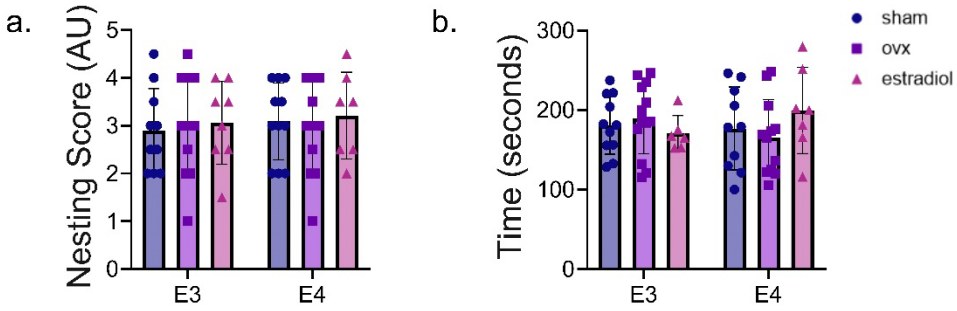

Figure 4.10. Instinctual behavior and motor function are not impacted by estrogen status or *APOE* genotype. a) Instinctual behavior, determined by the score on a nest building task, and b) motor coordination, measured by the time spent on an accelerating rotarod, was not different between groups. n=5-12/group. Data are mean ± SD.

4.4 Discussion

Contrary to our original hypotheses, this study demonstrates that the cerebral vasculature in female mice with the *E4* genotype shows resistance to the positive effects of 17β-estradiol, particularly in relation to endothelial and mitochondrial function. Endothelial-dependent dilation in *E3* mice was impaired with ovariectomy and rescued by estradiol supplementation. However, *E4* mice had no detriments or benefits with ovariectomy or estradiol supplementation. CI and CI+CII mitochondrial respiration was impaired in the *E3* OVX group, and greater in the *E3* OVX+estradiol group. Again, the *E4* mice had no detriments or benefits with ovariectomy or estradiol supplementation. Mitochondrial DNA to nuclear DNA ratio was greater in *E3* OVX+estradiol in part explaining the elevated mitochondrial respiration in this group. *E4* mice also had lower mitochondrial DNA than *E3* mice. The genotype differences in mitochondrial and endothelial function may be driven by inflammatory signaling and differences in receptor expression. Hippocampal protein expression for NF-κB subunits p65 & p50 were elevated in *E4* NF-κB p105 trended toward elevation with ovariectomy . Receptor LRP1 was higher in *E4* mice,

while apoE protein was lower in the *E4* mice in the hippocampus. Furthermore, in the aorta, r peNOS (S1177) trended higher in the *E3* mice, while pAkt(S473) was higher in the *E4* mice. Lastly, ovariectomy led to stiffening of the carotid artery in E3 mice, which was rescued by estradiol treatment; but there were no effects of ovariectomy or estradiol in the E4 mice. Contrary to our hypotheses, genotype and estrogen status did not impact *in vivo* metabolism, cognitive function, or motor function to the extent we hypothesized.

E4's resistance to estrogen: What do we know?

While we are the first to investigate the interaction effect of estrogen and *APOE* genotype on the cerebral vasculature, researchers have previously investigated this interaction in other tissues and reported *E4's* resistance to estrogen status. A few of these investigations were conducted in the APOE x 5XFAD Alzheimer's disease mouse model. Specifically, one group found in their *APOE* x5XFAD model, that estradiol infusion improved memory and dendritic spine density in *E3/E3* and *E3/E4* mice, but not in *E4/E4* mice(133). This group furthered their investigations to look at the influence of ovariectomy on these mice (138). Their results indicated that *E3* OVX mice had less exploratory behavior than *E3* shams, but *E4* mice were unaffected by estrogen status (138). A different group of researchers studied how estradiol supplementation affected Aβ levels in *APOE* x5XFAD mice. In *E2* and *E3* 5XFAD mice, estradiol supplementation decreased the number of Aβ plaques, whereas in *E4* mice, estradiol supplementation increased the number of Aβ plaques (141). Recently, Balu and colleagues found that estrogen supplementation in *E4* 5XFAD mice did not affect learning, memory, or Aβ pathology, but estrogen supplementation improved these outcomes in *E3* mice (282). Additionally, researchers have also studied the *E3* and *E4* targeted replacement (TR) mice. These studies reported that ovx led to less CA1 spine density in *E3's*, while ovx increased spine density

in *E4* mice (139). These authors proposed that *E3s* respond to the loss of estrogen and *E4s* respond to the loss of progesterone with ovariectomy; however, this hypothesis requires further investigation. Another research group using the ApoE TR mice investigated the effects of a diet targeting Erβ in female mice. They reported that an Erβ-targeted diet led to higher brain-derived neurotropic factor (BDNF) in *E2* and *E3* mice but not *E4* mice (140). Brown and colleagues discovered that the interaction between *APOE* genotype and estradiol influences NO and cytokine production in activated microglia (142). More specifically, estradiol decreased inflammation (TNFα and IL-6) in *E3* but not *E4* mice (142). Additionally, human trials also suggest that hormone replacement therapy has negative effects on cognition, memory, cholesterol alterations, and brain volumes in individuals with the *E4* genotype (266, 283–285). Contrary to the previously mentioned studies, some literature supports that HRT is beneficial for *E4* hippocampal volumes, and even decreases Aβ (137, 266). The majority of these previous studies support the idea of *E4's* resistance to estrogen status, but no one until now has 1) investigated if this resistance extends into the vasculature and 2) explored the mechanisms as to why *E4* is resistant to the beneficial effects of estrogen.

Endothelial Function

Our lab and others have consistently shown that the removal of ovaries leads to a subsequent decrease in endothelial function (216, 217, 279). What is less known though is the influence of estrogen and *APOE* genotype on endothelial function. Our data suggests lower NO-mediated dilation in *E3* OVX mice, while OVX+estradiol supplementation in *E3* females preserved NO-mediated dilation. Interestingly, unlike the *E3* mice, ovariectomy and estradiol supplementation had no effect on the endothelial function of *E4* mice. However, these patterns for responses were not consistent for other endothelium-dependent vasodilators. NO-mediated

dilation to insulin had a main effect on genotype, where *E4* mice had lower dilation to insulin than E3 mice. Estradiol did not influence the dilation to insulin for *E3* mice, suggesting different mechanisms for dilation. A previous study from our lab showed that high soy diet preserves cerebral artery dilation to insulin after ovariectomy (279), highlighting that the high fat diet our E3 OVX mice were on may play a role in the differing results. Overall, the responses to endothelial-dependent dilators suggest that cerebral artery endothelial function is not influenced by estrogen for *E4* mice and that *E4* mice have endothelial dysfunction when compared with *E3* mice.

To better understand the mechanisms underlying the differences in NO-mediated dilation, protein expression was measured for total eNOS and phosphorylated eNOS at serine 1177 (peNOS S1177) in the aorta . While the aorta differs in composition from the smaller cerebral arteries, protein expression measurement in the cerebral arteries is not feasible due to too little protein. We observe a trend in peNOS (S1177) levels in the aortas of these mice, with *E3* mice exhibiting higher peNOS levels compared to *E4* mice. However, contrary to previous literature, we saw no effect of estrogen status on peNOS (279). Aortic eNOS and peNOS/eNOS ratio had no statistical differences between groups. These observations don't support our findings for the NO component of cerebrovascular EDD, and this can be potentially explained by our inability to measure eNOS in the cerebral vasculature directly.

Protein kinase B (Akt) and the mitochondria have a multifaceted relationship that is critical for function across cell types. Through a vascular lens, Akt plays a major role in activating eNOS and NO production. Phosphorylated-Akt was higher in the aortas from *E4* mice compared to E3 mice. However, the E4 females did not have elevated aortic peNOS, perhaps because the p-Akt/Akt ratio was not different between groups, suggesting no difference in Akt

activation despite higher levels of p-Akt. P-Akt is also a major player in signaling for vascular smooth muscle cell proliferation (286), which in excess can be negative in terms of vascular function, warranting further investigation to determine the downstream consequences of elevated pAkt.

The impact of cerebral vascular mitochondrial function on cerebral vessel dynamics

Mitochondrial dysfunction is a primary culprit of oxidative stress, which significantly influences cerebral vascular function (278), making the proper functioning of the mitochondria critically important. Endothelial cells rely on mitochondrial ATP to maintain vascular tone and function (287, 288). The mitochondria, primarily CI and CIII, are the primary sites of ROS production. Even though estradiol supplementation increases CI respiration in *E3* mice, this does not necessarily result in greater oxidative stress as estrogen also prepares the cells by increasing antioxidant enzyme expression (271).

Cerebrovascular mitochondrial respiration and whole-body metabolism

Mitochondria content varies across vascular beds, and brain endothelial cells contain more mitochondria than other vascular beds (289). Isolation of cerebral arteries and respirometry by oroboros has only been performed once previously, to our knowledge (278), highlighting the novelty of this technique. Cerebral vascular mitochondrial respiration can provide information about the health and function of the mitochondrial complexes. Our findings suggest that estrogen supplementation in *E3* mice increases CI and CI+CII respiration, but estrogen supplementation does not impact CI or CI+CII respiration in *E4* mice. Changes observed in CI+CII were driven by the initial increase in CI respiration. We also find that estradiol supplementation in *E3* mice resulted in higher mitochondrial DNA content, relative to nuclear DNA, a finding also not seen in *E4* mice. The major findings regarding our respirometry data are twofold: 1) Estradiol

enhances CI respiration in *E3* mice but not *E4* mice, and 2) Estradiol increases mitochondrial DNA in *E3* mice, suggesting that estradiol results in either more or larger mitochondria, but estradiol did not have this effect in *E4* mice. Mitochondrial fission and fusion dynamics are potential mediators of these findings, but future investigations are needed to determine these dynamics in the cerebrovasculature of *APOE* and estradiol-supplemented mice.

Since most of the mitochondrial differences were related to CI, we measured CI protein NDSUF1 in the hippocampus. We saw no differences in NDSFU1 expression between groups, potentially because this protein is transcribed from nuclear DNA, not mitochondrial DNA. A previous study found that mtDNA-encoded CI in cerebral blood vessels was elevated by estradiol treatment in rats (65). Another study found that nDNA-encoded CI protein NDUFB8 was more highly expressed in *E4* compared to *E3* brain endothelial cells (100). Future research should consider testing multiple CI-related proteins to aid in a more complete understanding of how estrogen and *APOE* influence this complex. We also measured citrate synthase expression in the hippocampus, the rate-limiting enzyme of the citric acid cycle, and found it was not modulated by estrogen or *APOE* genotype. Potentially explaining the lack of significance from this finding is that we did not have enough tissue to measure citrate synthase activity rather than abundance. Also, all the above measures were performed in the hippocampus, but our respiration studies were conducted on cerebral arteries, and thus, it could be that *APOE* genotype and estrogen have a specific impact on the vasculature.

APOE's effects on mitochondrial function have the potential to impact whole-body metabolism. A 2021 study measured in-vivo whole-body metabolism in *E3* and *E4* female mice on a normal chow or a high carbohydrate diet. The study found that *E4* mice have lower energy expenditure and failed to increase oxygen consumption following a high carbohydrate diet (290).

In contrast, we found no differences in *in-vivo* whole-body metabolism for average, light, or dark cycles between *E3* and *E4* mice on a high fat diet. We also found no differences in glucose tolerance tests between *E3* and *E4* mice. In addition to our small group numbers, another limitation is that we did not measure the activity of the mice, which can greatly alter oxygen consumption and CO2 production. Overall, *in vivo* metabolic outcomes were not altered to the extent of which we hypothesized.

Other mechanisms that contribute to vascular function

Key mechanistic proteins altered by the *E4* genotype at the level of the blood-brain barrier include apoE and LRP1 (125, 126). Our findings indicated that apoE expression in the hippocampus is influenced by an interaction between genotype and estrogen status. *E4* mice trended to have lower apoE expression, matching other literature in the field (100, 291), but we did not find an effect of estradiol on hippocampal apoE expression. In 1997, Srivastava and colleagues reported that apoE gene expression is upregulated by estrogen (292). This pioneering study in the field differs from our results, but it is important to note that their measurements were in liver slices and plasma, where we measured protein expression in the hippocampus (292). ApoE's primary receptor in the brain is LRP1. We found that LRP1 is elevated in the *E4* females and not influenced by estrogen status. The *E4* variant of apoE binds less efficiently to LRP1 than the other variant, and perhaps this lower binding triggered the increase in expression of LRP1 we see in *E4*. The insufficient binding of *E4* on LRP1 is proposed to activate cyclophilin-A-NF-kB-MMP9 pathways, promoting BBB breakdown (125). It was previously shown that *E4* mice have five- to six-fold higher CypA levels in cerebral microvessels (125). Thus, sufficient binding of ApoE/LRP1 in *E3's* can lead to NF-κB inhibition. Thus, the reduced efficiency of *E4* ApoE binding to LRP1 potentially explains the elevations in NF-κB in *E4* mice in our study.

Estrogen receptors can also inhibit NF-κB signaling in the vasculature (293, 294). For aortic protein expression of phosphorylated Erα (S167), we see a trend of genotype, where Erα phosphorylation is greater in *E3* mice than *E4* mice. The trend of this lower Erα activation in *E4* mice could explain the elevations in NF-κB; although, NF-κB and Erα should be measured in both the aorta and hippocampus to confirm this hypothesis.

Endothelial cells are also primed to use ROS as signaling molecules, influencing the expression of COX proteins. COX1 and COX2 are integral to the production of prostaglandins and can modulate inflammation and, thus, vascular tone. COX1 is often more involved in normal cellular functions, whereas COX2 is inducible via inflammation. While we did not see significant differences in protein expression of COX1 or 2 in the hippocampus, that does not mean their expression isn't altered in the cerebral vasculature. ApoE can upregulate COX2 in smooth muscle cells (295). In *E4* mice, COX2 can be upregulated, and COX2 inhibition has been explored as a treatment for AD (296), but the results of treatment were inconclusive. Estrogen can also influence COX activity. In endothelial cells, estrogen upregulates COX-1 (297) and decreases COX2 (47). The regulation of COX expression by *APOE* and estrogen are opposing, where estrogen favors COX1 expression and *E4* favors increases in COX2 expression, thus additional research is required to further understand these findings.

Stiffness

The age-related increase in large artery stiffness is a predictor of cognitive decline (298, 299). Despite previous literature suggesting increases in PWV with ovariectomy (41) and elevated pulse pressure with the *E4* genotype (300), our data did not support this. Although we did not find differences in PWV, we did observe a higher carotid passive stiffness with ovariectomy that was rescued by estradiol treatment, primarily driven by the *E3* groups. This

aligns with a recent study where ovariectomy increased carotid passive incremental modulus in OVX mice (41). In the cerebral arteries, we found an interaction effect of genotype and estrogen status on passive stiffness. This suggests again that estrogen status and *APOE* genotype influence vascular stiffness, although the exact mechanisms explaining this remain unknown.

Cognitive and motor function

E4 is associated with lower cognition. *E4* knock-in mice show cognitive deficits in multiple behavioral and learning tasks (301). One study used female *E4* FAD mice on a HFD and treated with estradiol and tested novel object placement (NOP) and novel object recognition (NOR)(302). These authors demonstrated that with NOP there were significant main effects of *APOE* genotype and hormone treatment. Interestingly, cognitive function in *E3* animals was not improved by estrogen, and cognitive function improved in *E4* mice with estrogen treatment, but not when the mice were fed a high-fat diet (302). We measured learning and spatial memory via Morris water maze. Our probe trial revealed the *E4* estradiol group spent more time in the other quadrants than the target quadrant during the probe trial, indicating poor learning and memory behavior. We also see that the latency to the platform during the probe trial has an interaction effect, where *E3* OVX+estradiol mice found the platform quickest, suggesting improvements in memory and learning. Swimming distance and velocity were higher in *E4* mice compared to *E3* mice. One previous study in 16-mo old mice reported that *E4* females perform worse on the Morris water maze probe trial than *E3* females. This previous study, however, did not account for sex hormone status, and contrary to our findings, reported no differences between groups for swimming speed (303). Overall, other variables like age or additional genotype stressors in tandem with *E4* may be necessary to observe declines in memory and learning.

Limitations

Although this study was rigorously designed, there are some limitations that should be noted. The first major limitation is the absence of a vehicle control group. The vehicle control would ensure that any changes we saw were due to estradiol and not a result of the implantation surgery. However, the implantation surgeries were approximately 5-10 minutes, and mice with implants showed no additional signs of stress or behavior deficits. The second limitation of our study is regarding the normalization of the Oroboros outcomes by tissue mass. The mass of the cerebral vessels was measured as accurately as possible, but given the small size, there is likely some error. As such, we also computed the Oroboros outcomes normalized to nDNA and leak and saw similar patterns of group differences regardless of the normalization protocol (data not shown). Third, we did not measure testosterone or aromatase; thus, we do not know the impact of these on our outcomes. Fourth, we did not measure superoxide or antioxidants directly, which are likely important mechanisms for the group differences we see. Fifth, the *APOE* mice are on a C57BL/6 background strain, and recent studies indicate that other strains, particularly ones that are more genetically diverse, are better for studies of Alzheimer's disease-related outcomes. Lastly, mice lack the cholesterol ester transfer protein (CETP) gene. CETP exchanges cholesterol and triglycerides between lipoproteins, and the absence of this gene in mice results in them carrying the majority of their lipid cargo in HDL rather than atherogenic LDL particles. Thus, future studies investigating ApoE or lipids in mice should be done in the presence of CETP in efforts to increase the translation to humans.

4.5 Conclusion

Overall, our results indicate that *APOE* genotype modulates the impact of estrogen on the cerebrovasculature. We found that 17β-estradiol enhances cerebrovascular function and mitochondrial function in *E3* mice but not *E4* mice. The results suggest that estradiol

supplementation may have a more therapeutic benefit for *E4* non-carriers. Further research should delve into the mechanisms by which *E4* is resistant to estradiol supplementation to help improve our understanding of disease progression and help generate better therapeutic targets.

Table 4.1. Animal Characteristics

	E3 Sham	E3 OVX	E3 estradiol	E4 Sham	E4 OVX	E4 estradiol
n	16	16	18	12	16	12
Age (months)	6.7 ± 0.5	6.7 ± 0.4	6.6 ± 0.5	6.6 ± 0.7	6.8 ± 0.7	6.7 ± 0.7
Body mass (g)[b]	23.6 ± 3.2	26.0 ± 4.5	24.3 ± 2.0	27.0 ± 4.9	29 ± 5.2*‡	27.8 ± 5.6
Heart mass (mg)	0.11 ± 0.01	0.12 ± 0.01	0.12 ± 0.02	0.13 ± 0.02	0.12 ± 0.02	0.12 ± 0.01
Percent heart: body mass	0.5 ± 0.07	0.5 ± 0.1	0.5 ± 0.1	0.49 ± 0.08	0.42 ± 0.02	0.45 ± 0.09
Liver mass (g)[a]	2.1 ± 0.3	2.2 ± 0.4	2.4 ± 0.4	2.1 ± 0.4	2.3 ± 0.4	2.5 ± 0.4
Percent liver: body mass [a,b]	9.0 ± 1.6	8.6 ± 2.0	10.1 ± 1.8	7.7 ± 1.1‡	8.1 ± 1.5‡	9.2 ± 2.1
Spleen mass (g)[a]	0.13 ± 0.02	0.14 ± 0.03	0.17 ± 0.1	0.11 ± 0.01‡	0.14 ± 0.04	0.16 ± 0.04#
Percent spleen: body mass	0.46 ± 0.3	0.6 ± 0.2	0.56 ± 0.2	0.42 ± 0.07	0.5 ± 0.2	0.61 ± 0.3
WAT mass (g)[a,b]	0.45 ± 0.3	0.86 ± 0.5	0.37 ± 0.2	0.85 ± 0.7	1.4 ± 0.8*‡	0.9 ± 0.7
Percent WAT: body mass[a,b]	1.8 ± 1.1	3.1 ± 1.4	1.5 ± 0.7	3.0 ± 1.8	4.4 ± 2.2*‡	2.8 ± 1.9$
Gastroc mass (g)[b]	0.15 ± 0.03	0.14 ± 0.04	0.13 ± 0.04	0.16 ± 0.03	0.16 ± 0.04	0.16 ± 0.04
Percent gastroc: body mass	0.64 ± 0.07	0.56 ± 0.1	0.55 ± 0.1	0.8 ± 0.6	0.56 ± 0.1	0.58 ± 0.1
Soleus mass (g)	0.01 ± 0.002	0.01 ± 0.002	0.008 ± 0.002	0.02 ± 0.02	0.02 ± 0.03	0.01 ± 0.004
Percent soleus: body mass	0.04 ± 0.007	0.04 ± 0.007	0.03 ± 0.008	0.07 ± 0.07	0.05 ± 0.07	0.03 ± 0.01
Uterus mass (g) [a]	0.10 ± 0.04	0.03 ± 0.04	0.09 ± 0.08	0.08 ± 0.04	0.03 ± 0.02	0.16 ± 0.2†$
Percent uterus mass: body weight [a]	0.40 ± 0.1	0.13 ± 0.2	0.37 ± 0.3	0.3 ± 0.1	0.11 ± 0.09	0.5 ± 0.6
17β-estradiol (ng/mL)[a, c]	0.0040 ± 0.0020	0.0009 ± 0.0003*	0.0007 ± 0.0007*	0.0015 ± 0.0020	0.0006 ± 0.0003*	0.0025 ± 0.0020
Esterone (ng/mL)	0.0010 ± 0.0003	0.0009 ± 0.0003	0.0008 ± 0.0002	0.0007 ± 0.0002	0.0010 ± 0.0020	0.0020 ± 0.0010
E2/E1 ratio	3.6 ± 1.5	1.4 ± 0.6	1.6 ± 0.8	3.3 ± 0.7	1.1 ± 0.05	4.4 ± 3.3
Progesterone (ng/mL)[a]	2.0 ± 1.9	1.6 ± 0.8	1.2 ± 0.5	2.9 ± 1.3	1.2 ± 0.5	1.3 ± 0.8
Total cholesterol (μM)[a]	3897 ± 814	4063 ± 615	5233 ± 1103	4442 ± 1152	5027 ± 1524	5685 ± 1317

Data are mean ± SD. WAT, white adipose tissue. [a] $p<0.05$ main effect of estrogen, [b] $p<0.05$ main effect of genotype, [c] $p<0.05$ interaction effect, * $p<0.05$ vs E3 sham, † $p<0.05$ vs. E3 ovx, ‡ $p<0.05$ vs. E3 estradiol, # $p<0.05$ vs E4 sham, $ $p<0.05$ vs E4 ovx

V. THE EFFECT OF AGE AND *APOE* GENOTYPE ON COGNITION, VASCULAR FUNCTION, AND CEREBRAL BLOOD FLOW

5.1 Introduction

Age remains the greatest risk factor for developing Alzheimer's disease (AD). Between 2015 and 2030, the number of people in the world over 60 years of age is projected to grow by 56% and by 2050 the global aged population is projected to more than double (304). During aging, cellular dysfunction leads to metabolic dysregulation, cholesterol dyshomeostasis, vascular stiffness, depression, memory and cognition complaints, all linked to neurodegenerative diseases later in life (265, 305–309). While aging and neurodegenerative disease are multidimensional, a focus on genetic predispositions related to AD has emerged as a main target to understand AD pathology and discover potential therapeutics.

The *APOE* gene is a longevity gene, and its *E4* variant raises risk for the development of AD compared to the most prevalent variant *E3* (113). Although AD is typically characterized by the presence of amyloid beta (Aβ) and hyperphosphorylated tau, it is now clear that vascular and metabolic impairments contribute to the disease (3). The *E4* variant accelerates Aβ and tau tangle deposition (310, 311). It also accelerates blood brain barrier (BBB) break down (126) by degenerating brain capillary pericytes (312), and reduces cerebral blood flow (CBF) (313, 314). The BBB interfaces cerebral vascular health and brain function. The interface is composed largely of endothelial cells, microglia, and astrocytes. In the presence of pathology, an oxidative and inflammatory environment exists, and augments endothelial cell dysfunction, BBB disruption. While small vessel disease and cognitive function have been investigated (315, 316), the upstream resistance arteries, like the posterior cerebral artery (PCA), remain largely uninvestigated.

Current literature on *E4* is missing a big piece of the puzzle by only including young mice in their investigations, leaving it a mystery to the physiology that occurs in these mice with age. Previously our lab revealed that 24-month-old Bl-C57 mice have greater cerebral endothelial dysfunction and vascular stiffness compared to young mice (233). Additionally, these mice also displayed greater cognitive deficits (233). These studies in 24-month-old mice are necessary for determining how natural aging contributes to vascular dysfunction and cognitive decline. We know that *E4* plays prominent roles in promoting oxidative stress and inflammation (110, 317), however, could *E4* be exacerbating the effect of aging, contributing to further vascular dysfunction and great cognitive decline?

Thus, the purpose of this study was to investigate the interaction of aging and *APOE* genotype on cerebral vascular function and cognition. We hypothesized that old mice would have greater cognitive deficits, worse motor function and instinctual behavior than their young counterparts, and that old *E4* mice would display greater cognitive dysfunction than the old *E3* group. Additionally, we hypothesized that old mice would have poorer endothelial function and greater vascular stiffness than their young counterparts, again being exacerbated in the old *E4* animals. We hypothesized that old *E4* mice would also have lower CBF measured by MRI compared with old *E3* mice. Lastly, due to altered metabolism with age, we hypothesized that the old *APOE* mice would have a lower RER than the young mice, and *E4* mice would have a higher RER than the old *E3's* due to insufficient fat utilization.

5.2 Methods

Animals

We purchased *E3* (JAX#029018) and *E4* (JAX#027894) mice from The Jackson Laboratories to establish a breeding colony. We studied male and female homozygous *E3* and *E4*

mice. Young mice were studied at ~6 to 7 mo of age, and old mice were studied ~24 mo. Please see table 1 for animal characteristics. Mice were fed a standard chow diet (Lab Diet, PicoLab Rodent Diet 20, 5053). Food and water were provided ad libitum, and mice were housed on a 12/12-hour light-dark cycle at 24°C. Mice were euthanized by exsanguination under isoflurane immediately prior to vascular studies. All animal procedures conform with the Guide for the Car and Use of Laboratory Animals (8^{th} edition revised 2011) and were approved by the Institutional Animal Care and Use Committee at the University of Oregon.

Vascular Reactivity

Endothelium-dependent vasodilation was assessed in ex vivo isolated pressurized PCAs, as described in detail previously (231, 279). Arteries were excised and cannulated onto glass micropipettes in a myograph chamber (Danish MyoTechnology Inc.) filled with a physiological salt solution. All the arteries were pre-constricted with phenylephrine (1-6 μM) to obtain 20-40% pre-constriction of starting luminal diameter. Increases in luminal diameter in response to increasing concentrations of endothelium-dependent dilators acetylcholine (ACh: 1x10-9 to 1x10-4 M) and insulin (1 to 10000 ng/mL) were determined. After ACh and insulin responses, arteries were incubated for 30 minutes with 0.1 mM of N omega-Nitro-L-arginine methyl ester hydrochloride (L-NAME). ACh and insulin responses were repeated in the presence of LNAME to determine the contribution of NOS to endothelium-dependent dilation. Endothelial constriction responses were performed in response to potassium chloride (KCl: 10-80M) and endothelin-1 (ET1: 1x10-11 to 1x10-7), where decreases in luminal diameter were measured. Endothelium-independent dilation was measured by the increases in luminal diameter to sodium nitroprusside (SNP) (1x10-10 to 1x10-4 M).

MRI

Cerebral perfusion was collected in anesthetized (10mg/mL Ketamine 1mg/mL xylazine) mice by arterial spin-labeled MRI under basal (100% O2) and hypercapnic (95%/5% O2/CO2) conditions in an 11.75T BrukerBiospin Animal MRI system. Perfusion data was analyzed using Paravision 6 (Bruker) and Jim 9 MRI analysis software (Xinapse Systems). Cerebrovascular reactivity (CVR) was calculated as the percent increase in perfusion with hypercapnia.

Passive Stiffness

Passive arterial stiffness was measured ex vivo in the PCA's and carotid arteries by the changes to lumen diameter and medial wall thickness in response to increasing intraluminal pressure (232). Passive stiffness was measured following a 60-minute incubation of calcium free solution to eliminate myogenic tone. Measurements were recorded in 5 cmH2O increments from 5 to 100 cmH2O (3.7-73.5mmHg). From these data, stress-strain curves, Beta-stiffness, and elastic modulus were calculated as previously described (233).

Aortic Stiffness

Aortic stiffness was measured in vivo by pulse wave velocity (PWV) (279). Mice were anesthetized using isoflurane (2% isoflurane in 100% oxygen) and placed supine on a temperature-controlled heating pad (37°C). Electrodes were placed on distal portions of limbs that record ECG, while two Doppler transducers were positioned on the aortic arch and abdominal aorta. The distance between the transducers was recorded. Using the Doppler signal processing workstation program (DSPW; Indus Industries, Webster, TX, USA), the time of a pulse to travel from the arch to the abdominal aorta was analyzed, and the time was then divided by the distance between the transducers. Two researchers analyzed the files independently, and the average was taken. Young female mice's estrous stage was noted at the time of PWV measure (230).

Instinctual behavior

Nest building is a test of instinctual behavior and was performed over a 12-hour period. Mice were singly housed overnight in a fresh cage containing a condensed cotton nestlet. The following morning, the researcher scored the nests. The same researcher scored all nests. The intrapersonal coefficient of variation in our laboratory is 0% for this test. Nests were scored on a scale of 0-5 with the following criteria: 0- nestlet is untouched; 1- nestlet has been moved but no significant tearing; 2- significant tearing, but no formation of a nest; 3- significant tearing, indication of nest OR nest is in the corner of the cage; 4- significant tearing, formation of nest in the corner; 5- significant tearing, formation of nest in corner and the nest walls are high making a bowl like nest (159).

Motor Coordination

Motor coordination testing was performed using a rotarod (47650 Rota-Rod NG, Ugo Basile, Gemonio, Italy) over a two-day period. The first day was a training session, mice were required to stay on the rod rotating at 4 rpm for 90 seconds. The second day consisted of three trials, with a 10-minute rest between trials, where the rod accelerated during each trial from 4 to 40 rpm with a cut-off time at 5 minutes. The time was recorded for when the mouse fell from the rod or rotated around the rod two consecutive times (318).

Frailty

Mouse frailty was assessed using a previously studied 31-item FI based on established clinical signs of deterioration in C57BL/6J mice (319). FI assessments included evaluation of the integumentary, musculoskeletal, vestibulocochlear/auditory, ocular, nasal, digestive, urogenital, and respiratory systems as well as signs of discomfort, body weight, and body surface temperature. The severity of each deficit was assessed and assigned either a 0, 0.5, or 1, with the

higher score indicating more severe frailty. Each mouse was examined at approximately the same time in the day, following the same order of assessments. To calculate FRIGHT age and AFRAID score, we organized our data into the format of the Example_Frailty_Data.csv from the website: http://frailtyclocks.sinclairlab.org/ (320). For each mouse, we added age in days (age_days), body mass in grams (bw), the standard deviation of the body mass (bwSD), and scores for each deficit (between 0 and 1). As we did not measure the body mass at 21 months, we entered 0 for %twc and %rwc. We also did not collect vision loss data, and thus this score was entered as a 0 for all mice. We then uploaded the .csv file onto the above website and the outputs (Analyzed Data) are presented in this manuscript.

Cognitive function testing

Learning and spatial memory was assessed via Morris Water Maze. Mice underwent a 3-day training period, where they performed 3 trails every session, with 2 sessions per day. On the fourth day, a probe trial was performed in the morning, where the mice swam for 60-seconds. Also, on the fourth day in the afternoon session the beacon trial was preformed, where the platform was marked and the time it took the mouse to get to the platform was acquired. All sessions were analyzed and recorded on EthoVision XT12 software (Noldus, Wageningen, the Netherlands) (281).

Anxiety was measured via open field testing. Mice were placed in a $40cm^2$ square arena with a white matte floor and walls. Mice were in the arena for 10 minutes and their exploration was recorded using Ethovision XT12 software. The center of the 20x20 cm square was marked with software, and exploration criteria were defined as the amount of time the center of the mouse's body was inside the square area. Mice that spent more time exploring have lower levels of anxiety (281).

Indirect Calorimetry

Prior to *ex-vivo* studies mice were singly housed in an environmental cabinet for 5 days. Using metabolic cages (Promethion, Sable Systems, Las Vegas NV), we measured food and water intake, body weight, oxygen consumption (VO2), carbon dioxide production (VCO2), and water vapor during the 12:12-h light-dark cycles. Metascreen software (Sable Systems Inc.) was used for data collection. Data was then processed with ExpeData and Macro Interpreter (Sable Systems Inc.), analyzed on an hourly basis. VO2, VCO2 production, and expenditure (kcals/hour) were normalized to body weight (kg). The first 24 hours were excluded from data analysis for an acclimatization period.

Statistical analysis

Statistical analyses were performed with IBM SPSS (Version 26, Armonk, NY) and GraphPad Prism 10. A two-way analysis of variance (ANOVA) was used to determine the interaction effects and independent effects of age and genotype. In the case of a significant F-value, post-hoc analyses were performed using a Tukey correction for preplanned comparisons. An additional sub-analysis was performed separately for young mice and old mice by two-way ANOVA for the interaction of genotype and sex. A repeated measures ANOVA was used to determine group differences for dose responses. Significance was set at $p<0.05$, and values are represented as mean ± SD. Outliers were identified as a z score >2 and were removed from the data set.

5.3 Results

Animal Characteristics:

Old mice had significantly greater body mass, heart mass, spleen mass, and white adipose tissue (WAT) mass compared with the young groups, independent of *APOE* genotype ($p<0.05$;

table 5.1). Liver, gastrocnemius, and soleus weights did not differ among groups. None of the animal characteristics revealed an effect of *APOE* genotype, suggesting aging effects on animal characteristics are independent of *APOE* genotype.

Cerebral artery endothelial dilation is dependent on age but not APOE genotype

The PCAs from old mice had impaired endothelium-dependent dilation to ACh (main effect of age, $p<0.0001$, Figure 5.1A and B) and insulin (main effect of insulin, $p<0.001$, Figure 5.1E and F) compared to the young groups, but there was no main effect of *APOE* genotype ($p>0.05$). Specifically, old *E3* had ~7% less dilation to ACh (max: $p=0.2$, dose-response: $p<0.0001$)(Figure 5.1A and B), and ~13% less dilation to insulin (max: $p=0.005$, dose-response: $p<0.0001$)(Figure 5.1F and E) compared with young *E3* mice. Old *E4* mice had ~16% less dilation to ACh (max: $p=0.0004$, dose-response: $p<0.0001$)(Figure 5.1A and B) and ~12% lower dilation to insulin (max: $p=0.01$, dose-response: $p<0.0001$)(Figure 5.1E and F) compared with young *E4* mice. Interestingly, a sub-analysis for sex revealed that young female mice have better EDD to ACh (max: $p=0.0007$) (Figure 5.1C) and a trend to better insulin response (max $p=0.07$)(Figure 5.1G) compared to their young male counterparts, but there was no main effect of *APOE* genotype ($p>0.05$). Interestingly though, despite the sex difference observed in the young mice, no sex differences were observed in the old mice to ACh or insulin (maximal and dose-responses all $p>0.05$)(Figures 5.1D and H). All dilation seen in response to increasing doses of ACh and insulin, was mediated by nitric oxide, as indicated by the little to no dilation in the presence of NO inhibitor, LNAME. Specifically, with LNAME present, there were no differences between groups for ACh- or insulin-mediated dilation (dose-response and maximal responses, all $p>0.05$)(Figures 5.1A and E). Endothelium-independent dilation was not different between groups (dose-response and maximal responses, all $p>0.05$)(Figures 5.1 I), indicating

that the differences in vasodilation were due to endothelial cell impairment in old animals, regardless of their genotype. Sensitivity (EC50) to vasodilators did not differ per group (all p>0.05, Table 5.2). Lastly, the amount of preconstriction did not differ per group (all p>0.05, Table 5.2).

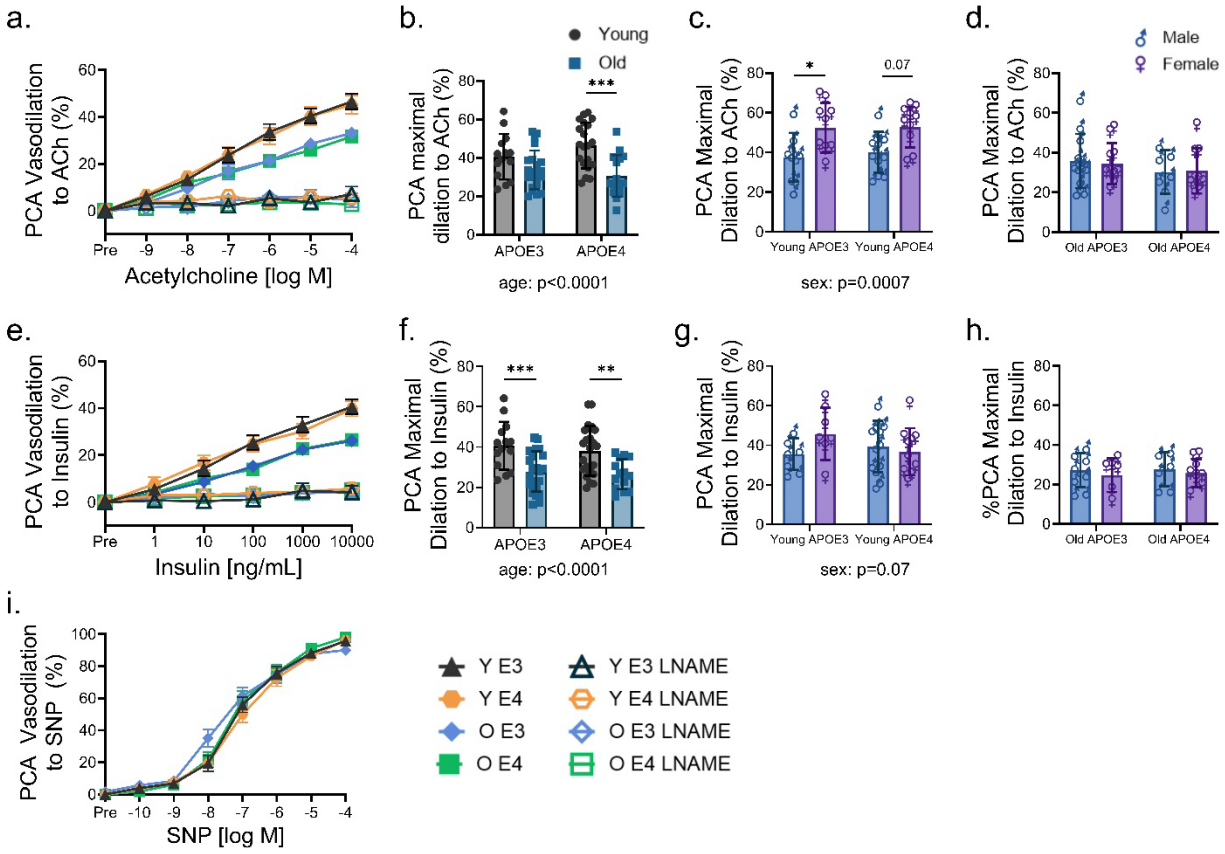

Figure 5.1. Cerebral artery endothelial function is impaired with old age, and greater in young females compared to young males, both not affected by *APOE* genotype. Young and Old homozygous *E3* and *E4* mice were studied at 6 mo and 24 mo. In isolated posterior cerebral arteries (PCAs), endothelium-dependent dilation was measured to a) increasing doses of acetylcholine (ACh) in the presence and absence of nitric oxide inhibitor, LNAME b) age x *APOE* genotype, c) in young mice, sex x *APOE* genotype and d) in old mice, sex x *APOE* genotype. E) Endothelium-dependent dilation to increasing doses of insulin, in the presence and absence of LNAME. Max dilations f) age x *APOE* genotype, g) in young mice, sex x *APOE* genotype and, h) in old mice, sex x *APOE*. i) Endothelium-independent dilation in response to increasing doses to SNP. A repeated measures ANOVA for the dose responses and a two-way ANOVA for the maximal responses was used to determine independent and interaction effects, and a Tukey's post-hoc analysis was performed.*p<0.05, **p<0.01, ***p<0.001. n=12-22/group, data are mean ± SEM.

Cerebral artery constriction is dependent on age and APOE genotype

PCA's from old mice had less constriction to KCl, however this was dependent on *APOE* genotype (interaction effect: p=0.001, age effect: p<0.0001)(Figure 5.2A and B). Old *E3* mice constricted 33% less to KCl when compared to the *E3* young cohort (max: p<0.0001, dose-response: p=0.0002)(Figure 5.2A and B). Old *E4* mice to their young *E4* counterparts had no differences (max: p=0.8, dose-response: p=0.02)(Figure 5.2A and B). Young *E4* mice constricted about 18% less to KCl than their young *E3* counterparts (max: p=0.009, dose-response: p=0.02)(Figure V.2A and B). Old *E3* mice trended toward less constriction than the old *E4* mice (max constriction, p=0.08) (Figure 5.2D). In a sub-analysis for sex there was a main effect of genotype in the young mice (p=0.004), in the young mice, KCl constriction was lower in the *E4* male mice compared to young *E3* males (max p=0.01)(Figure 5.2C).

Regarding constriction to ET1 in PCA's, there was an interaction effect between *APOE* genotype and age, and a main effect of age (interaction: p=0.02, age: p=0,03)(Figure 5.2F). ET1 constriction was 18% less in old *E3* mice compared to young *E3* mice (max: p=0.009, dose-response: p=0.001)(Figure 5.2G and F). Old *E4* mice did not differ in constriction when compared to young *E4* mice (maximal and dose response all p>0.05)(Figure 5.2E and F). In the sub-analysis for sex differences, there was a main effect of sex in the young cohort, where young females had greater ET1 constriction compared to young males (p=0.003)(Figure 5.2G). Specifically, young female *E4* mice had 25% greater constriction than young *E4* males (p=0.02)(Figure 5.2G). However, in the old mice, no sex differences were seen, but there was a trend for a genotype effect where maximal ET1 constriction in the old *E4's* was greater than that of the old *E3's* (p=0.08)(Figure 5.2H). These constriction results suggest that *E4* mice maintain responsiveness to vasoconstrictors in old age.

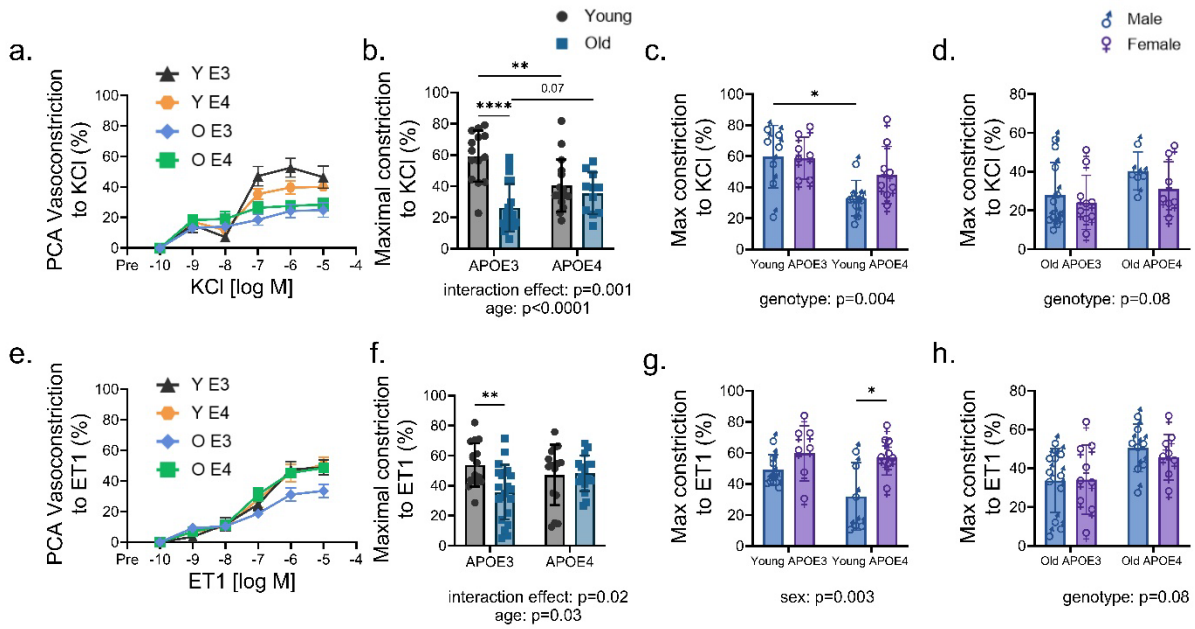

Figure 5.2. Posterior cerebral artery (PCA) responsiveness to constrictors is maintained with age in *APOE E4* mice but diminishes with age in *APOE E3* mice. In isolated posterior cerebral arteries (PCAs), the constriction response to a) potassium chloride (KCl) was measured. b) Maximal constriction to KCl for age x *APOE* genotype, c) in young mice, sex x *APOE* genotype and, d) in old mice sex x *APOE* genotype. E) PCA vasoconstriction to endothelin-1 (ET1) was also measured. Maximal constriction to ET-1 for f) age x *APOE* genotype, g) young mice for sex x *APOE* genotype, and h) old mice for sex x *APOE* genotype. *APOE* genotype and age interact to maintain constriction in old *E4* animals in response to KCl and ET1. A repeated measures ANOVA of dose responses and a two-way ANOVA with Tukey's multiple comparisons was used to determine independent and interaction effects of age and genotype. A sub-analysis using a two-way ANOVA to determine the effect of sex differences and *APOE* genotype on constriction responses.*p<0.05, **p<0.01, ****p<0.0001. n= 14-20/group, data are mean ± SEM

Cerebral vascular reactivity is better in old female mice

Cerebral perfusion was measured via arterial spin labeling MRI in a subset of old mice. There was a non-significant trend in the interaction effect of *E4* genotype and female sex in lowering resting cerebral perfusion in the whole brain, hippocampus, cortex and thalamus (all p>0.05)(Figure 5.3C, F, I, & L). Cerebral perfusion was measured during hypercapnia, which revealed similar trends as the resting state (p>0.05, Figure 5.3 D, G, J, & M). The percent change was calculated from resting to hypercapnic, a measure of cerebrovascular reactivity. Females had greater reactivity in the whole brain (p=0.02), hippocampus (p=0.05), and cortex (p=0.04)(Figure

5.3 E, H, K, & N), but there was no effect of *APOE* genotype (p>0.05). Thus, despite the old *E4* females trending to lower resting cerebral perfusion, they maintained CVR.

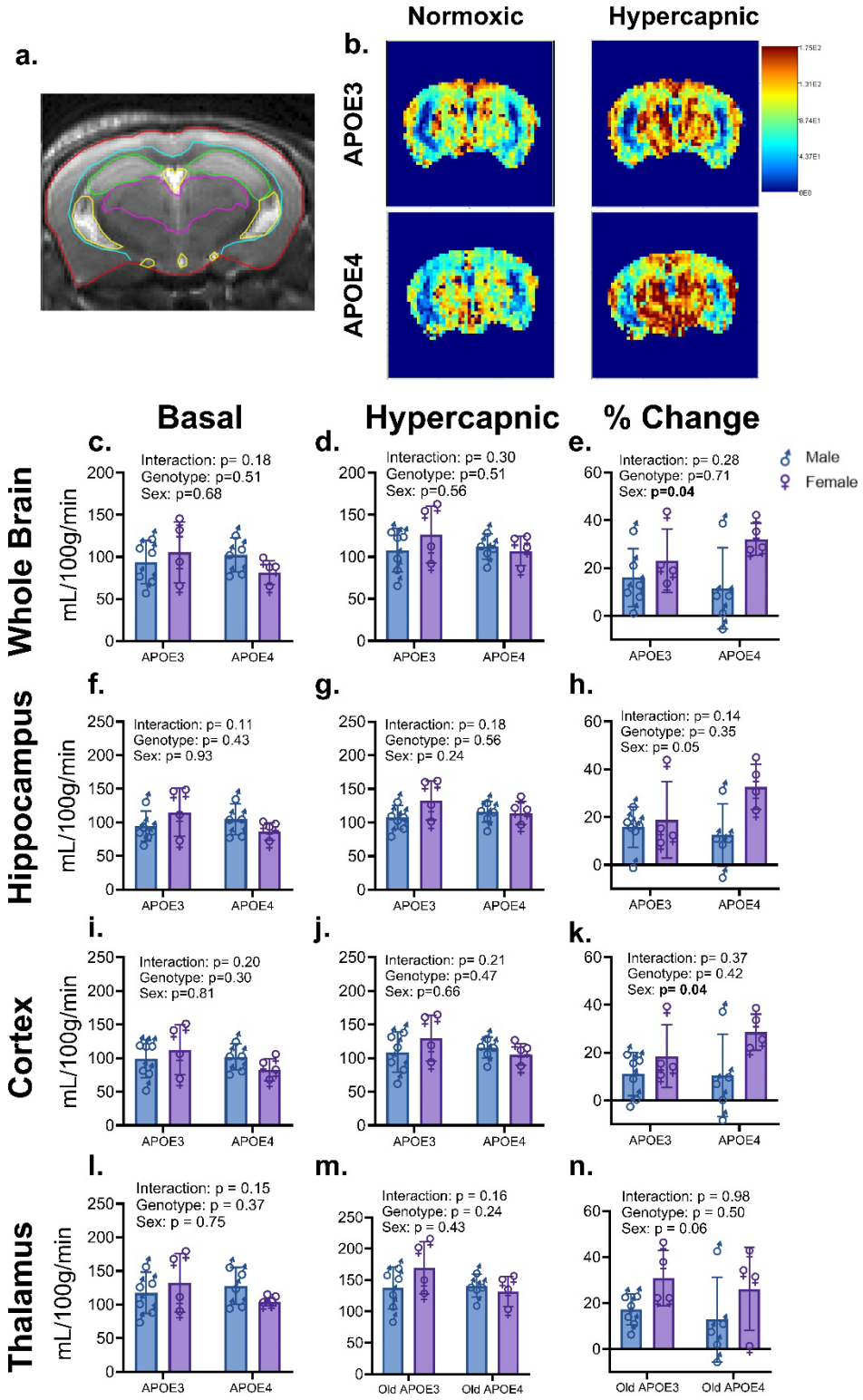

Figure 5.3. Cerebral vascular reactivity is better in old female mice. a) Regions of interest were drawn for the whole brain, hippocampus, cortex, and thalamus. b) Representative CBF images. Whole brain CBF was measured in c) normoxic conditions, d) hypercapnia, and e) % CVR was calculated. This was repeated for the (f-h) hippocampus, (i-k) cortex and (l-n) thalamus. A two-way ANOVA was used to determine main and interaction effects of sex and genotype on CBF in normal, hypercapnia, and %CVR. measures.*p<0.05. n=4-6/group, data are mean ± SEM.

Cerebral artery stiffness and large artery stiffness are influenced by age

PCA and common carotid arteries were studied for passive stiffness *ex vivo*. PCA β stiffness was greater with age (p<0.0001). Old *E3* mice have greater PCA β stiffness than their young counterparts (p=0.05), and old *E4* mice have greater PCA β stiffness than the *E4* young (p<0.0001)(Figure 5.4A). There were no sex differences among young mice (all β stiffness p>0.05), however old mice had an interaction of *APOE* genotype and sex on PCA β stiffness (p=0.04)(Figure 5.4C). Lastly, PCA elastic modulus at low pressure had a main effect of age (p=0.01)(Figure 5.4D). No differences were seen in carotid artery β stiffness or in elastic modulus at low or high pressure (all p>0.05)(Figure 5.5A-F). Large artery stiffness, measured by

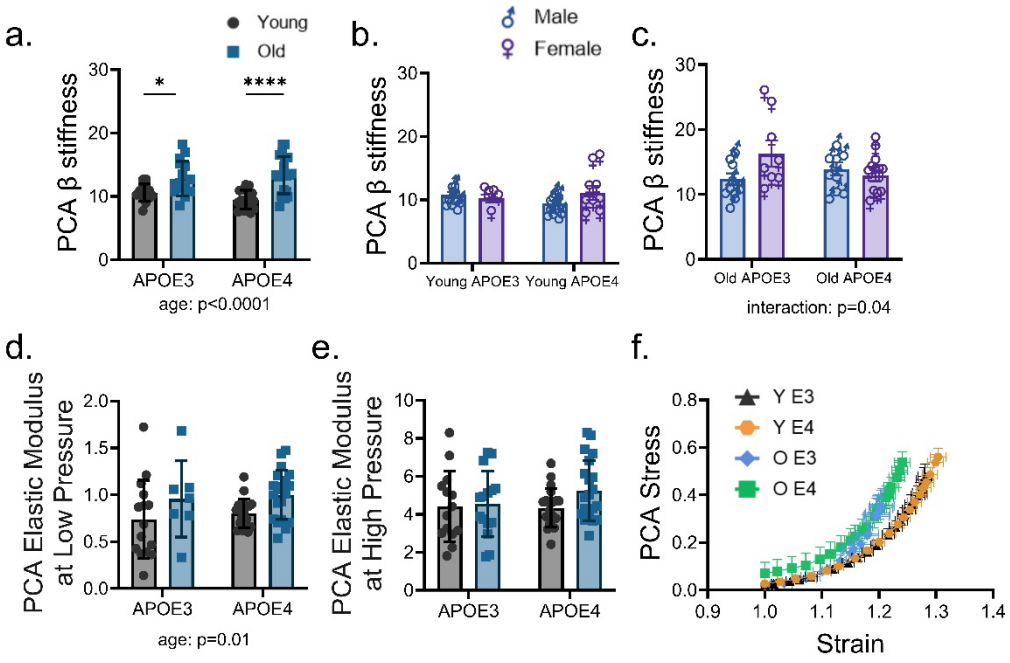

Figure 5.4. Posterior cerebral artery stiffness is elevated with age but is not affected by *APOE* genotype. In posterior cerebral arteries incubated in a calcium-free solution, a passive response to determine the structural components on the artery was performed, generating a f) stress strain curve. From this curve, β -stiffness and elastic modulus were calculated. a) PCA β-stiffness was elevated in old mice, but no genotype effect was seen. b) PCA β-stiffness did not differ by sex in young mice, but c) in old mice there was an interaction effect of age and sex. Elastic modulus d) at low pressure was higher in old mice, however no differences at e) high pressure were seen. A two-way ANOVA was used to determine main and interaction effects of age and genotype on PCA β-stiffness. A sub-analysis using a two-way ANOVA was used

aortic pulse wave velocity, was elevated with age (p=0.001)(Figure 5.6A), but there was no main effect of genotype.

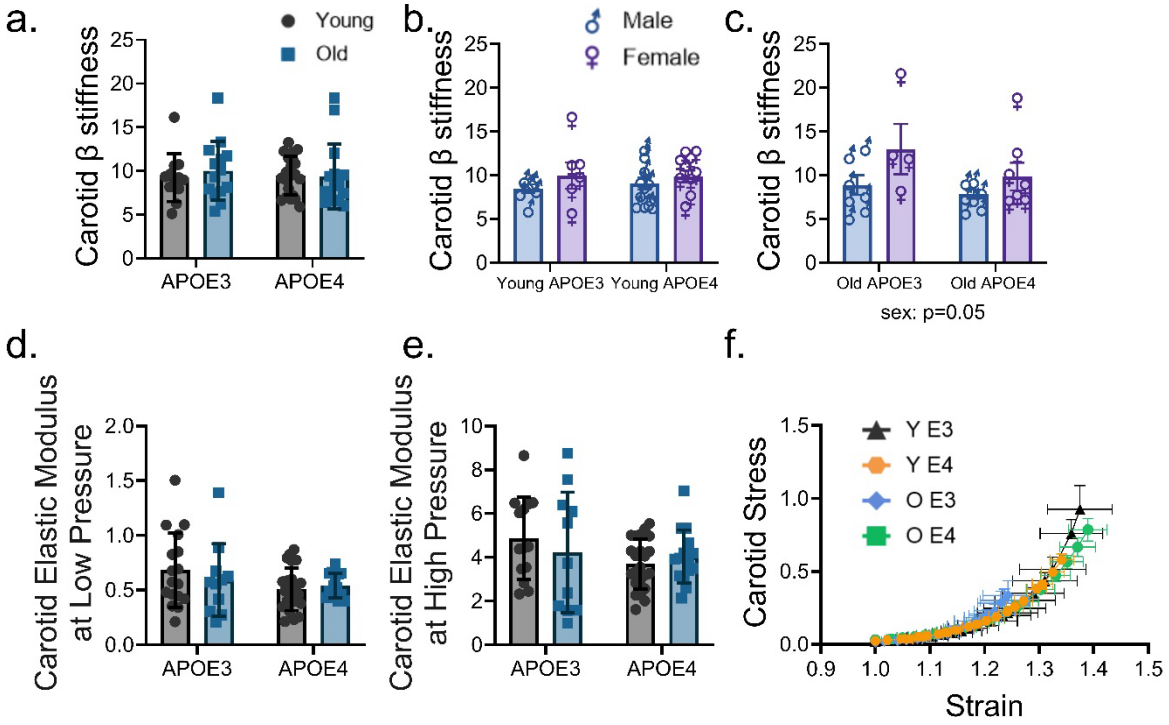

Figure 5.5. Carotid artery stiffness is not affected by age or *APOE* genotype. Carotid arteries were incubated in a calcium free solution, and a passive response was performed. A f) stress strain curve was generated in which to calculate β-stiffness and elastic modulus. a) Carotid β-stiffness was not different between groups. b) Carotid β-stiffness did not differ by sex in young mice, but c) old mice had a interaction effect of age and sex. Elastic modulus d) at low pressure and e) high pressure were not different between groups. A two-way ANOVA was used to determine independent and interaction effects of age and genotype on Carotid β-stiffness. A sub-analysis using a two-way ANOVA was used to determine the effect of sex and *APOE* genotype on carotid stiffness measures.*p<0.05. n=10-18/group, data are mean ± SEM.

Instinctual behavior, and motor coordination are impacted by age but not APOE genotype

Instinctual behavior, a measure of cognitive function, measured by nest building, was lower with age (p<0.0001), but again there was no main effect of *APOE* genotype (Figure 5.6B). Lastly, motor coordination, measured by rotarod, was lower with age (p=0.0002) (Figure 5.6C).

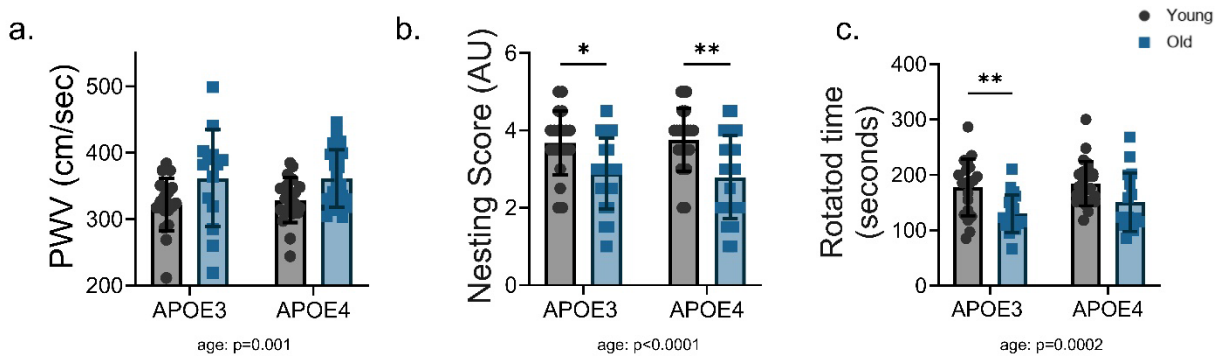

Figure 5.6. *In vivo* stiffness, instinctual behavior, and motor coordination worsen with age, but are not affected by *APOE* genotype. a) Aortic stiffness, measured by pulse wave velocity (PWV), is elevated with age. b) Instinctual behavior, determined by the score on a nest building task, and c) motor coordination, measured as the time spent on an accelerating rotarod, was worse in the old mice. Two-way ANOVA with Tukey's multiple comparison analysis. *p<0.05, **p<0.01. n=21-27/ group. Data are mean ± SEM.

Cognitive function is impaired with age

Morris water maze was used to assess learning and spatial memory. In training trials 5 (E3 p=0.002, E4 p=0.09)& 6 (E3 p=0.004, E4 p=0.2), the old mice took longer to locate the platform compared to their young cohorts (Figure 5.7C), but there was no main effect of *APOE* genotype (p>0.05). In the 60 second probe trial, analyzed for seconds 10 – 50, the young mice spent more time in the target quadrant than the other quadrants, where the old mice did not spend more time in the target quadrant (Figure 5.7E), indicating impaired memory in the old mice. For the beacon trial, there was an effect of age on the total distance moved, where old mice took longer to reach the platform than their young cohorts (p=0.03)(Figure 5.7K), with no main effect of *APOE* genotype (p>0.05). Latency to platform for the beacon trial was slowest in the old *E3* mice (p<0.0001). Lastly, in the training trials, probe trial, and beacon trial, old mice had a slower swimming velocity than their young counter parts (all p<0.05)(Figure 5.7D, H, J), indicating potential impairments in motor function with age, again with no main effect of *APOE* genotype.

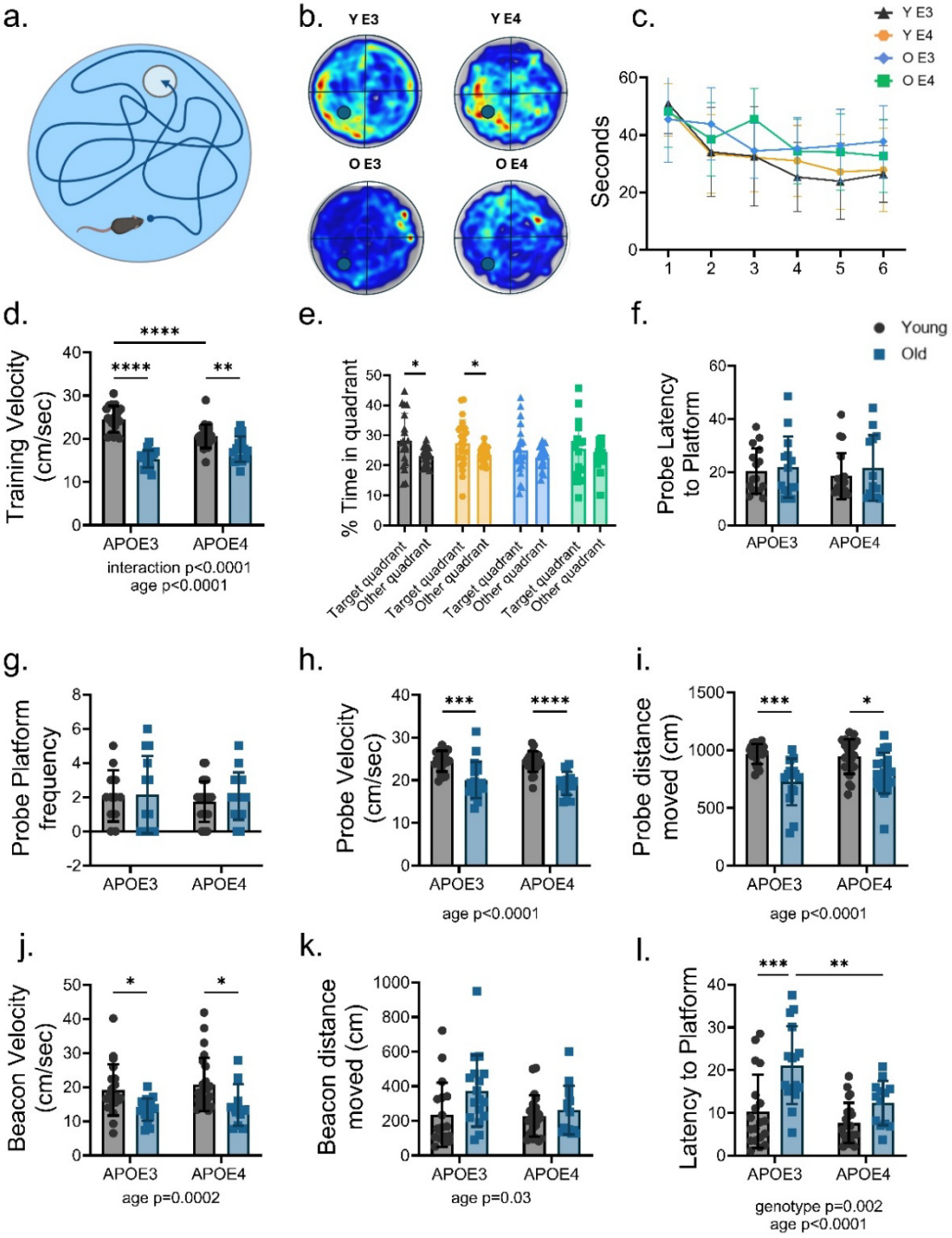

Figure 5.7. Learning and spatial memory is impaired with age but not *APOE* genotype. a) Schematic of morris water maze. b) Heat maps of morris water maze probe trials. c) Training trials were not different between any of the groups. d) Training velocity was lower in with age. e) The young cohorts spent more time in the target quadrant than the old group during the probe trial. f) Latency to platform and g) platform frequency was not different between groups. h) Probe velocity and i) probe distance moved was lower with age. j) Beacon velocity, k) distance moved, and l) latency to platform were all lower with age. Two way ANOVA was with Tukey's multiple comparison analysis was used to determine the effect of age and genotype. A repeated-measures ANOVA was used to determine the difference between training trials. A one tailed t-test was used to determine differences between target and other quadrants. .*p<0.05, **p<0.01, ****p<0.0001. n=16-22/group. Data are mean ± SEM.

Differences in swimming velocity and beacon performance are potential cofounders for the interpretation of the probe trial results.

With age increased anxiety is associated with cognitive decline in mice (321). Anxiety was measured by the open field test, where mice that spent more time exploring are assumed to have less anxiety. There was a main effect of age on time spent in the center of the quadrant, were time spent in the center was lower in the old mice, and there was no main effect of genotype (p=0.02)(Figure 5.8D). A sub-analysis of sex uncovered an interaction effect (p=0.01) in the old mice, where old *E4* male mice spent less time in the center compared to the *E4* females (p=0.01)(Figure 5.8F), however

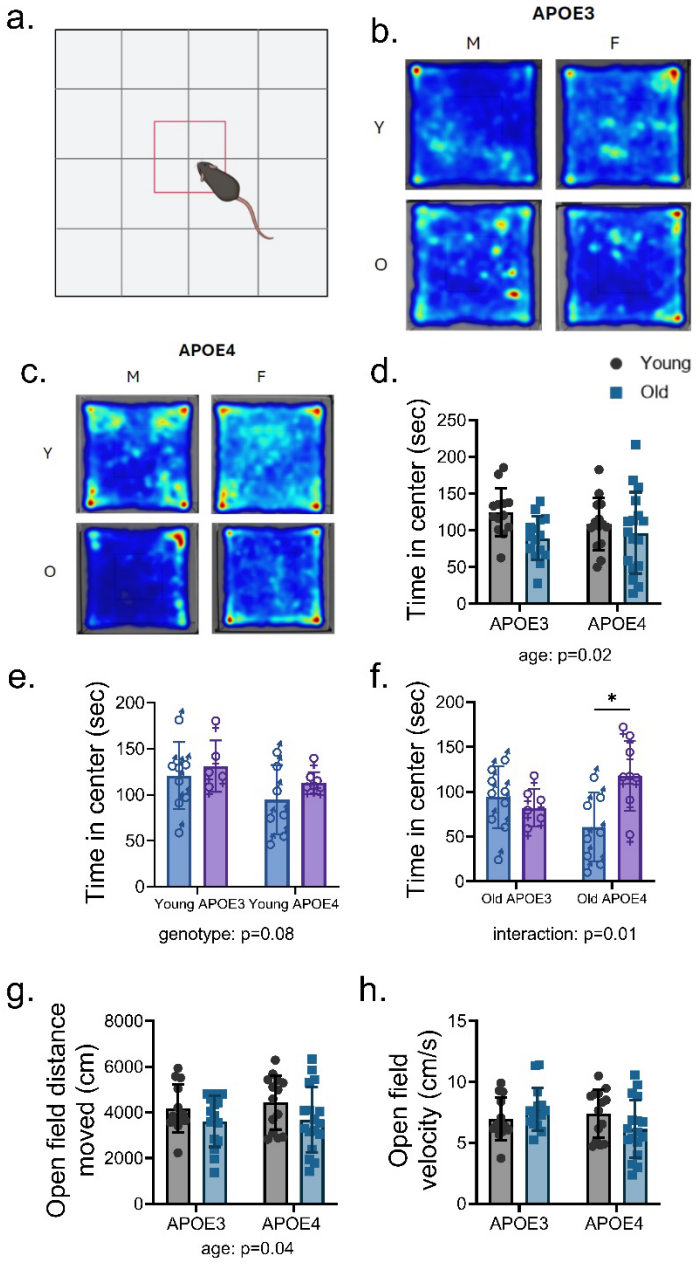

Figure 5.8. Anxiety was higher with age. a) A schematic of the open field test. Representative heat maps for b) young and c) old mice. d) Time spent in the center of the arena was lower with age. e) Young mice by sex on time spent in the center. f) Old mice by sex on time spent in the center of the arena. g) Open field distance moved and h) open field velocity. A two-way ANOVA was used to determine main and interaction effects of age and genotype on anxiety. A sub-analysis using a two-way ANOVA was used to determine the effect of sex and *APOE* genotype on anxiety.*p<0.05, **p<0.01, ****p<0.0001. n=16-22/group, data are mean ± SEM.

this was not seen in the *E3* mice. Lastly, the total distance moved was less in old mice (p=0.04)(Figure 5.8G), while there were no differences in velocity, indicating that old mice did not explore as much due to elevated levels of anxiety(Figure 5.8).

Indirect Calorimetry is altered by age

In vivo whole-body metabolism was measured in a subset of mice, via metabolic cages. Age influenced dark cycle VO2 uptake (p=0.02; Figure 5.9C), and total and dark cycle VCO2 production (p=0.0005, p=0.004; Figure 5.9D, F) in young mice, and there was no main effect of

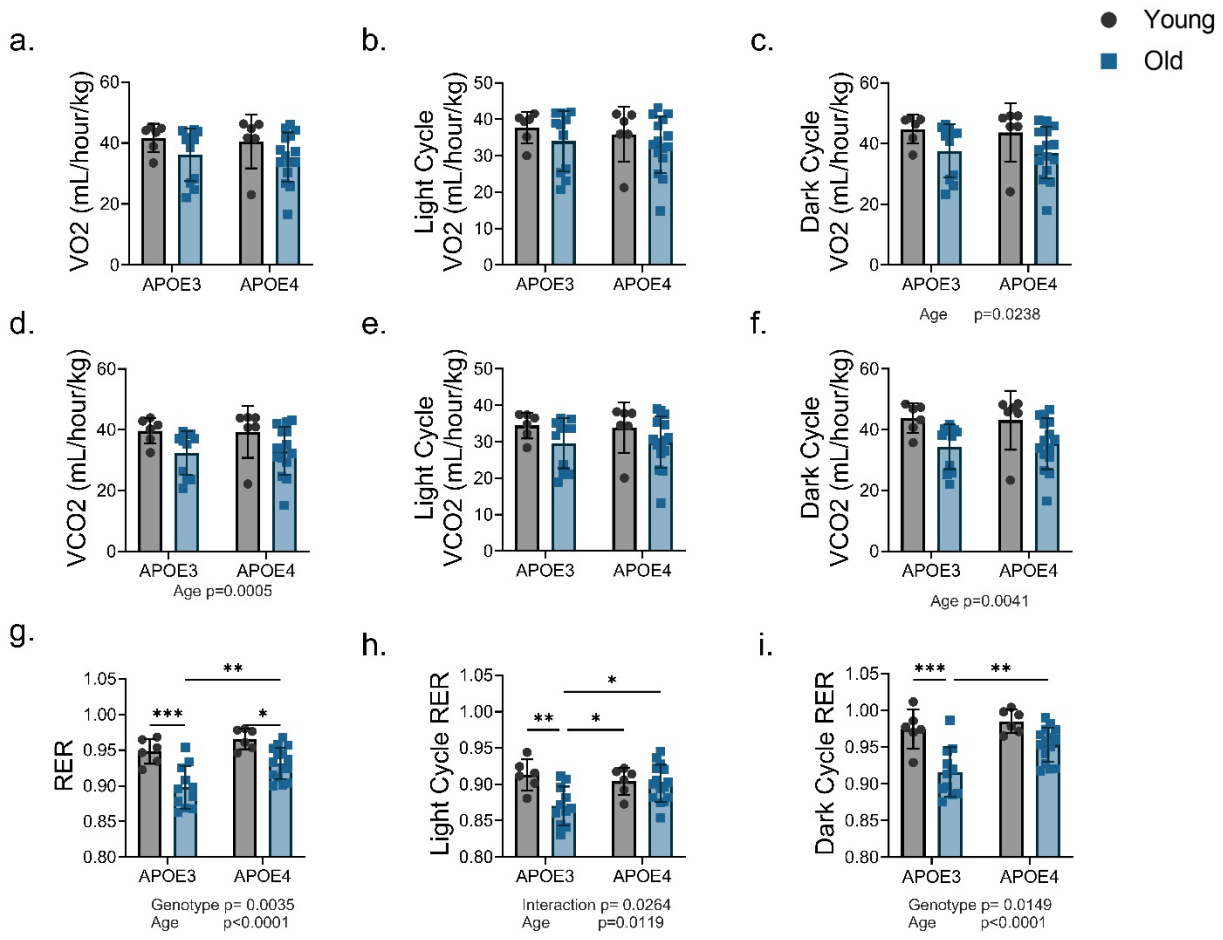

Figure 5.9. Age impacts oxygen consumption, and carbon dioxide production, while respiratory exchange ratio is influenced by age and *APOE* genotype. a-c) VO2 and d-f) VCO2 normalized to body weight in ml/hr/kg for young and aged *ε3* and *ε4* spanning a,d) total, b,e) light cycle, and c,f) dark cycles. g-i) Respiratory exchange ratio (RER) in young and aged *ε3* and *ε4* mice spanning g) total, f) light cycle, and i) dark cycle values. *p<0.05, **p<0.01, ***p<0.001. n=6-12/ group. Data are mean ± SEM.

genotype. Total RER, light cycle RER, and dark cycle RER were lower in old mice ($p<0.0001$, $p=0.01$, $p<0.0001$). Interestingly, the lowest RER was observed in the old *E3* mice compared to old *E4* mice for average, light, and dark cycle RER ($p=0.003$, 0.02, $p=0.01$; Figure 5.9G-H). Overall, our data suggests that *E4* mice had a higher RER than old *E3* mice. Thus, age and *APOE* genotype are important factors to consider in metabolic outcomes, especially in old mice.

5.4 Discussion

The major findings of this study are that age greatly influenced cerebrovascular function, arterial stiffness, cognition, and motor function. *APOE* genotype did not affect most outcomes in this study, apart from the cerebral artery vasoconstrictor responsiveness and cerebrovascular reactivity. PCA's from old mice constricted less to KCl and ET1, however this lower constriction was seen in the old *E3* mice, whereas old *E4* mice maintained their ability to constrict to these stimuli. Further, female *E4* mice trended towards lower cerebral perfusion compared with female *E3* mice, but old female *E4* mice preserved the capacity to respond to hypercapnia. These data also show that old female mice had greater cerebrovascular reactivity than their male counterparts. Lastly, RER was lower in old mice than young, and old *E4* mice had a higher RER than old *E3* mice, suggesting potential alterations in carbohydrate metabolism. The lack of an effect of *APOE* genotype on endothelial function, arterial stiffness, and cognitive function indicates that additional stressors may be necessary to elicit the previously seen negative effects of *E4* genotype with age (313).

Cerebrovascular dilation and constriction: The delicate dance of vascular homeostasis

In this study, age strikes again as a predominant disrupter of healthy vascular function. Previous studies have demonstrated oxidative stress and inflammation are the primary culprits in aging that disrupt vascular function. As this study and others have shown vasodilation knowingly

decreases with age, due to lower NO bioavailability. This is a consequence of elevated reactive oxygen species production (ROS), however we did not measure this in this study (322). The production of super oxide radicals can enhance eNOS uncoupling, and can also react with NO generating perioxynitrate, forming a reactive nitrogen species, reaping havoc on the vascular system (30). The elevation of ROS feeds into further ROS production and promotes inflammation, ultimately leading to endothelial cellular senescence (323). These are potential mechanisms for the lower EDD in the present study but need verified with further analysis. Age also influenced the stiffness of our PCA's, but no changes were observed in smooth muscle function, as indicated by our SNP results. Additional investigation into changes in the ECM could explain the changes in stiffness.

As we age, we have a reduced ability to vasoconstrict blood vessels effectively. In 24-month-old rats, coronary resistance arterioles to ET1 and KCl reactivity decreased compared to young rats (324). These are similar to our findings where there was a main effect of age for the response to ET1 and KCl in cerebral arteries. Previous literature also suggests that age reduces the expression of voltage Ca++-activated K+ channels in coronary arteries (324, 325), potentially explaining the decreased responsiveness seen in old mice. The lower ET1 constriction with as is potentially explained by receptor changes in ETA and ETB expression on VSMCs (326), however further testing on our samples would be needed to verify this. All the previously discussed changes occur with age but little to no investigation has been done on vasoconstriction and vasodilation responses with regards to *APOE* genotype, adding novelty to our study.

E4 genotype has previously demonstrated to elevate levels of inflammation and oxidative stress in cerebral vascular endothelial cells (100). Thus, we hypothesized the *E4* genotype would be associated with impaired endothelial function, but contrary to our hypothesis, we found no

effect of *APOE* genotype. However, our results indicated that old *E4* mice maintained constriction responsiveness with age, while the old *E3* mice did not. A potential explanation for our results is *E4* mediated alterations in lipid homeostasis. *E4* has prominent effects on lipid metabolism, often resulting in excess lipid accumulation, a result of poor lipid exportation(106). In VSMC's, this accumulation of lipids can lead to a phenotypic change, impacting contractile properties as seen in our results (327, 328). Another alternative is that lipid metabolism can increase oxidative stress and decrease NO, furthering ROS production, enhancing contractility (329). However, we saw no differences in NO mediated dilation between genotypes, and no dilation in the presence of NO inhibitor LNAME, suggesting that it is unlikely that *E4* is impacting oxidative stress and NO. Future testing for inflammatory markers is warranted, and further experiments should measure the expression of ETA vs ETB, and levels of ET1.

CBF and CVR: A story of age and sex

Human literature indicates that old *E4* females have lower CBF than old *E3* females (330, 331). Our data trends to lower resting CBF in old *E4* females compared to *E3* females. Despite having lower resting CBF though, the *E4* females, have better CVR than their old male counterparts. *E3* females also have better CVR than their old male group, suggesting old females independent of *APOE* genotype have better CVR with age. Potential explanations for females having preserved CVR could be related to more effective cerebral autoregulation (332). Additionally, a role for androgens in cerebrovascular function has been proposed, suggesting that androgens may be negating proper CVR. A study in male rats showed that castration increases vasodilation in middle cerebral arteries (333). Thus, additional investigations are needed to tease apart the mechanisms for the lower basal perfusion with *E4* and greater CVR in females.

Cognitive Function

Contrary to our hypothesis and previous literature (301), the *E4* genotype did not worsen cognitive function. A meta-analysis of cognitively healthy older adults indicates that *E4* carriers have worse cognitive performance than non-carriers, with larger differences emerging in old age (301, 334). A more recent meta-analysis shares that *E4*-knock-in mice, in an otherwise healthy brain condition, are endowed with some cognitive deficits irrespective of sex or age, dependent on experimental test condition (301). Conflicting our findings, one study in *E4* mice treated with an RXR agonist (which is responsible for expression of ABCA1 and apoE), had improved memory compared to *E4* mice not treated with the agonist. Also, control *E4* animals had a greater impairment in cognition measured by water maze and novel object when compared to *E4* animals treated with an RXR agonist (335). One future avenue to investigate the swim pattern of all the mice, which may indicate more floating or more slowing down to orient themselves to compensate for a reduction in spatial mapping in the hippocampus (301). Regardless of the absence of *APOE* effect seen in our results, we do see a prominent age effect in morris water maze (MWM) results, and nest building, a measure for cognitive function and executive function (159). In a previous study in our lab, old mice had lower nesting scores than the young controls (233). Additional stressors may be required to impact cognitive function in old *E4* mice. Aging is a major driver of cognitive impairment, and *E4* in the absence of Aβ or other hallmarks of AD is not enough to further the impairment that is already seen with old age.

Open field was used as a measurement of anxiety, which occurs in 50-75% of AD patients(336–338). We observed that with age there are greater measures of anxiety, which is consistent with previous literature in mice (339). A study performed in GFAP-*E4* transgenic mice demonstrated anxiety like behaviors compared to their GFAP-*E3* controls, measured by open field (340). These *APOE*-GFAP mice were only 3-months of age and male, while our

young mice were 6-months old and both male and females. Also, contrary to this study, our *E4* males did not have increased anxiety like the *E4*-GFAP mice, suggesting again that additional stressors may be necessary to exacerbate the effect of the *E4* genotype. We find that old *E4* female mice had less anxiety behaviors than the old *E4* males, this finding was not seen in the *E3* mice though. This could be due to the lack of literature in old *E4* mice, and thus mechanisms need elucidation. In our study, we also found that measures of motor function were significantly impaired with old age as measured by rotor rod and swimming velocity. A study in 2021 similarly saw a decline rotor rod gait velocity and swimming speed from 6 months to 22 months in male B6-C57 mice (341). Overall, our findings suggest that age more strongly alters anxiety and motor function than *APOE* genotype.

Indirect Calorimetry: RER varies by APOE genotype

The main finding from our indirect calorimetry experiments is that *E4* mice exhibited a higher RER than *E3* mice for both age groups, suggesting an impaired ability to utilize lipids. The differences seen in RER are due to a slight increase in VCO2 and slight decreases in VO2, resulting in larger differences in RER. In a recent study from 2024, 18-month-old male mice had no differences in RER in *E3* compared to *E4* mice on a normal diet (342). This study differs from ours by 1) they only used male mice that were 18 months-old; 2) RER was only measured for a 24-hour period, analyzed every 20 minutes. In contrast, our study observed RER over a 4-day period. A major limitation to our metabolic findings is that we did not measure activity. Thus, the differences in RER could be a result of old *E4* being more active than the old *E3* mice, thus further investigations are warranted.

Limitations

One major limitation in our study is the diet contained soybean meal. Our previous study and other literature has suggested the soybean meal, particularly genistein (a phytoestrogen) can improve vascular function and cognitive function. Thus, future studies should be conscious of their diet and avoid diets high in soy to avoid potential cofounding effects. The phytoestrogens in soy could improve vascular and cognitive function in *E4* mice, this negating genotype differences. Another limitation is the *APOE* mice are on a C57BL/6 background strain as other studies have shown that background strain interacts with AD gene variants to impact outcomes (343). It is also of importance to note that mice have different lipid trafficking than humans. Mice lack the cholesterol ester transfer protein (CETP) gene. This gene transports cholesterol and triglycerides between lipoproteins, and the absence of this gene in mice results in them carrying majority of their lipid cargo in HDL, rather than the more atherogenic LDL particles. Also, a mouses normal chow contains low fat and cholesterol, unlike a traditional human diet. Thus, future studies investigating apoE (a primary lipid trafficking protein) should be investigated in the presence of CETP in efforts to increase translation to human physiology and pathology.

5.5 Conclusion

The results of these studies demonstrate that age has a greater influence on cerebral vascular, vascular structure, and cognitive function than the *E4* genotype. For the first time, we demonstrated that old *E4* animals maintain their ability to vasoconstrict with age compared to old *E3* mice. This could impact the ability to regulate blood flow, but this was not indicated by our cerebral perfusion measures and could have impacted outcomes not measured. These results demonstrated that old female mice maintain a better cerebral vascular reactivity than the males. Altogether, these results imply that age continues as the greatest disruptor of vascular and

cognitive function, and that other stressors in tandem with the *E4* genotype are necessary to induce genotypic changes that are seen in the human data.

Table 5.1. Animal Characteristics

	Young E3	Young E4	Old E3	Old E4
n	20	24	26	22
Age (months)	6.7 ± 0.2	6.5 ± 0.2	24 ± 0.4	23 ± 0.9
Sex (%F)	20 (45%)	24 (46%)	26 (50%)	22 (50%)
Body mass (g)[a]	28.1 ± 5.6	28.3 ± 4.7	34.0 ± 4.4*†	35.8 ± 9.3*†
Heart mass (mg)[a]	0.15 ± 0.03	0.15 ± 0.02	0.18 ± 0.03*†	0.19 ± 0.03*†
Percent heart: body mass	0.56 ± 0.1	0.52 ± 0.01	0.52 ± 0.1	0.55 ± 0.1
Liver mass (mg)[a]	1.53 ± 0.4	1.53 ± 0.4	1.82 ± 0.4	1.68 ± 0.7
Percent liver: body mass	5.39 ± 0.6	5.37 ± 0.7	5.39 ± 1.2	4.67 ± 1.4
Spleen mass (mg)[a]	0.1 ± 0.01	0.09 ± 0.01	0.16 ± 0.1†	0.16 ± 0.1*†
Percent spleen: body mass	0.38 ± 0.08	0.33 ± 0.07	0.48 ± 0.4	0.47 ± 0.3
WAT mass (mg)[a]	0.65 ± 0.4	0.85 ± 0.4	1.43 ± 0.7*	1.66 ± 1.6*†
Percent WAT: body mass	2.17 ± 1.0	2.95 ± 1.0	4.07 ± 1.6	4.18 ± 3.1
Gastroc mass (mg)	0.16 ± 0.03	0.17 ± 0.03	0.15 ± 0.02	0.15 ± 0.03
Percent gastroc: body mass[a]	0.56 ± 0.08	0.60 ± 0.08	0.40 ± 0.16	0.44 ± 0.08
Soleus mass (mg)	0.01 ± 0.0	0.01 ± 0.0	0.06 ± 0.2	0.01 ± 0.0
Percent soleus: body mass	0.04 ± 0.0	0.04 ± 0.0	0.14 ± 0.6	0.03 ± 0.0
Uterus mass (mg)	0.12 ± 0.0	0.10 ± 0.0	0.12 ± 0.05	0.12 ± 0.05
Percent uterus mass: body weight	0.5 ± 0.1	0.37 ± 0.1	0.38 ± 0.1	0.4 ± 0.2
Frailty Index			0.23 ± 0.07	0.22 ± 0.08
FRIGHT age (days)			788 ± 40	785 ± 49
AFRAID score (days)			187 ± 22	188 ± 17

Data are mean ± SD. WAT, white adipose tissue. [a] $p<0.05$ main effect of age, [b] $p<0.05$ main effect of genotype, [c] $p<0.05$ interaction effect, * $P<0.05$ vs. young E3, † $P<0.05$ vs. young E4

Table 5.2. Artery Characteristics

Variable	Y E3	Y E4	O E3	O E4
Posterior Cerebral Artery				
Maximal Diameter (μm)	141 ± 14	145 ± 11	132 ± 22	147 ± 18
EC50, log M				
ACh	-7.0 ± 0.4	-7.1 ± 0.4	-6.9 ± 0.4	-7.1 ± 0.3
Insulin	1.6 ± 0.5	1.4 ±0.4	1.6 ± 0.5	1.6 ± 0.5
ET1	-7.2 ± 0.8	-7.2 ± 0.7	-7.5 ± 0.5	-7.3 ± 0.7
KCl	-7.6 ± 1.6	-8.1 ± 0.5	-8.3 ± 0.3	-9.5 ± 0.3
SNP	-7.1 ± 0.6	-7.0 ± 0.5	-7.5 ± 0.5	-7.1 ± 0.6
Preconstriction (%)				
ACh	37 ± 9	38 ± 13	35 ± 8	40 ± 10
Insulin	41 ± 10	38 ± 14	36 ± 11	40 ± 9
SNP	45 ± 14	50 ± 12	46 ± 14	49 ± 12

Data are mean ± SD. ACh, acetylcholine; ET1, endothelin-1; KCl, potassium chloride; SNP, sodium nitroprusside. No significant effects for 2x2 ANOVA analysis

VI. DISCUSSION

Chapters 2 & 3 provided insight into Chapters 4 & 5. The first two chapters allowed me to confirm 1) ovariectomy decreases cerebrovascular function and 2) understand how the estrous cycle influences vascular function. The results of these first two studies were pivotal for properly designing the studies performed in Chapters 4 & 5.

6.1 Summary and conclusions of chapter 2 & 3

6.1.1 Impact of estrous cycle on vascular function

I found that the estrous cycle should be accounted for when measuring in vivo large artery stiffness in young female mice. It is important to consider sex as a biological variable and account for hormonal fluctuation during *in vivo* measurements of vascular function to improve the overall quality of the study. These findings could also explain the current variability found within the literature.

6.1.2 Impact of dietary soy on vascular function

I found that dietary soy can influence vascular function, insulin signaling, and cognitive function. I confirmed previous findings that ovariectomy impairs cerebral artery endothelial function. For the first time, I demonstrated that a diet containing soy prevents the adverse effects of ovariectomy on insulin-mediated vasodilation. My results also provide insights into the potential mechanisms for these vascular effects, such as increased insulin receptor expression with soy diet and decreased estrogen receptor and antioxidant expression after ovariectomy. I also found that dietary soy improves instinctual behavior, suggesting potential benefits to cognitive function. The results of these studies highlight the need to consider soy content in the diet when studying cerebrovascular function in rodents. Together, these results imply that the

effects of diet on vascular function may explain potential inconsistencies found between studies, particularly in female rodents.

6.2 Conclusions of Chapters 4 & 5

6.2.1 The *E4* genotype resists estrogen status

The results from Chapter 4 are some of the most intriguing of this dissertation. My results indicated that *APOE* genotype modulated the response to estrogen on cerebral vascular and mitochondrial function. In *E3* OVX mice, 17β-estradiol supplementation prevented ovariectomy-induced declines in cerebral vascular function and led to greater mitochondrial respiration. Mice with the *E4* genotype, however, saw no benefit or detriment due to estrogen status on cerebral vascular function. Ultimately, these results suggest that estradiol supplementation may have a more therapeutic benefit for *E4* non-carriers. Further research should delve into the mechanisms by which *E4* is resistant to change in estradiol to help improve our understanding of disease progression and generate better therapeutic targets.

6.2.2 Age disrupts cerebral vascular function greater than *APOE* genotype

The results of these studies demonstrate that age has a greater influence on cerebral vascular function, vascular structure, and cognitive function than the *E4* genotype. I demonstrated that the old *E4* animals maintain their ability to vasoconstrict with age compared to *E3* mice. Thus, their ability to regulate CBF could be altered, but this was not supported by cerebral perfusion measures. Altogether, these results imply that age continues as the greatest disruptor of vascular and cognitive function, and that other stressors in tandem with the *E4* genotype are necessary to induce the physiologic differences that are seen in the human data. Future directions for this study should investigate the mechanisms by which constriction is being altered in old *E4* mice.

6.3 Future Directions

While each study brought new insights to the literature, the most intriguing discovery worth further exploration is how the *E4* allele confers resistance to estrogen status. Again, other literature supports this idea of *E4* resistance to hormone therapy, but the mechanisms as to why remain unknown. While the *E4/E4* genotype showed resistance to estrogen supplementation, future studies should consider how the *E3/E4* genotype would influence these outcomes. Additionally, studies like this should be performed in male mice to further investigate the complex interaction of sex steroid hormones and *APOE* genotype. Considering existing literature may help unlock the answer to why *E4* genotype confers resistance to estrogen.

One key to the lock could be changes in plasma membrane cholesterol. ApoE is a major cholesterol and lipid transporter, determining to an extent the amount of cholesterol in the plasma membrane of cells, and recent literature suggests excessive cholesterol in the plasma membrane can influence vasodilatory signaling (344). Concurrent with this theory, I know that sex steroid hormones, like estrogen, are derived from cholesterol. Postmenopausal women experience an increase in cholesterol levels, and this cholesterol excess, particularly in *E4* women, may contribute to the observed dysfunctions. Thus, *E4*-bearing postmenopausal females could be pocketing excess cholesterol in cell membranes, altering physiological functions and leading to not only altered cerebrovascular function but a myriad of other diseases.

Key number two is that future research should verify these studies in a different mouse model of menopause, like the ovarian failure (VCD) model and in older mice. Our question – how the interaction of estrogen and *APOE* influences cerebrovascular and mitochondrial outcomes – drove our model of ovariectomy. However, physiological aging and asynchrony of perimenopause causes extensive changes throughout the body. Studies done at different ages and

with different menopausal models would allow us to tease apart the influence of age, the menopause transition, and other sex steroid hormones on vascular and mitochondrial function.

6.4 This dissertation in a paragraph

All in all, this work highlights three things: 1) Researchers need to always consider how sex steroid hormones and diet can influence their results, chiefly for vascular research. 2) *APOE* genotype interacts with estrogen status to influence cerebral vascular and mitochondrial function, where *E4* is resistant to the beneficial effects of estradiol. 3) Age continues to be the greatest disrupter of vascular and cognitive function. The importance of these studies is that they contribute new knowledge to the bigger picture of health and equity for females in aging diseases.

VII. APPENDIX A: SUPPLEMENTAL MATERIAL

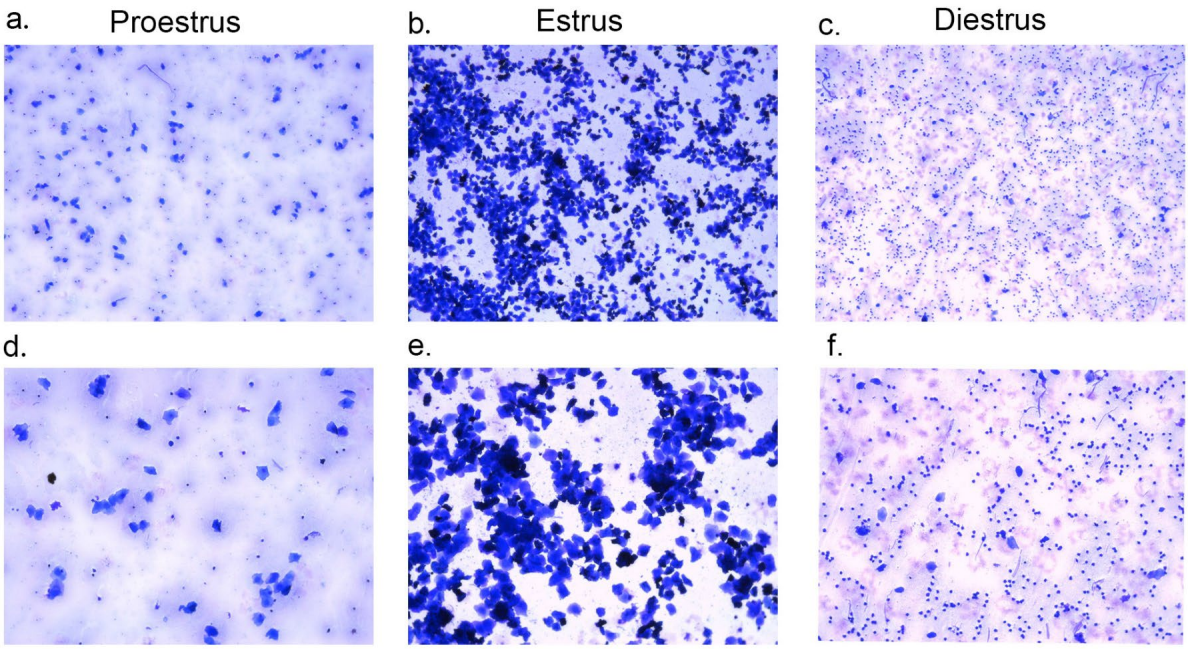

Supplemental Figure S2.1. Vaginal smears from C57BL/6J mice for each stage of the mouse estrous cycle. Three cells are identified: leukocytes, cornified epithelial cells, and nucleated epithelial cells. Proestrus is represented in (a) 10x and (d) 20x with nucleated epithelial cells. Estrus is shown in (b) 10x and (e) 20x magnification predominantly showing cornified epithelial cells. Diestrus is shown in (c) 10x and (f) 20x magnification, predominantly showing leukocytes.

Supplemental Table S2.1

	Primer Sequences
18S	Primer F: TAGAGGGACAAGTGGCGTTCPrimer R: CGCTGAGCCAGTCAGTGT
Ers1	Primer F: CCTCCCGCCTTCTACAGGT Primer R: CACACGGCACAGTAGCGAG
Ers2	Primer F: CTGTGATGAACTACAGTGTTCCC Primer R: CACATTTGGGCTTGCAGTCTG
Gper1	Primer F: ATGGATGCGACTACTCCAGC Primer R: AAGAGGGCAATCACGTACTGC

Supplemental Table S2.2

Target antigen	Vendor or Source	Product #	Working concentration	Antibody Validation
Gapdh Rabbit mAb	Cell Signaling	2118S	1:2000	Cell Signaling Technology Cat# 2118, RRID:AB_561053
Rabbit monoclonal eNOS (phosopho S1177)	Abcam	ab215717	1:1000	Abcam Cat# ab215717, RRID:AB_2893314
eNOS (D9A5L) Rabbit mAb	Cell Signaling	32027S	1:1000	Cell Signaling Technology Cat# 32027, RRID:AB_2728756
Phospho-Akt (Ser 473) Antibody Rabbit	Cell Signaling	9271S	1:1000	Cell Signaling Technology Cat# 9271, RRID:AB_32982
Akt antibody Rabbit	Cell Signaling	9272S	1:1000	Cell Signaling Technology Cat# 9272, RRID:AB_329827
Phospho-Estrogen Receptor α (Ser118) Mouse mAb	Cell Signaling	2511	1:1000	Cell Signaling Technology Cat# 2511, RRID:AB_331289
Recombinant Anti-Estrogen Receptor α antibody (ChIP Grade)	Abcam	ab32063	1:500	Abcam Cat# ab32063, RRID:AB_732249

Supplemental Table S2.3
Artery Characteristics

Variable	Proestrus	Estrus	Diestrus
Posterior Cerebral Artery			
Maximal Diameter (μm)	140 ± 21	156 ± 10	140 ± 16
EC_{50}, log M			
ACh	-7.6 ± 0.5	-6.9 ± 0.6	-7.5 ± 0.7
Insulin	-7.6 ± 0.6	-8.0 ± 0. 6	-7.8 ± 0.6
SNP	-7.2 ± 0.5	-7.2 ± 0.2	-7.5 ± 0.9
Preconstriction (%)			
ACh	32 ± 15	25 ± 10	22 ± 5
Insulin	37 ± 18	28 ± 19	23 ± 3
SNP	35 ± 13	40 ± 16	40 ± 17
Mesenteric Artery			
Maximal Diameter (μm)	182 ± 25	157 ± 13	155 ± 26
EC_{50}, log M			
ACh	-6.3 ± 0.4	-6.8 ± 0.4	-6.3 ± 0.4
Insulin	-8.0 ± 0.9	-8.0 ± 1.0	-7.7 ± 0.7
SNP	-7.7 ± 0.6	-7.6 ± 0.6	-7.7 ± 0.8
Preconstriction (%)			
ACh	43 ± 12	38 ± 9	34 ± 9
Insulin	38 ± 11	38 ± 7	35 ± 14
SNP	37 ± 11	54 ± 21	62 ± 6*

Data are mean ± SD. ACh, acetylcholine; SNP, sodium nitroprusside. No significant effects for 2x2 ANOVA analysis

Supplemental Table S3.1

Diet Comparisons

Diet	Soy Diet (5053)	Soy Free Diet (2020x)
Calories from Protein (%)	24.495	24
Calories from Fat (%)	13.122	16
Calories from Carbohydrate (%)	62.382	60

Ingredients for Soy Diet (5053): Ground Corn, Dehulled Soybean Meal, Wheat Middlings, Ground Wheat, Fish Meal, Wheat Germ, Dried Plain Beet Pulp, Cane Molasses, Brewers Dried Yeast, Ground Oats, Dehydrated Alfalfa Meal, Soybean Oil, Dried Whey, Calcium Carbonate, Salt, DL-Methionine, Menadione Dimethylpyrimidinol Bisulfite (Vitamin K), Choline Chloride, Pyridoxine Hydrochloride, Cholecalciferol (Vitamin D3), Vitamin A Acetate, DL-Alpha Tocopherol Acetate (Vitamin E), Biotin, Folic Acid, Thiamine Mononitrate, Manganous Oxide, Vitamin B12 Supplement, Zinc Oxide, Ferrous Carbonate, Nicotinic Acid, Riboflavin Supplement, Calcium Pantothenate, Copper Sulfate, Zinc Sulfate, Calcium Iodate, Cobalt Carbonate, Sodium Selenite.

Ingredients for Soy Free Diet (2020x): (in descending order of inclusion) Ground wheat, ground corn, corn gluten meal, wheat middlings, soybean oil, calcium carbonate, dicalcium phosphate, brewers dried yeast, L-lysine, iodized salt, magnesium oxide, choline chloride, DL-methionine, calcium propionate, L-tryptophan, vitamin E, acetate, menadione sodium bisulfite complex (source of vitamin K activity), manganous oxide, ferrous sulfate, zinc oxide, niacin, calcium pantothenate, copper sulfate, pyridoxine hydrochloride, riboflavin, thiamin mononitrate, vitamin A acetate, calcium iodate, vitamin B12 supplement, folic acid, biotin, vitamin D3 supplement, cobalt carbonate

Supplemental Table S3.2

Gene expression primer sequences

Gene	Primer Sequences
18S	Primer F: TAGAGGGACAAGTGGCGTTC Primer R: CGCTGAGCCAGTCAGTGT
Ers1	Primer F: CCTCCCGCCTTCTACAGGT Primer R: CACACGGCACAGTAGCGAG
Sod1	Primer F: AACCAGTTGTGTTGTCAGGAC Primer R: CCACCATGTTTCTTAGAGTGAGG
Sod2	Primer F: CAGACCTGCCTTACGACTATGG Primer R: CTCGGTGGCGTTGAGATTGTT
Sod 3	Primer F: CCTTCTTGTTCTACGGCTTGC Primer R: TCGCCTATCTTCTCAACCAGG
Slca2	Primer F: CAGTTCGGCTATAACACTGGTG Primer R: GCCCCCGACAGAGAAGATG
Insr	Primer F: ATGGGCTTCGGGAGAGGAT Primer R: GGATGTCCATACCAGGGCAC

Supplemental Table S3.3

Western Blot Antibodies

Target antigen	Vendor or Source	Product #	Working concentration	Antibody Validation
Gapdh Rabbit mAb	Cell Signaling	2118S	1:2000	Cell Signaling Technology Cat# 2118, RRID:AB_561053
IRS1	Cell Signaling	3407T	1:1000	Cell Signaling Technology Cat# 3407T RRID: AB_2127860
Phospho-Akt (Ser 473) Antibody Rabbit	Cell Signaling	9271S	1:1000	Cell Signaling Technology Cat# 9271, RRID:AB_32982
Akt antibody Rabbit	Cell Signaling	9272S	1:1000	Cell Signaling Technology Cat# 9272, RRID:AB_329827
Phospho-Estrogen Receptor α (Ser118) Mouse mAb	Cell Signaling	2511	1:1000	Cell Signaling Technology Cat# 2511, RRID:AB_331289
Recombinant Anti-Estrogen Receptor α antibody (ChIP Grade)	Abcam	ab32063	1:500	Abcam Cat# ab32063, RRID:AB_732249
P85 (PI3k)	Cell Signaling	4292S	1:1000	Cell Signaling Technology Cat# 4292 RRID: AB_329869

Supplemental Table S3.4

Artery Characteristics

Variable	Sham	OVX	OVX+Soy
Posterior Cerebral Artery			
Maximal Diameter (μm)	138 ± 21	140 ± 15	147 ± 13
EC_{50}, log M			
ACh	-6.8 ± 0.5	-6.6 ± 0.5	-7.0 ± 0.4
Insulin	-7.7 ± 0.6	-7.3 ± 0.5	-7.8 ± 0.5
SNP	-7.4 ± 0.4	-6.8 ± 0.4	-6.9 ± 0.4
Preconstriction (%)			
ACh	25.6 ± 4.7	23.7 ± 5.5	26.04 ± 7.0
Insulin	28.9 ± 10.3	27.9 ± 13.7	28.7 ± 11.9
SNP	32.7 ± 13.5	37.3 ± 13.4	25.0 ± 6.1

Data are mean ± SD. ACh, acetylcholine; SNP, sodium nitroprusside. No significant effects for 2x2 ANOVA analysis

Supplemental Figure S4.1

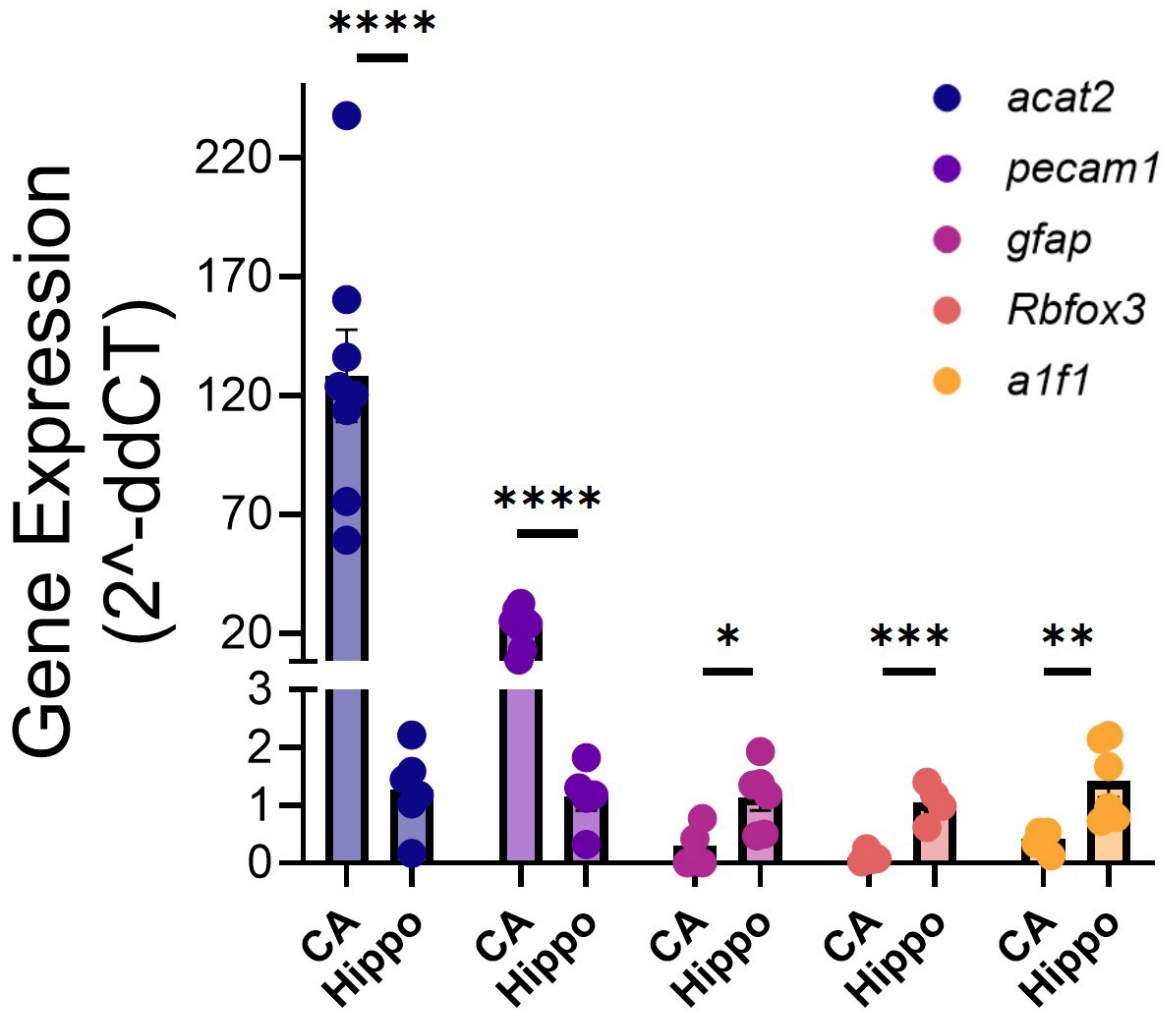

Supplemental Figure S4.1. Respiration samples contained primarily smooth muscle cells and endothelial cells. Cerebral arteries (CAs) dissected as for the Oroboros were measured for gene expression of *acat2* (smooth muscle cells), *pecam1* (endothelial cells), *gfap* (astrocytes), *rbfox3* (neurons), and *a1f1* (microglia) and compared to expression in the hippocampus (hippo) to ensure respiration samples were enriched for the cerebral vasculature. Samples were normalized to hippocampal measures. A one-tailed t-test was used to determine significance between CA and hippocampal samples. *p<0.05, **p<0.01, ***p<0.001, ***p<0.0001. N=4-8/group. Data are mean ± SD.

Supplemental Table S4.1

Artery Characteristics

Variable	E3 sham	E3 ovx	E3 estradiol	E4 sham	E4 ovx	E4 estradiol
Posterior Cerebral Artery						
Maximal Diameter (μm)	154 ± 8.0	140 ± 20.0	161 ± 21.7	138 ± 16.1	144 ± 10.1	169 ± 16.8
EC50, log M						
ACh	-7.2 ± 0.5	-7.2 ± 0.4	-7.5 ± 0.5	-6.9 ± 0.4	-7.0 ± 0.5	-7.3 ± 0.5
Insulin	0.75 ± 0.5	0.75 ± 0.6	1.3 ± 0.5	1.1 ± 0.5	1.1 ± 0.5	1.1 ± 0.6
SNP	-7.4 ± 0.6	-7.1 ± 0.6	-6.5 ± 0.6	-7.7 ± 0.7	-7.6 ± 0.7	-7.6 ± 0.5
Preconstriction (%)						
ACh	27.8 ± 6.5	34.0 ±7.2	29.9 ± 7.7	31.3 ± 5.9	30.4 ± 5.2	43.4 ± 4.6
Insulin	28.9 ± 7.2	30.1 ± 13.8	32.7 ± 9.9	28.3 ± 10.2	30.2 ± 6.8	38.9 ± 10.5
SNP	36.5 ± 10.1	30.3 ± 5.1	34.9 ± 8.4	39.2 ± 15.1	34.1 ± 12.6	38.6 ± 11.5

Supplemental Table S4.2

Gene primer sequences

Gene	Primer Sequences
18S	Primer F: TAGAGGGACAAGTGGCGTTC Primer R: CGCTGAGCCAGTCAGTGT
Pecam1	Primer F: ACGCTGGTGCTCTATGCAAG Primer R: TCAGTTGCTGCCCATTCATCA
Acat2	Primer F: GGCACCACTGAACCCTAAGG Primer R: ACAATACCAGTTGTACGTCCAGA
Gfap	Primer F: CCCTGGCTCGTGTGGATTT Primer R: GACCGATACCACTCCTCTGTC
A1F1	Primer F: AGCTGCCCGAAGTCAAGAAG Primer R: CATAGGGGTCAGCAGTACAGG
Rbfox3	Primer F: ATCGTAGAGGGACGGAAAATTGA Primer R: GTTCCCAGGCTTCTTATTGGTC
16s	Primer F: CCGCAAGGGAAAGATGAAAGAC Primer R: TCGTTTGGTTTCGGGGTTTC
ND1	Primer F: CTAGCAGAAACAAACCGGGC Primer R: CCGGCTGCGTATTCTACGTT
HK2	Primer F: GCCAGCCTCTCCTGATTTTAGTGT Primer R: GGGAACACAAAAGACCTCTTCTGG

Supplemental Table S4.3
Western Blot Antibodies

Target antigen	Vendor or Source	Product #	Working concentration	Antibody Validation
Anti-rabbit IgG	Cell signaling	7074	1:10000	Cell Signaling Technology Cat 7074, RRID: AB_2099233
Gapdh Rabbit mAb	Cell Signaling	2118S	1:2000	Cell Signaling Technology Cat# 2118, RRID:AB_561053
LRP1	Cell Signaling	64099S	1:1000	Cell Signaling Technology Cat# 64099 RRID: AB_2799654
Phospho-Akt (Ser 473) Antibody Rabbit	Cell Signaling	9271S	1:1000	Cell Signaling Technology Cat# 9271, RRID:AB_32982
Akt antibody Rabbit	Cell Signaling	9272S	1:1000	Cell Signaling Technology Cat# 9272, RRID:AB_329827
Phospho-Estrogen Receptor α (Ser118) Mouse mAb	Cell Signaling	2511	1:1000	Cell Signaling Technology Cat# 2511, RRID:AB_331289
COX1	Cell Signaling	4847S	1:1000	Cell Signaling Cat# 4841 RRID:AB_2084807_
COX2	Cell Signaling	12282T	1:1000	Cell Signaling Technology Cat# 12282 RRID: AB_2571729
Rabbit monoclonal eNOS (phosopho S1177)	Abcam	ab215717	1:1000	Abcam Cat# ab215717, RRID:AB_2893314
eNOS (D9A5L) Rabbit mAb	Cell Signaling	32027S	1:1000	Cell Signaling Technology Cat# 32027, RRID:AB_2728756
Citrate Synthase	Cell Signaling	14039T	1:1000	Cell Signaling Technology Cat# 14309 RRID:AB_2665545
NDSFU1 (E4K3E) Rabbit mAb	Cell Signaling	70246T	1:1000	Cell Signaling Technology Cat# 70264 RRID:AB_3086727
NFkB1, p105,p50 Polyclonal antibody	Proteintech	1422-1-AP	1:1000	Proteintech Cat # 14220-1-AP RRID:AB_2153393
NF-kB p65 Polyclonal antibody	Proteintech	10745-1-AP	1:1000	Proteintech Cat# 10745-1-AP RRID:AB_2920357

VIII. REFERENCES

1. **Farrer LA**, **Cupples LA**, **Haines JL**, **Hyman B**, **Kukull WA**, **Mayeux R**, **Myers RH**, **Pericak-Vance MA**, **Risch N**, **van Duijn CM**. Effects of age, sex, and ethnicity on the association between apolipoprotein E genotype and Alzheimer disease. A meta-analysis. APOE and Alzheimer Disease Meta Analysis Consortium. *JAMA* 278: 1349–1356, 1997.

2. **Haan MN**, **Mayeda ER**. Apolipoprotein E Genotype and Cardiovascular Diseases in the Elderly. *Curr Cardiovasc Risk Rep* 4: 361–368, 2010. doi: 10.1007/s12170-010-0118-4.

3. **Iturria-Medina Y**, **Sotero RC**, **Toussaint PJ**, **Mateos-Pérez JM**, **Evans AC**. Early role of vascular dysregulation on late-onset Alzheimer's disease based on multifactorial data-driven analysis. *Nat Commun* 7: 11934, 2016. doi: 10.1038/ncomms11934.

4. **Moir ME**, **Corkery AT**, **Senese KA**, **Miller KB**, **Pearson AG**, **Loggie NA**, **Howery AJ**, **Gaynor-Metzinger SHA**, **Cody KA**, **Eisenmenger LB**, **Johnson SC**, **Barnes JN**. Age at natural menopause impacts cerebrovascular reactivity and brain structure. *American Journal of Physiology-Regulatory, Integrative and Comparative Physiology* 324: R207–R215, 2023. doi: 10.1152/ajpregu.00228.2022.

5. **Abi-Ghanem C**, **Robison LS**, **Zuloaga KL**. Androgens' effects on cerebrovascular function in health and disease. *Biology of Sex Differences* 11: 35, 2020. doi: 10.1186/s13293-020-00309-4.

6. **Razmara A**, **Krause DN**, **Duckles SP**. Testosterone augments endotoxin-mediated cerebrovascular inflammation in male rats. *American Journal of Physiology-Heart and Circulatory Physiology* 289: H1843–H1850, 2005. doi: 10.1152/ajpheart.00465.2005.

7. **Rettberg JR**, **Yao J**, **Brinton RD**. Estrogen: a master regulator of bioenergetic systems in the brain and body. *Front Neuroendocrinol* 35: 8–30, 2014. doi: 10.1016/j.yfrne.2013.08.001.

8. **Mendelsohn ME**. Mechanisms of estrogen action in the cardiovascular system. *The Journal of Steroid Biochemistry and Molecular Biology* 74: 337–343, 2000. doi: 10.1016/S0960-0760(00)00110-2.

9. **Miller VM**, **Duckles SP**. Vascular Actions of Estrogens: Functional Implications. *Pharmacol Rev* 60: 210–241, 2008. doi: 10.1124/pr.107.08002.

10. **McCarthy M**, **Raval AP**. The peri-menopause in a woman's life: a systemic inflammatory phase that enables later neurodegenerative disease. *J Neuroinflammation* 17: 317, 2020. doi: 10.1186/s12974-020-01998-9.

11. **Stachenfeld NS**. Hormonal Changes During Menopause and the Impact on Fluid Regulation. *Reprod Sci* 21: 555–561, 2014. doi: 10.1177/1933719113518992.

12. **Marongiu R**. Accelerated Ovarian Failure as a Unique Model to Study Peri-Menopause Influence on Alzheimer's Disease. *Front Aging Neurosci* 11: 242, 2019. doi: 10.3389/fnagi.2019.00242.

13. **Morrison JH**, **Brinton RD**, **Schmidt PJ**, **Gore AC**. Estrogen, Menopause, and the Aging Brain: How Basic Neuroscience Can Inform Hormone Therapy in Women. *J Neurosci* 26: 10332–10348, 2006. doi: 10.1523/JNEUROSCI.3369-06.2006.

14. The menopausal transition. *Fertility and Sterility* 90: S61–S65, 2008. doi: 10.1016/j.fertnstert.2008.08.095.

15. **Writing Group for the Women's Health Initiative Investigators**. Risks and Benefits of Estrogen Plus Progestin in Healthy Postmenopausal WomenPrincipal Results From the Women's Health Initiative Randomized Controlled Trial. *JAMA* 288: 321–333, 2002. doi: 10.1001/jama.288.3.321.

16. **Chester RC**, **Kling JM**, **Manson JE**. What the Women's Health Initiative has taught us about menopausal hormone therapy. *Clin Cardiol* 41: 247–252, 2018. doi: 10.1002/clc.22891.

17. **Stute P**, **Marsden J**, **Salih N**, **Cagnacci A**. Reappraising 21 years of the WHI study: Putting the findings in context for clinical practice. *Maturitas* 174: 8–13, 2023. doi: 10.1016/j.maturitas.2023.04.271.

18. **Deer RR**, **Stallone JN**. Effects of estrogen on cerebrovascular function: age-dependent shifts from beneficial to detrimental in small cerebral arteries of the rat. *Am J Physiol Heart Circ Physiol* 310: H1285-1294, 2016. doi: 10.1152/ajpheart.00645.2015.

19. **Grady D**, **Herrington D**, **Bittner V**, **Blumenthal R**, **Davidson M**, **Hlatky M**, **Hsia J**, **Hulley S**, **Herd A**, **Khan S**, **Newby LK**, **Waters D**, **Vittinghoff E**, **Wenger N**, **HERS Research Group**. Cardiovascular disease outcomes during 6.8 years of hormone therapy: Heart and Estrogen/progestin Replacement Study follow-up (HERS II). *JAMA* 288: 49–57, 2002. doi: 10.1001/jama.288.1.49.

20. **Hendrix SL**, **Wassertheil-Smoller S**, **Johnson KC**, **Howard BV**, **Kooperberg C**, **Rossouw JE**, **Trevisan M**, **Aragaki A**, **Baird AE**, **Bray PF**, **Buring JE**, **Criqui MH**, **Herrington D**, **Lynch JK**, **Rapp SR**, **Torner J**, **WHI Investigators**. Effects of conjugated equine estrogen on stroke in the Women's Health Initiative. *Circulation* 113: 2425–2434, 2006. doi: 10.1161/CIRCULATIONAHA.105.594077.

21. **Hulley S**, **Furberg C**, **Barrett-Connor E**, **Cauley J**, **Grady D**, **Haskell W**, **Knopp R**, **Lowery M**, **Satterfield S**, **Schrott H**, **Vittinghoff E**, **Hunninghake D**, **HERS Research Group**. Noncardiovascular disease outcomes during 6.8 years of hormone therapy: Heart and Estrogen/progestin Replacement Study follow-up (HERS II). *JAMA* 288: 58–66, 2002. doi: 10.1001/jama.288.1.58.

22. **Hulley S**, **Grady D**, **Bush T**, **Furberg C**, **Herrington D**, **Riggs B**, **Vittinghoff E**. Randomized trial of estrogen plus progestin for secondary prevention of coronary heart

disease in postmenopausal women. Heart and Estrogen/progestin Replacement Study (HERS) Research Group. *JAMA* 280: 605–613, 1998. doi: 10.1001/jama.280.7.605.

23. **Wassertheil-Smoller S**, **Hendrix SL**, **Limacher M**, **Heiss G**, **Kooperberg C**, **Baird A**, **Kotchen T**, **Curb JD**, **Black H**, **Rossouw JE**, **Aragaki A**, **Safford M**, **Stein E**, **Laowattana S**, **Mysiw WJ**, **WHI Investigators**. Effect of estrogen plus progestin on stroke in postmenopausal women: the Women's Health Initiative: a randomized trial. *JAMA* 289: 2673–2684, 2003. doi: 10.1001/jama.289.20.2673.

24. **Maki PM**. The Critical Window Hypothesis of Hormone Therapy and Cognition: A Scientific Update on Clinical Studies. *Menopause* 20: 695–709, 2013. doi: 10.1097/GME.0b013e3182960cf8.

25. **Sabayan B**, **Westendorp RG**, **Grond J van der**, **Stott DJ**, **Sattar N**, **van Osch MJP**, **van Buchem MA**, **de Craen AJM**. Markers of endothelial dysfunction and cerebral blood flow in older adults. *Neurobiology of Aging* 35: 373–377, 2014. doi: 10.1016/j.neurobiolaging.2013.08.020.

26. **Ashby JW**, **Mack JJ**. Endothelial Control of Cerebral Blood Flow. *Am J Pathol* 191: 1906–1916, 2021. doi: 10.1016/j.ajpath.2021.02.023.

27. **Pober JS**, **Sessa WC**. Evolving functions of endothelial cells in inflammation. *Nat Rev Immunol* 7: 803–815, 2007. doi: 10.1038/nri2171.

28. **Wang F**, **Cao Y**, **Ma L**, **Pei H**, **Rausch WD**, **Li H**. Dysfunction of Cerebrovascular Endothelial Cells: Prelude to Vascular Dementia. *Front Aging Neurosci* 10: 376, 2018. doi: 10.3389/fnagi.2018.00376.

29. **Donato AJ**, **Morgan RG**, **Walker AE**, **Lesniewski LA**. Cellular and Molecular Biology of Aging Endothelial Cells. *J Mol Cell Cardiol* 89: 122–135, 2015. doi: 10.1016/j.yjmcc.2015.01.021.

30. **Lesniewski LA**, **Connell ML**, **Durrant JR**, **Folian BJ**, **Anderson MC**, **Donato AJ**, **Seals DR**. B6D2F1 Mice are a suitable model of oxidative stress-mediated impaired endothelium-dependent dilation with aging. *J Gerontol A Biol Sci Med Sci* 64: 9–20, 2009. doi: 10.1093/gerona/gln049.

31. **Moreau KL**, **Hildreth KL**, **Klawitter J**, **Blatchford P**, **Kohrt WM**. Decline in endothelial function across the menopause transition in healthy women is related to decreased estradiol and increased oxidative stress. *GeroScience* 42: 1699–1714, 2020. doi: 10.1007/s11357-020-00236-7.

32. **Kehmeier MN**, **Walker AE**. Sex Differences in Large Artery Stiffness: Implications for Cerebrovascular Dysfunction and Alzheimer's Disease. *Front Aging* 2: 791208, 2021. doi: 10.3389/fragi.2021.791208.

33. **Mosconi L**, **Berti V**, **Guyara-Quinn C**, **McHugh P**, **Petrongolo G**, **Osorio RS**, **Connaughty C**, **Pupi A**, **Vallabhajosula S**, **Isaacson RS**, **de Leon MJ**, **Swerdlow RH**,

Brinton RD. Perimenopause and emergence of an Alzheimer's bioenergetic phenotype in brain and periphery. *PLoS ONE* 12: e0185926, 2017. doi: 10.1371/journal.pone.0185926.

34. **Lew R**, **Komesaroff P**, **Williams M**, **Dawood T**, **Sudhir K**. Endogenous estrogens influence endothelial function in young men. *Circ Res* 93: 1127–1133, 2003. doi: 10.1161/01.RES.0000103633.57225.BC.

35. **Raz L**. Estrogen and cerebrovascular regulation in menopause. *Mol Cell Endocrinol* 389: 22–30, 2014. doi: 10.1016/j.mce.2014.01.015.

36. **Stirone C**, **Duckles SP**, **Krause DN**. Multiple forms of estrogen receptor-alpha in cerebral blood vessels: regulation by estrogen. *Am J Physiol Endocrinol Metab* 284: E184-192, 2003. doi: 10.1152/ajpendo.00165.2002.

37. **Kim KH**, **Young BD**, **Bender JR**. Endothelial Estrogen Receptor Isoforms and Cardiovascular Disease. *Mol Cell Endocrinol* 389: 65–70, 2014. doi: 10.1016/j.mce.2014.02.001.

38. **Michell BJ**, **Griffiths JE**, **Mitchelhill KI**, **Rodriguez-Crespo I**, **Tiganis T**, **Bozinovski S**, **de Montellano PRO**, **Kemp BE**, **Pearson RB**. The Akt kinase signals directly to endothelial nitric oxide synthase. *Current Biology* 9: 845-S1, 1999. doi: 10.1016/S0960-9822(99)80371-6.

39. **Ogola BO**, **Abshire CM**, **Visniauskas B**, **Kiley JX**, **Horton AC**, **Clark-Patterson GL**, **Kilanowski-Doroh I**, **Diaz Z**, **Bicego AN**, **McNally AB**, **Zimmerman MA**, **Groban L**, **Trask AJ**, **Miller KS**, **Lindsey SH**. Sex differences in vascular aging and impact of GPER deletion. *American Journal of Physiology-Heart and Circulatory Physiology* 323: H336–H349, 2022. doi: 10.1152/ajpheart.00238.2022.

40. **Zimmerman MA**, **Budish RA**, **Kashyap S**, **Lindsey SH**. GPER - novel membrane estrogen receptor. *Clin Sci (Lond)* 130: 1005–1016, 2016. doi: 10.1042/CS20160114.

41. **Kilanowski-Doroh IM**, **McNally AB**, **Wong T**, **Visniauskas B**, **Blessinger SA**, **Imulinde Sugi A**, **Richard C**, **Diaz Z**, **Horton A**, **Natale CA**, **Ogola BO**, **Lindsey SH**. Ovariectomy-Induced Arterial Stiffening Differs From Vascular Aging and Is Reversed by GPER Activation. .

42. **SenthilKumar G**, **Katunaric B**, **Bordas-Murphy H**, **Young M**, **Doren EL**, **Schulz ME**, **Widlansky ME**, **Freed JK**. 17β-Estradiol promotes sex-specific dysfunction in isolated human arterioles. *American Journal of Physiology-Heart and Circulatory Physiology* 324: H330–H337, 2023. doi: 10.1152/ajpheart.00708.2022.

43. **Meyer MR**, **Fredette NC**, **Howard TA**, **Hu C**, **Ramesh C**, **Daniel C**, **Amann K**, **Arterburn JB**, **Barton M**, **Prossnitz ER**. G Protein-coupled Estrogen Receptor Protects from Atherosclerosis. *Sci Rep* 4: 7564, 2014. doi: 10.1038/srep07564.

44. **Novensà L**, **Novella S**, **Medina P**, **Segarra G**, **Castillo N**, **Heras M**, **Hermenegildo C**, **Dantas AP**. Aging Negatively Affects Estrogens-Mediated Effects on Nitric Oxide

Bioavailability by Shifting ERα/ERβ Balance in Female Mice. *PLOS ONE* 6: e25335, 2011. doi: 10.1371/journal.pone.0025335.

45. **Tsang S-Y**, **Yao X**, **Chan FL**, **Wong C-M**, **Chen Z-Y**, **Laher I**, **Huang Y**. Estrogen and Tamoxifen Modulate Cerebrovascular Tone in Ovariectomized Female Rats. *Hypertension* 44: 78–82, 2004. doi: 10.1161/01.HYP.0000131659.27081.19.

46. **Zhou Y**, **Khan H**, **Xiao J**, **Cheang WS**. Effects of Arachidonic Acid Metabolites on Cardiovascular Health and Disease. *Int J Mol Sci* 22: 12029, 2021. doi: 10.3390/ijms222112029.

47. **Ospina JA**, **Duckles SP**, **Krause DN**. 17beta-estradiol decreases vascular tone in cerebral arteries by shifting COX-dependent vasoconstriction to vasodilation. *Am J Physiol Heart Circ Physiol* 285: H241-250, 2003. doi: 10.1152/ajpheart.00018.2003.

48. **Li M**, **Kuo L**, **Stallone JN**. Estrogen potentiates constrictor prostanoid function in female rat aorta by upregulation of cyclooxygenase-2 and thromboxane pathway expression. *Am J Physiol Heart Circ Physiol* 294: H2444-2455, 2008. doi: 10.1152/ajpheart.01121.2007.

49. **Davalli P**, **Mitic T**, **Caporali A**, **Lauriola A**, **D'Arca D**. ROS, Cell Senescence, and Novel Molecular Mechanisms in Aging and Age-Related Diseases. *Oxid Med Cell Longev* 2016: 3565127, 2016. doi: 10.1155/2016/3565127.

50. **Cimmino TP**, **Ammendola R**, **Cattaneo F**, **Esposito G**. NOX Dependent ROS Generation and Cell Metabolism. *International Journal of Molecular Sciences* 24, 2023. doi: 10.3390/ijms24032086.

51. **Janaszak-Jasiecka A**, **Płoska A**, **Wierońska JM**, **Dobrucki LW**, **Kalinowski L**. Endothelial dysfunction due to eNOS uncoupling: molecular mechanisms as potential therapeutic targets. *Cell Mol Biol Lett* 28: 21, 2023. doi: 10.1186/s11658-023-00423-2.

52. **Miller AA**, **Drummond GR**, **Mast AE**, **Schmidt HHHW**, **Sobey CG**. Effect of gender on NADPH-oxidase activity, expression, and function in the cerebral circulation: role of estrogen. *Stroke* 38: 2142–2149, 2007. doi: 10.1161/STROKEAHA.106.477406.

53. **Js B**, **Wh K**. Nitric oxide, superoxide, and peroxynitrite: the good, the bad, and ugly. *The American journal of physiology* 271, 1996. doi: 10.1152/ajpcell.1996.271.5.C1424.

54. **Gao YJ**, **Lee RMKW**. Hydrogen peroxide induces a greater contraction in mesenteric arteries of spontaneously hypertensive rats through thromboxane A2 production. *Br J Pharmacol* 134: 1639–1646, 2001. doi: 10.1038/sj.bjp.0704420.

55. **Pearson AG**, **Miller KB**, **Corkery AT**, **Eisenmann NA**, **Howery AJ**, **Carl AE**, **Eldridge MW**, **Barnes JN**. Impact of age and cyclooxygenase inhibition on the hemodynamic response to acute cognitive challenges. *American Journal of Physiology-Regulatory, Integrative and Comparative Physiology* 321: R208–R219, 2021. doi: 10.1152/ajpregu.00048.2021.

56. **Freed JK**, **Beyer AM**, **LoGiudice JA**, **Hockenberry JC**, **Gutterman DD**. Ceramide Changes the Mediator of Flow-Induced Vasodilation From Nitric Oxide to Hydrogen Peroxide in the Human Microcirculation. *Circulation Research* 115: 525–532, 2014. doi: 10.1161/CIRCRESAHA.115.303881.

57. **Miura H**, **Bosnjak JJ**, **Ning G**, **Saito T**, **Miura M**, **Gutterman DD**. Role for Hydrogen Peroxide in Flow-Induced Dilation of Human Coronary Arterioles. *Circulation Research* 92: e31–e40, 2003. doi: 10.1161/01.RES.0000054200.44505.AB.

58. **Rich LR**, **Harris W**, **Brown AM**. The Role of Brain Glycogen in Supporting Physiological Function. *Front Neurosci* 13, 2019. doi: 10.3389/fnins.2019.01176.

59. **Gupte AA**, **Pownall HJ**, **Hamilton DJ**. Estrogen: An Emerging Regulator of Insulin Action and Mitochondrial Function. *J Diabetes Res* 2015: 916585, 2015. doi: 10.1155/2015/916585.

60. **Mattingly KA**, **Ivanova MM**, **Riggs KA**, **Wickramasinghe NS**, **Barch MJ**, **Klinge CM**. Estradiol stimulates transcription of nuclear respiratory factor-1 and increases mitochondrial biogenesis. *Molecular Endocrinology* 22: 609–622, 2008. doi: 10.1210/me.2007-0029.

61. **Lopez Sanchez MIG**, **Shearwood A-MJ**, **Chia T**, **Davies SMK**, **Rackham O**, **Filipovska A**. Estrogen-Mediated Regulation of Mitochondrial Gene Expression. *Molecular Endocrinology* 29: 14–27, 2015. doi: 10.1210/me.2014-1077.

62. **Moreno AJM**, **Moreira PI**, **Custódio JBA**, **Santos MS**. Mechanism of inhibition of mitochondrial ATP synthase by 17β-estradiol. *J Bioenerg Biomembr* 45: 261–270, 2013. doi: 10.1007/s10863-012-9497-1.

63. **Brinton RD**. The healthy cell bias of estrogen action: mitochondrial bioenergetics and neurological implications. *Trends in Neurosciences* 31: 529–537, 2008. doi: 10.1016/j.tins.2008.07.003.

64. **Irwin RW**, **Yao J**, **To J**, **Hamilton RT**, **Cadenas E**, **Brinton RD**. Selective oestrogen receptor modulators differentially potentiate brain mitochondrial function. *J Neuroendocrinol* 24: 236–248, 2012. doi: 10.1111/j.1365-2826.2011.02251.x.

65. **Stirone C**, **Duckles SP**, **Krause DN**, **Procaccio V**. Estrogen Increases Mitochondrial Efficiency and Reduces Oxidative Stress in Cerebral Blood Vessels. *Mol Pharmacol* 68: 959–965, 2005. doi: 10.1124/mol.105.014662.

66. **Guo J**, **Krause DN**, **Horne J**, **Weiss JH**, **Li X**, **Duckles SP**. Estrogen-receptor-mediated protection of cerebral endothelial cell viability and mitochondrial function after ischemic insult in vitro. *J Cereb Blood Flow Metab* 30: 545–554, 2010. doi: 10.1038/jcbfm.2009.226.

67. **Duckles SP**, **Krause DN**. Mechanisms of Cerebrovascular Protection: Estrogen, Inflammation and Mitochondria. *Acta Physiol (Oxf)* 203: 149–154, 2011. doi: 10.1111/j.1748-1716.2010.02184.x.

68. **Razmara A**, **Sunday L**, **Stirone C**, **Wang X**, **Krause D**, **Duckles S**, **Procaccio V**. Mitochondrial Effects of Estrogen Are Mediated by Estrogen Receptor in Brain Endothelial Cells. *The Journal of pharmacology and experimental therapeutics* 325: 782–90, 2008. doi: 10.1124/jpet.107.134072.

69. **Nag S**. The blood–brain barrier and cerebral angiogenesis: lessons from the cold-injury model. *Trends in Molecular Medicine* 8: 38–44, 2002. doi: 10.1016/S1471-4914(01)02221-3.

70. **Girouard H**, **Iadecola C**. Neurovascular coupling in the normal brain and in hypertension, stroke, and Alzheimer disease. *Journal of Applied Physiology* 100: 328–335, 2006. doi: 10.1152/japplphysiol.00966.2005.

71. **Kelly DP**, **Scarpulla RC**. Transcriptional regulatory circuits controlling mitochondrial biogenesis and function. *Genes Dev* 18: 357–368, 2004. doi: 10.1101/gad.1177604.

72. **Scarpulla RC**. Nuclear Control of Respiratory Chain Expression by Nuclear Respiratory Factors and PGC-1-Related Coactivator. *Ann N Y Acad Sci* 1147: 321–334, 2008. doi: 10.1196/annals.1427.006.

73. **Torres MJ**, **Kew KA**, **Ryan TE**, **Pennington ER**, **Lin C-T**, **Buddo KA**, **Fix AM**, **Smith CA**, **Gilliam LA**, **Karvinen S**, **Lowe DA**, **Spangenburg EE**, **Zeczycki TN**, **Shaikh SR**, **Neufer PD**. 17β-Estradiol Directly Lowers Mitochondrial Membrane Microviscosity and Improves Bioenergetic Function in Skeletal Muscle. *Cell Metabolism* 27: 167-179.e7, 2018. doi: 10.1016/j.cmet.2017.10.003.

74. **Walker AE**, **Kaplon RE**, **Pierce GL**, **Nowlan MJ**, **Seals DR**. Prevention of age-related endothelial dysfunction by habitual aerobic exercise in healthy humans: Possible role of nuclear factor-κB. *Clin Sci (Lond)* 127: 645–654, 2014. doi: 10.1042/CS20140030.

75. **Moreau KL**, **Hildreth KL**. Vascular Aging across the Menopause Transition in Healthy Women. *Adv Vasc Med* 2014: 204390, 2014. doi: 10.1155/2014/204390.

76. **Xing D**, **Feng W**, **Miller AP**, **Weathington NM**, **Chen Y-F**, **Novak L**, **Blalock JE**, **Oparil S**. Estrogen modulates TNF-α-induced inflammatory responses in rat aortic smooth muscle cells through estrogen receptor-β activation. *American Journal of Physiology-Heart and Circulatory Physiology* 292: H2607–H2612, 2007. doi: 10.1152/ajpheart.01107.2006.

77. **Sunday L**, **Tran MM**, **Krause DN**, **Duckles SP**. Estrogen and progestagens differentially modulate vascular proinflammatory factors. *Am J Physiol Endocrinol Metab* 291: E261-267, 2006. doi: 10.1152/ajpendo.00550.2005.

78. **McNeill AM**, **Kim N**, **Duckles SP**, **Krause DN**. Chronic Estrogen Treatment Increases Levels of Endothelial Nitric Oxide Synthase Protein in Rat Cerebral Microvessels. *Stroke* 30: 2186–2190, 1999. doi: 10.1161/01.STR.30.10.2186.

79. **Ali N**, **Sohail R**, **Jaffer SR**, **Siddique S**, **Kaya B**, **Atowoju I**, **Imran A**, **Wright W**, **Pamulapati S**, **Choudhry F**, **Akbar A**, **Khawaja UA**. The Role of Estrogen Therapy as a Protective Factor for Alzheimer's Disease and Dementia in Postmenopausal Women: A Comprehensive Review of the Literature. *Cureus* 15: e43053, [date unknown]. doi: 10.7759/cureus.43053.

80. **Samargandy S**, **Matthews KA**, **Brooks MM**, **Barinas-Mitchell E**, **Magnani JW**, **Janssen I**, **Hollenberg SM**, **El Khoudary SR**. Arterial Stiffness Accelerates Within 1 Year of the Final Menstrual Period: The SWAN Heart Study. *Arterioscler Thromb Vasc Biol* 40: 1001–1008, 2020. doi: 10.1161/ATVBAHA.119.313622.

81. **Gavin KM**, **Jankowski C**, **Kohrt WM**, **Stauffer BL**, **Seals DR**, **Moreau KL**. Hysterectomy is associated with large artery stiffening in estrogen-deficient postmenopausal women. *Menopause* 19: 1000–1007, 2012. doi: 10.1097/gme.0b013e31825040f9.

82. **DuPont JJ**, **Kenney RM**, **Patel AR**, **Jaffe IZ**. Sex differences in mechanisms of arterial stiffness. *British Journal of Pharmacology* 176: 4208–4225, 2019. doi: 10.1111/bph.14624.

83. **Fonck E**, **Feigl GG**, **Fasel J**, **Sage D**, **Unser M**, **Rüfenacht DA**, **Stergiopulos N**. Effect of Aging on Elastin Functionality in Human Cerebral Arteries. *Stroke* 40: 2552–2556, 2009. doi: 10.1161/STROKEAHA.108.528091.

84. **Hayashi K**, **Hirayama E**. Age-related changes of wall composition and collagen cross-linking in the rat carotid artery – In relation with arterial mechanics. *Journal of the Mechanical Behavior of Biomedical Materials* 65: 881–889, 2017. doi: 10.1016/j.jmbbm.2016.10.007.

85. **Winder NR**, **Reeve EH**, **Walker AE**. Large artery stiffness and brain health: insights from animal models. *American Journal of Physiology-Heart and Circulatory Physiology* 320: H424–H431, 2021. doi: 10.1152/ajpheart.00696.2020.

86. **Lakatta EG**, **Levy D**. Arterial and Cardiac Aging: Major Shareholders in Cardiovascular Disease Enterprises. *Circulation* 107: 139–146, 2003. doi: 10.1161/01.CIR.0000048892.83521.58.

87. **Natoli AK**, **Medley TL**, **Ahimastos AA**, **Drew BG**, **Thearle DJ**, **Dilley RJ**, **Kingwell BA**. Sex Steroids Modulate Human Aortic Smooth Muscle Cell Matrix Protein Deposition and Matrix Metalloproteinase Expression. *Hypertension* 46: 1129–1134, 2005. doi: 10.1161/01.HYP.0000187016.06549.96.

88. **Qiu H**, **Depre C**, **Ghosh K**, **Resuello RG**, **Natividad FF**, **Rossi F**, **Peppas A**, **Shen Y-T**, **Vatner DE**, **Vatner SF**. Mechanism of Gender-Specific Differences in Aortic Stiffness

With Aging in Nonhuman Primates. *Circulation* 116: 669–676, 2007. doi: 10.1161/CIRCULATIONAHA.107.689208.

89. **Gardner JD**, **Murray DB**, **Voloshenyuk TG**, **Brower GL**, **Bradley JM**, **Janicki JS**. Estrogen attenuates chronic volume overload induced structural and functional remodeling in male rat hearts. *Am J Physiol Heart Circ Physiol* 298: H497–H504, 2010. doi: 10.1152/ajpheart.00336.2009.

90. **Dworatzek E**, **Mahmoodzadeh S**, **Schriever C**, **Kusumoto K**, **Kramer L**, **Santos G**, **Fliegner D**, **Leung Y-K**, **Ho S-M**, **Zimmermann W-H**, **Lutz S**, **Regitz-Zagrosek V**. Sex-specific regulation of collagen I and III expression by 17β-Estradiol in cardiac fibroblasts: role of estrogen receptors. *Cardiovasc Res* 115: 315–327, 2019. doi: 10.1093/cvr/cvy185.

91. **Westendorp ICD**, **Veld BAI**, **Bots ML**, **Akkerhuis JM**, **Hofman A**, **Grobbee DE**, **Witteman JCM**. Hormone Replacement Therapy and Intima-Media Thickness of the Common Carotid Artery. *Stroke* 30: 2562–2567, 1999. doi: 10.1161/01.STR.30.12.2562.

92. **Dubey RK**, **Jackson EK**, **Gillespie DG**, **Zacharia LC**, **Imthurn B**, **Keller PJ**. Clinically Used Estrogens Differentially Inhibit Human Aortic Smooth Muscle Cell Growth and Mitogen-Activated Protein Kinase Activity. *Arteriosclerosis, Thrombosis, and Vascular Biology* 20: 964–972, 2000. doi: 10.1161/01.ATV.20.4.964.

93. **Puglielli L**, **Tanzi RE**, **Kovacs DM**. Alzheimer's disease: the cholesterol connection. *Nat Neurosci* 6: 345–351, 2003. doi: 10.1038/nn0403-345.

94. **Weisgraber KH**, **Rall SC**, **Mahley RW**. Human E apoprotein heterogeneity. Cysteine-arginine interchanges in the amino acid sequence of the apo-E isoforms. *Journal of Biological Chemistry* 256: 9077–9083, 1981. doi: 10.1016/S0021-9258(19)52510-8.

95. **Liu C-C**, **Liu C-C**, **Kanekiyo T**, **Xu H**, **Bu G**. Apolipoprotein E and Alzheimer disease: risk, mechanisms and therapy. *Nat Rev Neurol* 9: 106–118, 2013. doi: 10.1038/nrneurol.2012.263.

96. **Tanzi RE**, **Bertram L**. New Frontiers in Alzheimer's Disease Genetics. *Neuron* 32: 181–184, 2001. doi: 10.1016/S0896-6273(01)00476-7.

97. **Dong LM**, **Weisgraber KH**. Human apolipoprotein E4 domain interaction. Arginine 61 and glutamic acid 255 interact to direct the preference for very low density lipoproteins. *J Biol Chem* 271: 19053–19057, 1996. doi: 10.1074/jbc.271.32.19053.

98. **Nguyen D**, **Dhanasekaran P**, **Phillips MC**, **Lund-Katz S**. Molecular Mechanism of Apolipoprotein E Binding to Lipoprotein Particles. *Biochemistry* 48: 3025–3032, 2009. doi: 10.1021/bi9000694.

99. **Windham IA**, **Cohen S**. The cell biology of APOE in the brain. *Trends in Cell Biology* 34: 338–348, 2024. doi: 10.1016/j.tcb.2023.09.004.

100. **Marottoli FM**, **Trevino TN**, **Geng X**, **Arbieva Z**, **Kanabar P**, **Maienschein-Cline M**, **Lee JC**, **Lutz SE**, **Tai LM**. Autocrine Effects of Brain Endothelial Cell-Produced Human Apolipoprotein E on Metabolism and Inflammation in vitro [Online]. *Frontiers in Cell and Developmental Biology* 9, 2021. https://www.frontiersin.org/article/10.3389/fcell.2021.668296 [28 Feb. 2022].

101. **Chernick D**, **Ortiz-Valle S**, **Jeong A**, **Qu W**, **Li L**. Peripheral versus central nervous system APOE in Alzheimer's disease: Interplay across the blood-brain barrier. *Neuroscience Letters* 708: 134306, 2019. doi: 10.1016/j.neulet.2019.134306.

102. **Dietschy JM**, **Turley SD**. Cholesterol metabolism in the brain. *Current Opinion in Lipidology* 12: 105, 2001.

103. **Mahley RW**. Central Nervous System Lipoproteins: ApoE and Regulation of Cholesterol Metabolism. *ATVB* 36: 1305–1315, 2016. doi: 10.1161/ATVBAHA.116.307023.

104. **Dietschy JM**, **Turley SD**. *Thematic review series: Brain Lipids.* Cholesterol metabolism in the central nervous system during early development and in the mature animal. *J Lipid Res* 45: 1375–1397, 2004. doi: 10.1194/jlr.R400004-JLR200.

105. **Dunk MM**, **Driscoll I**. Total Cholesterol and APOE-Related Risk for Alzheimer's Disease in the Alzheimer's Disease Neuroimaging Initiative. *J Alzheimers Dis* 85: 1519–1528, 2022. doi: 10.3233/JAD-215091.

106. **Yang LG**, **March ZM**, **Stephenson RA**, **Narayan PS**. Apolipoprotein E in lipid metabolism and neurodegenerative disease. *Trends in Endocrinology & Metabolism* 34: 430–445, 2023. doi: 10.1016/j.tem.2023.05.002.

107. **Barger SW**, **Harmon AD**. Microglial activation by Alzheimer amyloid precursor protein and modulation by apolipoprotein E. *Nature* 388: 878–881, 1997. doi: 10.1038/42257.

108. **Tao Q**, **Ang TFA**, **DeCarli C**, **Auerbach SH**, **Devine S**, **Stein TD**, **Zhang X**, **Massaro J**, **Au R**, **Qiu WQ**. Association of Chronic Low-grade Inflammation With Risk of Alzheimer Disease in ApoE4 Carriers. *JAMA Netw Open* 1: e183597, 2018. doi: 10.1001/jamanetworkopen.2018.3597.

109. **Lynch JR**, **Tang W**, **Wang H**, **Vitek MP**, **Bennett ER**, **Sullivan PM**, **Warner DS**, **Laskowitz DT**. APOE Genotype and an ApoE-mimetic Peptide Modify the Systemic and Central Nervous System Inflammatory Response*. *Journal of Biological Chemistry* 278: 48529–48533, 2003. doi: 10.1074/jbc.M306923200.

110. **Pires M**, **Rego AC**. Apoe4 and Alzheimer's Disease Pathogenesis—Mitochondrial Deregulation and Targeted Therapeutic Strategies. *International Journal of Molecular Sciences* 24, 2023. doi: 10.3390/ijms24010778.

111. **Theendakara V**, **Peters-Libeu CA**, **Spilman P**, **Poksay KS**, **Bredesen DE**, **Rao RV**. Direct Transcriptional Effects of Apolipoprotein E. *J Neurosci* 36: 685–700, 2016. doi: 10.1523/JNEUROSCI.3562-15.2016.

112. **Chung W-S**, **Verghese PB**, **Chakraborty C**, **Joung J**, **Hyman BT**, **Ulrich JD**, **Holtzman DM**, **Barres BA**. Novel allele-dependent role for APOE in controlling the rate of synapse pruning by astrocytes. *Proc Natl Acad Sci U S A* 113: 10186–10191, 2016. doi: 10.1073/pnas.1609896113.

113. **Hunsberger HC**, **Pinky PD**, **Smith W**, **Suppiramaniam V**, **Reed MN**. The role of APOE4 in Alzheimer's disease: strategies for future therapeutic interventions. *Neuronal Signal* 3: NS20180203, 2019. doi: 10.1042/NS20180203.

114. **Wang N**, **Cai L**, **Pei X**, **Lin Z**, **Huang L**, **Liang C**, **Wei M**, **Shao L**, **Guo T**, **Huang F**, **Luo H**, **Zheng H**, **Chen X**, **Leng L**, **Zhang Y**, **Wang X**, **Zhang J**, **Guo K**, **Wang Z**, **Zhang H**, **Zhao Y**, **Xu H**. Microglial apolipoprotein E particles contribute to neuronal senescence and synaptotoxicity. *iScience* 27: 110006, 2024. doi: 10.1016/j.isci.2024.110006.

115. **Jofre-Monseny L**, **Minihane A-M**, **Rimbach G**. Impact of apoE genotype on oxidative stress, inflammation and disease risk. *Mol Nutr Food Res* 52: 131–145, 2008. doi: 10.1002/mnfr.200700322.

116. **E T**, **H W**, **Jf C**, **P R**, **M R**, **J D**, **L B**, **E B**. Apolipoprotein E limits oxidative stress-induced cell dysfunctions in human adipocytes. *FEBS letters* 583, 2009. doi: 10.1016/j.febslet.2009.05.016.

117. **Dose J**, **Huebbe P**, **Nebel A**, **Rimbach G**. APOE genotype and stress response - a mini review. *Lipids in Health and Disease* 15: 121, 2016. doi: 10.1186/s12944-016-0288-2.

118. **Haney MS**, **Pálovics R**, **Munson CN**, **Long C**, **Johansson PK**, **Yip O**, **Dong W**, **Rawat E**, **West E**, **Schlachetzki JCM**, **Tsai A**, **Guldner IH**, **Lamichhane BS**, **Smith A**, **Schaum N**, **Calcuttawala K**, **Shin A**, **Wang Y-H**, **Wang C**, **Koutsodendris N**, **Serrano GE**, **Beach TG**, **Reiman EM**, **Glass CK**, **Abu-Remaileh M**, **Enejder A**, **Huang Y**, **Wyss-Coray T**. APOE4/4 is linked to damaging lipid droplets in Alzheimer's disease microglia. *Nature* 628: 154–161, 2024. doi: 10.1038/s41586-024-07185-7.

119. **Chang S**, **ran Ma T**, **Miranda RD**, **Balestra ME**, **Mahley RW**, **Huang Y**. Lipid- and receptor-binding regions of apolipoprotein E4 fragments act in concert to cause mitochondrial dysfunction and neurotoxicity. *Proc Natl Acad Sci U S A* 102: 18694–18699, 2005. doi: 10.1073/pnas.0508254102.

120. **Chen H-K**, **Ji Z-S**, **Dodson SE**, **Miranda RD**, **Rosenblum CI**, **Reynolds IJ**, **Freedman SB**, **Weisgraber KH**, **Huang Y**, **Mahley RW**. Apolipoprotein E4 Domain Interaction Mediates Detrimental Effects on Mitochondria and Is a Potential Therapeutic Target for Alzheimer Disease. *Journal of Biological Chemistry* 286: 5215–5221, 2011. doi: 10.1074/jbc.M110.151084.

121. **Ihara Y**, **Hayabara T**, **Sasaki K**, **Kawada R**, **Nakashima Y**, **Kuroda S**. Relationship between oxidative stress and apoE phenotype in Alzheimer's disease. *Acta Neurologica Scandinavica* 102: 346–349, 2000. doi: 10.1034/j.1600-0404.2000.102006346.x.

122. **Yin J**, **Reiman EM**, **Beach TG**, **Serrano GE**, **Sabbagh MN**, **Nielsen M**, **Caselli RJ**, **Shi J**. Effect of ApoE isoforms on mitochondria in Alzheimer disease. *Neurology* 94: e2404–e2411, 2020. doi: 10.1212/WNL.0000000000009582.

123. **Reiman EM**, **Chen K**, **Alexander GE**, **Caselli RJ**, **Bandy D**, **Osborne D**, **Saunders AM**, **Hardy J**. Functional brain abnormalities in young adults at genetic risk for late-onset Alzheimer's dementia. *Proc Natl Acad Sci U S A* 101: 284–289, 2004. doi: 10.1073/pnas.2635903100.

124. **Protas HD**, **Chen K**, **Langbaum JBS**, **Fleisher AS**, **Alexander GE**, **Lee W**, **Bandy D**, **de Leon MJ**, **Mosconi L**, **Buckley S**, **Truran-Sacrey D**, **Schuff N**, **Weiner MW**, **Caselli RJ**, **Reiman EM**. Posterior Cingulate Glucose Metabolism, Hippocampal Glucose Metabolism, and Hippocampal Volume in Cognitively Normal, Late-Middle-Aged Persons at 3 Levels of Genetic Risk for Alzheimer Disease. *JAMA Neurology* 70: 320–325, 2013. doi: 10.1001/2013.jamaneurol.286.

125. **BELL RD**, **WINKLER EA**, **SINGH I**, **SAGARE AP**, **DEANE R**, **WU Z**, **HOLTZMAN DM**, **BETSHOLTZ C**, **ARMULIK A**, **SALLSTROM J**, **BERK BC**, **ZLOKOVIC BV**. Apolipoprotein E controls cerebrovascular integrity via cyclophilin A. *Nature* 485: 512–516, 2012. doi: 10.1038/nature11087.

126. **Montagne A**, **Nikolakopoulou AM**, **Huuskonen MT**, **Sagare AP**, **Lawson EJ**, **Lazic D**, **Rege SV**, **Grond A**, **Zuniga E**, **Barnes SR**, **Prince J**, **Sagare M**, **Hsu C-J**, **LaDu MJ**, **Jacobs RE**, **Zlokovic BV**. APOE4 accelerates advanced-stage vascular and neurodegenerative disorder in old Alzheimer's mice via cyclophilin A independently of amyloid-β. *Nat Aging* 1: 506–520, 2021. doi: 10.1038/s43587-021-00073-z.

127. **Weeber EJ**, **Beffert U**, **Jones C**, **Christian JM**, **Förster E**, **Sweatt JD**, **Herz J**. Reelin and ApoE Receptors Cooperate to Enhance Hippocampal Synaptic Plasticity and Learning *. *Journal of Biological Chemistry* 277: 39944–39952, 2002. doi: 10.1074/jbc.M205147200.

128. **Shi Y**, **Yamada K**, **Liddelow SA**, **Smith ST**, **Zhao L**, **Luo W**, **Tsai RM**, **Spina S**, **Grinberg LT**, **Rojas JC**, **Gallardo G**, **Wang K**, **Roh J**, **Robinson G**, **Finn MB**, **Jiang H**, **Sullivan PM**, **Baufeld C**, **Wood MW**, **Sutphen C**, **McCue L**, **Xiong C**, **Del-Aguila JL**, **Morris JC**, **Cruchaga C**, **Fagan AM**, **Miller BL**, **Boxer AL**, **Seeley WW**, **Butovsky O**, **Barres BA**, **Paul SM**, **Holtzman DM**. ApoE4 markedly exacerbates tau-mediated neurodegeneration in a mouse model of tauopathy. *Nature* 549: 523–527, 2017. doi: 10.1038/nature24016.

129. **Valencia-Olvera AC**, **Maldonado Weng J**, **Christensen A**, **LaDu MJ**, **Pike CJ**. Role of estrogen in women's Alzheimer's disease risk as modified by APOE. *Journal of Neuroendocrinology* 35: e13209, 2023. doi: 10.1111/jne.13209.

130. **Serrano-Pozo A**, **Das S**, **Hyman BT**. APOE and Alzheimer's disease: advances in genetics, pathophysiology, and therapeutic approaches. *Lancet Neurol* 20: 68–80, 2021. doi: 10.1016/S1474-4422(20)30412-9.

131. **Giannisis A**, **Al-Grety A**, **Carlsson H**, **Patra K**, **Twohig D**, **Sando SB**, **Lauridsen C**, **Berge G**, **Grøntvedt GR**, **Bråthen G**, **White LR**, **Kultima K**, **Nielsen HM**. Plasma apolipoprotein E levels in longitudinally followed patients with mild cognitive impairment and Alzheimer's disease. *Alzheimers Res Ther* 14: 115, 2022. doi: 10.1186/s13195-022-01058-9.

132. **Wang JM**, **Irwin RW**, **Brinton RD**. Activation of estrogen receptor α increases and estrogen receptor β decreases apolipoprotein E expression in hippocampus *in vitro* and *in vivo*. *Proc Natl Acad Sci USA* 103: 16983–16988, 2006. doi: 10.1073/pnas.0608128103.

133. **Taxier LR**, **Philippi SM**, **Fleischer AW**, **York JM**, **LaDu MJ**, **Frick KM**. APOE4 homozygote females are resistant to the beneficial effects of 17β-estradiol on memory and CA1 dendritic spine density in the EFAD mouse model of Alzheimer's disease. *Neurobiol Aging* 118: 13–24, 2022. doi: 10.1016/j.neurobiolaging.2022.06.005.

134. **Ishunina TA**, **van Heerikhuize JJ**, **Ravid R**, **Swaab DF**. Estrogen receptors and metabolic activity in the human tuberomamillary nucleus: changes in relation to sex, aging and Alzheimer's disease. *Brain Research* 988: 84–96, 2003. doi: 10.1016/S0006-8993(03)03347-X.

135. **Almeida OP**, **Lautenschlager NT**, **Vasikaran S**, **Leedman P**, **Gelavis A**, **Flicker L**. A 20-week randomized controlled trial of estradiol replacement therapy for women aged 70 years and older: Effect on mood, cognition and quality of life. *Neurobiology of Aging* 27: 141–149, 2006. doi: 10.1016/j.neurobiolaging.2004.12.012.

136. **Garry PJ**, **Baumgartner RN**, **Brodie SG**, **Montoya GD**, **Liang HC**, **Lindeman RD**, **Williams TM**. Estrogen replacement therapy, serum lipids, and polymorphism of the apolipoprotein E gene. *Clin Chem* 45: 1214–1223, 1999.

137. **Kantarci K**, **Lowe VJ**, **Lesnick TG**, **Tosakulwong N**, **Bailey KR**, **Fields JA**, **Shuster LT**, **Zuk SM**, **Senjem ML**, **Mielke MM**, **Gleason C**, **Jack CR**, **Rocca WA**, **Miller VM**. Early Postmenopausal Transdermal 17β-Estradiol Therapy and Amyloid-β Deposition. *J Alzheimers Dis* 53: 547–556, [date unknown]. doi: 10.3233/JAD-160258.

138. **Taxier LR**, **Philippi SM**, **York JM**, **LaDu MJ**, **Frick KM**. *APOE4* genotype or ovarian hormone loss influence open field exploration in an EFAD mouse model of Alzheimer's disease. *Hormones and Behavior* 140: 105124, 2022. doi: 10.1016/j.yhbeh.2022.105124.

139. **Klein RC**, **Saini S**, **Risher M-L**, **Acheson SK**, **Fleming RL**, **Sexton HG**, **Swartzwelder HS**, **Moore SD**. Regional-Specific Effects of Ovarian Hormone Loss on Synaptic Plasticity in Adult Human APOE Targeted Replacement Mice. *PLoS One* 9: e94071, 2014. doi: 10.1371/journal.pone.0094071.

140. **Chhibber A**, **Zhao L**. ERβ and ApoE isoforms interact to regulate BDNF–5-HT2A signaling and synaptic function in the female brain. *Alzheimers Res Ther* 9: 79, 2017. doi: 10.1186/s13195-017-0305-3.

141. **Kunzler J**, **Youmans KL**, **Yu C**, **LaDu MJ**, **Tai LM**. APOE modulates the effect of estrogen therapy on Aβ accumulation EFAD-Tg mice. *Neuroscience Letters* 560: 131–136, 2014. doi: 10.1016/j.neulet.2013.12.032.

142. **Brown CM**, **Choi E**, **Xu Q**, **Vitek MP**, **Colton CA**. The APOE4 genotype alters the response of microglia and macrophages to 17β-estradiol. *Neurobiol Aging* 29: 1783–1794, 2008. doi: 10.1016/j.neurobiolaging.2007.04.018.

143. **Clayton JA**, **Collins FS**. NIH to balance sex in cell and animal studies. *Nature* 509: 282–283, 2014.

144. **Lindsey ML**, **LeBlanc AJ**, **Ripplinger CM**, **Carter JR**, **Kirk JA**, **Hansell Keehan K**, **Brunt KR**, **Kleinbongard P**, **Kassiri Z**. Reinforcing rigor and reproducibility expectations for use of sex and gender in cardiovascular research. *Am J Physiol Heart Circ Physiol* 321: H819–H824, 2021. doi: 10.1152/ajpheart.00418.2021.

145. **Robb AO**, **Mills NL**, **Din JN**, **Smith IBJ**, **Paterson F**, **Newby DE**, **Denison FC**. Influence of the Menstrual Cycle, Pregnancy, and Preeclampsia on Arterial Stiffness. *Hypertension* 53: 952–958, 2009. doi: 10.1161/HYPERTENSIONAHA.109.130898.

146. **Hong K**, **Choi Y**. Role of estrogen and RAS signaling in repeated implantation failure. *BMB Rep* 51: 225–229, 2018. doi: 10.5483/BMBRep.2018.51.5.045.

147. **Chirinos JA**, **Segers P**, **Hughes T**, **Townsend R**. Large-Artery Stiffness in Health and Disease. *Journal of the American College of Cardiology* 74: 1237–1263, 2019. doi: 10.1016/j.jacc.2019.07.012.

148. **Sandoo A**, **van Zanten JJCSV**, **Metsios GS**, **Carroll D**, **Kitas GD**. The endothelium and its role in regulating vascular tone. *Open Cardiovasc Med J* 4: 302–312, 2010. doi: 10.2174/1874192401004010302.

149. **Hadi HA**, **Carr CS**, **Al Suwaidi J**. Endothelial Dysfunction: Cardiovascular Risk Factors, Therapy, and Outcome. *Vasc Health Risk Manag* 1: 183–198, 2005.

150. **Stamatelopoulos KS**, **Georgiopoulos G**, **Papaioannou T**, **Lambrinoudaki I**, **Kouzoupis A**, **Vlachopoulos C**, **Georgiou SP**, **Manios E**, **Alevizaki M**, **Papamichael CM**, **Sfikakis PP**. Can premenstrual syndrome affect arterial stiffness or blood pressure? *Atherosclerosis* 224: 170–176, 2012. doi: 10.1016/j.atherosclerosis.2012.05.037.

151. **Madhura M**, **Sandhya T**. Effect of Different Phases of Menstrual Cycle on Reflection Index, Stiffness index and Pulse wave velocity in Healthy subjects. *J Clin Diagn Res* 8: BC01–BC04, 2014. doi: 10.7860/JCDR/2014/7385.4778.

152. **Natoli AK**, **Medley TL**, **Ahimastos AA**, **Drew BG**, **Thearle DJ**, **Dilley RJ**, **Kingwell BA**. Sex Steroids Modulate Human Aortic Smooth Muscle Cell Matrix Protein Deposition and Matrix Metalloproteinase Expression. *Hypertension* 46: 1129–1134, 2005. doi: 10.1161/01.HYP.0000187016.06549.96.

153. **Ogola BO**, **Clark GL**, **Abshire CM**, **Harris NR**, **Gentry KL**, **Gunda SS**, **Kilanowski-Doroh I**, **Wong TJ**, **Visniauskas B**, **Lawrence DJ**, **Zimmerman MA**, **Bayer CL**, **Groban L**, **Miller KS**, **Lindsey SH**. Sex and the G Protein–Coupled Estrogen Receptor Impact Vascular Stiffness. *Hypertension* 78: e1–e14, 2021. doi: 10.1161/HYPERTENSIONAHA.120.16915.

154. **Pastore MB**, **Talwar S**, **Conley MR**, **Magness RR**. Identification of Differential ER-Alpha Versus ER-Beta Mediated Activation of eNOS in Ovine Uterine Artery Endothelial Cells. *Biol Reprod* 94: 139, 2016. doi: 10.1095/biolreprod.115.137554.

155. **Lim W**, **Mayer B**, **Pawson T**. *Cell Signaling principles and mechanisms*. 1st ed. Garland Science, 2014.

156. **Salinero AE**, **Robison LS**, **Gannon OJ**, **Riccio D**, **Mansour F**, **Abi-Ghanem C**, **Zuloaga KL**. Sex-specific effects of high-fat diet on cognitive impairment in a mouse model of VCID. *The FASEB Journal* 34: 15108–15122, 2020. doi: https://doi.org/10.1096/fj.202000085R.

157. **Cora MC**, **Kooistra L**, **Travlos G**. Vaginal Cytology of the Laboratory Rat and Mouse: Review and Criteria for the Staging of the Estrous Cycle Using Stained Vaginal Smears. *Toxicol Pathol* 43: 776–793, 2015. doi: 10.1177/0192623315570339.

158. **Deacon RMJ**. Measuring Motor Coordination in Mice. *J Vis Exp* : 2609, 2013. doi: 10.3791/2609.

159. **Deacon R**. Assessing burrowing, nest construction, and hoarding in mice. *J Vis Exp* : e2607, 2012. doi: 10.3791/2607.

160. **Rossi P**, **Francès Y**, **Kingwell BA**, **Ahimastos AA**. Gender differences in artery wall biomechanical properties throughout life. *Journal of Hypertension* 29: 1023–1033, 2011. doi: 10.1097/HJH.0b013e328344da5e.

161. **Hougaku H**, **Fleg JL**, **Najjar SS**, **Lakatta EG**, **Harman SM**, **Blackman MR**, **Metter EJ**. Relationship between androgenic hormones and arterial stiffness, based on longitudinal hormone measurements. *American Journal of Physiology-Endocrinology and Metabolism* 290: E234–E242, 2006. doi: 10.1152/ajpendo.00059.2005.

162. **Williams MRI**, **Westerman RA**, **Kingwell BA**, **Paige J**, **Blombery PA**, **Sudhir K**, **Komesaroff PA**. Variations in Endothelial Function and Arterial Compliance during the Menstrual Cycle. *The Journal of Clinical Endocrinology & Metabolism* 86: 5389–5395, 2001. doi: 10.1210/jcem.86.11.8013.

163. **Hayashi K**, **Miyachi M**, **Seno N**, **Takahashi K**, **Yamazaki K**, **Sugawara J**, **Yokoi T**, **Onodera S**, **Mesaki N**. Variations in carotid arterial compliance during the menstrual cycle in young women. *Exp Physiol* 91: 465–472, 2006. doi: 10.1113/expphysiol.2005.032011.

164. **Adkisson EJ**, **Casey DP**, **Beck DT**, **Gurovich AN**, **Martin JS**, **Braith RW**. Central, peripheral and resistance arterial reactivity: fluctuates during the phases of the menstrual cycle. *Exp Biol Med (Maywood)* 235: 111–118, 2010. doi: 10.1258/ebm.2009.009186.

165. **Spaczyński RZ**, **Mitkowska A**, **Florczak M**, **Banaszewska B**, **Krauze T**, **Wykrętowicz A**, **Guzik P**, **Pawelczyk L**. Decreased large-artery stiffness in midluteal phase of the menstrual cycle in healthy women of reproductive age. *Ginekol Pol* 85: 771–777, 2014.

166. **Ounis-Skali N**, **Mitchell GF**, **Solomon CG**, **Solomon SD**, **Seely EW**. Changes in central arterial pressure waveforms during the normal menstrual cycle. *J Investig Med* 54: 321–326, 2006. doi: 10.2310/6650.2006.05055.

167. **Ajayi AF**, **Akhigbe RE**. Staging of the estrous cycle and induction of estrus in experimental rodents: an update. *Fertil Res and Pract* 6: 5, 2020. doi: 10.1186/s40738-020-00074-3.

168. **Man B**, **Cui C**, **Zhang X**, **Sugiyama D**, **Barinas-Mitchell E**, **Sekikawa A**. The effect of soy isoflavones on arterial stiffness: a systematic review and meta-analysis of randomized controlled trials. *Eur J Nutr* 60: 603–614, 2021. doi: 10.1007/s00394-020-02300-6.

169. **Gavin KM**, **Seals DR**, **Silver AE**, **Moreau KL**. Vascular Endothelial Estrogen Receptor α Is Modulated by Estrogen Status and Related to Endothelial Function and Endothelial Nitric Oxide Synthase in Healthy Women. *The Journal of Clinical Endocrinology & Metabolism* 94: 3513–3520, 2009. doi: 10.1210/jc.2009-0278.

170. **Lannigan DA**. Estrogen receptor phosphorylation. *Steroids* 68: 1–9, 2003. doi: 10.1016/S0039-128X(02)00110-1.

171. **Fuentes N**, **Silveyra P**. Estrogen receptor signaling mechanisms. *Adv Protein Chem Struct Biol* 116: 135–170, 2019. doi: 10.1016/bs.apcsb.2019.01.001.

172. **Liu Z**, **Gou Y**, **Zhang H**, **Zuo H**, **Zhang H**, **Liu Z**, **Yao D**. Estradiol improves cardiovascular function through up-regulation of SOD2 on vascular wall. *Redox Biology* 3: 88–99, 2014. doi: 10.1016/j.redox.2014.11.001.

173. **Knauf C**, **Ferreira SP**, **Hamdane M**, **Mailliot C**, **Prevot V**, **Beauvillain J-C**, **Croix D**. Variation of Endothelial Nitric Oxide Synthase Synthesis in the Median Eminence during the Rat Estrous Cycle: An Additional Argument for the Implication of Vascular Blood Vessel in the Control of GnRH Release. *Endocrinology* 142: 7, 2001.

174. **Zhang X**, **Lin HY**, **Liu GY**, **Wang HM**, **Li QL**, **Zhu C**. Expressions and regulation of endothelial and inducible nitric oxide synthases in mouse uterus during the estrous cycle and early pregnancy. *Front Biosci* 10: 3172–3182, 2005. doi: 10.2741/1773.

175. **Drazen DL**, **Klein SL**, **Burnett AL**, **Wallach EE**, **Crone JK**, **Huang PL**, **Nelson RJ**. Reproductive function in female mice lacking the gene for endothelial nitric oxide synthase. *Nitric Oxide* 3: 366–374, 1999. doi: 10.1006/niox.1999.0251.

176. **Gurrala R**, **Kilanowski-Doroh IM**, **Hutson DD**, **Ogola BO**, **Zimmerman MA**, **Katakam PVG**, **Satou R**, **Mostany R**, **Lindsey SH**. Alterations in the estrogen receptor profile of cardiovascular tissues during aging. *GeroScience* 43: 433–442, 2021. doi: 10.1007/s11357-021-00331-3.

177. **Ogola BO**, **Zimmerman MA**, **Sure VN**, **Gentry KM**, **Duong JL**, **Clark GL**, **Miller KS**, **Katakam PVG**, **Lindsey SH**. G Protein-Coupled Estrogen Receptor Protects From Angiotensin II-Induced Increases in Pulse Pressure and Oxidative Stress [Online]. *Frontiers in Endocrinology* 10, 2019. https://www.frontiersin.org/article/10.3389/fendo.2019.00586 [26 Jun. 2022].

178. **Hall JM**, **McDonnell DP**. The Estrogen Receptor β-Isoform (ERβ) of the Human Estrogen Receptor Modulates ERα Transcriptional Activity and Is a Key Regulator of the Cellular Response to Estrogens and Antiestrogens1. *Endocrinology* 140: 5566–5578, 1999. doi: 10.1210/endo.140.12.7179.

179. **Maggi A**, **Cignarella A**, **Brusadelli A**, **Bolego C**, **Pinna C**, **Puglisi L**. Diabetes Undermines Estrogen Control of Inducible Nitric Oxide Synthase Function in Rat Aortic Smooth Muscle Cells Through Overexpression of Estrogen Receptor-β. *Circulation* 108: 211–217, 2003. doi: 10.1161/01.CIR.0000079311.39939.94.

180. **Connelly PJ**, **Casey H**, **Montezano AC**, **Touyz RM**, **Delles C**. Sex steroids receptors, hypertension, and vascular ageing. *J Hum Hypertens* 36: 120–125, 2022. doi: 10.1038/s41371-021-00576-7.

181. **Peltonen GL**, **Harrell JW**, **Aleckson BP**, **LaPlante KM**, **Crain MK**, **Schrage WG**. Cerebral blood flow regulation in women across menstrual phase: differential contribution of cyclooxygenase to basal, hypoxic, and hypercapnic vascular tone. *American Journal of Physiology-Regulatory, Integrative and Comparative Physiology* 311: R222–R231, 2016. doi: 10.1152/ajpregu.00106.2016.

182. **Gibson CL**, **Murphy SP**. Progesterone Enhances Functional Recovery after Middle Cerebral Artery Occlusion in Male Mice. *J Cereb Blood Flow Metab* 24: 805–813, 2004. doi: 10.1097/01.WCB.0000125365.83980.00.

183. **Barbagallo M**, **Dominguez LJ**, **Licata G**, **Shan J**, **Bing L**, **Karpinski E**, **Pang PKT**, **Resnick LM**. Vascular Effects of Progesterone. *Hypertension* 37: 142–147, 2001. doi: 10.1161/01.HYP.37.1.142.

184. **Faulkner JL**, **Kennard S**, **Huby A-C**, **Antonova G**, **Lu Q**, **Jaffe IZ**, **Patel VS**, **Fulton DJR**, **Belin de Chantemèle EJ**. Progesterone Predisposes Females to Obesity-Associated Leptin-Mediated Endothelial Dysfunction via Upregulating Endothelial MR (Mineralocorticoid Receptor) Expression. *Hypertension* 74: 678–686, 2019. doi: 10.1161/HYPERTENSIONAHA.119.12802.

185. **Vlachopoulos C**, **Ioakeimidis N**, **Miner M**, **Aggelis A**, **Pietri P**, **Terentes-Printzios D**, **Tsekoura D**, **Stefanadis C**. Testosterone deficiency: A determinant of aortic stiffness in men. *Atherosclerosis* 233: 278–283, 2014. doi: 10.1016/j.atherosclerosis.2013.12.010.

186. **Williams JS**, **Dunford EC**, **MacDonald MJ**. Impact of the menstrual cycle on peripheral vascular function in premenopausal women: systematic review and meta-analysis. *American Journal of Physiology-Heart and Circulatory Physiology* 319: H1327–H1337, 2020. doi: 10.1152/ajpheart.00341.2020.

187. **Higashi Y**, **Sanada M**, **Sasaki S**, **Nakagawa K**, **Goto C**, **Matsuura H**, **Ohama K**, **Chayama K**, **Oshima T**. Effect of estrogen replacement therapy on endothelial function in peripheral resistance arteries in normotensive and hypertensive postmenopausal women. *Hypertension* 37: 651–657, 2001. doi: 10.1161/01.hyp.37.2.651.

188. **Capone C**, **Anrather J**, **Milner TA**, **Iadecola C**. Estrous Cycle–Dependent Neurovascular Dysfunction Induced by Angiotensin II in the Mouse Neocortex. *Hypertension* 54: 302–307, 2009. doi: 10.1161/HYPERTENSIONAHA.109.133249.

189. **Arias-Loza P-A**, **Muehlfelder M**, **Pelzer T**. Estrogen and estrogen receptors in cardiovascular oxidative stress. *Pflugers Arch* 465: 739–746, 2013. doi: 10.1007/s00424-013-1247-7.

190. **Bellanti F**, **Matteo M**, **Rollo T**, **Rosario FD**, **Greco P**, **Vendemiale G**, **Serviddio G**. Sex hormones modulate circulating antioxidant enzymes: Impact of estrogen therapy. *Redox biology* 1: 340–346, 2013. doi: 10.1016/j.redox.2013.05.003.

191. **Maioli S**, **Leander K**, **Nilsson P**, **Nalvarte I**. Estrogen receptors and the aging brain. *Essays Biochem* 65: 913–925, 2021. doi: 10.1042/EBC20200162.

192. **Deacon RM**. Assessing nest building in mice. *Nat Protoc* 1: 1117–1119, 2006. doi: 10.1038/nprot.2006.170.

193. **Meziane H**, **Ouagazzal A-M**, **Aubert L**, **Wietrzych M**, **Krezel W**. Estrous cycle effects on behavior of C57BL/6J and BALB/cByJ female mice: implications for phenotyping strategies. *Genes, Brain and Behavior* 6: 192–200, 2007. doi: 10.1111/j.1601-183X.2006.00249.x.

194. **Chari T**, **Griswold S**, **Andrews NA**, **Fagiolini M**. The Stage of the Estrus Cycle Is Critical for Interpretation of Female Mouse Social Interaction Behavior. *Front Behav Neurosci* 14: 113, 2020. doi: 10.3389/fnbeh.2020.00113.

195. **Stanczyk FZ**, **Clarke NJ**. Advantages and challenges of mass spectrometry assays for steroid hormones. *The Journal of Steroid Biochemistry and Molecular Biology* 121: 491–495, 2010. doi: 10.1016/j.jsbmb.2010.05.001.

196. **Stanczyk FZ**, **Jurow J**, **Hsing AW**. Limitations of Direct Immunoassays for Measuring Circulating Estradiol Levels in Postmenopausal Women and Men in Epidemiologic Studies. *Cancer Epidemiology, Biomarkers & Prevention* 19: 903–906, 2010. doi: 10.1158/1055-9965.EPI-10-0081.

197. **Schiøler V**, **Thode J**. Six direct radioimmunoassays of estradiol evaluated. *Clin Chem* 34: 949–952, 1988.

198. **Stanczyk FZ**, **Lee JS**, **Santen RJ**. Standardization of steroid hormone assays: why, how, and when? *Cancer Epidemiol Biomarkers Prev* 16: 1713–1719, 2007. doi: 10.1158/1055-9965.EPI-06-0765.

199. **Lee JS**, **Ettinger B**, **Stanczyk FZ**, **Vittinghoff E**, **Hanes V**, **Cauley JA**, **Chandler W**, **Settlage J**, **Beattie MS**, **Folkerd E**, **Dowsett M**, **Grady D**, **Cummings SR**. Comparison of methods to measure low serum estradiol levels in postmenopausal women. *J Clin Endocrinol Metab* 91: 3791–3797, 2006. doi: 10.1210/jc.2005-2378.

200. **Cook NJ**, **Read GF**. Oestradiol measurement in women on oral hormone replacement therapy: the validity of commercial test kits. *Br J Biomed Sci* 52: 97–101, 1995.

201. **Dowsett M**, **Folkerd E**. Deficits in plasma oestradiol measurement in studies and management of breast cancer. *Breast Cancer Res* 7: 1–4, 2005. doi: 10.1186/bcr960.

202. **Krasowski MD**, **Drees D**, **Morris CS**, **Maakestad J**, **Blau JL**, **Ekins S**. Cross-reactivity of steroid hormone immunoassays: clinical significance and two-dimensional molecular similarity prediction. *BMC Clin Pathol* 14: 33, 2014. doi: 10.1186/1472-6890-14-33.

203. **Handelsman DJ**, **Wartofsky L**. Requirement for Mass Spectrometry Sex Steroid Assays in the Journal of Clinical Endocrinology and Metabolism. *The Journal of Clinical Endocrinology & Metabolism* 98: 3971–3973, 2013. doi: 10.1210/jc.2013-3375.

204. **Kubota K**, **Cui W**, **Dhakal P**, **Wolfe MW**, **Rumi MAK**, **Vivian JL**, **Roby KF**, **Soares MJ**. Rethinking progesterone regulation of female reproductive cyclicity. *Proc Natl Acad Sci U S A* 113: 4212–4217, 2016. doi: 10.1073/pnas.1601825113.

205. **Wood GA**, **Fata JE**, **Watson KLM**, **Khokha R**. Circulating hormones and estrous stage predict cellular and stromal remodeling in murine uterus. *Reproduction* 133: 1035–1044, 2007. doi: 10.1530/REP-06-0302.

206. **Visser JA**, **Durlinger ALL**, **Peters IJJ**, **van den Heuvel ER**, **Rose UM**, **Kramer P**, **de Jong FH**, **Themmen APN**. Increased Oocyte Degeneration and Follicular Atresia during the Estrous Cycle in Anti-Müllerian Hormone Null Mice. *Endocrinology* 148: 2301–2308, 2007. doi: 10.1210/en.2006-1265.

207. **Asai S**, **Ohta R**, **Shirota M**, **Sato M**, **Watanabe G**, **Taya K**. Reproductive endocrinology in Hatano high- and low-avoidance rats during the estrous cycle. *Endocrine* 18: 161–166, 2002. doi: 10.1385/ENDO:18:2:161.

208. **Inoue S**. Neural basis for estrous cycle-dependent control of female behaviors. *Neuroscience Research* 176: 1–8, 2022. doi: 10.1016/j.neures.2021.07.001.

209. **Zenclussen ML**, **Casalis PA**, **Jensen F**, **Woidacki K**, **Zenclussen AC**. Hormonal Fluctuations during the Estrous Cycle Modulate Heme Oxygenase-1 Expression in the Uterus. *Front Endocrinol (Lausanne)* 5: 32, 2014. doi: 10.3389/fendo.2014.00032.

210. **McQuillan HJ**, **Han SY**, **Cheong I**, **Herbison AE**. GnRH Pulse Generator Activity Across the Estrous Cycle of Female Mice. *Endocrinology* 160: 1480–1491, 2019. doi: 10.1210/en.2019-00193.

211. **Smith MS**, **Freeman ME**, **Neill JD**. The control of progesterone secretion during the estrous cycle and early pseudopregnancy in the rat: prolactin, gonadotropin and steroid levels associated with rescue of the corpus luteum of pseudopregnancy. *Endocrinology* 96: 219–226, 1975. doi: 10.1210/endo-96-1-219.

212. **El Khoudary SR**, **Aggarwal B**, **Beckie TM**, **Hodis HN**, **Johnson AE**, **Langer RD**, **Limacher MC**, **Manson JE**, **Stefanick ML**, **Allison MA**, **American Heart Association Prevention Science Committee of the Council on Epidemiology and Prevention; and Council on Cardiovascular and Stroke Nursing**. Menopause Transition and Cardiovascular Disease Risk: Implications for Timing of Early Prevention: A Scientific Statement From the American Heart Association. *Circulation* 142: e506–e532, 2020. doi: 10.1161/CIR.0000000000000912.

213. **Appt SE**, **Ethun KF**. Reproductive aging and risk for chronic disease: Insights from studies of nonhuman primates. *Maturitas* 67: 7–14, 2010. doi: 10.1016/j.maturitas.2010.03.028.

214. **Webber KM**, **Casadesus G**, **Marlatt MW**, **Perry G**, **Hamlin CR**, **Atwood CS**, **Bowen RL**, **Smith MA**. Estrogen Bows to a New Master: The Role of Gonadotropins in Alzheimer Pathogenesis. *Annals of the New York Academy of Sciences* 1052: 201–209, 2005. doi: 10.1196/annals.1347.020.

215. **Moir ME**, **Corkery AT**, **Senese KA**, **Miller KB**, **Pearson AG**, **Loggie NA**, **Howery AJ**, **Gaynor-Metzinger SHA**, **Cody KA**, **Eisenmenger LB**, **Johnson SC**, **Barnes JN**. Age at natural menopause impacts cerebrovascular reactivity and brain structure. *American Journal of Physiology-Regulatory, Integrative and Comparative Physiology* 324: R207–R215, 2023. doi: 10.1152/ajpregu.00228.2022.

216. **Keaney JF**, **Shwaery GT**, **Xu A**, **Nicolosi RJ**, **Loscalzo J**, **Foxall TL**, **Vita JA**. 17 beta-estradiol preserves endothelial vasodilator function and limits low-density lipoprotein oxidation in hypercholesterolemic swine. *Circulation* 89: 2251–2259, 1994. doi: 10.1161/01.cir.89.5.2251.

217. **Moien-Afshari F**, **Kenyon E**, **Choy JC**, **Battistini B**, **McManus BM**, **Laher I**. Long-term effects of ovariectomy and estrogen replacement treatment on endothelial function in mature rats. *Maturitas* 45: 213–223, 2003. doi: 10.1016/s0378-5122(03)00149-x.

218. **Liu Z**, **Gou Y**, **Zhang H**, **Zuo H**, **Zhang H**, **Liu Z**, **Yao D**. Estradiol improves cardiovascular function through up-regulation of SOD2 on vascular wall. *Redox Biology* 3: 88–99, 2014. doi: 10.1016/j.redox.2014.11.001.

219. **Vitale DC**, **Piazza C**, **Melilli B**, **Drago F**, **Salomone S**. Isoflavones: estrogenic activity, biological effect and bioavailability. *Eur J Drug Metab Pharmacokinet* 38: 15–25, 2013. doi: 10.1007/s13318-012-0112-y.

220. **Kuiper GGJM**, **Lemmen JG**, **Carlsson B**, **Corton JC**, **Safe SH**, **Van Der Saag PT**, **Van Der Burg B**, **Gustafsson J-Å**. Interaction of Estrogenic Chemicals and Phytoestrogens with Estrogen Receptor β. *Endocrinology* 139: 4252–4263, 1998. doi: 10.1210/endo.139.10.6216.

221. **Azadbakht L**, **Kimiagar M**, **Mehrabi Y**, **Esmaillzadeh A**, **Hu FB**, **Willett WC**. Soy Consumption, Markers of Inflammation, and Endothelial Function: A cross-over study in postmenopausal women with the metabolic syndrome. *Diabetes Care* 30: 967–973, 2007. doi: 10.2337/dc06-2126.

222. **Hamden K**, **Carreau S**, **Ayadi F**, **Masmoudi H**, **El Feki A**. Inhibitory effect of estrogens, phytoestrogens, and caloric restriction on oxidative stress and hepato-toxicity in aged rats. *Biomed Environ Sci* 22: 381–387, 2009. doi: 10.1016/S0895-3988(10)60015-3.

223. **Schreihofer DA**, **Deutsch C**, **Lovekamp-Swan T**, **Sullivan JC**, **Dorrance AM**. Effect of high soy diet on the cerebrovasculature and endothelial nitric oxide synthase in the ovariectomized rat. *Vascul Pharmacol* 52: 236–242, 2010. doi: 10.1016/j.vph.2010.02.003.

224. **Jeong HG**, **Park H**. Metabolic Disorders in Menopause. *Metabolites* 12: 954, 2022. doi: 10.3390/metabo12100954.

225. **Olver TD**, **McDonald MW**, **Klakotskaia D**, **Richardson RA**, **Jasperse JL**, **Melling CWJ**, **Schachtman TR**, **Yang HT**, **Emter CA**, **Laughlin MH**. A chronic physical activity treatment in obese rats normalizes the contributions of ET-1 and NO to insulin-mediated posterior cerebral artery vasodilation. *Journal of Applied Physiology* 122: 1040–1050, 2017. doi: 10.1152/japplphysiol.00811.2016.

226. **Katakam PVG**, **Domoki F**, **Lenti L**, **Gáspár T**, **Institoris A**, **Snipes JA**, **Busija DW**. Cerebrovascular responses to insulin in rats. *J Cereb Blood Flow Metab* 29: 1955, 2009. doi: 10.1038/jcbfm.2009.177.

227. **Akintola AA**, **van Opstal AM**, **Westendorp RG**, **Postmus I**, **van der Grond J**, **van Heemst D**. Effect of intranasally administered insulin on cerebral blood flow and perfusion; a randomized experiment in young and older adults. *Aging (Albany NY)* 9: 790–802, 2017. doi: 10.18632/aging.101192.

228. **Nijssen KMR**, **Mensink RP**, **Joris PJ**. Effects of Intranasal Insulin Administration on Cerebral Blood Flow and Cognitive Performance in Adults: A Systematic Review of Randomized, Placebo-Controlled Intervention Studies. *Neuroendocrinology* 113: 1–13, 2023. doi: 10.1159/000526717.

229. **Gray SM**, **Aylor KW**, **Barrett EJ**. Unravelling the regulation of insulin transport across the brain endothelial cell. *Diabetologia* 60: 1512–1521, 2017. doi: 10.1007/s00125-017-4285-4.

230. **Kehmeier MN**, **Bedell BR**, **Cullen AE**, **Khurana A**, **D'Amico HJ**, **Henson GD**, **Walker AE**. In vivo arterial stiffness, but not isolated artery endothelial function, varies with the

mouse estrous cycle. *American Journal of Physiology-Heart and Circulatory Physiology* 323: H1057–H1067, 2022. doi: 10.1152/ajpheart.00369.2022.

231. **Cole JA**, **Kehmeier MN**, **Bedell BR**, **Krishna Kumaran S**, **Henson GD**, **Walker AE**. Sex Differences in the Relation Between Frailty and Endothelial Dysfunction in Old Mice. *The Journals of Gerontology: Series A* 77: 416–423, 2022. doi: 10.1093/gerona/glab317.

232. **Walker AE**, **Henson GD**, **Reihl KD**, **Morgan RG**, **Dobson PS**, **Nielson EI**, **Ling J**, **Mecham RP**, **Li DY**, **Lesniewski LA**, **Donato AJ**. Greater impairments in cerebral artery compared with skeletal muscle feed artery endothelial function in a mouse model of increased large artery stiffness. *J Physiol* 593: 1931–1943, 2015. doi: 10.1113/jphysiol.2014.285338.

233. **Reeve EH**, **Kronquist EK**, **Wolf JR**, **Lee B**, **Khurana A**, **Pham H**, **Cullen AE**, **Peterson JA**, **Meza A**, **Colton Bramwell R**, **Villasana L**, **Machin DR**, **Henson GD**, **Walker AE**. Pyridoxamine treatment ameliorates large artery stiffening and cerebral artery endothelial dysfunction in old mice. *J Cereb Blood Flow Metab* 43: 281–295, 2023. doi: 10.1177/0271678X221130124.

234. **De Paoli M**, **Zakharia A**, **Werstuck GH**. The Role of Estrogen in Insulin Resistance: A Review of Clinical and Preclinical Data. *The American Journal of Pathology* 191: 1490–1498, 2021. doi: 10.1016/j.ajpath.2021.05.011.

235. **Bansal S**, **Chopra K**. Construction of time-response curve for neuronal and vascular endothelial dysfunction in ovariectomized rats. *Indian J Pharmacol* 53: 31–38, 2021. doi: 10.4103/ijp.IJP_233_18.

236. **Somani YB**, **Pawelczyk JA**, **De Souza MJ**, **Kris-Etherton PM**, **Proctor DN**. Aging women and their endothelium: probing the relative role of estrogen on vasodilator function. *Am J Physiol Heart Circ Physiol* 317: H395–H404, 2019. doi: 10.1152/ajpheart.00430.2018.

237. **Catania MA**, **Crupi A**, **Firenzuoli F**, **Parisi A**, **Sturiale A**, **Squadrito F**, **Caputi AP**, **Calapai G**. Oral Administration of a Soy Extract Improves Endothelial Dysfunction in Ovariectomized Rats. *Planta med* 68: 1142–1144, 2002. doi: 10.1055/s-2002-36349.

238. **Wang D**, **Wang C**, **Wu X**, **Zheng W**, **Sandberg K**, **Ji H**, **Welch WJ**, **Wilcox CS**. Endothelial dysfunction and enhanced contractility in microvessels from ovariectomised rats: roles of oxidative stress and perivascular adipose tissue. *Hypertension* 63: 1063–1069, 2014. doi: 10.1161/HYPERTENSIONAHA.113.02284.

239. **LeBlanc AJ**, **Reyes R**, **Kang LS**, **Dailey RA**, **Stallone JN**, **Moningka NC**, **Muller-Delp JM**. Estrogen replacement restores flow-induced vasodilation in coronary arterioles of aged and ovariectomized rats. *American Journal of Physiology-Regulatory, Integrative and Comparative Physiology* 297: R1713–R1723, 2009. doi: 10.1152/ajpregu.00178.2009.

240. **Miller AA**, **Drummond GR**, **Mast AE**, **Schmidt HHHW**, **Sobey CG**. Effect of gender on NADPH-oxidase activity, expression, and function in the cerebral circulation: role of estrogen. *Stroke* 38: 2142–2149, 2007. doi: 10.1161/STROKEAHA.106.477406.

241. **DuBose LE**, **Ozemek C**, **Wick T**, **Richardson V**, **Hildreth KL**, **Moreau KL**. Role of BH4 deficiency as a mediator of oxidative stress-related endothelial dysfunction in menopausal women. *Am J Physiol Heart Circ Physiol* 323: H975–H982, 2022. doi: 10.1152/ajpheart.00435.2022.

242. **Lam K-K**, **Lee Y-M**, **Hsiao G**, **Chen S-Y**, **Yen M-H**. Estrogen therapy replenishes vascular tetrahydrobiopterin and reduces oxidative stress in ovariectomized rats. *Menopause* 13: 294–302, 2006. doi: 10.1097/01.gme.0000182806.99137.5e.

243. **Clegg D**, **Hevener AL**, **Moreau KL**, **Morselli E**, **Criollo A**, **Van Pelt RE**, **Vieira-Potter VJ**. Sex Hormones and Cardiometabolic Health: Role of Estrogen and Estrogen Receptors. *Endocrinology* 158: 1095–1105, 2017. doi: 10.1210/en.2016-1677.

244. **Jackman KA**, **Woodman OL**, **Chrissobolis S**, **Sobey CG**. Vasorelaxant and antioxidant activity of the isoflavone metabolite equol in carotid and cerebral arteries. *Brain Res* 1141: 99–107, 2007. doi: 10.1016/j.brainres.2007.01.007.

245. **Rosenfeld CR**, **Chen C**, **Roy T**, **Liu X tie**. Estrogen selectively up-regulates eNOS and nNOS in reproductive arteries by transcriptional mechanisms. *J Soc Gynecol Investig* 10: 205–215, 2003. doi: 10.1016/s1071-5576(03)00049-2.

246. **Si H**, **Liu D**. Genistein, a Soy Phytoestrogen, Upregulates the Expression of Human Endothelial Nitric Oxide Synthase and Lowers Blood Pressure in Spontaneously Hypertensive Rats1,2. *The Journal of Nutrition* 138: 297–304, 2008. doi: 10.1093/jn/138.2.297.

247. **Fisslthaler B**, **Benzing T**, **Busse R**, **Fleming I**. Insulin enhances the expression of the endothelial nitric oxide synthase in native endothelial cells: a dual role for Akt and AP-1. *Nitric Oxide* 8: 253–261, 2003. doi: 10.1016/s1089-8603(03)00042-9.

248. **Padilla J**, **Olver TD**, **Thyfault JP**, **Fadel PJ**. Role of habitual physical activity in modulating vascular actions of insulin. *Exp Physiol* 100: 759–771, 2015. doi: 10.1113/EP085107.

249. **Pernow J**, **Shemyakin A**, **Böhm F**. New perspectives on endothelin-1 in atherosclerosis and diabetes mellitus. *Life Sci* 91: 507–516, 2012. doi: 10.1016/j.lfs.2012.03.029.

250. **Eringa EC**, **Stehouwer CDA**, **Roos MH**, **Westerhof N**, **Sipkema P**. Selective resistance to vasoactive effects of insulin in muscle resistance arteries of obese Zucker (fa/fa) rats. *American Journal of Physiology-Endocrinology and Metabolism* 293: E1134–E1139, 2007. doi: 10.1152/ajpendo.00516.2006.

251. **Manrique-Acevedo C**, **Soares RN**, **Smith JA**, **Park LK**, **Burr K**, **Ramirez-Perez FI**, **McMillan NJ**, **Ferreira-Santos L**, **Sharma N**, **Olver TD**, **Emter CA**, **Parks EJ**,

Limberg JK, **Martinez-Lemus LA**, **Padilla J**. Impact of sex and diet-induced weight loss on vascular insulin sensitivity in type 2 diabetes. *American Journal of Physiology-Regulatory, Integrative and Comparative Physiology* 324: R293–R304, 2023. doi: 10.1152/ajpregu.00249.2022.

252. **Cross T-WL**, **Zidon TM**, **Welly RJ**, **Park Y-M**, **Britton SL**, **Koch LG**, **Rottinghaus GE**, **de Godoy MRC**, **Padilla J**, **Swanson KS**, **Vieira-Potter VJ**. Soy Improves Cardiometabolic Health and Cecal Microbiota in Female Low-Fit Rats. *Sci Rep* 7: 9261, 2017. doi: 10.1038/s41598-017-08965-0.

253. **Chirinos JA**, **Segers P**, **Hughes T**, **Townsend R**. Large-Artery Stiffness in Health and Disease. *Journal of the American College of Cardiology* 74: 1237–1263, 2019. doi: 10.1016/j.jacc.2019.07.012.

254. **Pase MP**, **Grima NA**, **Sarris J**. The effects of dietary and nutrient interventions on arterial stiffness: a systematic review. *Am J Clin Nutr* 93: 446–454, 2011. doi: 10.3945/ajcn.110.002725.

255. **Moreau KL**, **Hildreth KL**. Vascular Aging across the Menopause Transition in Healthy Women. *Advances in Vascular Medicine* 2014: e204390, 2014. doi: 10.1155/2014/204390.

256. **Losurdo P**, **Grillo A**, **Panizon E**, **Gortan Cappellari G**, **Fabris B**, **Bardelli M**, **Biolo G**, **Zanetti M**, **Carretta R**. Supplementation of omega-3 polyunsaturated fatty acids prevents increase in arterial stiffness after experimental menopause. *J Cardiovasc Pharmacol Ther* 19: 114–120, 2014. doi: 10.1177/1074248413500716.

257. **Tatchum-Talom R**, **Martel C**, **Marette A**. Influence of estrogen on aortic stiffness and endothelial function in female rats. *American Journal of Physiology-Heart and Circulatory Physiology* 282: H491–H498, 2002. doi: 10.1152/ajpheart.00589.2001.

258. **Westmark CJ**, **Brower J**, **Held PK**. Improving Reproducibility to Enhance Scientific Rigor through Consideration of Mouse Diet. *Animals* 12: 3448, 2022. doi: 10.3390/ani12243448.

259. **Russell JK**, **Jones CK**, **Newhouse PA**. The Role of Estrogen in Brain and Cognitive Aging. *Neurotherapeutics* 16: 649–665, 2019. doi: 10.1007/s13311-019-00766-9.

260. **ter Horst GJ**. Estrogen in the limbic system. *Vitam Horm* 82: 319–338, 2010. doi: 10.1016/S0083-6729(10)82017-5.

261. **Polonsky KS**, **Given BD**, **Van Cauter E**. Twenty-four-hour profiles and pulsatile patterns of insulin secretion in normal and obese subjects. *J Clin Invest* 81: 442–448, 1988. doi: 10.1172/JCI113339.

262. **Parra MD**, **de Morentin BEM**, **Martínez JA**. Postprandial insulin response and mitochondrial oxidation in obese men nutritionally treated to lose weight. *Eur J Clin Nutr* 59: 334–340, 2005. doi: 10.1038/sj.ejcn.1602078.

263. **Andrikopoulos S**, **Blair AR**, **Deluca N**, **Fam BC**, **Proietto J**. Evaluating the glucose tolerance test in mice. *Am J Physiol Endocrinol Metab* 295: E1323-1332, 2008. doi: 10.1152/ajpendo.90617.2008.

264. **Mosconi L**, **Berti V**, **Quinn C**, **McHugh P**, **Petrongolo G**, **Varsavsky I**, **Osorio RS**, **Pupi A**, **Vallabhajosula S**, **Isaacson RS**, **de Leon MJ**, **Brinton RD**. Sex differences in Alzheimer risk: Brain imaging of endocrine vs chronologic aging. *Neurology* 89: 1382–1390, 2017. doi: 10.1212/WNL.0000000000004425.

265. **Riedel BC**, **Thompson PM**, **Brinton RD**. Age, APOE and sex: Triad of risk of Alzheimer's disease. *The Journal of Steroid Biochemistry and Molecular Biology* 160: 134–147, 2016. doi: 10.1016/j.jsbmb.2016.03.012.

266. **Yue Y**, **Hu L**, **Tian Q**, **Jiang J**, **Dong Y**, **Jin Z**, **Cheng Y**, **Hong X**, **Ge Q**, **Zuo P**. Effects of long-term, low-dose sex hormone replacement therapy on hippocampus and cognition of postmenopausal women of different apoE genotypes. *Acta Pharmacol Sin* 28: 1129–1135, 2007. doi: 10.1111/j.1745-7254.2007.00618.x.

267. **Yun SH**, **Park KA**, **Kwon S**, **Woolley CS**, **Sullivan PM**, **Pasternak JF**, **Trommer BL**. Estradiol enhances long term potentiation in hippocampal slices from aged apoE4-TR mice. *Hippocampus* 17: 1153–1157, 2007. doi: 10.1002/hipo.20357.

268. **Rippon GA**, **Tang M-X**, **Lee JH**, **Lantigua R**, **Medrano M**, **Mayeux R**. Familial Alzheimer Disease in Latinos: Interaction Between APOE, Stroke and Estrogen Replacement. *Neurology* 66: 35, 2006. doi: 10.1212/01.wnl.0000191300.38571.3e.

269. **Zlokovic BV**. Neurovascular pathways to neurodegeneration in Alzheimer's disease and other disorders. *Nat Rev Neurosci* 12: 723–738, 2011. doi: 10.1038/nrn3114.

270. **Katusic ZS**, **d'Uscio LV**, **He T**. Emerging Roles of Endothelial Nitric Oxide in Preservation of Cognitive Health. *Stroke* 54: 686–696, 2023. doi: 10.1161/STROKEAHA.122.041444.

271. **Liu Z**, **Gou Y**, **Zhang H**, **Zuo H**, **Zhang H**, **Liu Z**, **Yao D**. Estradiol improves cardiovascular function through up-regulation of SOD2 on vascular wall. *Redox Biol* 3: 88–99, 2014. doi: 10.1016/j.redox.2014.11.001.

272. **Hevener AL**, **Ribas V**, **Moore TM**, **Zhou Z**. ERα in the Control of Mitochondrial Function and Metabolic Health. *Trends in Molecular Medicine* 27: 31–46, 2021. doi: 10.1016/j.molmed.2020.09.006.

273. **Caminiti SP**, **Ballarini T**, **Sala A**, **Cerami C**, **Presotto L**, **Santangelo R**, **Fallanca F**, **Vanoli EG**, **Gianolli L**, **Iannaccone S**, **Magnani G**, **Perani D**, **Project B**. FDG-PET and CSF biomarker accuracy in prediction of conversion to different dementias in a large multicentre MCI cohort. *NeuroImage : Clinical* 18: 167, 2018. doi: 10.1016/j.nicl.2018.01.019.

274. **Mosconi L**, **Rahman A**, **Diaz I**, **Wu X**, **Scheyer O**, **Hristov HW**, **Vallabhajosula S**, **Isaacson RS**, **de Leon MJ**, **Brinton RD**. Increased Alzheimer's risk during the menopause transition: A 3-year longitudinal brain imaging study. *PLoS ONE* 13: e0207885, 2018. doi: 10.1371/journal.pone.0207885.

275. **Mishra A**, **Wang Y**, **Yin F**, **Vitali F**, **Rodgers KE**, **Soto M**, **Mosconi L**, **Wang T**, **Brinton RD**. A tale of two systems: Lessons learned from female mid-life aging with implications for Alzheimer's prevention & treatment. *Ageing Res Rev* 74: 101542, 2022. doi: 10.1016/j.arr.2021.101542.

276. **Schmukler E**, **Solomon S**, **Simonovitch S**, **Goldshmit Y**, **Wolfson E**, **Michaelson DM**, **Pinkas-Kramarski R**. Altered mitochondrial dynamics and function in APOE4-expressing astrocytes. *Cell Death Dis* 11: 578, 2020. doi: 10.1038/s41419-020-02776-4.

277. **Busija DW**, **Rutkai I**, **Dutta S**, **Katakam PV**. Role of Mitochondria in Cerebral Vascular Function: Energy Production, Cellular Protection, and Regulation of Vascular Tone. *Compr Physiol* 6: 1529–1548, 2016. doi: 10.1002/cphy.c150051.

278. **Tyrrell DJ**, **Blin MG**, **Song J**, **Wood SC**, **Goldstein DR**. Aging Impairs Mitochondrial Function and Mitophagy and Elevates Interleukin 6 Within the Cerebral Vasculature. *J Am Heart Assoc* 9: e017820, 2020. doi: 10.1161/JAHA.120.017820.

279. **Kehmeier MN**, **Khurana A**, **Bedell BR**, **Cullen AE**, **Cannon AT**, **Henson GD**, **Walker AE**. Effects of dietary soy content on cerebral artery function and behavior in ovariectomized female mice. *Am J Physiol Heart Circ Physiol* 326: H636–H647, 2024. doi: 10.1152/ajpheart.00618.2023.

280. **Quiros PM**, **Goyal A**, **Jha P**, **Auwerx J**. Analysis of mtDNA/nDNA ratio in mice. *Curr Protoc Mouse Biol* 7: 47–54, 2017. doi: 10.1002/cpmo.21.

281. **Duvoisin RM**, **Villasana L**, **Pfankuch T**, **Raber J**. Sex-Dependent Cognitive Phenotype of Mice Lacking mGluR8. *Behav Brain Res* 209: 21–26, 2010. doi: 10.1016/j.bbr.2010.01.006.

282. **Balu D**, **Valencia-Olvera AC**, **Deshpande A**, **Narayanam S**, **Konasani S**, **Pattisapu S**, **York JM**, **Thatcher GRJ**, **LaDu MJ**, **Tai LM**. Estradiol improves behavior in FAD transgenic mice that express APOE3 but not APOE4 after ovariectomy. *Front Endocrinol (Lausanne)* 15: 1374825, 2024. doi: 10.3389/fendo.2024.1374825.

283. **Burkhardt MS**, **Foster JK**, **Laws SM**, **Baker LD**, **Craft S**, **Gandy SE**, **Stuckey BGA**, **Clarnette R**, **Nolan D**, **Hewson-Bower B**, **Martins RN**. Oestrogen replacement therapy may improve memory functioning in the absence of APOE epsilon4. *J Alzheimers Dis* 6: 221–228, 2004. doi: 10.3233/jad-2004-6302.

284. **Yaffe K**, **Haan M**, **Byers A**, **Tangen C**, **Kuller L**. Estrogen use, APOE, and cognitive decline: Evidence of gene–environment interaction. *Neurology* 54: 1949–1954, 2000. doi: 10.1212/WNL.54.10.1949.

285. **Wugalter KA**, **Schroeder RA**, **Thurston RC**, **Wu M**, **Aizenstein HJ**, **Cohen AD**, **Kamboh MI**, **Karikari TK**, **Derby CA**, **Maki PM**. Associations of endogenous estrogens, plasma Alzheimer's disease biomarkers, and APOE4 carrier status on regional brain volumes in postmenopausal women. *Frontiers in Aging Neuroscience* 16: 1426070, 2024. doi: 10.3389/fnagi.2024.1426070.

286. **Cullen AE**, **Centner AM**, **Deitado R**, **Ismaeel A**, **Koutakis P**, **Muller-Delp J**, **Salazar G**. AKT Mediates Adiponectin-Dependent Regulation of VSMC Phenotype. *Cells* 12: 2493, 2023. doi: 10.3390/cells12202493.

287. **Oldendorf WH**, **Cornford ME**, **Brown WJ**. The large apparent work capability of the blood-brain barrier: a study of the mitochondrial content of capillary endothelial cells in brain and other tissues of the rat. *Ann Neurol* 1: 409–417, 1977. doi: 10.1002/ana.410010502.

288. **Kirkman DL**, **Robinson AT**, **Rossman MJ**, **Seals DR**, **Edwards DG**. Mitochondrial contributions to vascular endothelial dysfunction, arterial stiffness, and cardiovascular diseases. *American Journal of Physiology-Heart and Circulatory Physiology* 320: H2080–H2100, 2021. doi: 10.1152/ajpheart.00917.2020.

289. **Caja S**, **Enríquez JA**. Mitochondria in endothelial cells: Sensors and integrators of environmental cues. *Redox Biology* 12: 821–827, 2017. doi: 10.1016/j.redox.2017.04.021.

290. **Farmer BC**, **Williams HC**, **Devanney NA**, **Piron MA**, **Nation GK**, **Carter DJ**, **Walsh AE**, **Khanal R**, **Young LEA**, **Kluemper JC**, **Hernandez G**, **Allenger EJ**, **Mooney R**, **Golden LR**, **Smith CT**, **Brandon JA**, **Gupta VA**, **Kern PA**, **Gentry MS**, **Morganti JM**, **Sun RC**, **Johnson LA**. APOE4 lowers energy expenditure in females and impairs glucose oxidation by increasing flux through aerobic glycolysis. *Mol Neurodegeneration* 16: 62, 2021. doi: 10.1186/s13024-021-00483-y.

291. **Riddell DR**, **Zhou H**, **Atchison K**, **Warwick HK**, **Atkinson PJ**, **Jefferson J**, **Xu L**, **Aschmies S**, **Kirksey Y**, **Hu Y**, **Wagner E**, **Parratt A**, **Xu J**, **Li Z**, **Zaleska MM**, **Jacobsen JS**, **Pangalos MN**, **Reinhart PH**. Impact of Apolipoprotein E (ApoE) Polymorphism on Brain ApoE Levels. *J Neurosci* 28: 11445–11453, 2008. doi: 10.1523/JNEUROSCI.1972-08.2008.

292. **Srivastava RA**, **Srivastava N**, **Averna M**, **Lin RC**, **Korach KS**, **Lubahn DB**, **Schonfeld G**. Estrogen up-regulates apolipoprotein E (ApoE) gene expression by increasing ApoE mRNA in the translating pool via the estrogen receptor alpha-mediated pathway. *J Biol Chem* 272: 33360–33366, 1997. doi: 10.1074/jbc.272.52.33360.

293. **Xing D**, **Oparil S**, **Yu H**, **Gong K**, **Feng W**, **Black J**, **Chen Y-F**, **Nozell S**. Estrogen Modulates NFκB Signaling by Enhancing IκBα Levels and Blocking p65 Binding at the Promoters of Inflammatory Genes via Estrogen Receptor-β. *PLoS One* 7: e36890, 2012. doi: 10.1371/journal.pone.0036890.

294. **Moreau KL**, **Deane KD**, **Meditz AL**, **Kohrt WM**. TUMOR NECROSIS FACTOR-α INHIBITION IMPROVES ENDOTHELIAL FUNCTION AND DECREASES

ARTERIAL STIFFNESS IN ESTROGEN-DEFICIENT POSTMENOPAUSAL WOMEN. *Atherosclerosis* 230: 10.1016/j.atherosclerosis.2013.07.057, 2013. doi: 10.1016/j.atherosclerosis.2013.07.057.

295. **Ali K**, **Lund-Katz S**, **Lawson J**, **Phillips MC**, **Rader DJ**. Structure-function properties of the apoE-dependent COX-2 pathway in vascular smooth muscle cells. *Atherosclerosis* 196: 201–209, 2008. doi: 10.1016/j.atherosclerosis.2007.03.038.

296. **Moussa N**, **Dayoub N**. Exploring the role of COX-2 in Alzheimer's disease: Potential therapeutic implications of COX-2 inhibitors. *Saudi Pharm J* 31: 101729, 2023. doi: 10.1016/j.jsps.2023.101729.

297. **Gibson LL**, **Hahner L**, **Osborne-Lawrence S**, **German Z**, **Wu KK**, **Chambliss KL**, **Shaul PW**. Molecular Basis of Estrogen-Induced Cyclooxygenase Type 1 Upregulation in Endothelial Cells. *Circulation Research* 96: 518–525, 2005. doi: 10.1161/01.RES.0000158967.96231.88.

298. **Cooper LL**, **Mitchell GF**. Aortic Stiffness, Cerebrovascular Dysfunction, and Memory. *Pulse* 4: 69, 2016. doi: 10.1159/000448176.

299. **Palta P**, **Sharrett AR**, **Wei J**, **Meyer ML**, **Kucharska-Newton A**, **Power MC**, **Deal JA**, **Jack CR**, **Knopman D**, **Wright J**, **Griswold M**, **Tanaka H**, **Mosley TH**, **Heiss G**. Central Arterial Stiffness Is Associated With Structural Brain Damage and Poorer Cognitive Performance: The ARIC Study. *JAHA* 8: e011045, 2019. doi: 10.1161/JAHA.118.011045.

300. **Werhane ML**, **Thomas KR**, **Edmonds EC**, **Bangen KJ**, **Tran M**, **Clark AL**, **Nation DA**, **Gilbert PE**, **Bondi MW**, **Delano-Wood L**, **Alzheimer's Disease Neuroimaging Initiative**. Differential Effect of APOE ε4 Status and Elevated Pulse Pressure on Functional Decline in Cognitively Normal Older Adults. *J Alzheimers Dis* 62: 1567–1578, 2018. doi: 10.3233/JAD-170918.

301. **van Heuvelen MJG**, **van der Lei MB**, **Alferink PM**, **Roemers P**, **van der Zee EA**. Cognitive deficits in human ApoE4 knock-in mice: A systematic review and meta-analysis. *Behavioural Brain Research* 471: 115123, 2024. doi: 10.1016/j.bbr.2024.115123.

302. **Christensen A**, **McGill CJ**, **Qian W**, **Pike CJ**. Effects of obesogenic diet and 17β-estradiol in female mice with APOE 3/3, 3/4, and 4/4 genotypes. *Front Aging Neurosci* 16: 1415072, 2024. doi: 10.3389/fnagi.2024.1415072.

303. **Leung L**, **Andrews-Zwilling Y**, **Yoon SY**, **Jain S**, **Ring K**, **Dai J**, **Wang MM**, **Tong L**, **Walker D**, **Huang Y**. Apolipoprotein E4 Causes Age- and Sex-Dependent Impairments of Hilar GABAergic Interneurons and Learning and Memory Deficits in Mice. *PLOS ONE* 7: e53569, 2012. doi: 10.1371/journal.pone.0053569.

304. Ageing and disability | Division for Inclusive Social Development (DISD) [Online]. [date unknown]. https://social.desa.un.org/issues/disability/disability-issues/ageing-and-disability [14 Oct. 2024].

305. **Kumar V**, **Kim S-H**, **Bishayee K**. Dysfunctional Glucose Metabolism in Alzheimer's Disease Onset and Potential Pharmacological Interventions. *International Journal of Molecular Sciences* 23, 2022. doi: 10.3390/ijms23179540.

306. **Shin KC**, **Ali Moussa HY**, **Park Y**. Cholesterol imbalance and neurotransmission defects in neurodegeneration. *Exp Mol Med* 56: 1685–1690, 2024. doi: 10.1038/s12276-024-01273-4.

307. **Cortes-Canteli M**, **Iadecola C**. Alzheimer's Disease and Vascular Aging. *J Am Coll Cardiol* 75: 942–951, 2020. doi: 10.1016/j.jacc.2019.10.062.

308. **Amidfar M**, **Garcez ML**, **Kim Y-K**. The shared molecular mechanisms underlying aging of the brain, major depressive disorder, and Alzheimer's disease: The role of circadian rhythm disturbances. *Progress in Neuro-Psychopharmacology and Biological Psychiatry* 123: 110721, 2023. doi: 10.1016/j.pnpbp.2023.110721.

309. **Brinton RD**, **Yao J**, **Yin F**, **Mack WJ**, **Cadenas E**. Perimenopause as a neurological transition state. *Nat Rev Endocrinol* 11: 393–405, 2015. doi: 10.1038/nrendo.2015.82.

310. **Liu C-C**, **Zhao N**, **Fu Y**, **Wang N**, **Linares C**, **Tsai C-W**, **Bu G**. ApoE4 accelerates early seeding of amyloid pathology. *Neuron* 96: 1024, 2017. doi: 10.1016/j.neuron.2017.11.013.

311. **Koutsodendris N**, **Blumenfeld J**, **Agrawal A**, **Traglia M**, **Grone B**, **Zilberter M**, **Yip O**, **Rao A**, **Nelson MR**, **Hao Y**, **Thomas R**, **Yoon SY**, **Arriola P**, **Huang Y**. Neuronal APOE4 removal protects against tau-mediated gliosis, neurodegeneration and myelin deficits. *Nat Aging* 3: 275–296, 2023. doi: 10.1038/s43587-023-00368-3.

312. **Halliday MR**, **Rege SV**, **Ma Q**, **Zhao Z**, **Miller CA**, **Winkler EA**, **Zlokovic BV**. Accelerated pericyte degeneration and blood–brain barrier breakdown in apolipoprotein E4 carriers with Alzheimer's disease. *J Cereb Blood Flow Metab* 36: 216–227, 2016. doi: 10.1038/jcbfm.2015.44.

313. **Tai LM**, **Thomas R**, **Marottoli FM**, **Koster KP**, **Kanekiyo T**, **Morris AW**, **Bu G**. The Role of APOE in Cerebrovascular Dysfunction. *Acta Neuropathol* 131: 709–723, 2016. doi: 10.1007/s00401-016-1547-z.

314. **Wierenga CE**, **Clark LR**, **Dev SI**, **Shin DD**, **Jurick SM**, **Rissman RA**, **Liu TT**, **Bondi MW**. Interaction of Age and APOE Genotype on Cerebral Blood Flow at Rest. *J Alzheimers Dis* 34: 921–935, 2013. doi: 10.3233/JAD-121897.

315. **Hainsworth AH**, **Markus HS**, **Schneider JA**. Cerebral Small Vessel Disease, Hypertension, and Vascular Contributions to Cognitive Impairment and Dementia. *Hypertension* 81: 75–86, 2024. doi: 10.1161/HYPERTENSIONAHA.123.19943.

316. **Zanon Zotin MC**, **Sveikata L**, **Viswanathan A**, **Yilmaz P**. Cerebral small vessel disease and vascular cognitive impairment: from diagnosis to management. *Curr Opin Neurol* 34: 246–257, 2021. doi: 10.1097/WCO.0000000000000913.

317. **Butterfield DA**, **Mattson MP**. Apolipoprotein E and oxidative stress in brain with relevance to Alzheimer's disease. *Neurobiology of Disease* 138: 104795, 2020. doi: 10.1016/j.nbd.2020.104795.

318. **Deacon RMJ**. Measuring Motor Coordination in Mice. *J Vis Exp* : 2609, 2013. doi: 10.3791/2609.

319. **Whitehead JC**, **Hildebrand BA**, **Sun M**, **Rockwood MR**, **Rose RA**, **Rockwood K**, **Howlett SE**. A Clinical Frailty Index in Aging Mice: Comparisons With Frailty Index Data in Humans. *J Gerontol A Biol Sci Med Sci* 69: 621–632, 2014. doi: 10.1093/gerona/glt136.

320. **Schultz MB**, **Kane AE**, **Mitchell SJ**, **MacArthur MR**, **Warner E**, **Vogel DS**, **Mitchell JR**, **Howlett SE**, **Bonkowski MS**, **Sinclair DA**. Age and life expectancy clocks based on machine learning analysis of mouse frailty. *Nat Commun* 11: 4618, 2020. doi: 10.1038/s41467-020-18446-0.

321. **Gray NE**, **Hack W**, **Brandes MS**, **Zweig JA**, **Yang L**, **Marney L**, **Choi J**, **Magana AA**, **Cerruti N**, **McFerrin J**, **Koike S**, **Nguyen T**, **Raber J**, **Quinn JF**, **Maier CS**, **Soumyanath A**. Amelioration of age-related cognitive decline and anxiety in mice by Centella asiatica extract varies by sex, dose and mode of administration. .

322. **Taddei S**, **Virdis A**, **Ghiadoni L**, **Salvetti G**, **Bernini G**, **Magagna A**, **Salvetti A**. Age-related reduction of NO availability and oxidative stress in humans. *Hypertension* 38: 274–279, 2001. doi: 10.1161/01.hyp.38.2.274.

323. **Morgan RG**, **Donato AJ**, **Walker AE**. Telomere uncapping and vascular aging. *Am J Physiol Heart Circ Physiol* 315: H1–H5, 2018. doi: 10.1152/ajpheart.00008.2018.

324. **Shipley R**, **Mullerdelp J**. Aging decreases vasoconstrictor responses of coronary resistance arterioles through endothelium-dependent mechanisms. *Cardiovascular Research* 66: 374–383, 2005. doi: 10.1016/j.cardiores.2004.11.005.

325. **Marijic J**, **Li Q**, **Song M**, **Nishimaru K**, **Stefani E**, **Toro L**. Decreased expression of voltage- and Ca(2+)-activated K(+) channels in coronary smooth muscle during aging. *Circ Res* 88: 210–216, 2001. doi: 10.1161/01.res.88.2.210.

326. **Schiffrin EL**. Role of endothelin-1 in hypertension and vascular disease*. *American Journal of Hypertension* 14: 83S-89S, 2001. doi: 10.1016/S0895-7061(01)02074-X.

327. **Jh C**, **L P**, **Pj N**, **Gr C**. Lipid accumulation in arterial smooth muscle cells. Influence of phenotype. *Atherosclerosis* 47, 1983. doi: 10.1016/0021-9150(83)90059-x.

328. **Cao G**, **Xuan X**, **Hu J**, **Zhang R**, **Jin H**, **Dong H**. How vascular smooth muscle cell phenotype switching contributes to vascular disease. *Cell Communication and Signaling* 20: 180, 2022. doi: 10.1186/s12964-022-00993-2.

329. **Kim J**, **Montagnani M**, **Chandrasekran S**, **Quon MJ**. Role of Lipotoxicity in Endothelial Dysfunction. *Heart Failure Clinics* 8: 589–607, 2012. doi: 10.1016/j.hfc.2012.06.012.

330. **Wang R**, **Oh JM**, **Motovylyak A**, **Ma Y**, **Sager MA**, **Rowley HA**, **Johnson KM**, **Gallagher CL**, **Carlsson CM**, **Bendlin BB**, **Johnson SC**, **Asthana S**, **Eisenmenger L**, **Okonkwo OC**. Impact of sex and APOE ε4 on age-related cerebral perfusion trajectories in cognitively asymptomatic middle-aged and older adults: A longitudinal study. *J Cereb Blood Flow Metab* 41: 3016–3027, 2021. doi: 10.1177/0271678X211021313.

331. **Damestani NL**, **Jacoby J**, **Yadav SM**, **Lovely AE**, **Michael A**, **Terpstra M**, **Eshghi M**, **Rashid B**, **Cruchaga C**, **Salat DH**, **Juttukonda MR**. Associations between age, sex, APOE genotype, and regional vascular physiology in typically aging adults. *NeuroImage* 275: 120167, 2023. doi: 10.1016/j.neuroimage.2023.120167.

332. **Favre J**, **Gao J**, **Henry J-P**, **Remy-Jouet I**, **Fourquaux I**, **Billon-Gales A**, **Thuillez C**, **Arnal J-F**, **Lenfant F**, **Richard V**. Endothelial Estrogen Receptor α Plays an Essential Role in the Coronary and Myocardial Protective Effects of Estradiol in Ischemia/Reperfusion. *Arteriosclerosis, Thrombosis, and Vascular Biology* 30: 2562–2567, 2010. doi: 10.1161/ATVBAHA.110.213637.

333. **Gonzales RJ**, **Ghaffari AA**, **Duckles SP**, **Krause DN**. Testosterone treatment increases thromboxane function in rat cerebral arteries. *American Journal of Physiology-Heart and Circulatory Physiology* 289: H578–H585, 2005. doi: 10.1152/ajpheart.00958.2004.

334. **Wisdom NM**, **Callahan JL**, **Hawkins KA**. The effects of apolipoprotein E on non-impaired cognitive functioning: A meta-analysis. *Neurobiology of Aging* 32: 63–74, 2011. doi: 10.1016/j.neurobiolaging.2009.02.003.

335. **Boehm-Cagan A**, **Michaelson DM**. Reversal of apoE4-Driven Brain Pathology and Behavioral Deficits by Bexarotene. *J Neurosci* 34: 7293–7301, 2014. doi: 10.1523/JNEUROSCI.5198-13.2014.

336. **Gustavson AR**, **Cummings JL**. Assessment and Treatment of Neuropsychiatric Symptoms in Alzheimer's Disease. In: *Alzheimer's Disease: A Physician's Guide to Practical Management*, edited by Richter RW, Richter BZ. Humana Press, p. 371–385.

337. **de Toledo M**, **Bermejo-Pareja F**, **Vega-Quiroga S**, **Muñoz-García D**. [Behavioural disorders in Alzheimer's disease. Data from a populational study]. *Rev Neurol* 38: 901–905, 2004.

338. **Raber J**. Role of Apolipoprotein E in Anxiety. *Neural Plasticity* 2007: 091236, 2007. doi: 10.1155/2007/91236.

339. **Nolte ED**, **Nolte KA**, **Yan SS**. Anxiety and task performance changes in an aging mouse model. *Biochemical and Biophysical Research Communications* 514: 246–251, 2019. doi: 10.1016/j.bbrc.2019.04.049.

340. **Meng F-T**, **Zhao J**, **Fang H**, **Zhang L-F**, **Wu H-M**, **Liu Y-J**. Upregulation of Mineralocorticoid Receptor in the Hypothalamus Associated with a High Anxiety-like Level in Apolipoprotein E4 Transgenic Mice. *Behav Genet* 47: 416–424, 2017. doi: 10.1007/s10519-017-9843-5.

341. **Yanai S**, **Endo S**. Functional Aging in Male C57BL/6J Mice Across the Life-Span: A Systematic Behavioral Analysis of Motor, Emotional, and Memory Function to Define an Aging Phenotype. *Front Aging Neurosci* 13, 2021. doi: 10.3389/fnagi.2021.697621.

342. **Zhang X**, **Xie T**, **Zhou S**, **Yuan Y**, **Chen W**, **Zheng J**, **Liu X**, **Yuan T**, **Lu Y**, **Liu Z**. Effects of the ApoE genotype on cognitive function in aging mice fed with a high-fat diet and the protective potential of n-3 polyunsaturated fatty acids. *Food Funct* 15: 2249–2264, 2024. doi: 10.1039/D3FO03965J.

343. **Soni N**, **Hohsfield LA**, **Tran KM**, **Kawauchi S**, **Walker A**, **Javonillo D**, **Phan J**, **Matheos D**, **Da Cunha C**, **Uyar A**, **Milinkeviciute G**, **Gomez-Arboledas A**, **Tran K**, **Kaczorowski CC**, **Wood MA**, **Tenner AJ**, **LaFerla FM**, **Carter GW**, **Mortazavi A**, **Swarup V**, **MacGregor GR**, **Green KN**. Genetic diversity promotes resilience in a mouse model of Alzheimer's disease. *Alzheimers Dement* 20: 2794–2816, 2024. doi: 10.1002/alz.13753.

344. **Hakim MA**, **Behringer EJ**. Methyl-Beta-Cyclodextrin Restores KIR Channel Function in Brain Endothelium of Female Alzheimer's Disease Mice. *Journal of Alzheimer's Disease Reports* 5: 693, 2021. doi: 10.3233/ADR-210016.